Henri M. Duvernoy

The Human Hippocampus

Functional Anatomy, Vascularization and Serial Sections with MRI

Third Edition

Springer

Henri M. Duvernoy, The Human Hippocampus

Henri M. Duvernoy

The Human Hippocampus

Functional Anatomy, Vascularization and Serial Sections with MRI

Third Edition

In collaboration with F. Cattin, G. Fatterpekar, Th. Naidich, Ch. Raybaud, P.Y. Risold, U. Salvolini and T. Scarabino

Drawings by J. L. Vannson

With 260 Figures

Springer

H. Duvernoy
Anatomie, Université de Franche-Comté
Personal address:
Chemin des Relançons
25000 Besançon, France
email: henri.duvernoy@wanadoo.fr

F. Cattin
Service de Neuroradiologie, Centre Hospitalier Universitaire J. Minjoz
25000 Besançon, France

Th. Naidich and G. Fatterpekar
The Mount Sinai Medical Center
One Gustave L. Levy Place, New-York, USA

Ch. Raybaud
Hopital de la Timone, 264 rue Saint-Pierre
13385 Marseille Cedex 05, France

P.Y. Risold
Laboratoire d'Histologie, Faculté de Médecine
25000 Besançon, France

U. Salvolini
Instituto di Radiologia, Facultá di Medicina, Università Polytecnica
della Marche, Ancona, Italia

T. Scarabino
Neurologia, Casa Sollevo della Sofferenza
71013 San Giovanni Rotondo (FG), Italia

ISBN 3-540-23191-9 Springer-Verlag Berlin Heidelberg New York

Library of Congress Control Number: 2004112752

Springer-Verlag Berlin Heidelberg New York
Springer is a part of Springer Science+Business Media
http://www.springeronline.com

Printed in Germany

Cover Design: eStudio Calamar, Spain
Typesetting: FotoSatz Pfeifer GmbH, D-82166 Gräfelfing
Printed on acid-free paper – 24/3150 – 5 4 3 2 1 0

Preface

Since the first edition of this book was published (Duvernoy 1988), considerable advances have been made. The new edition therefore includes current concepts about functions of the hippocampus and a study of its external and internal vascularization. Head sections and magnetic resonance imaging (MRI) views have also been added to the previous atlas of sections.

The book is divided into five sections, preceded by an introduction (Chap. 1) and a short comment on the material and methods (Chap. 2). The first section (Chap. 3) deals briefly with the structure, functions, and connections of the hippocampus. This is followed in Chap. 4 by a description of the anatomy of the hippocampus and its relations with adjacent structures. The next section (Chap. 5) is concerned with the vascularization of the hippocampus, and the final sections (Chap. 6 and 7) are devoted to sectional anatomy and MRI.

This work has benefitted from the invaluable help of many of my colleagues. First of all, I would like to express my gratitude to the late Professor Roger Warwick, who helped me clarify the difficult description of hippocampal anatomy.

I will also acknowledge the help of Dr. F. Cattin, Prof. Ch. Raybaud, Dr. P.Y. Risold, and the members of the Department of Anatomy in Besançon.

My thanks go to Prof. T. Naidich, Dr. G. Fatterpekar, Prof. U. Salvolini and Prof. T. Scarabino who provide us with 9.4T and 3.T MRI views.

My deepest thanks to Michel Gaudron for his support as well as Ms. Françoise Gillet and Ms. Anne Richard.

Thanks are also due to Ms. S. Benko, Ms. G. Schröder, and Mr. J.W. Schmidt (Springer-Verlag, Heidelberg) for their support.

This book is dedicated to my wife Odile and to my sons Charles and David.

Henri Duvernoy

Contents

Introduction

The aim of this study is to give a precise description of human hippocampal anatomy in view of neurosurgical progress and the wealth of medical imaging methods available. Two major problems render this study more difficult: (1) the complexity of the hippocampal structure, making it one of the most mysterious regions in the central nervous system, and (2) the great confusion which plagues its terminology, a confusion which appeared in the earliest descriptions.

From among those who have studied the history of hippocampal terminology (e.g., Tilney 1939; Benninghoff 1940; Klinger 1948; Clara 1959; Meyer 1971), the views of Lewis (1923) have been chosen to be summarized here.

The first description of the hippocampus was written by Arantius in 1587 (cited in Lewis 1923), who compared the protrusion on the floor of the temporal horn to a hippocampus, or sea horse (see Fig. 3). It should be noted, however, that he hesitated between the terms "sea horse" and "silkworm." In 1729, J.G. Duvernoy (cited in Lewis 1923) first illustrated the hippocampus and he, too, hesitated between "hippocampus" and "silkworm." In 1732, Winslow suggested the term "ram's horn" (see Winslow 1752). *Hippocampus, silkworm*, and *ram's horn* were thus the terms used at the end of this initial period, all based on the intraventricular appearance of the hippocampus.

A second period was characterized by an excessive imagery among anatomists, who compared the hippocampus to mythological symbols:

- The "ram's horn" became the *cornu Ammonis*, after the Egyptian god Ammon (Ammun Kneph). This name, probably first used by De Garengeot (1742; cited by Lewis 1923), has remained in use.
- The term *pes hippocampi* was introduced next, although it is not known who added "foot" to the hippocampus. Lewis (1923) cites Diemerbroeck (1672), while others have challenged this claim. This curious terminology may derive from a comparison between the sea horse and the mythical animal that is supposed to have drawn Poseidon's chariot over the sea. The posterior part of this animal is shaped like a fish, and the anterior part, which is like a horse, has two feet folded back; each foot was compared to the intraventricular relief of the temporal horn, hence the appearance of the term "pes hippocampi." The end of this foot was webbed, like the enlarged anterior end of the intraventricular hippocampus or "digitationes hippocampi."

To complicate matters, the hippocampus was then described as having two feet: *pes hippocampi major* for the hippocampus and *pes hippocampi minor* for the calcar avis, a bulge in the occipital horn. The terms "large hippocampus" and "small hippocampus" have sometimes been used for these two structures.

In current usage, the terms "cornu Ammonis" and "pes hippocampi" are often regarded as synonymous (Kopsch 1940), although the latter is sometimes reserved for the digitationes hippocampi, which raise the anterior end of the hippocampus (Williams 1995).

After these periods of confusion, the terminology that is currently most commonly used needs to be clarified. The name hippocampus applies to the entire ventricular protrusion. Thus the hippocampus comprises two cortical laminae rolled up one inside the other: the cornu Ammonis and the gyrus dentatus (see Fig. 5). The subiculum, or transitional cortex between the cornu Ammonis and the rest of the temporal lobe, is sometimes viewed as part of the hippocampus, constituting a functional unit (Chronister and White 1975). However, since the hippocampus and subiculum do not form a distinct topographical unit, the subiculum is not included in this study.

Material and Methods

Sixty hippocampi were examined, the average age of the brains being 57 years (range, 19 – 85 years). To simplify this account, the hemisphere studied (right or left) and the sex of the subject it was taken from were omitted; previous studies have shown no differences stemming from the particular techniques used (Mani et al. 1986).

The brains were removed between 5 and 12 h after death and were fixed in a 10% formalin solution. Most had already received an intravascular injection of India ink. In the following, the specific methods used in each chapter are described.

In Chaps. 3 and 4 on the structure and anatomy of the hippocampus, two methods were used:

1. *Dissection of the hippocampus*. With the help of an operating microscope, the hippocampus was examined after ablation of blood vessels and leptomeninges. The temporal horn was opened, and the choroid plexuses removed to inspect the ventricular aspect of the hippocampus.
2. *Bodian's method of silver impregnation.* After fixation in formalin, the hippocampus was cut into sections of 10 – 20 µm and then impregnated by the silver proteinate method. This method is applicable after intravascular injection, and a correlation can thus be established between the neural architecture and the vascular network. Compared with the usual staining by cresyl violet, Bodian's technique has the advantage of showing not only neuronal somata, but also their processes. Conversely, and due to density of impregnation, photographs of large areas show insufficient contrast and are of little use.

In Chap. 5 on the hippocampal vascularization, two methods were applied:

1. *Intravascular injection of India ink.* Once the brain had been removed, 400 cc India ink solution diluted by distilled water to 50% was injected into the carotid and vertebral arteries. Gelatin (5% – 10%) was added to the mixture. In our opinion, this method of total vascular injection of the brain through the main arterial trunks is the best way to obtain a good view not only of the arteries, but also of the capillaries and, in particular, the veins. In the literature, the cerebral veins have always been studied by specific retrograde venous injections. Using this last method, however, it is rarely possible to obtain good filling of the venous tree. The method of intravascular India ink injection permits the vascular anatomy to be observed in three different ways:

a) *Observation of the superficial (leptomeningeal) vessels.* The superficial vessels were dissected with the help of an operating microscope. Arteries and veins were identified, and the point of penetration of arteries and emergence of veins noted (16 hemispheres were used for this study). The preparations were then photographed while immersed in distilled water to prevent reflection and bubbles.

b) *Identification of the deep path of intrahippocampal arteries and veins.* Blocks 3 – 4 mm thick were cut and cleared using the Spalteholz technique (a mixture of methyl salicylate and benzyl benzoate). The superficial arteries and veins identified during the preceding step were followed into the hippocampal tissue. By this method, it is possible to recognize the intrahippocampal arteries and veins and to follow them along their entire course.

c) *Thick sections.* After fixation, the brains were cut into coronal, sagittal, or axial sections in relation to the bicommissural plane linking the middle part of the anterior and posterior commissures. Sections (500 µm thick) were made after dehydration, immersion in toluene, and embedding in paraffin. To obtain thick sections without cracks, the block was heated between each cut. Sections were then mounted on slides in gelatin and dried under pressure. This method provides a picture of the total cerebral vascular pattern (Chap. 6) and allows the intrahippocampal vascular network to be studied. However, the possible deformation of the nervous tissue due to considerable shrinkage following immersion in alcohols and toluene must be taken in account. Thick sections facilitate the identification of cerebral structures according to differences in the vascular density. White and grey substances are clearly differentiated. In addition, the grey matter nuclei do not have a vascular network of equal density. This technique has already been used to study the vascularization of circumventricular organs and brain stem, cerebral, cerebellar cortices and pineal gland (Duvernoy 1972, 1975, 1978, 1995a, 1999a,b; Duvernoy and Koritke 1964, 1965; Duvernoy et al. 1969, 1971, 1972, 1981, 1983, 2000).

2. *Intravascular injection with low-viscosity resin (Mercox)*. This technique was used to complete the observation of the vessels carried out by intravascular injection of India ink. After total vascular injection of the brain with the resin (Mercox), the tissues were destroyed, and the cast of the vascular network was examined with a scanning electron microscope. Thus accurate observations of the fine vascular network and its spatial organization became possible.

In Chap. 7 on sectional anatomy, each plate includes several figures:

1. *A three-dimensional section of the hippocampus.* The principle of this method is to gradually erode the hemisphere by sectioning it from anterior to posterior for coronal sections, from medial to lateral for sagittal sections, and from superior to inferior for axial sections. Eroded tissue is discarded, and the newly exposed surface of the hemisphere is observed for the purpose of anatomical analysis.
2. *A head section*
3. *One or several MRI views*

The bicommissural plane acted as a reference for all these sections. The 3T MRI views were provided by Prof. U. Salvolini and Prof. T. Scarabino. Prof. T. Naidich and Dr. G. Fatterpekar supplied us with the 9.4T views obtained from anatomical preparation.

Structure, Functions, and Connections

3.1 Preliminary Remarks

The general situation of the hippocampus in relation to the hemisphere is indicated in Figs. 1 and 2. The intraventricular aspect of the hippocampus is shown in Fig. 3.

Features of the Limbic Lobe
As the hippocampus is part of the limbic lobe, this latter structure will be described first. The limbic lobe (see Figs. 1, 4) is situated on the inferomedial aspect of the hemisphere, separated from adjoining cortex by the limbic fissure. This fissure is a discontinuous sulcus composed successively of the cingulate, subparietal, anterior calcarine, collateral, and rhinal sulci. Broca (1878) divided the limbic lobe into the limbic and intralimbic gyri, something which has become an established tradition.

The *limbic gyrus* consists of the subcallosal, cingulate, and parahippocampal gyri. (The term "parahippocampal" will be used here, rather than "hippocampal gyrus," which can lead to confusion with the hippocampus itself.) The retrosplenial cortex and a narrowed lobule, the *isthmus*, join the cingulate and parahippocampal gyri behind and below the splenium of the corpus callosum (B.A. Vogt 1993). The parahippocampal gyrus can be divided into two segments: (1) the posterior segment is narrow, and its flat superior surface, the *subiculum*, is separated from the hippocampus by the hippocampal sulcus (see Fig. 5); (2) the anterior segment is more voluminous and is called the *piriform lobe*, comprising the *uncus* and the *entorhinal area*. The *uncus* curves posteriorly to rest on the parahippocampal gyrus itself, from which it is separated by the uncal sulcus. The uncus is functionally divided into anterior and posterior parts. The posterior part, which belongs to the hippocampus, will be studied later (see p. 41). The anterior part displays two protrusions: the *semilunar gyrus* and the *ambient gyrus* (Figs. 4, 28), which are separated by the *semianular sulcus*, both covering a deep nucleus, the *amygdala* (see Fig. 14). The *entorhinal area* is the lower part of the piriform lobe extending to the posterior segment of the parahippocampal gyrus.

The *intralimbic gyrus* arches within the limbic gyrus (Fig. 4). Its anterior segment includes a narrow zone in the subcallosal region, the prehippocampal rudiment, partially belonging to the paraterminal gyrus and to the septal region (Brodal 1947); its superior segment, a continuation of the prehippocampal rudiment, is the *indusium griseum*, situated on the superior surface of the corpus callosum. The indusium griseum is a neuronal lamina covering the corpus callosum as far as its splenium, itself covered on each side of the midline by two small white fasciculi, the medial and lateral longitudinal striae (see Fig. 32). Passing around the splenium, the indusium griseum reaches the inferior segment of the intralimbic gyrus, the hippocampus, which is the only part that is well developed.

The hippocampus, separated from the subiculum by the hippocampal sulcus, extends forward to the uncus to occupy its posterior segment. The hippocampus is bordered by the *fimbria* (Figs. 4, 5).

In relation to the corpus callosum, the intralimbic gyrus is sometimes divided into three parts (Elliot Smith 1897): (1) the precommissural hippocampus (prehippocampal rudiment), (2) the supracommissural hippocampus (indusium griseum), and (3) the retrocommissural hippocampus (the hippocampus proper). This terminology takes into account the migration of the hippocampus during development. The human hippocampus follows the progress of the lateral telencephalic vesicle, which starts from the region of the interventricular foramen and curves up and back and then down and under to form the *temporal lobe*. This development is incomplete in most mammals, as rotation of the primitive telencephalic vesicle ceases before a complete temporal lobe is formed. Thus in the rat, for instance, the retrocommissural hippocampus remains largely dorsal to the thalamus, whereas the human hippocampus curves beneath the thalamus (Fig. 6). It will be noted below that these differences contribute to the complexity and confusion of hippocampal terminology.

The development of conceptions about the anatomy and functions of the limbic lobe was clearly presented by Nieuwenhuys (1985).

Broca (1878) first described and named the limbic lobe. From its comparative anatomy, he attributed olfactory functions to these structures. It was therefore later named the rhinencephalon (W. Turner 1891).

In a subsequent phase in speculation on the limbic lobe by observers such as Papez (1937) and Brodal (1947), it was suggested that, in humans, this lobe is only partially olfactory and is mainly concerned with emotional behavior. In addition, the amygdala was seen as part of the limbic lobe. MacLean (1970) subsequently included numerous subcortical structures such as the septum, midline thalamus, habenula, and hypothalamus in the limbic lobe, something which was later criticized by LeDoux (1989). Thus from the single entity of Broca, the limbic lobe became an organization, the so-called *limbic system*, composed of disparate anatomical units with common functions. Nauta (1958) developed this concept further, insisting on the functional importance of certain regions of the neural axis, such as the septum, preoptic area, hypothalamus, and mesencephalon, regions closely related to the hippocampus. The hypothalamus makes a link between the limbic and endocrine system reasonable. The mesencephalon, said to form a "mesolimbic system" through its paramedian structures, could enable visceral information ascending in the brain stem to influence general functioning of the limbic system.

General Features of Hippocampal Anatomy

The general arrangement of the hippocampus is shown in Fig. 3. It bulges into the temporal horn of the lateral ventricle, and its general appearance does indeed resemble a sea horse in shape. It is arched around the mesencephalon (see Fig. 40), and the arch can be divided into three segments:

1. A body, or middle segment, which is sagittally oriented
2. A head, or anterior segment, which is transversely oriented and dilated and which shows elevations, the digitationes hippocampi
3. A tail, or posterior segment, which is also oriented transversely and which narrows, disappearing beneath the splenium

3.2 Structure

The characteristics of hippocampal structure are merely summarized here; for more detailed information, the reader is referred to the fundamental works by the following authors: Ramon y Cajal 1911 1968; Lorente de No 1934; Vogt and Vogt 1937; Blackstad 1956, 1958. In addition, the following works may be consulted: Gastaut and Lammers 1961; Isaacson 1974; Angevine 1975; Chronister and White 1975; Tryhubczak 1975; O'Keefe and Nadel 1978; Carpenter and Sutin 1983; Schwerdtfeger 1984; Kahle 1986; Amaral and Insausti 1990; Williams 1995.

The hippocampus is bilaminar, consisting of the cornu Ammonis (or hippocampus proper) and the gyrus dentatus (or fascia dentata), with one lamina rolled up inside the other (Fig. 5B). Elliot Smith (1897) and Williams (1995) looked for an explanation for this during cerebral development. In early development, the two laminae are continuous. For reasons still uncertain, the anlage of the cornu Ammonis bulges into the ventricular cavity to an increasing extent. Formation of the hippocampal sulcus at the cortical surface corresponds to this fold (Fig. 5A). The gyrus dentatus becomes concave and seems to slip beneath the medial end of the cornu Ammonis, perhaps due to asymmetry of development between the two structures. A final position is arrived at in which the cornu Ammonis and the gyrus dentatus resemble two interlocking, U-shaped laminae, one fitting into the other (see Fig. 21) and separated from each other by the hippocampal sulcus.

The hippocampal sulcus may be divided into deep and superficial parts. The deep part of the hippocampal sulcus soon disappears or remains visible as the *vestigial hippocampal sulcus* (Humphrey 1967), and its superficial part is clearly seen on the temporal lobe surface as the *superficial hippocampal sulcus*.

Two formations are thus studied here: the cornu Ammonis and the gyrus dentatus. Their typical position in the hippocampal body remains in the head and tail, possibly with slight variations (see Fig. 21).

The cornu Ammonis and the gyrus dentatus are the simplest part of the cortex, the *allocortex* (or archaeocortex), as compared with the more complex *isocortex* (or neocortex) (see p. 9).

3.2.1 Cornu Ammonis (Hippocampus Proper)

From its deepest level to the surface, i.e., from the ventricular cavity towards the vestigial hippocampal sulcus, the cornu Ammonis may be divided into six layers: the alveus, stratum oriens, stratum pyramidale, stratum radiatum, stratum lacunosum, and stratum moleculare (Figs. 7 – 10).

The *alveus* covers the intraventricular surface and contains axons of the hippocampal and subicular neurons, which are the main efferent pathway of these structures. These fibers then enter the fimbria (see Fig. 15). The alveus also contains afferent fibers largely from the septum (see Fig. 19).

The limits of the *stratum oriens* are poorly defined because the latter blends with the underlying stratum pyramidale, particularly in humans (Stephan and Manolescu 1980). It is composed of scattered nervous cells (basket cells) and is crossed by the axons of pyramidal neurons as they arrive at the alveus.

The *stratum pyramidale* contains the pyramidal neurons, the main element of the cornu Ammonis. A pyramidal soma is typically triangular, its base facing the alveus and its apex facing towards the vestigial hippocampal sulcus (see Fig. 13). From its base, the axon traverses the stratum oriens to the alveus. Such pyramidal axons mainly project to septal nuclei, but some are association fibers for other pyramidal neurons and perhaps cross to the contralateral hippocampus. While on course, such axons have Schaffer collaterals (Schaffer 1892), which curve back into the stratum radiatum and reach other pyramidal neurons (see Figs. 13, 15). The fundamental role of these collaterals is described on p. 28. At the apex of each pyramidal neuron is an *apical dendrite*, the length of which is remarkable, because it traverses the entire thickness of the cornu Ammonis to reach the stratum moleculare near the vestigial hippocampal sulcus. In addition to the apical dendrite, there are basal dendrites from the soma's basal angles; some of these arborize in the stratum oriens. Thus hippocampal pyramidal neurons have sometimes been called "double pyramidal" because of their double dendritic trees (Isaacson 1974). The soma is surrounded by a dense plexus of arborizations from basket cells with somata in the stratum oriens (see Fig. 13). Basket-type interneurons and stellate neurons are also scattered throughout the stratum pyramidale itself (Olbrich and Braak 1985), as in other layers of the cornu Ammonis (Braak 1974).

The *stratum radiatum* consists mainly of apical dendrites from pyramidal neurons, the parallel arrangement of which gives this layer a striated appearance. In the stratum radiatum, apical dendrites connect with Schaffer collaterals, fibers from septal nuclei, and commissural fibers.

The *stratum lacunosum* contains numerous axonal fasciculi parallel to the surface of the cornu Ammonis, formed mainly of perforant fibers and Schaffer collaterals.

The *stratum moleculare* adjoins the vestigial hippocampal sulcus. Because of the rapid sulcal disappearance during development, the stratum moleculare of the cornu Ammonis blends with that of the gyrus dentatus. The stratum moleculare contains few neurons, and here, too, these are considered as interneurons. It contains the original arborizations of apical dendrites of pyramidal neurons. Thus, by their prolongation, pyramidal neurons reach all layers of the cornu Ammonis. Their dendrites receive a great deal of information, as summarized in Fig. 13.

As the allocortex usually shows only three layers, the six layers of the cornu Ammonis described above are grouped into three layers: the stratum oriens, the stratum pyramidale, and a layer which combines the strata radiatum, lacunosum, and moleculare, i.e., the molecular zone (Ramon y Cajal 1911, 1968; Lorente de No 1934).

Regional Variations

In coronal sections, the cornu Ammonis has a heterogenous structure due to different aspects of its pyramidal neurons. The cornu Ammonis has thus been described as having four fields (Fig. 7), which Lorente de No (1934) named CA1 – CA4.

CA1 continues from the subiculum. Its pyramidal somata are typically triangular (Fig. 11) and generally small and scattered (Mouritzen Dam 1979). The stratum pyramidale of human CA1 is large, but it is narrow and dense in rats (Stephan 1983). Two sublayers have been distinguished in the stratum pyramidale of human CA1: a stratum profundum and a stratum superficiale (Braak 1974), the former in contact with the stratum oriens, with few pyramidal neurons, while the latter contains numerous ones.

CA2 is composed of large, ovoid, densely packed somata (Figs. 7, 11), making the stratum pyramidale dense and narrow, in sharp contrast to CA1 (Braak 1980). Its presence, a matter of debate in numerous species (Blackstad 1956; Schwerdtfeger 1984), is clear in human and simian hippocampi (Amaral et al. 1984).

CA3 corresponds to the curve, or genu, of the cornu Ammonis, where it enters the concavity of the gyrus dentatus. Its pyramidal somata are like those in CA2, but their density is less pronounced (Figs. 7, 11).

A typical feature of CA3 is the presence of fine, nonmyelinated fibers, the mossy fibers, which arise from the gyrus dentatus. These fibers surround the pyramidal somata and are also compressed between the strata radiatum and pyramidale, thus forming a supplementary layer, the stratum lucidum that is characteristic of CA3 (see Figs. 7, 9).

CA4 is situated within the concavity of the gyrus dentatus, which distinguishes it from CA3. Somata in this field are ovoid, large, few in number, and scattered among intertwined large and mossy myelinated fibers characteristic of CA4 (Fig. 11).

Other divisions have been suggested, in particular by Rose (1927), who divided the cornu Ammonis into five sectors, H1 – H5 (H, hippocampus). H1 corresponds to CA1, but also extends into the adjacent subiculum. H2 and H3 correspond to CA2 and CA3, respectively, whereas H4 and H5 corespond to CA4, slightly overlapping into CA3. Vogt and Vogt (1937) simplified this terminology by limiting themselves to three fields: H1 for CA1, H2 for CA2 and CA3, and H3 for CA4.

Taking into account the different sensitivity to hypoxia in different fields in the cornu Ammonis, CA1 is said to be a "vulnerable sector," or Sommer sector (Sommer 1880), whereas CA3 is called a "resistant sector," or Spielmeyer sector (Spielmeyer 1927), CA4 being a sector of medium vulnerability, or Bratz sector (Bratz 1899) (see p. 31). The rich abundance of terminology concerning the cornu Ammonis is noteworthy.

Terminological confusion is augmented by variations in the position of the hippocampus in different species. Thus, during development, the rat hippocampus, which is involved in an only partial hemispheric rotation, remains dorsal (Powell and Hines 1975; König and Klippel 1963). In this species, a division is often distinguished in the hippocampus or cornu Ammonis, separating it into superior and inferior regions (Ramon y Cajal 1911, 1968; Blackstad 1956; Isaacson 1974; Stephan 1983). The superior region contains CA1, and the inferior region CA3. In humans, however, the rotation is complete (Tilney 1939). The hippocampus is ventral, and the relation of CA1 to CA3 is thus the opposite of that found in rats (Fig. 6).

3.2.2
Gyrus Dentatus (Fascia Dentata, Gyrus Involutus)

In coronal sections of the hippocampal body, the gyrus dentatus is a narrow, dorsally concave lamina. Its concavity envelopes the CA4 segment of the cornu Ammonis (Figs. 7, 9).

The gyrus dentatus is separated from CA1 – CA 3 by the hippocampal sulcus, which disappears soon after its development and becomes vestigial. A few residual cavities may persist (see Figs. 7, 10, 67). The cornu Ammonis and the gyrus dentatus are thus fused together, separated only by the vestigial hippocampal sulcus. At the far end of this sulcus, the layers of the gyrus dentatus and the cornu Ammonis are so closely approximated that it becomes impossible to distinguish between them.

A narrow segment of gyrus dentatus, the margo denticulatus (Klinger 1948) is visible on the temporal lobe surface. In humans, it has a characteristic toothed appearance (see Fig. 23). The margo denticulatus is the border of primitive cortex. It overlaps the subiculum, separated from it by the superficial hippocampal sulcus and from the fimbria by the fimbriodentate sulcus (Fig. 7).

In structure, the gyrus dentatus is simpler than the cornu Ammonis. The three layers of the allocortex are plainly visible, i.e., the strata moleculare and granulosum and the polymorphic layer (Figs. 7, 9). The *stratum granulosum*, the main layer, contains somata of granular neurons, which are small and round but densely packed, making the layer easy to distinguish (Fig. 12). Their axons are "mossy" and traverse the polymorphic layer to CA4 and CA3. A single dendrite escapes from the basal pole of each granular soma and extends into the stratum moleculare (Fig. 13). The *stratum moleculare* is thick and separated from the stratum moleculare of the cornu Ammonis by the vestigial hippocampal sulcus. Its external two thirds near the hippocampal sulcus receive fibers from the perforant pathway (Fig. 13), whereas the inner third, in contact with the stratum granulosum, is occupied by commissural and septal fibers (Lynch and Cotman 1975; Cerbone et al. 1993). The *polymorphic layer* (or plexiform layer) unites the granular layer to CA4 and is crossed by axons of granular neurons. In the molecular and polymorphic layers, there are few interneurons.

The gyrus dentatus (fascia dentata) and CA4, which it encloses, constitute an entity that Blackstad (1956) designated the *area dentata* (Fig. 9), whereas CA4 alone is sometimes called the end-folium, the end-blade, or the hilus of the fascia dentata.

Figures 8 and 10 show a transverse section of hippocampus after intravascular injection of India ink; the hippocampal organization is partially revealed by differences in density of the capillary network. The special features of the capillary density of different hippocampal regions will be studied in Chap. 5.

3.2.3 Structures Joined to the Hippocampus

The hippocampus is prolonged by the *subiculum* (the "bed" of the hippocampus), which, from an anatomical point of view, forms part of the parahippocampal gyrus. The end of the stratum radiatum of CA1 is considered to mark the division between the cornu Ammonis and the subiculum (Figs. 7, 8) (Lorente de No 1934; Blackstad 1956; Braak 1980). The subiculum itself is divided into several segments (Fig. 5; Powell and Hines 1975; Williams 1995): (1) the *prosubiculum*, which continues CA1 (and whose existence is not accepted by all), (2) the *subiculum proper*, partly hidden by the gyrus dentatus, (3) the *presubiculum*, whose small, superficial pyramidal neurons are packed in clusters, making it characteristically maculate (see Figs. 113B, 114B; Braak 1980; Amaral et al. 1984), and (4) the *parasubiculum*, which passes around the margin of the parahippocampal gyrus to the entorhinal area on the medial aspect of the gyrus. The *entorhinal area* (Brodmann's area 28) is itself poorly demarcated (Amaral et al. 1987). Although its presence in the uncus and anterior end of the parahippocampal gyrus (Figs. 4, 16, 18) is generally accepted, its posterior extension along the parahippocampal gyrus is uncertain. This posterior extension is thought to be marked in humans where the entorhinal area is well developed (Jacobs et al. 1979; Braak 1980; Hyman et al. 1986). Its special structure will be described later together with its functions (see p. 26, 28).

The *amygdala*, which belongs to the limbic lobe, is often described together with the hippocampus as far as its function is concerned. Its structure, as described by Braak and Braak (1983) and Amaral et al. (1992), is shown in Fig. 14. The cortical and medial nuclei are olfactory centers, whereas the basal, lateral, and central nuclei have limbic functions (Aggleton 1992), which are described on p. 30.

From an anatomical point of view, the limbic lobe may be divided into limbic and intralimbic gyri. According to its structure, however, the limbic lobe is usually divided into the *allocortex*, including the hippocampus (cornu Ammonis and gyrus dentatus), the proximal part of the subiculum, and the indusium griseum (the amygdala is often included in this group), and the *periallocortex*, made up of the transitional cortex between the allocortex and isocortex, including the cingulate and parahippocampal gyri (Schwerdtfeger 1984; Chronister and White 1975; Jacobs et al. 1979; Braak 1980; Van Hoesen 1982; Swanson 1983; Kier et al. 1995).

(Text continued on p. 26)

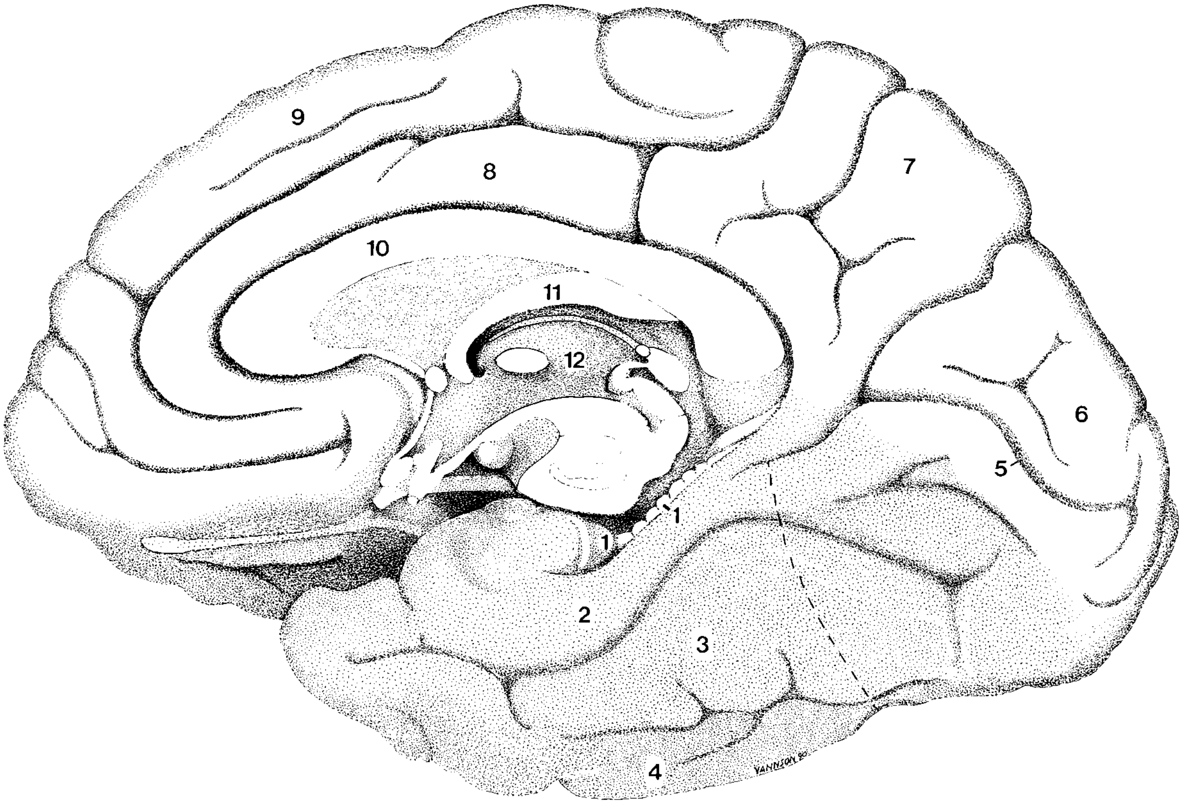

Fig. 1. A Drawing and **B** dissection showing the inferomedial aspect of the right hemisphere. **Bar,** 10 mm
1, hippocampus, only partly visible on the inferomedial surface of the temporal lobe; **2**, parahippocampal gyrus (T5); **3**, fusiform gyrus (T4); **4**, inferior temporal gyrus (T3); **5**, calcarine sulcus; **6**, occipital lobe (cuneus); **7**, parietal lobe, medial aspect (precuneus); **8**, cingulate gyrus; **9**, frontal lobe, medial aspect (superior frontal gyrus); **10**, corpus callosum; **11**, fornix; **12**, third ventricle

Fig. 1 B

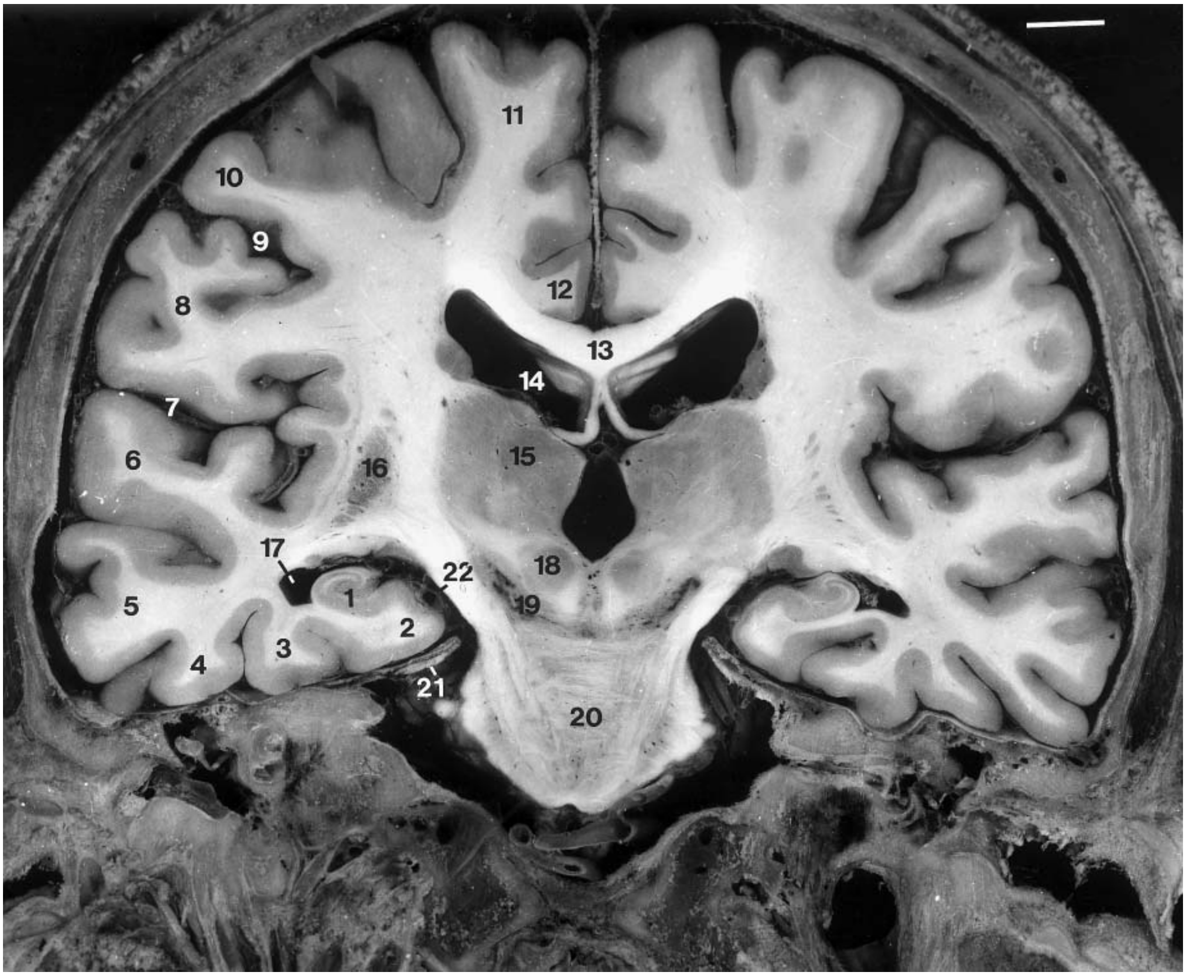

Fig. 2. A, B Coronal section of the brain. **A** Head section. **Bar**, 10 mm. **B** 3T MRI view, T^1-weighted image
1, hippocampus; **2**, parahippocampal gyrus; **3**, fusiform gyrus; **4**, inferior temporal gyrus; **5**, middle temporal gyrus; **6**, superior temporal gyrus; **7**, lateral fissure; **8**, postcentral gyrus; **9**, central sulcus; **10**, precentral gyrus; **11**, superior frontal gyrus; **12**, cingulate gyrus; **13**, corpus callosum; **14**, lateral ventricle; **14′** caudate nucleus; **15**, thalamus; **16**, putamen; **17**, temporal (inferior) horn of the lateral ventricle; **18**, red nucleus; **19**, substantia nigra; **20**, pons; **21**, tentorium cerebelli; **22**, ambient cistern

Fig. 2. B 3T MRI view

▷
Fig. 3. Intraventricular aspect of the hippocampus. The temporal horn has been opened and the choroid plexuses removed. **Bar**, 6.5 mm
1, hippocampal body; **2**, head and digitationes hippocampi (internal digitations); **3**, hippocampal tail; **4**, fimbria; **5**, crus of fornix; **6**, subiculum; **7**, splenium of the corpus callosum; **8**, calcar avis; **9**, collateral trigone; **10**, collateral eminence; **11**, uncal recess of the temporal horn

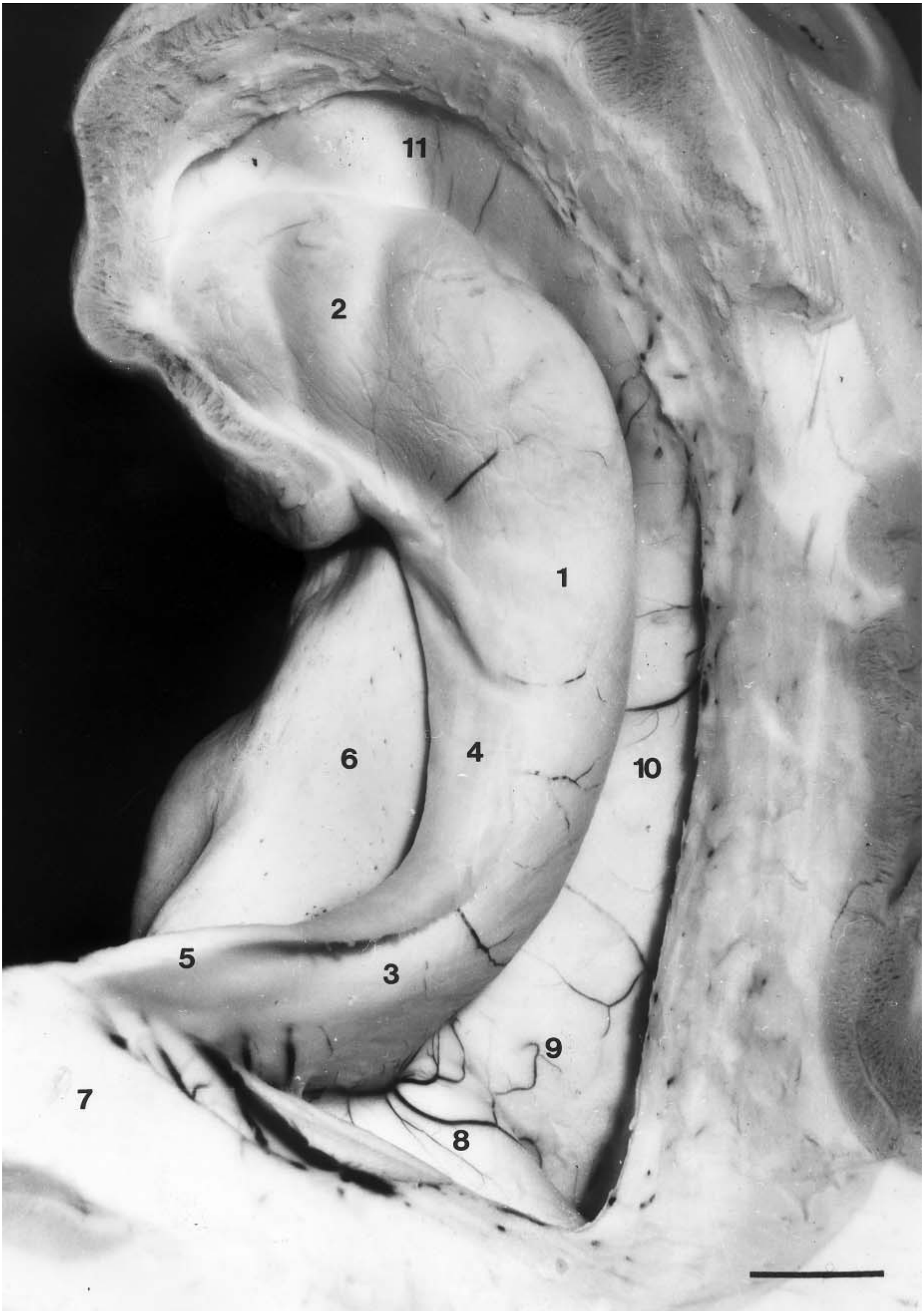
11
2
1
6
4
10
5
3
9
7
8

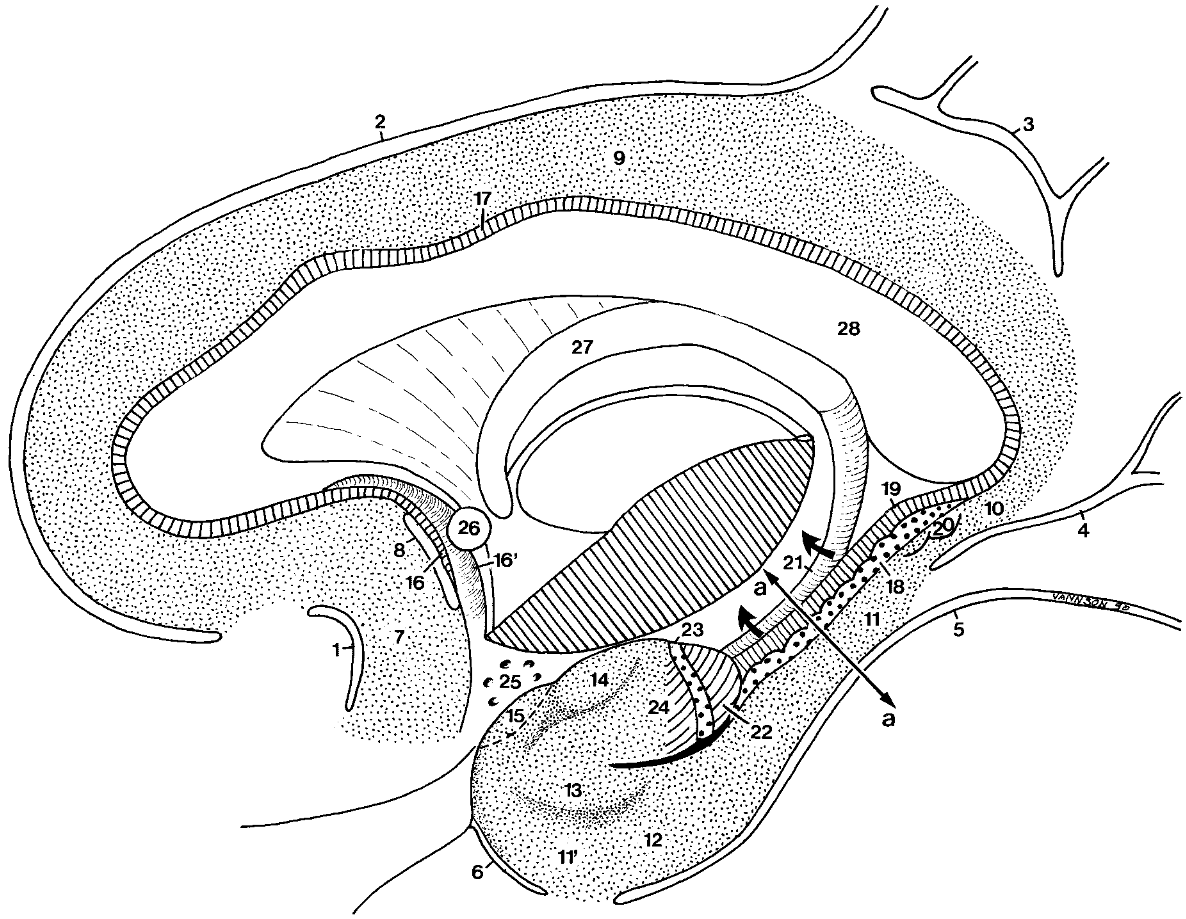

Fig. 4. A Drawing and **B** dissection showing a sagittal section, right hemisphere. The limbic lobe is separated from the isocortex by the limbic fissure and may be divided into two gyri: the limbic and intralimbic gyri. The line **a–a** indicates the plane of the section on Fig. 5. **Bar**, 7.7 mm
Limbic fissure: **1**, anterior paraolfactory sulcus (subcallosal sulcus); **2**, cingulate sulcus; **3**, subparietal sulcus; **4**, anterior calcarine sulcus; **5**, collateral sulcus; **6**, rhinal sulcus. Limbic gyrus: **7**, subcallosal gyrus; **8**, posterior paraolfactory sulcus; **9**, cingulate gyrus; **10**, isthmus; **11**, parahippocampal gyrus, posterior part; **11′**, parahippocampal gyrus, anterior part (piriform lobe). Piriform lobe: **12**, entorhinal area; **13**, ambient gyrus; **14**, semilunar gyrus; **15**, prepiriform cortex. Intralimbic gyrus: **16**, prehippocampal rudiment; **16′**, paraterminal gyrus; **17**, indusium griseum. Hippocampus: **18**, gyrus dentatus; **19**, cornu Ammonis; **20**, gyri of Andreas Retzius; **21**, fimbria (displaced upwards, **arrows**); **22**, uncal apex; **23**, band of Giacomini; **24**, uncinate gyrus; **25**, anterior perforated substance; **26**, anterior commissure; **27**, fornix; **28**, corpus callosum

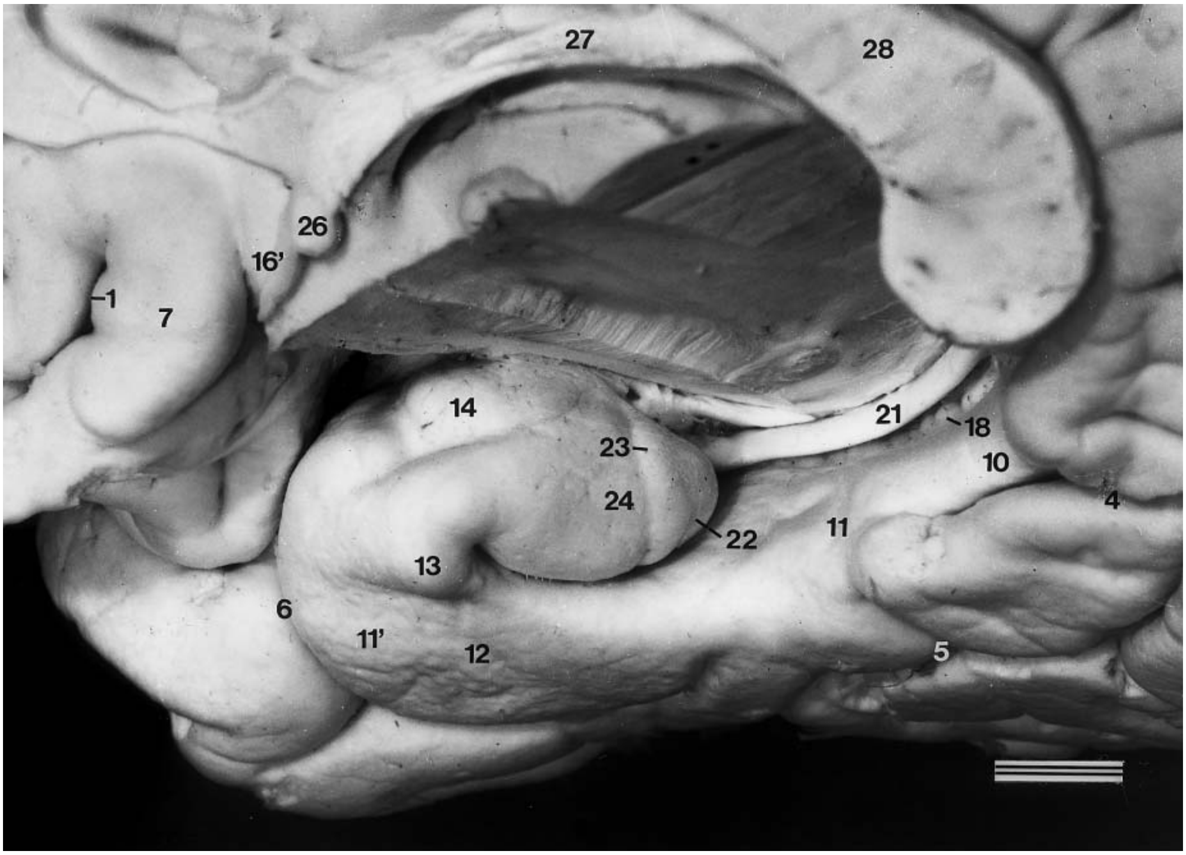

Fig. 4. B

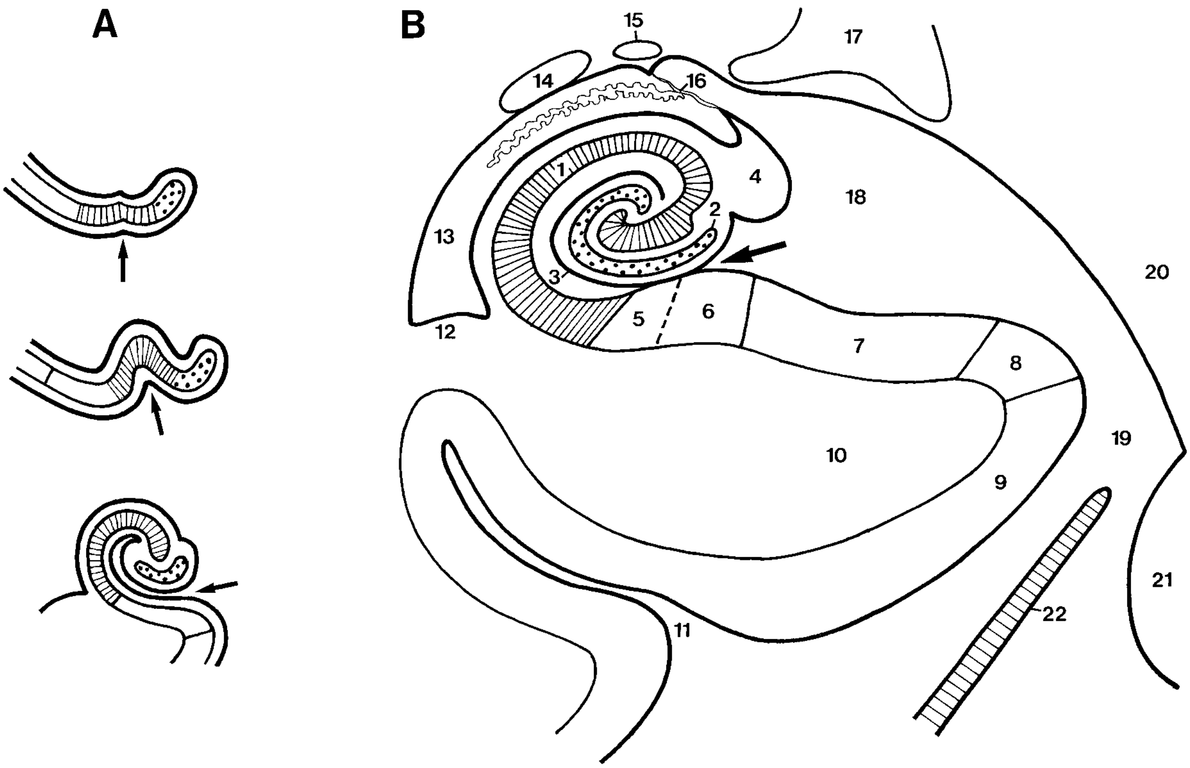

Fig. 5. A Development of the gyrus dentatus (**dotted area**) and of the cornu Ammonis (**hatched area**) towards **B** their definitive disposition. **Arrows** indicate the hippocampal sulcus (superficial part). (Modified after Williams 1995)
1, cornu Ammonis; **2**, gyrus dentatus; **3**, hippocampal sulcus (deep or vestigial part); **4**, fimbria; **5**, prosubiculum; **6**, subiculum proper; **7**, presubiculum; **8**, parasubiculum; **9**, entorhinal area; **10**, parahippocampal gyrus; **11**, collateral sulcus; **12**, collateral eminence; **13**, temporal (inferior) horn of the lateral ventricle; **14**, tail of caudate nucleus; **15**, stria terminalis; **16**, choroid fissure and choroid plexuses; **17**, lateral geniculate body; **18**, lateral part of the transverse fissure (wing of ambient cistern); **19**, ambient cistern; **20**, mesencephalon; **21**, pons; **22**, tentorium cerebelli

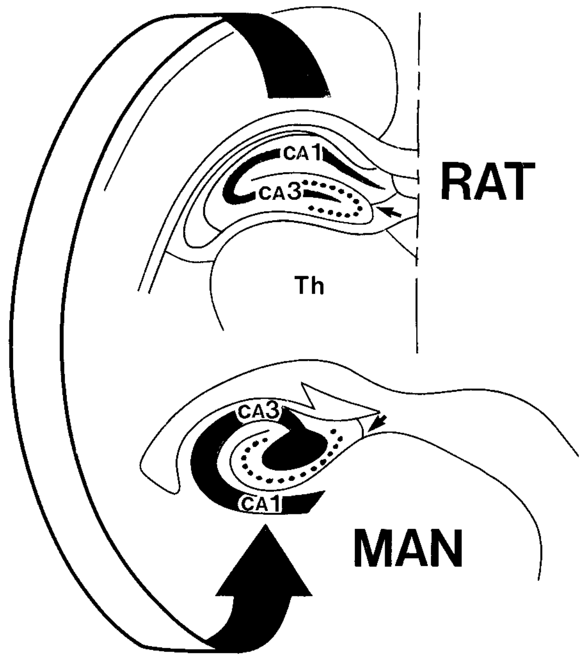

Fig. 6. Site of CA1 and CA3 in rats and humans (see p. 8). **Arrowheads** show the hippocampal sulcus. The **arrow** indicates the inversion of arrangements in the hippocampus in these two species
CA1, superior region; **CA3**, inferior region; **Th**, thalamus

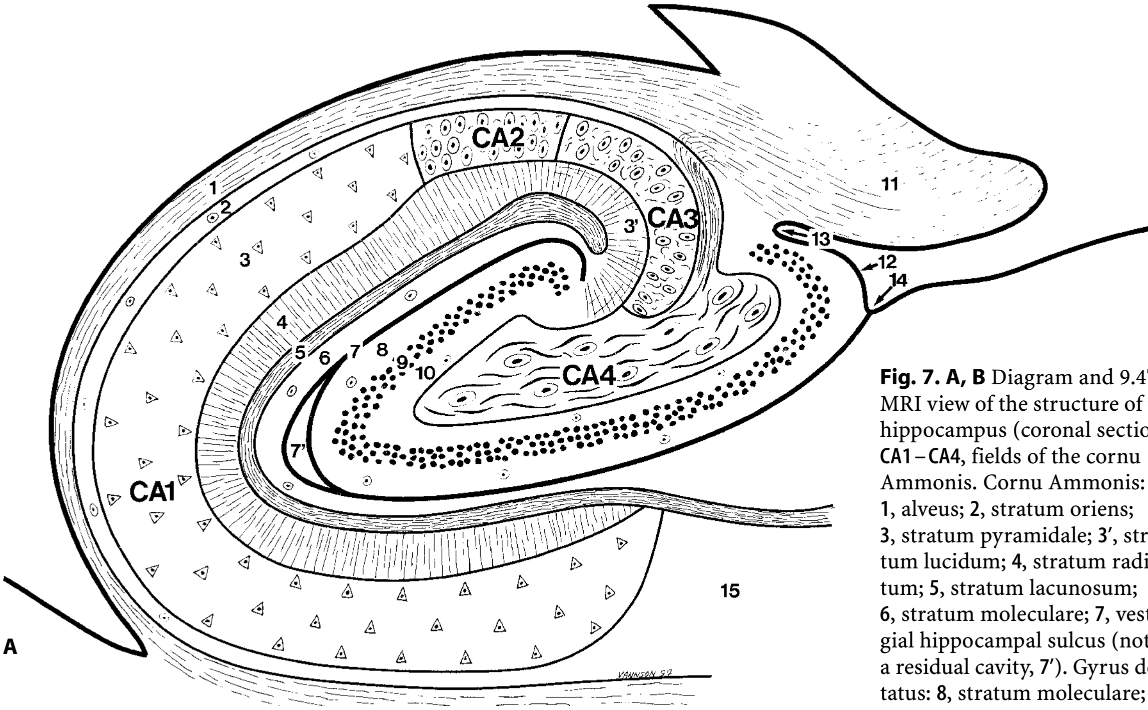

Fig. 7. A, B Diagram and 9.4T MRI view of the structure of the hippocampus (coronal section) **CA1–CA4**, fields of the cornu Ammonis. Cornu Ammonis: **1**, alveus; **2**, stratum oriens; **3**, stratum pyramidale; **3′**, stratum lucidum; **4**, stratum radiatum; **5**, stratum lacunosum; **6**, stratum moleculare; **7**, vestigial hippocampal sulcus (note a residual cavity, **7′**). Gyrus dentatus: **8**, stratum moleculare; **9**, stratum granulosum; **10**, polymorphic layer; **11**, fimbria; **12**, margo denticulatus; **13**, fimbriodentate sulcus; **14**, superficial hippocampal sulcus; **15**, subiculum; **16**, choroid plexuses; **17**, tail of caudate nucleus; **18**, temporal (inferior) horn of the lateral ventricle

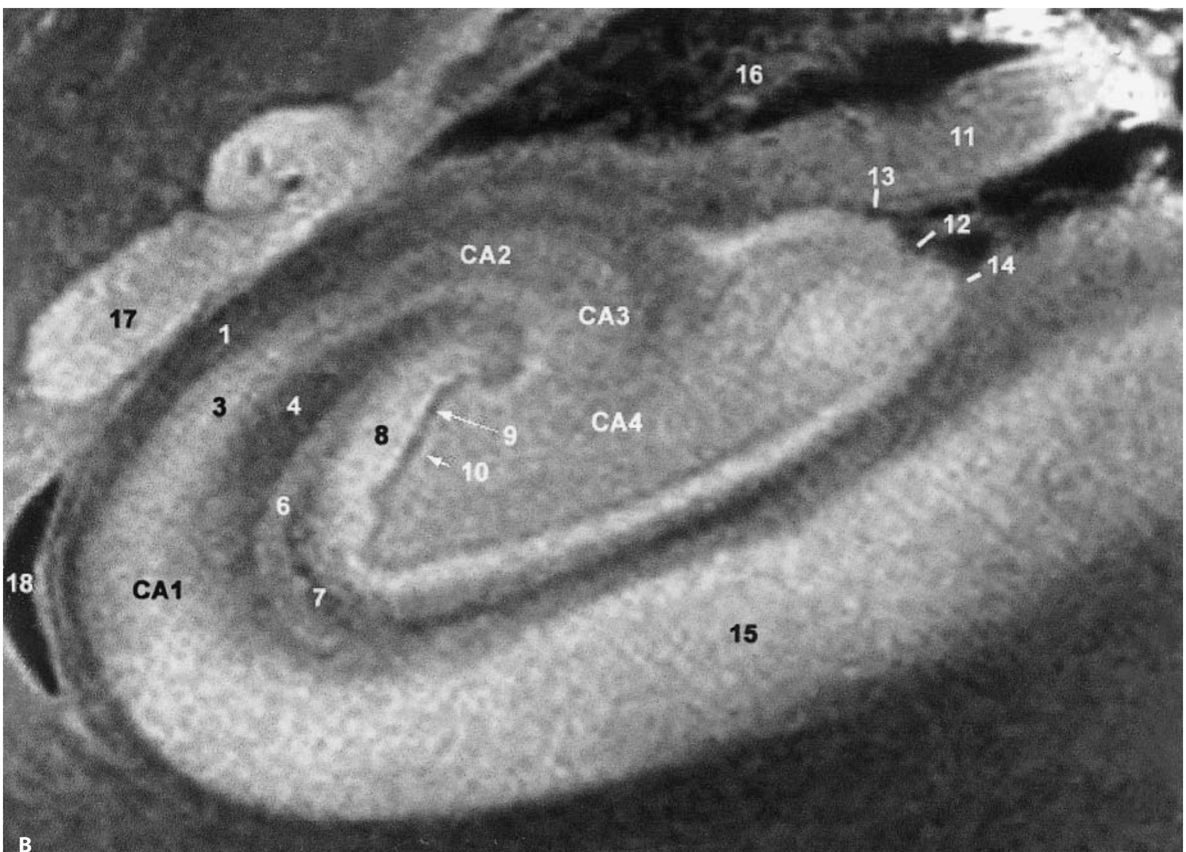

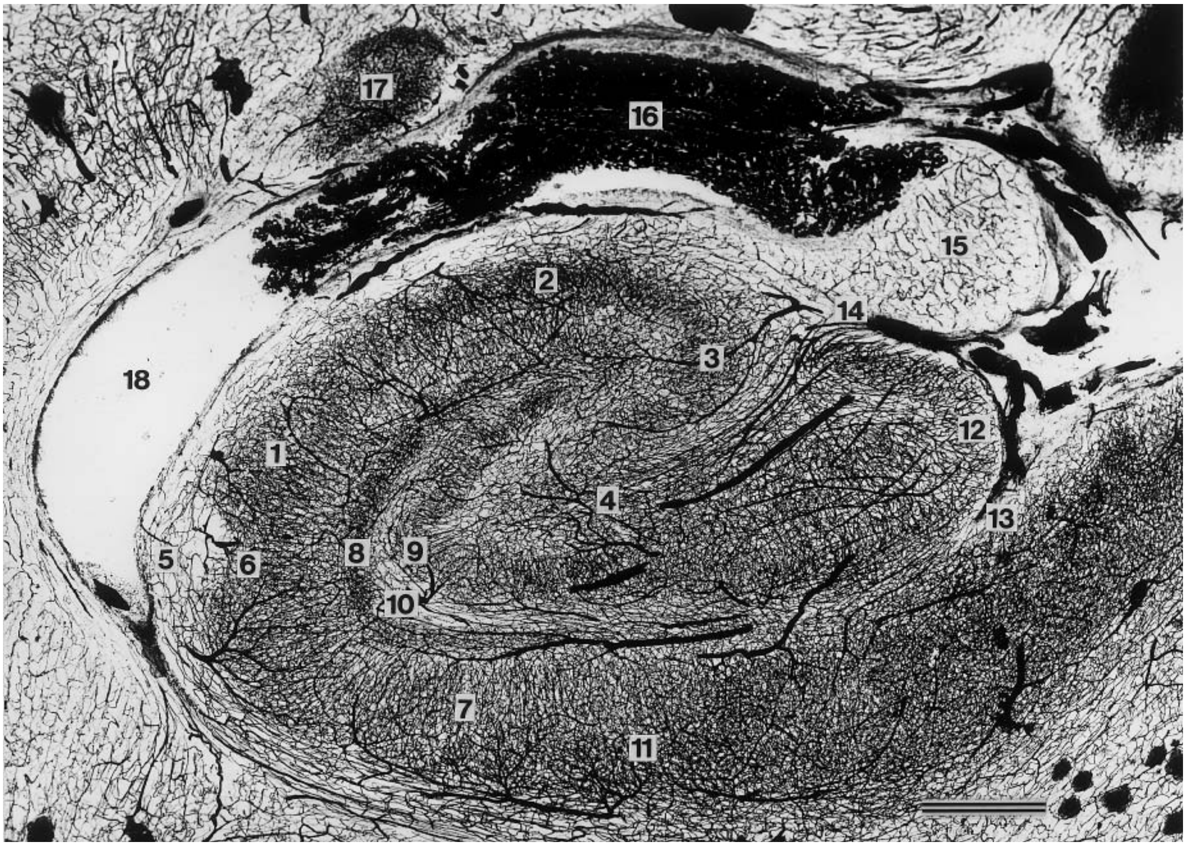

Fig. 8. Coronal section of the hippocampal body after intravascular India ink injection. The layers of the hippocampus (see Fig. 7) can be distinguished due to differences in their vascular density. The stratum moleculare of the cornu Ammonis (**8**) and that of the gyrus dentatus (**9**) are separated by the vestigial hippocampal sulcus (**10**). Note the high vascular density of the subiculum (**11**) in comparison to that of the adjacent stratum radiatum of CA1 (**7**), **Bar**, 1.5 mm

Cornu Ammonis: **1–4**, CA1–CA4 (fields of the cornu Ammonis). Sublayers of CA1: **5**, alveus; **6**, stratum pyramidale; **7**, strata radiatum and lacunosum; **8**, stratum moleculare. Gyrus dentatus: **9**, stratum moleculare; **10**, vestigial hippocampal sulcus; **11**, subiculum; **12**, margo denticulatus; **13**, superficial hippocampal sulcus; **14**, fimbriodentate sulcus; **15**, fimbria; **16**, choroid plexuses; **17**, tail of caudate nucleus; **18**, temporal (inferior) horn of the lateral ventricle

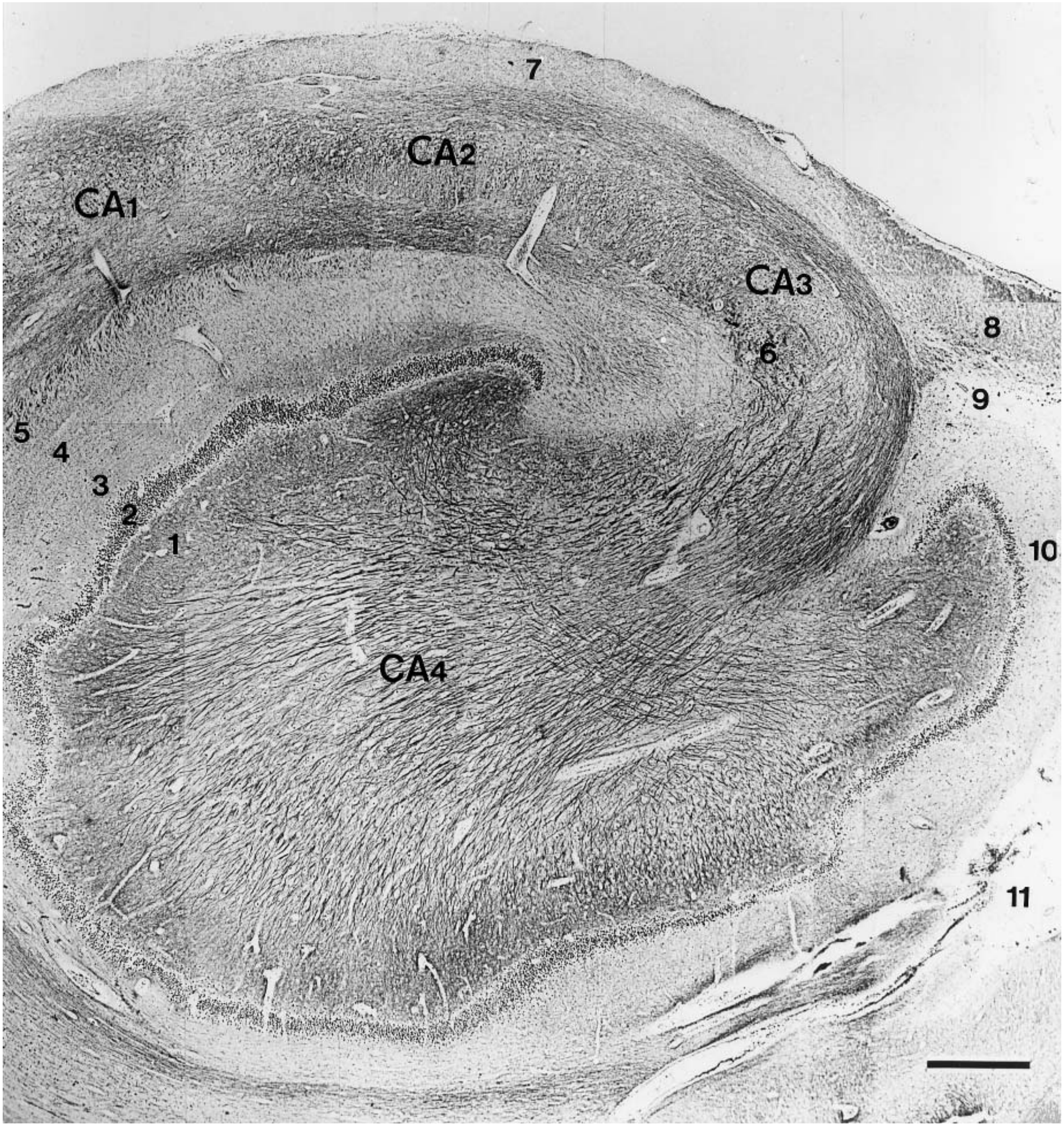

Fig. 9. Enlargement of the dentata area. The gyrus dentatus and CA4 together form the area dentata. Silver impregnation, Bodian. **Bar**, 590 µm
CA1–CA4, fields of the cornu Ammonis. Gyrus dentatus: **1**, polymorphic layer; **2**, stratum granulosum; **3**, stratum moleculare. Cornu Ammonis: **4**, stratum moleculare; **5**, stratum lacunosum; **6**, stratum lucidum; **7**, alveus; **8**, fimbria; **9**, fimbriodentate sulcus; **10**, margo denticulatus; **11**, superficial hippocampal sulcus

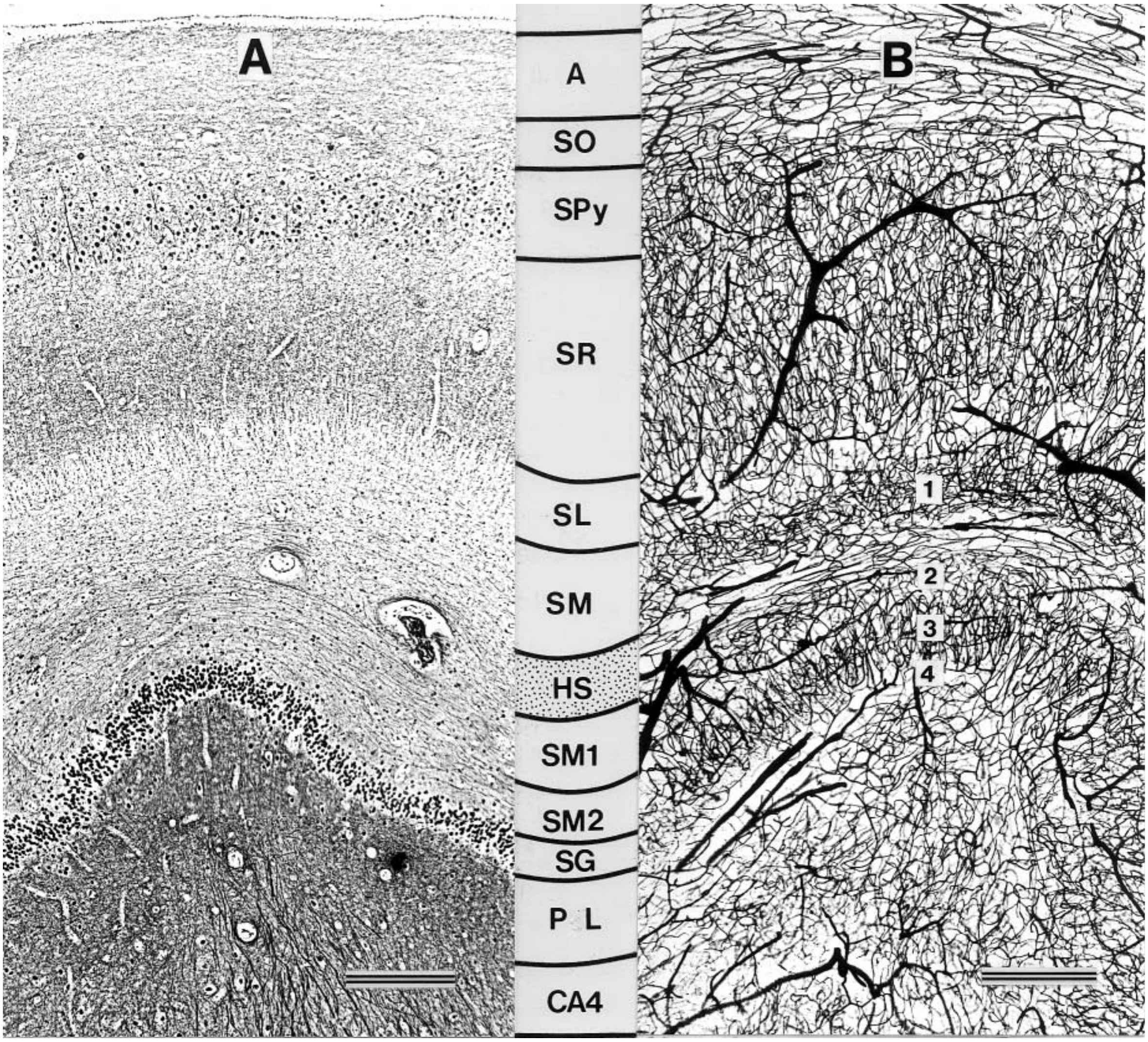

Fig. 10. A, B Structure of the hippocampus. **A** Silver impregnation (Bodian). **B** Intravascular India ink injection, showing the varying density of the vascular network in different hippocampal layers. Note high vascular density in the stratum moleculare of the cornu Ammonis (**1**). **Bar**, 600 μm
Cornu Ammonis: **A**, alveus; **SO**, stratum oriens; **SPy**, stratum pyramidale; **SR**, stratum radiatum; **SL**, stratum lacunosum; **SM**, stratum moleculare; **HS**, vestigial hippocampal sulcus. Gyrus dentatus: **SM1**, stratum moleculare, external two thirds; **SM2**, stratum moleculare, inner third; **SG**, stratum granulosum; **PL**, polymorphic layer; **CA4**, field of the cornu Ammonis. **1**, Stratum moleculare; **2**, external part of stratum moleculare of the gyrus dentatus; **3**, inner part, highly vascularized; **4**, stratum granulosum, poorly vascularized

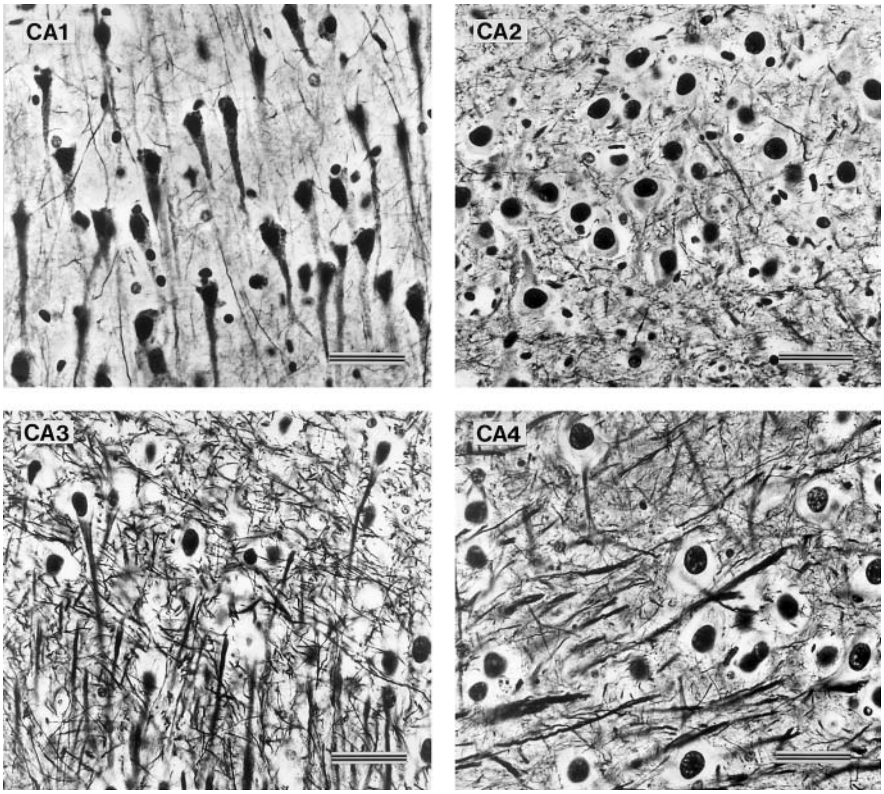

Fig. 11. Neuronal types in the cornu Ammonis. Silver impregnation, Bodian.
Bar, 52 µm
CA1 – CA4, fields of the cornu Ammonis

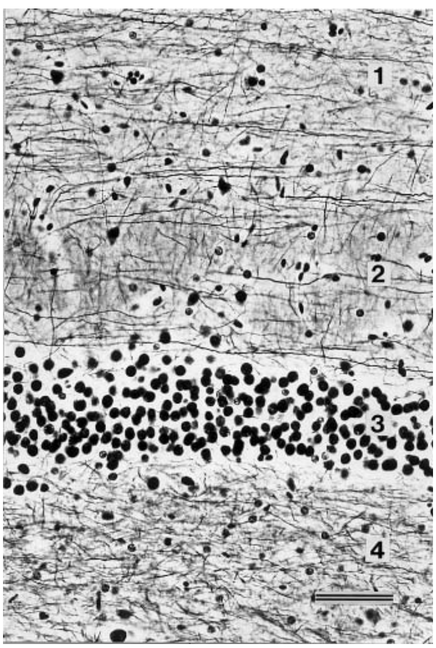

Fig. 12. Neuronal types in the gyrus dentatus. Silver impregnation, Bodian.
Bar, 85 µm
1, stratum moleculare, external part; **2,** stratum moleculare, inner part; **3,** stratum granulosum; **4,** polymorphic layer

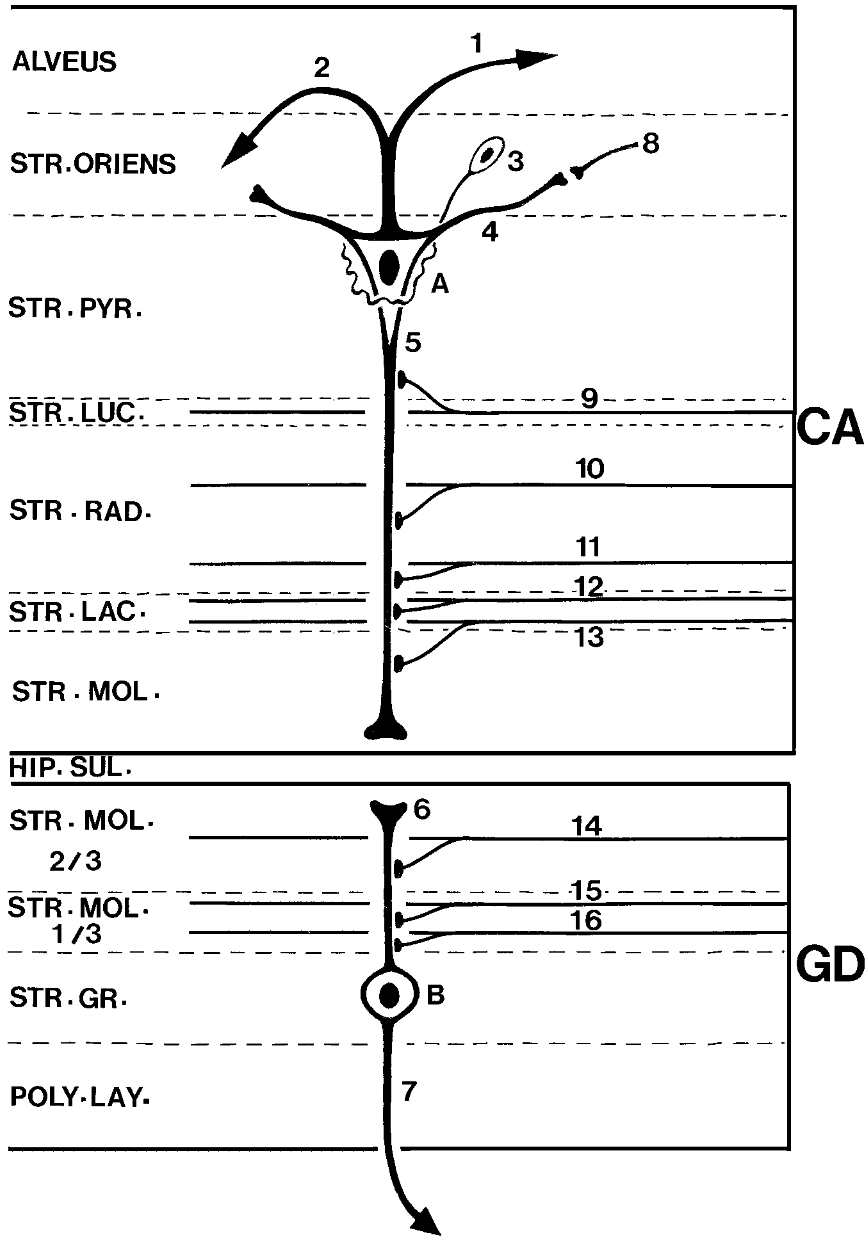

Fig. 13. Overview of the principal connections of pyramidal (A) and granular (B) neurons
CA, cornu Ammonis; GD, gyrus dentatus. 1, axon of a pyramidal neuron; 2, Schaffer collateral; 3, basket cell; 4, basal dendrite; 5, apical dendrite; 6, apical dendrite of a granular neuron; 7, axon (mossy fiber) of a granular neuron; 8, connections of a basal dendrite of a pyramidal neuron with other pyramidal neurons and with septal and commissural fibers; 9, mossy fibers (stratum lucidum into CA3); 10, septal and commissural fibers; 11, 12, Schaffer collaterals; 13, 14, perforant path; 15, commissural fibers; 16, septal fibers. Layers of the cornu Ammonis: alveus, stratum oriens (STR. ORIENS), stratum pyramidale (STR. PYR.), stratum lucidum (STR. LUC.), stratum radiatum (STR. RAD.), stratum lacunosum (STR. LAC.), stratum moleculare (STR. MOL.), vestigial hippocampal sulcus (HIP. SUL.). Layers of the gyrus dentatus: stratum moleculare, external two thirds (STR. MOL. 2/3), stratum moleculare, inner third (STR. MOL. 1/3), stratum granulosum (STR. GR.), polymorphic layer (POLY. LAY.)

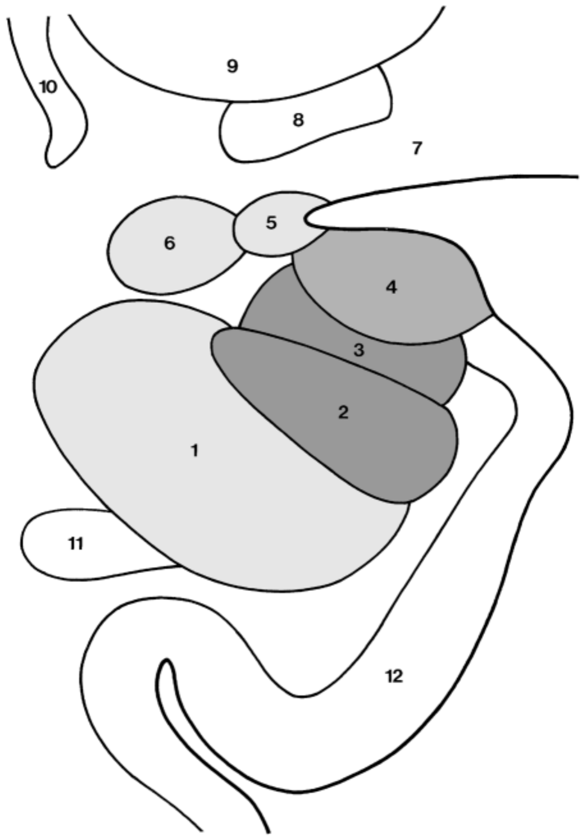

Fig. 14. A, B Structure of the amygdala. **A** Drawing of a coronal section. **B** Intravascular India ink injection. **Bar,** 1.8 mm **1**, lateral nucleus; **2**, basal nucleus; **3**, accessory basal nucleus; **4**, cortical nucleus; **5**, medial nucleus; **6**, central nucleus; **7**, anterior perforated substance; **8**, anterior commissure, lateral part; **9**, putamen; **10**, claustrum; **11**, uncal recess of the temporal horn; **12**, ambient gyrus

▷
Fig. 14 B

3.3 Functions and Connections

This section, which goes beyond the author's field of research, is based on an abundant body of work found in the literature, in particular the following: Ramon y Cajal 1911; Lorente de No 1934; Papez 1937; Blackstad 1958; Crosby et al. 1962; Hjorth-Simonsen and Jeune 1972; P. Andersen 1975; Chronister and White 1975; O'Keefe and Nadel 1978; Walaas 1983; Lopes da Silva et al. 1984; Schwerdtfeger 1984; Crunelli et al. 1985; Teyler and DiScenna 1985; Van Hoesen 1985; Rosene and Van Hoesen 1987; Nieuwenhuys et al. 1988; Amaral and Insausti 1990; Maclean 1992; Eichenbaum et al. 1994; Markowitsch 1995a,b; Williams 1995.

Based on this significant amount of research, only a general survey of the hippocampal functions shall be given here. It should be noted that some of the results presented here are controversial and may thus be subject to discussion. However, it may be helpful for the reader to find an overview of the hippocampal functions, as currently described, even if some of these hypotheses are not considered to be valid ones in the future. The possible functions of the hippocampus are divided into four categories: (1) learning and memory, (2) regulation of emotional behavior, (3) certain aspects of motor control, and (4) regulation of hypothalamic functions.

3.3.1 Learning and Memory

It is generally admitted that the hippocampus has a critical role in learning and memory. Information arising from large isocortical zones converges to the entorhinal area and then to the hippocampus. Thus newly acquired items cross the hippocampal filter before being fixed in the isocortex. It is possible to distinguish the memory of new or recent items, which depends on the hippocampus (short-term memory), from that of old ones (long-term memory), which depends on the isocortex. The entorhinal area, despite its small size, is the principal input to

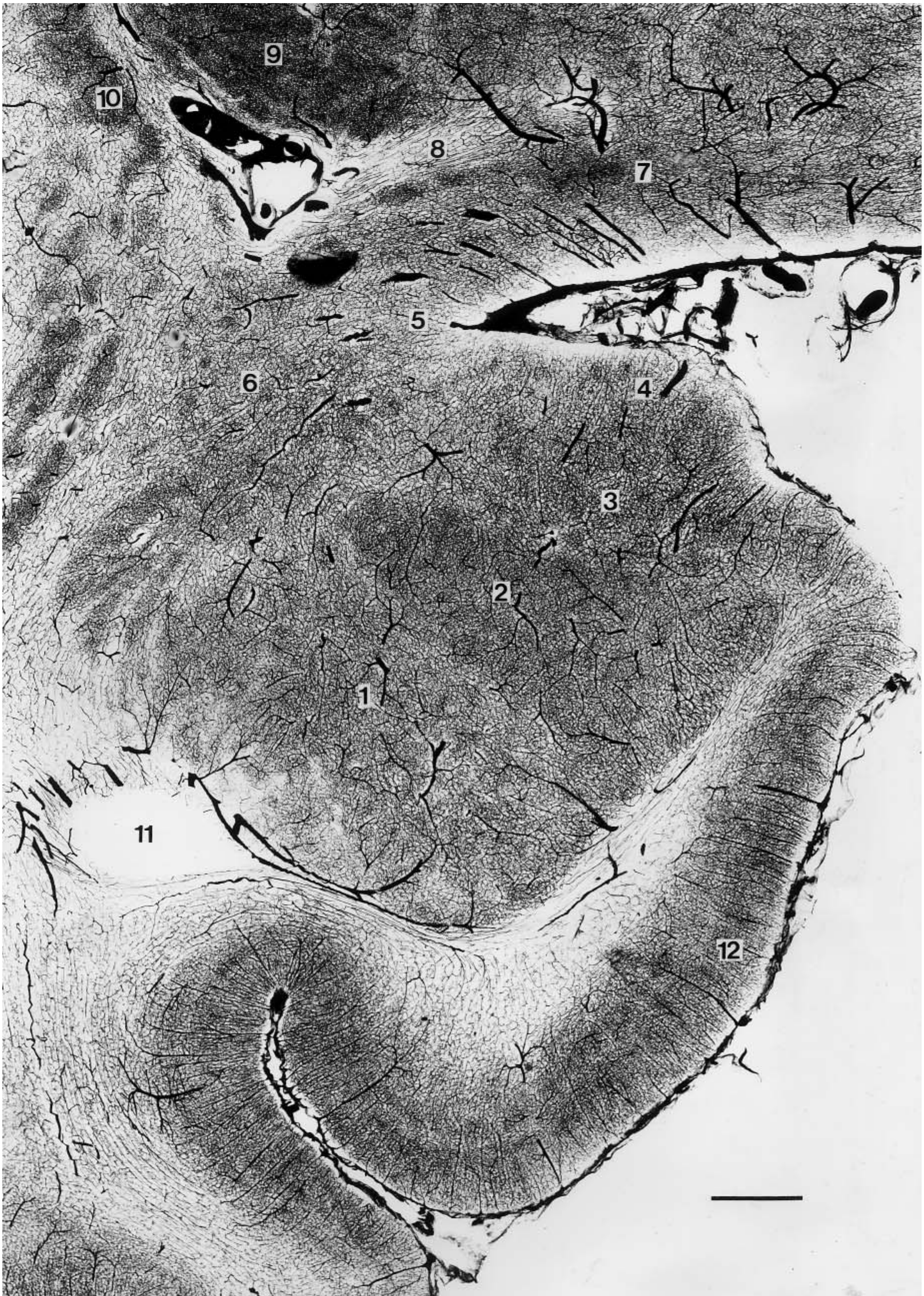
9
10
8
7
5
6
4
3
2
1
11
12

the hippocampus. It is composed of the periallocortex and is divided into deep and superficial layers (Hevner and Wong-Riley 1992; Insausti et al. 1995; Solodkin and Van Hoesen 1996). The superficial layers mainly comprise layers II and III (see Figs. 15, 17). In layer II, clusters of large pyramidal neurons (Hyman et al. 1986; Green and Mesulam 1988) are visible on the surface of the entorhinal area, which has a granular aspect (verrucae gyri hippocampi; Fig. 28). This aspect allows macroscopical delineation of the limits of the entorhinal area, which is situated mainly on the piriform lobe and extends caudally along the subiculum to the parahippocampal gyrus.

The hippocampus is implicated in all aspects of the declarative memory, i.e., the *semantic memory*, which involves memory of facts and concepts, the *episodic memory*, which permits conscious recollection of events and the relations between them, and the *spatial memory*, which involves spatial location recognition (Kopelman 1993; Eichenbaum et al. 1994; Kesner 1994; Markowitsch 1995a,b). Thus it should be noted that the hippocampal allocortex, composed of only three layers, has very high cognitive functions. Moreover, the hippocampal neurons have a remarkable plasticity: repetitive stimulations produce a persistent modification of their physiological state (long-term potentation; Trillet 1992).

After passing through the hippocampus, the information to be memorized is stored in the association cortex. The hippocampal projections involve large neocortical areas, including in particular the prefrontal and retrosplenial cortices (Markowitsch 1995a,b), as shown by positron emission tomography (PET) and functional MRI methods. At present, the storage mechanisms are largely unknown. They may be based on persistent changes in the biochemical structure of neurons obtained through a chain of biological modifications. Certain neurotransmitters are involved in these modifications, such as acetylcholine (ACh), arginine vasopressine (AVP), and endorphins.

The hippocampal pathways involved in learning and memory, their control, and a brief survey of clinical implications will be studied below.

3.3.1.1 Hippocampal Pathways Involved in Memory

Based on the course of the intrahippocampal fibers, it is possible to divide the intrahippocampal circuitry into two pathways: the *polysynaptic pathway*, which links all parts of the hippocampus by a long neuronal chain, and the *direct pathway*, which directly reaches the output neurons of the hippocampus. For more information, the reader is referred to the following works: Amaral and Insausti 1990; Maclean 1992; Witter and Groenewegen 1992; Eichenbaum et al. 1994; Leonard et al. 1995; Markowitsch 1995a,b.

Polysynaptic Intrahippocampal Pathway (Figs. 15, 16)

The intrahippocampal circuitry is composed of a long neuronal chain made up of the entorhinal area, the gyrus dentatus, CA3, CA1, and the subiculum. First of all, its organization will be studied, and its cortical projections and its functions will then be described.

The origin of the polysynaptic pathway is layer II of the *entorhinal cortex* (Amaral and Insausti 1990), from which the perforant path arises. The *perforant path* "perforates" the subiculum to reach the gyrus dentatus. The majority of the fibers making up the perforant path reaches the stratum moleculare of the *gyrus dentatus* after traversing the vestigial hippocampal sulcus. In the external two thirds of the molecular layer, they are in contact with the dendrites of granular cells (Cerbone et al. 1993). Thus the perforant path, composed of glutaminergic fibers, has an excitatory action on the gyrus dentatus.

The next link in the chain is the *gyrus dentatus*, whose axons of granular neurons, the mossy fibers, are glutaminergic and have a large content of zinc (McLardy 1962; Frederickson et al. 1983). These fibers traverse the polymorphic layer and stimulate the dendrites of CA4 and especially those of CA3 (Treves 1995).

The axons of CA3 and CA4 enter the alveus and then the fimbria; however, they first emit the Schaffer collaterals, which reach the apical dendrites of CA1 in the strata radiatum and lacunosum (Fig. 13). The CA2 field, which has not yet been discussed here but is in fact quite distinct in humans, has an obscure role. Its marked cellular density and its intense vascularization (see Chap. 5) might, however, correspond to a particular function (Veazey et al. 1982).

Since Ramon y Cajal's description (Ramon y Cajal 1909–1911), axons of CA1 have been considered the main output of the hippocampus by way of the alveus and then of the fimbria. Currently, a supplementary link is considered to be joined to the chain, a link formed by the subiculum. Thus, by entering the alveus, the axons of CA1 produce collaterals which reach the subiculum.

The *subiculum* therefore emits the definitive response, by fibers constituting the major part of the alveus and then the fimbria. The neurons of the subiculum are glutaminergic, as are those of the preceding parts of the polysynaptic chain (Francis et al. 1994).

The polysynaptic pathway is thus composed of the following elements: the entorhinal area, the gyrus dentatus, the cornu Ammonis, and the subiculum. For this reason these structures, with their disparate anatomy, are sometimes grouped together as the "hippocampal formation," a single functional unit (Powell and Hines 1975; Rakic and Nowakoswki 1981; Teyler and DiScenna 1984; Amaral and Campbell 1986; Squire 1986).

Since the studies carried out by Blackstad et al. (1970), P. Andersen et al. (1971), Hjordt-Simonsen and Jeune (1972) and P. Andersen (1975), precise arrangements have been attributed to the hippocampal pathways; the hippocampus may hence contain many lamellae arranged transverse to the hippocampal axis. Each lamella is a functional unit, with a narrow strip of gyrus dentatus linked to a narrow strip of CA3 and then CA1. Likewise, neurons in the entorhinal area may be precisely arranged in relation to each lamella. Finally, all lamellae may be associated by longitudinal fibers, as described by Schaffer (1892), Ramon y Cajal (1911, 1968), and Lorente de No (1934). This lamellar arrangment, which appears to be restricted to mossy fibers, has been recently discussed (Amaral and Witter 1989; Witter and Groenewegen 1992; Amaral and Insausti 1990).

Hippocampal Output to the Cortex (Fig. 16).
The principal outputs of the polysynaptic pathway to the cortex follow the fimbria, the crus and body of the fornix, and the columns of the fornix, also known as the postcommissural fornix (behind the anterior commissure). The nervous impulses then reach the anterior thalamic nucleus, either directly (Devinsky and Luciano 1993) or via the mamillary bodies, extending from there into the mamillothalamic tract. Other thalamic nuclei, such as the intralaminar nuclei, and the hypothalamus may possibly be reached (O'Keefe and Nadel 1978; Teyler and DiScenna 1984; Bentivoglio et al. 1993).

From the thalamus, impulses reach the posterior cingulate cortex (area 23) and the retrosplenial cortex (areas 29 and 30). Some projections reaching the anterior cingulate cortex (area 24) will be discussed later.

Input from the Cortex (Fig. 16). These fibers originate in a large cortical area that includes the posterior parietal association cortex (area 7) and the neighboring temporal and occipital cortices (areas 40, 39, and 22). In the monkey, this cortex is restricted to the sides of the superior temporal sulcus, i.e., the middle temporal (MT) and medial superior temporal cortices (MST). The posterior parietal association cortex sends fibers to the entorhinal area through the parahippocampal gyrus. The main function attributed to the posterior parietal association cortex, related to the superior visual system, is perception of the position of an object in space (R.A. Andersen et al. 1990; Mountcastle 1995). This spatial perception is thought to then be memorized through the polysynaptic pathway, and the episodic memory and the memory of facts in relation to each other apparently also depend on this system. The polysynaptic pathway and its cortical projections are often referred to as the *medial limbic system of Papez* (Papez 1937) or the *Delay and Brion system* (Delay and Brion 1969).

Direct Intrahippocampal Pathway (Figs. 17, 18)
The direct intrahippocampal pathway is referred to as being direct because the fibers reach CA1 and the hippocampal outputs directly without following the usual polysynaptic chain.

The origin of the direct pathway is found in layer III of the entorhinal cortex (Fig. 17). From this layer, fibers directly reach the pyramidal neurons of CA1 by a different pathway from that of the perforant path (Du et al. 1993). The CA1 neurons project onto the subiculum, the axons of which return to the deep layers of the entorinal area (Maclean 1992).

Hippocampal Output to the Cortex. The output of the direct pathway to the cortex is believed to reach the inferior temporal association cortex, the temporal pole, and the prefrontal cortex (Fig. 18).

Input from the Cortex. The main input from the cortex,(Fig. 18) is the inferior temporal association cortex (areas 37, 20), which reaches the entorhinal area through the perirhinal cortex (areas 35, 36). The functions of this cortex, which is connected to the inferior visual system, are the recognition and description of objects, the memorization of which may depend on the direct pathway. More generally, the semantic memory is believed to involve this system.

In conclusion, the fundamental function of hippocampus and entorhinal cortex in the memorization process is generally accepted. It depends on two systems, each with specific functions (Squire et al. 1994): the *polysynaptic pathway*, the most primitive one, is mainly involved in episodic and spatial memory, whereas the *direct pathway*, the most important in humans, is mainly involved in semantic memory.

Before converging on the entorhinal cortex, the cortical fibers related to the polysynaptic pathway relay to the parahippocampal gyrus, whereas those connected to the direct pathway reach the hippocampus through the perirhinal cortex (Suzuki 1994; Susuki and Amaral 1993, 1994; Leonard et al. 1995; Williams 1995). In both pathways, the entorhinal area has a crucial role. It is the sole input to the hippocampus, with the subiculum as its main output. It seems that the entorhinal area and subiculum are divided into specific functionnal zones (Amaral et al. 1987; Witter and Groenewegen 1992).

The role of the amygdala in memorization is controversial. It may act in parallel with the hippocampal pathways (Aggleton 1986; Devinsky and Luciano 1993; Markowitsch 1995a,b). From the basal and lateral nuclei of the amygdala (see Figs. 14, 20B), the ventral amygdalofugal tract reaches the dorsomedial thalamic nucleus, whose functions in memory are well known (Squire and Zola-Morgan 1988). However, the involvement of the amygdala in memory is a matter of debate and is even denied by some (Zola-Morgan et al. 1989).

3.3.1.2
Regulatory Circuits

Numerous circuits may regulate the main principal pathways and can thus be described as internal regulatory circuits, entirely within the hippocampus, and external regulatory circuits, which involve extrahippocampal structures.

Internal Regulatory Circuits

Basket Neurons. The basic elements in these circuits are the interneurons, so-called basket neurons, described by Ramon y Cajal (1911, 1968), which occur in the cornu Ammonis and gyrus dentatus. In the cornu Ammonis, they are largely situated in the stratum oriens, but are also scattered throughout other layers. They receive impulses from pyramidal neurons, and their axons return to numerous such neurons, forming basket arborizations around their bodies (Fig. 13). Through their GABA-containing fibers, the basket neurons powerfully inhibit pyramidal neurons (Haefely and Polc 1986; Nunzi et al. 1986). In the gyrus dentatus (Amaral and Campbell 1986), basket neurons situated in the molecular and polymorphic layers may influence granular neurons, just as basket neurons in the cornu Ammonis influence pyramidal neurons. In other words, basket neurons, stimulated at first by collaterals of mossy fibers, go on to inhibit granular neurons by retroaction. Thus the GABAergic interneurons modulate the hippocampal functions (Buckmaster and Soltesz 1996).

Neurotransmitters. Interneurons producing neurotransmitters other than GABA have been described in the hippocampus. The cornu Ammonis and gyrus dentatus do in fact contain neurons producing substance P, vasoactive intestinal polypeptide (VIP), cholecystokinin (CCK), somatostatin, corticotropin-releasing factor (CRF), and neuropeptide Y. All such neurons intervene in local inhibitory or excitatory circuits (Amaral and Campbell 1986; Köhler et al. 1986; Nunzi et al. 1986; Chan Palay 1987). In addition, granular neurons from the gyrus dentatus may produce enkephalins and dynorphins, which may reach the cornu Ammonis through mossy fibers (Siggins et al. 1986). However, some investigators believe that enkephalin-containing neurons are present in only very small numbers in humans and thus distribution of neuropeptides could be highly variable according to species (Sakamoto et al. 1987).

Pyramidal neurons. Finally, it seems possible that the pyramidal neurons might influence each other. In fact, collaterals of their axons connect with basal dendrites of other pyramidal neurons (Fig. 13).

External Regulatory Circuits

The external regulatory circuits involve the septal nuclei, the contralateral hippocampus by commissural fibers, neuromediators of extrahippocampal origin, and certain areas of cerebral cortex.

Septal Nuclei. Chief circuits uniting septal nuclei and the hippocampus (Fig. 19) have been known since the studies performed by Green and Arduini (1954) and later by Petsche et al. (1962), Lynch et al. (1978), and Swanson (1978).

Axons of hippocampal and subicular pyramidal neurons are the origin of these circuits (Fig. 15). Via the fimbria and then the precommissural fornix (in relation to the anterior commissure), such fibers reach the lateral septal nucleus, from which impulses reach the medial septal nucleus and the nucleus of the vertical limb of the diagonal band (Fig. 20A). These two nuclei are important cholinergic centers: Ch1 for the medial septal nucleus and Ch2 for the nucleus of the vertical limb. From these nuclei, cholinergic and GABAergic fibers project back to the hippocampus by the same route, i.e., the precommissural fornix and fimbria (Fig. 19).

Septal fibers end on granular neurons in the gyrus dentatus, and pyramidal neurons in the cornu

Ammonis (Fig. 13). The septal cholinergic fibers are excitatory, acting on pyramidal and granular neurons (Bilkey and Goddard 1985) either directly or indirectly by inhibiting the inhibitory action of hippocampal interneurons. They enhance the capacity for memorization, especially for spatial memory and learning (Stackman and Walsh 1995; Alonso et al. 1996).

Through these projections, the septum may control a special hippocampal activity, the rhythmic slow wave activity or theta rhythm. The septum itself may be controlled by excitatory or inhibitory influences from the brain stem's reticular formation (Vanderwolf et al. 1985). Rhythmic slow wave activity, controlled by the septum, is thought to be localized in the gyrus dentatus and CA1. Unlike the fast and continuously desynchronized rhythm of wakefulness, the theta rhythm is slow and only present during specific types of behavior, such as exploration of an unknown environment (O'Keefe and Nadel 1978; Vertes 1985). It has also been implicated in learning (Schwerdtfeger 1984). It should be noted, however, that the hippocampal theta rhythm has not been clearly detected in humans or other primates. Finally, the septum may have a modulatory role (as a pacemaker) on information arriving in the hippocampus from the entorhinal cortex (Lynch et al. 1978; O'Keefe and Nadel 1978; Lopes da Silva et al. 1984, 1985; Bland 1986; Ridley et al. 1996).

Commissural Fibers. The two hippocampi are joined via the fornix by commissural fibers. In rodents, all hippocampal regions are connected to the corresponding contralateral regions. In primates, however, commissural fibers are few and only reach limited regions of the hippocampus (Amaral et al. 1984; Fig. 13).

Neuromediators. Numerous endings of nerve fibers of extrahippocampal origin which liberate neuromediators have been described in the hippocampus, where they certainly play a regulatory role.

In addition to cholinergic septal fibers, terminals of monoaminergic pathways have been described in the hippocampus (Moore 1975). Thus noradrenergic fibers arising from the locus ceruleus and belonging to the dorsal noradrenergic bundle (Davis et al. 1989) may reach the hippocampus via the fornix, but also via the longitudinal striae (Nieuwenhuys 1985). Serotoninergic fibers from the nuclei of raphe may also reach the hippocampus via the longitudinal striae, perhaps with an inhibitory role (O'Keefe and Nadel 1978). The presence of dopamine is more doubtful; although in rodents only a limited number of fibers have been described coming from the substantia nigra (A9) and ventral tegmental area (A10) (Bischoff 1986), in humans the dopaminergic projections seem to be more abundant (Samson et al. 1990).

Many neuropeptidergic terminals have been found in the hippocampus, such as vasopressin, somatostatin, substance P, neuropeptide Y, and α-melanocyte-stimulating hormone (α-MSH), although their functions have not been explained (Nieuwenhuys 1985).

Cortical Regulation. Direct connections seem to exist between the neocortex and the hippocampus (Schwerdtfeger 1979). Thus the cingulate gyrus projects directly to hippocampus. Direct afferents from temporal and prefrontal lobes have also been described.

3.3.1.3
Clinical Implications

Clinical observations after surgical ablation and in neurological diseases show that, in humans, the deficits brought about by hippocampal damage mainly produce disorders of memory, particularly short-term memory (Vanderwolf et al. 1985). Marked defects in remembering events that occur after appearance of the lesion (producing anterograde amnesia) can be observed, but the most frequent defects are in spatial memory.

The etiology of many hippocampal disorders has been the root of much controversy, particularly in explaining lesions that cause temporal lobe epilepsy. It has long been observed that the CA1 field (and adjacent subiculum) has a specific sensitivity to anoxia. CA1 is therefore known as the vulnerable sector or Sommer sector (Sommer 1880). In contrast, CA3 remains healthy and is known as the resistant Spielmeyer sector (Spielmeyer 1927). CA4 (end-folium) is only partially affected (Bratz sector; Bratz 1899). The sensitivity to anoxia of CA2 is controversial: for some researchers it belongs to the resistant sector (Rutecki et al. 1989; Kotapka et al. 1994), and for others to the vulnerable sector (Zola-Morgan et al. 1992; Kartsounis et al. 1995). Lesions of CA1, and to a lesser degree of CA4, constitute the classic sclerosis of the cornu Ammonis, or hippocampal sclerosis, and frequently produce memory impairment (Zola-Morgan et al. 1986).

The selective vulnerability of certain hippocampal regions to anoxia has not yet been fully explained (Margerison and Corsellis 1966). It was first proposed that vascular arrangements might be the cause of this selective vulnerability (vascular theory; Scharrer 1940; Gastaut and Lammers 1961). The studies by Uchimura (1928) showed that the vulnerable sector (CA1) was supplied by *long arteries*, which are more sensitive to variations in blood pressure than those of the resistant sector supplied by *short arteries* (see Chap. 5). Spielmeyer (1927) believed that epileptic seizures produce vascular spasms causing secondary damage to this vulnerable sector, but Penfield and Jasper (1954) were of the opinion that a primary vascular disorder produces the lesion, perhaps due to trauma at birth leading to herniation of the temporal lobe through the *tentorial incisure* and compression of vessels supplying the hippocampus. Gastaut and Lammers (1961) extended this idea of vascular damage to any cause of temporal herniation, such as cranial trauma or cerebral infarct. The hippocampal lesion produced by this mechanism was called *incisural sclerosis* (Earle et al. 1953).

The specific arrangements of the CA1 arteries (see Chap. 5) resemble those of arteries supplying Purkinje neurons in the cerebellum (Duvernoy et al. 1983). However, selective ischemic lesions of CA1 have the same appearance as those found in the region of Purkinje neurons (Spielmeyer 1930; Scharrer 1944; Corsellis and Meldrum 1976; Corsellis and Bruton 1983).

However, despite the specific arrangement of the vessels, the vascular theory explaining the selective vulnerability of the hippocampus to anoxia was criticized by Vogt and Vogt as early as 1937 and has now been abandoned (Nilges 1944; Fleischhauer 1959; Friede 1966; De Reuck et al. 1979), yielding to a theory based on metabolic characteristics of neurons or on features of synapses and, more particularly, of receptors on pyramidal neurons.

A sudden and transient experimental cerebral ischemia in rats produces delayed and irreversible cell damage in the CA1 field of the hippocampus. The lesion does not appear until after an interval of about 4 days, whereas a lesion in CA4 is rapid but reversible (Kirino 1982; Kirino et al. 1986). The *delayed neuronal death* appearing in CA1 can be avoided experimentally by the previous destruction of CA3, the current explanation for which is that glutaminergic synapses of Schaffer collaterals originating in CA3 may have a toxic effect on CA1 during anoxia (Onodera et al. 1986). Thus blockage of synaptic terminals on a neuron might protect it from the consequences of anoxia (Johansen et al. 1984; Rothman 1984). The toxic excitatory action of the glutaminergic neurons of CA3 on CA1 may be due to a lesion of GABAergic interneurons (Khazipov et al. 1993). At present, the oversecretion of glutamate by CA3 is criticized (Schmidt-Kastner and Freund 1991), and the selective vulnerability of CA1 seems to be due to an overactivity of glutamate receptors (*N*-methyl-D-aspartate receptors, NMDA; Du et al. 1993), which are especially numerous on CA1 neurons, and to an increased intracellular concentration of Ca^{2+}, which produces degenerative processes in these neurons (Kudo et al. 1990; Olney et al. 1993; Kotapka et al. 1994; Ikonomovic et al. 1995; Schreibel and Baudry 1995). The origin of the selective vulnerability of specific hippocampal neurons to anoxia remains unclear.

Selective damage also occurs in certain hippocampal regions from causes other than anoxia (Pinard et al. 1984). Kainic acid produces selective lesions in CA3, which might be due to a dysfunction of synapses between terminals of mossy fibers and pyramidal neurons in this field (Collins 1986). Damage in the gyrus dentatus has also been observed in hypoglycemia (Collins 1986).

Hippocampal neuronal loss in aging and Alzheimer's disease seems to be different, although some discrepancies exist between the findings of different researchers, perhaps due to interindividual variations: in *aging*, the main site of neuronal loss is described as being either in CA1 and CA4 (Mani et al. 1986; West 1993) or restricted to CA1 and the subiculum (Simic et al. 1997). In *Alzheimer's disease*, although a lesion of the subiculum is always found, the occurrence of such damage in either CA1 (Bell and Ball 1981; Haigler et al. 1985; Doebler et al. 1987; West 1993) or the gyrus dentatus (Simic 1997) is debated. Only the CA2 field seems to escape damage.

Obviously, all these observations cannot be explained by the peculiar arrangement of vessels, but they do support the idea of a cell-specific structure of the different hippocampal fields (Babb et al. 1984; Haigler et al. 1985; Mani et al. 1986). The lesions specific to each of these different fields suggest that each has specific functions (Lopes da Silva and Arnolds 1978). This fine specialization is a remarkable feature of the hippocampal allocortex.

3.3.2 Emotional Behavior

Since the studies carried out by Papez (1937), regulation of emotional behavior has been considered the chief function of the hippocampus. At present, this function is mainly ascribed to the amygdala (LeDoux 1993; Gallagher and Holland 1994). Fibers arising from the basolateral amygdalar nucleus, which project to the dorsomedial thalamic nucleus and then to the prefrontal cortex, are thought to regulate an individual's behavior. Moreover, the central nucleus of the amygdala is believed to modulate the autonomic reactions produced by emotions (Martin et al. 1991). It is, however, accepted that the hippocampus may intervene in the regulation of some emotional behavior, especially that produced by pain; projections from the polysynaptic hippocampal pathway converge on the anterior cingulate cortex (area 24; Fig. 16), where the spinoreticulothalamocortical pathways involved in the perception of some aspects of pain end (Maclean 1992; B.A. Vogt et al. 1993; Graybiel et al. 1994; Adolphs et al. 1995; Ono et al. 1995; Williams 1995).

3.3.3 Motor Control

The hippocampus is believed to participate in the control of the *ventral striatal loop* (or limbic loop) belonging to the limbic system (Groenewegen et al. 1991;Witter and Groennewegen 1992; Maclean 1992). The ventral striatal loop (Fig. 20) is organized like the well-known dorsal striatal loop, but involves different structures. The main center of this loop is the ventral striatum or nucleus accumbens (Fig. 20A), which receives projections from the prefrontal cortex and controls the ventral pallidum. The ventral pallidum, which is of ill-defined location in humans (Fig. 20B), projects to the dorsomedial thalamic nucleus, although this projection is controversial in primates (Haber et al. 1993). From the dorsomedial nucleus, fibers return to the prefrontal cortex. The ventral striatum (nucleus accumbens) is itself controlled by dopaminergic fibers arising from the ventral tegmental area (cell group A10) and belonging to the dopaminergic mesolimbic system, as well as by the amygdala and the hippocampus. Fibers from the hippocampus reach the ventral striatum by way of the precommissural fornix (Lavin and Grace 1994). The ventral striatal loop may play a role in the control of motor behavior (e.g., motor reactions to emotion) and are thought to be involved in the mechanisms of drug addiction (Williams 1995).

3.3.4 Hypothalamus

The hippocampus is involved in the regulation of the hypothalamo-hypophyseal axis. Through its projections to the paraventricular hypothalamic nucleus, it may inhibit the hypophysial secretion of adrenocorticotrophic hormone (ACTH) (Jacobs et al. 1979; Teyler et al. 1980; Herman et al. 1989; Diamond et al. 1996).

3.3.5 Comparative Studies

This survey of the main hippocampal functions is of course incomplete, and some of these functions are controversial. Comparative studies do not shed much light on hippocampal functions. The size of the hippocampus generally increases in higher species (O'Keefe and Nadel 1978; Stephan 1983; West and Schwerdtfeger 1985). The very large size of the primate hippocampus, in contrast to that of insectivores, might be correlated with improved learning and memory. However, some highly evolved species, such as dolphins (Addison 1915; Jacobs et al. 1979) and whales (Stephan and Manolescu 1980; Schwerdtfeger 1984), have a small hippocampus. Moreover, hippocampal functions may differ among species (Howe and Courage 1993; Markowitsch 1995a). Notable support for this hypothesis is provided by the following: the particular development of certain zones, such as CA1 and the gyrus dentatus in humans and monkeys (Tilney 1939; Stephan and Manolescu 1980; Amaral and Campbell 1986; Schwerdtfeger 1986); the nearly total absence of commissural fibers in humans as compared to rodents (Wilson et al. 1987); and the great variations in the distribution of neuropeptides according to species (Sakamoto et al. 1987).

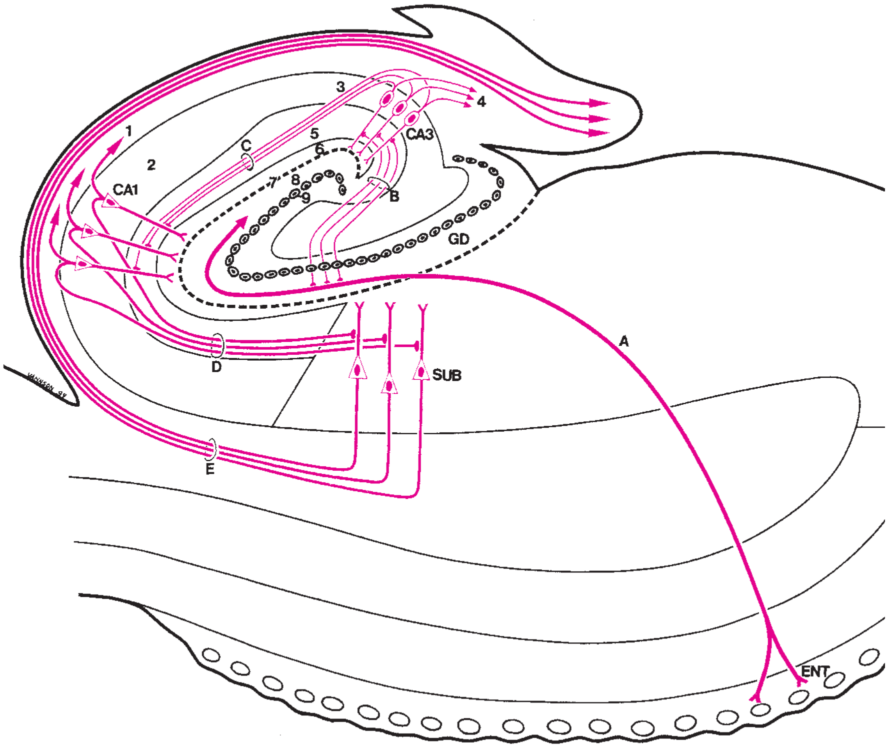

Cornu Ammonis: **1**, alveus; **2**, stratum pyramidale; **3**, Schaffer collaterals; **4**, axons of pyramidal neurons (mainly to septal nuclei); **5**, strata lacunosum and radiatum; **6**, stratum moleculare; **7**, vestigial hippocampal sulcus. Gyrus dentatus (**GD**): **8**, stratum moleculare; **9**, stratum granulosum. **CA1**, **CA3**, fields of the cornu Ammonis; **SUB**, subiculum

Fig. 15. Polysynaptic intrahippocampal pathway. **A–E** are parts of the neural chain forming the polysynaptic intrahippocampal pathway (see p. 28). Layer II of the entorhinal area (**ENT**) is the origin of this chain; its large pyramidal neurons are grouped in clusters, giving a granular aspect at the entorhinal surface

Fig. 16. Cortical connections of the polysynaptic intrahippocampal pathway. Hippocampal outputs fibers to the cortex: arising from the hippocampus (**1**), fibers successively reach the body (**2**) and column (**3**) of fornix (**3′**, anterior commissure), the mamillary body (**4**), and then, via the mamillothalamic tract (**5**), the anterior thalamic nucleus (**6**); some fibers reach this nucleus directly (**6′**); from the anterior thalamic nucleus, the main cortical projections are the posterior cingulate (**area 23**) and retrosplenial (**areas 29, 30**) cortices; some fibers may project to the anterior cingulate cortex (**area 24**) (see p. 33). Input fibers from the cortex to hippocampus: the posterior parietal association cortex (**7**) in relation to the superior visual system (**8**) projects via the parahippocampal gyrus (**9**) to the entorhinal area (**10**); **10′**, perforant fibers

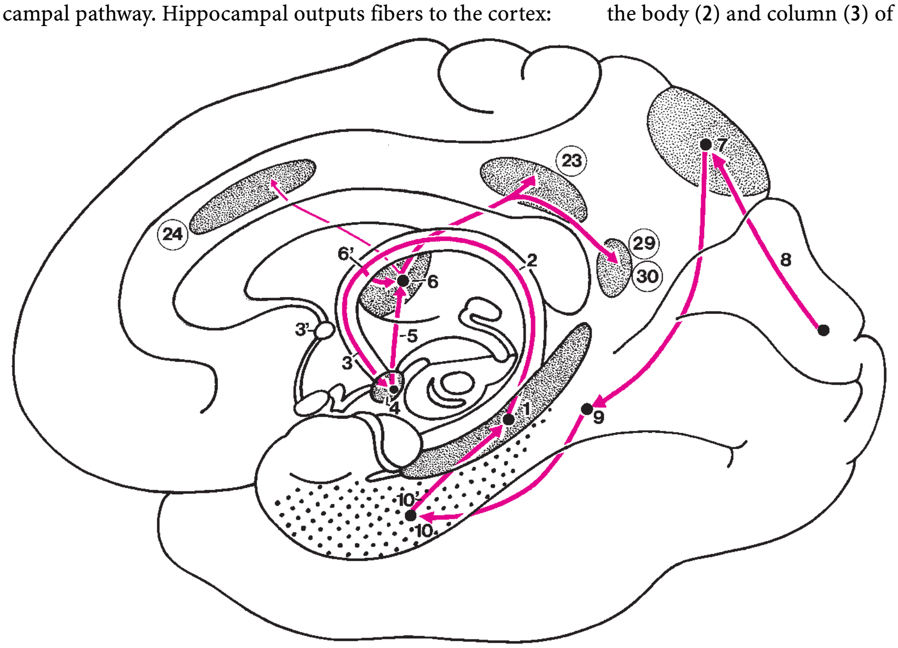

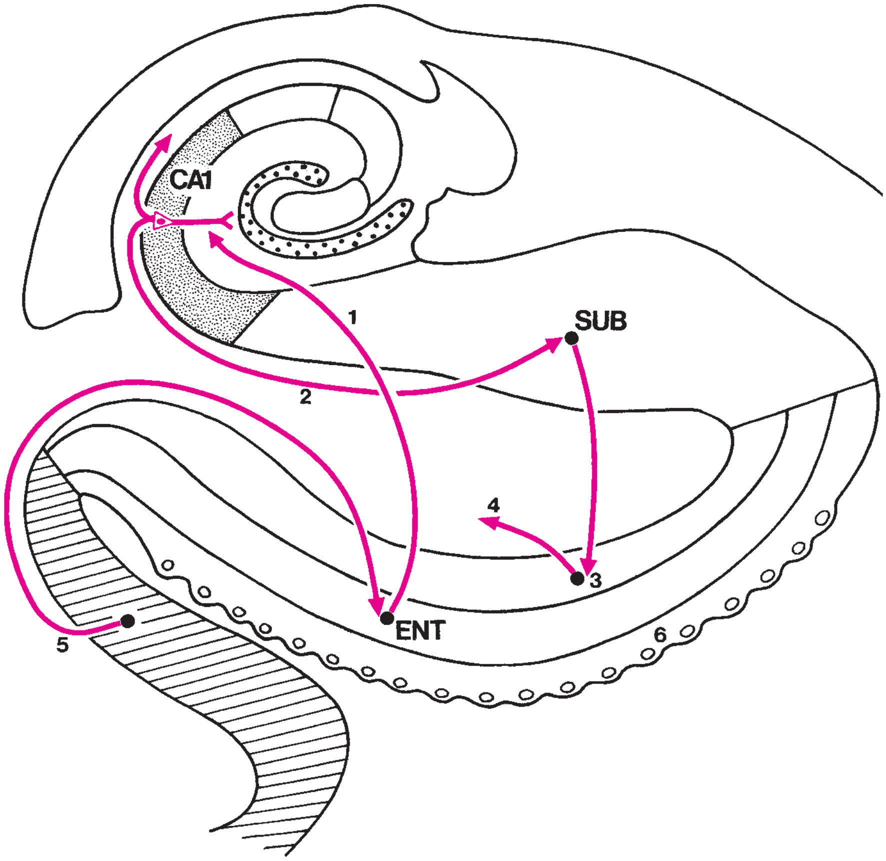

Fig. 17. Direct intrahippocampal pathway. The entorhinal area (**ENT**) (layer III) projects directly (**1**) onto CA1 pyramidal neurons, which innervate (**2**) the subiculum (**SUB**). Subicular axons project back to the deep layers of the entorhinal cortex (**3**). The neurons of these layers send axons to the association cortex (**4**) (see Fig. 18). The direct pathway receives inputs through the perirhinal cortex (**5**) (see Fig. 18). **6**, layer II of the entorhinal cortex

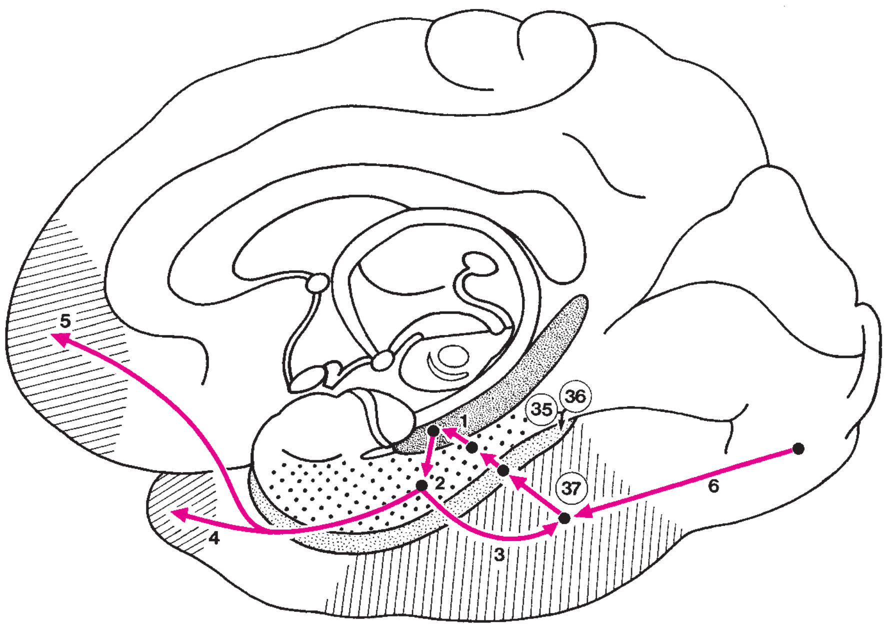

Fig. 18. Cortical connections of the direct intrahippocampal pathway. **1**, intrahippocampal circuitry (see Fig. 17). Hippocampal outputs fibers to the cortex: from the deep layers of the entorhinal cortex (**2**), fibers reach the inferior temporal association cortex (**3**), the temporal pole (**4**), and the prefrontal cortex (**5**). Inputs fibers from the cortex to hippocampus: the main origin of these fibers is the inferior temporal association cortex (**area 37**) in relation to the inferior visual system (**6**), reaching the entorhinal cortex through the perirhinal cortex (**areas 35, 36**)

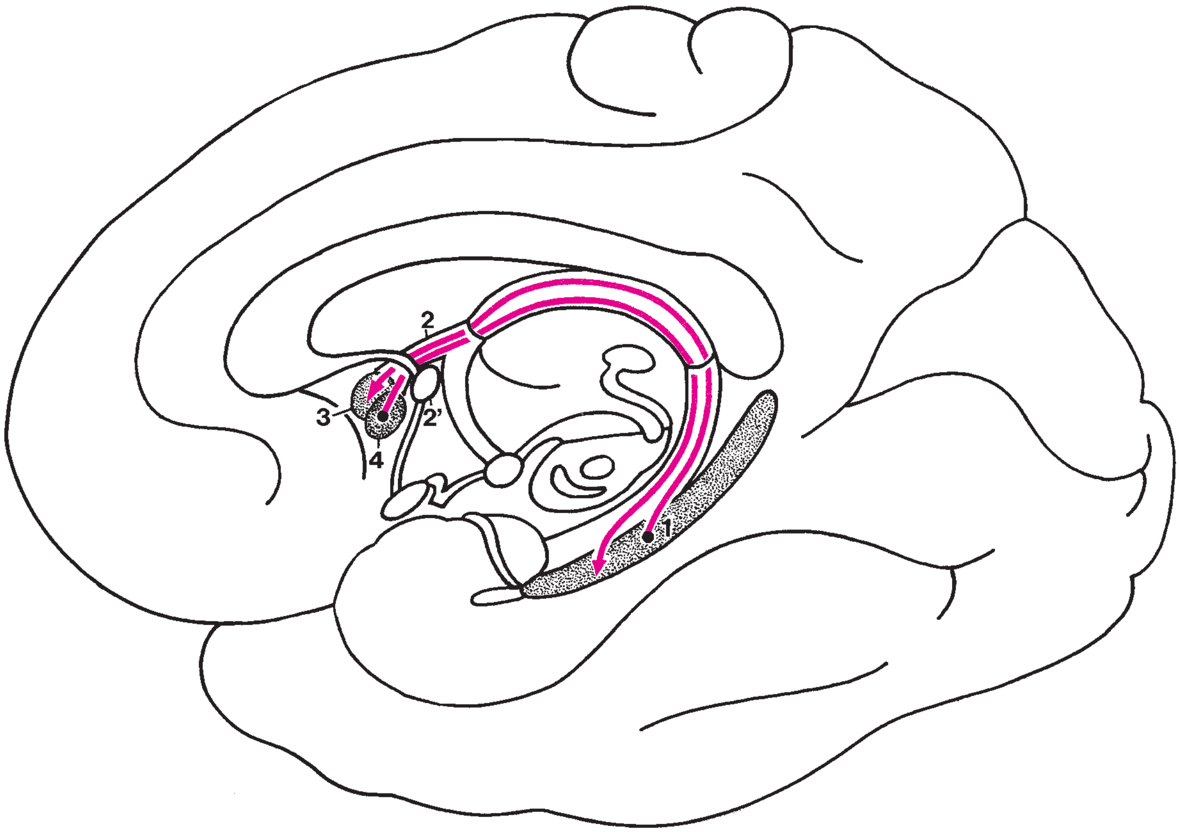

Fig. 19. Septal connections of the hippocampus. Axons of the cornu Ammonis (see Fig. 15), via the precommissural fornix (**2**), reach the lateral septal nucleus (**3**). The fibers from the medial septal nucleus (**4**) go back to the hippocampus by the same way. **2′**, anterior commissure

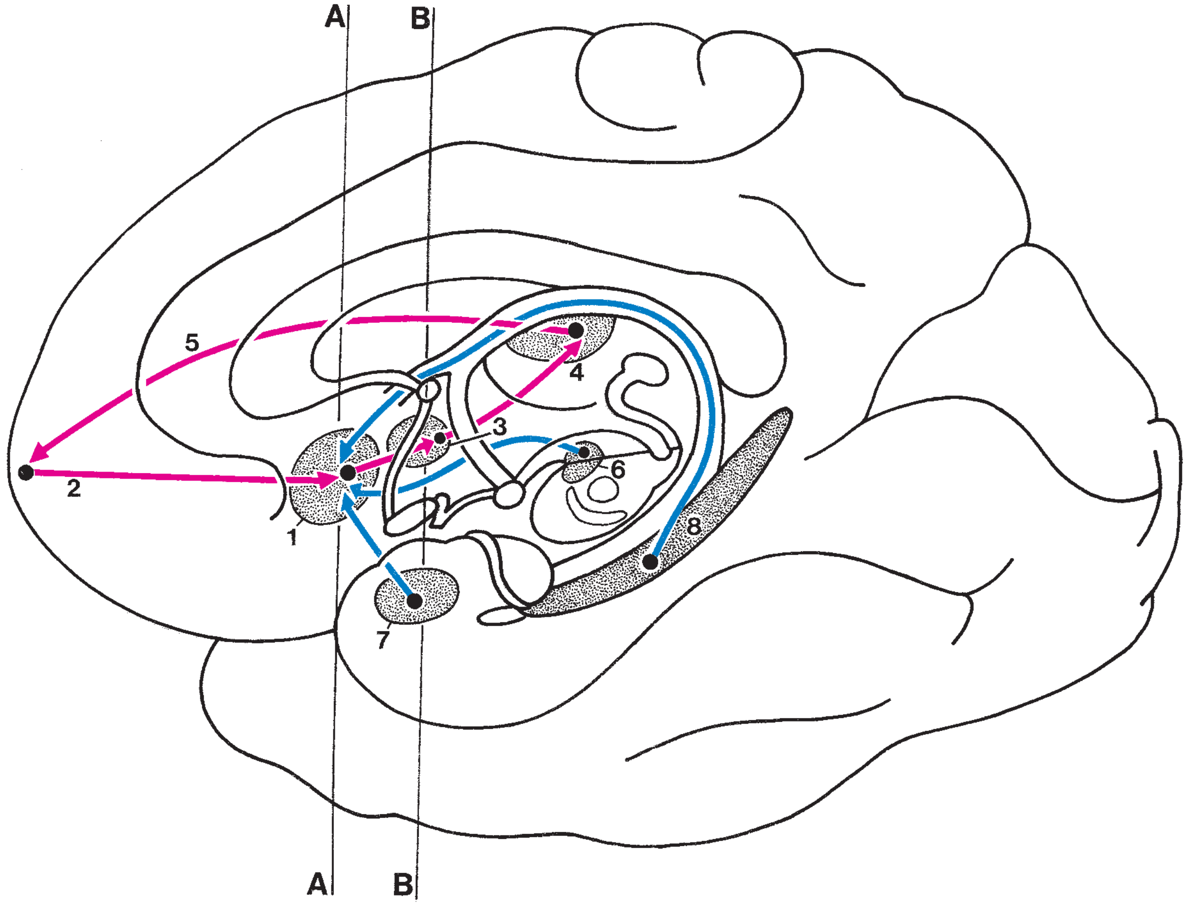

Fig. 20. Top, ventral (limbic) striatal loop. The ventral striatum (nucleus accumbens) (1) receives fibers from the prefrontal cortex (2) and controls the ventral pallidum (3). The ventral pallidum projects to the dorsomedial thalamic nucleus (4), whose fibers return to the prefrontal cortex (5). The ventral tegmental area (6) (dopaminergic mesolimbic system A10), the amygdala (7), and the hippocampus (8) control the ventral striatal loop. **Bottom**, planes of subjacent coronal sections corresponding to A and B in the top panel.

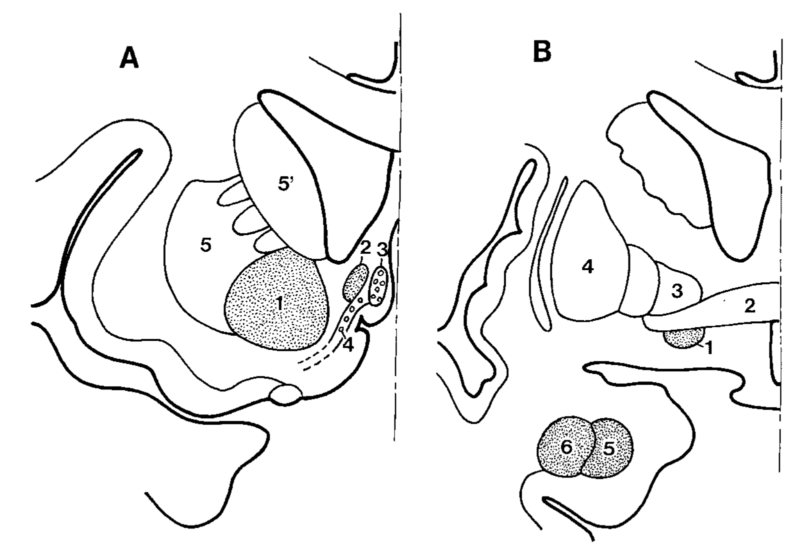

A Coronal section showing the situation of the ventral striatum (n. accumbens) (1), lateral septal nucleus (2), medial septal nucleus (3), nucleus of the vertical limb of the diagonal band (4), putamen (5) and caudate nucleus (5′) (5 and 5′: dorsal striatum).
B Coronal section showing the situation of the ventral pallidum (1), anterior commissure (2), globus pallidus (dorsal pallidum, 3), putamen (4; dorsal striatum), amygdala, basal nucleus (5), and amygdala, lateral nucleus (5′)

Anatomy

4.1 Preliminary Remarks

Hippocampal anatomy is so complex that its description can only be understood with the aid of the figures grouped at the end of this chapter (Figs. 21–45).

The hippocampus forms an arc whose anterior extremity is enlarged and whose posterior extremity narrows like a comma (Fig. 3). As with some other hemispheric structures, e.g., the caudate nucleus, the hippocampus can be divided into three parts: (1) an anterior part, or *head*, (2) a middle part, or *body*, and (3) a posterior part, or *tail*. It has a total length of between 4 and 4.5 cm; the body is on average 1 cm wide, and the head is 1.5–2 cm wide (Poirier and Charpy 1921; Testut and Latarjet 1948; Dejerine 1980). Although not particularly studied in this work, no important macroscopical differences have been observed between the right and left hippocampi or between hippocampi taken from male and female individuals.

Figure 21 shows the general position of the two components of the hippocampus. The cornu Ammonis and the gyrus dentatus form two interlokking, U-shaped laminae. As shown by Giacomini (1884) and later by Mutel (1923), the position of these two cortical laminae is the same in all three parts of the hippocampus. Thus, because of the curvature of the hippocampus, the gyrus dentatus and the cornu Ammonis have the same reciprocal position in a coronal section of the body as in a sagittal section of the head or of the tail (Figs. 101, 111).

Figure 22 shows the general form of the gyrus dentatus. It is folded, perhaps because of some obstacle during development; folding is especially marked in higher mammals. On the surface, these folds form the well-known “teeth” or dentes of the gyrus, whose deep part has extensions into the hippocampal body, head, and tail. Note that its anterior end (in the uncus) and posterior end (in contact with splenium) have a similar appearance, like a narrow and concave lamina devoid of dentes.

Having presented this global aspect of hippocampal morphology, the body, head, and tail will now be studied in succession.

4.2 Hippocampal Body

Two aspects of the hippocampal body will be considered: the intraventricular, or deep part, and the extraventricular, or superficial part.

4.2.1 Intraventricular Part (Figs. 3, 23)

The intraventricular part is an element of the floor in the lateral ventricle (temporal or inferior horn). It is a strongly convex protrusion, smooth and padded with ependyma covering the alveus. Numerous subependymal veins radiate on its surface (Fig. 54; Wolf and Huang 1964; see p. 76). In depth, the intraventricular part corresponds to the CA1–CA3 fields of the cornu Ammonis (Fig. 7). The hippocampal body is bordered medially by the fimbria and laterally by the narrow collateral eminence, which marks the intraventricular protrusion of cortex covering the collateral sulcus (Figs. 3, 5, 23). The roof of the temporal horn overhangs the intraventricular part of the hippocampal body; it is composed of the temporal stem, the tail of the caudate nucleus, and the stria terminalis (Figs. 5, 8). The temporal stem is a narrow lamina of white matter between the ventricular cavity and the fundus of the superior temporal sulcus (Figs. 102D, 103D, 104D, 105D, 106D).

Note that the intraventricular hippocampal surface is almost entirely hidden by voluminous choroid plexuses; only the hippocampal head is devoid of these plexuses (Figs. 38, 53). The choroid plexuses in the temporal horn are the inferior extremity of a unique formation, the choroid plexuses of the prosencephalon, which are all visible in Fig. 37. Choroid plexuses of the temporal horn are attached to a double layer, formed of ependyma and pia, which together make up the tela choroidea of the temporal horn (Fig. 36A).

Precise definition of the prosencephalic tela choroidea is controversial and needs to be discussed here. Most classic texts refer to the tela choroidea of prosencephalon as *two pial layers* trapped in the median part of the transverse fissure during development of the commissures and telencephalic vesicles (Villiger and Ludwig 1946; Testut and Latarjet 1948; Clara 1959; Kahle 1986; Yasargil 1987; Williams 1995). One layer covers the inferior surfaces of fornix and splenium, while the other covers the third ventricle and thalamus. Lateral extensions of the tela form the choroid plexuses in the bodies of lateral ventricles. The two pial layers delimit a space between them, the velum interpositum, which contains the internal cerebral veins. Curiously, however, this definition of the tela has not been extended to the temporal horns and lateral parts of the transverse fissure. Consequently, there is a lack of nomenclature here. For this reason, another description, used by several authorities, particularly Crosby et al. (1962), Bargmann (1964), and Carpenter and Sutin (1983), has been followed here.

The tela choroidea is thus the juxtaposition of *one ependymal layer* and *one pial layer* (Fig. 36A). The tela choroidea of the lateral ventricle closes the choroid fissure and fixes the choroid plexuses. The tela is attached to a thickening of the ventricular wall, the taenia of the tela choroidea. This description has the advantage of setting clear limits to the tela choroidea and of being applicable to the different ventricles.

The tela choroidea in the temporal horn is stretched between two taeniae, the taenia of the stria terminalis and that of the fimbria. Whereas the former is only slightly visible, the latter can often be clearly seen (Fig. 36A).

At the junction of hippocampal body and head, when the uncus appears, the taeniae of the fimbria and stria terminalis unite. This union is the velum terminale of Aeby (Aeby 1871) or inferior choroidal point (Nagata et al. 1988), a triangular lamella attached to superior surface of the uncus and of variable development (Fig. 29).

4.2.2 Extraventricular or Superficial Part

The extraventricular part of the hippocampus, visible on the medial surface of the temporal lobe, is reduced in size. It is limited to the gyrus dentatus, fimbria, and superficial hippocampal sulcus (Figs. 4A, 23).

The superficial part of the gyrus dentatus is the *margo denticulatus*, composed of rounded protrusions which form the dentes of the gyrus. There are usually about 15 dentes (Poirier and Charpy 1921; Stephan 1975), those in the middle being the largest. They diminish in size caudally and cranially. Numerous vessels penetrate the sulci between them and thus supply the hippocampus (see Chap. 5). The dentes of the margo denticulatus are surface manifestations of general folding in the gyrus dentatus (Fig. 22). The occurrence of dentes on the margo denticulatus is specific to humans and higher primates (Tilney 1939).

The fimbria is a narrow, white strip (Figs. 3, 23) which more or less hides the margo denticulatus, having individual variations. A deep fimbriodentate sulcus separates these two structures (Fig. 7).

The margo denticulatus is bordered inferiorly by the *superficial hippocampal sulcus*, which separates it from subjacent subiculum (Figs. 5, 7, 23).

4.2.3 Relations with Adjacent Structures

The extraventricular, superficial part of the hippocampus and the tela choroidea of the temporal horn together form the fundus of a deep fissure, the *lateral part of the transverse fissure* (Figs. 5, 107D). The roof of the latter is formed by the lateral geniculate body rostrally and the pulvinar caudally (Figs. 106D, 107D). Its floor is the flattened surface of the subiculum in its pre- and parasubicular segments. Since Liliequist (1959), the subarachnoid space in the transverse fissure has often been called the wing of the ambient cistern. In fact, this subarachnoid space communicates medially with the ambient cistern, situated between the temporal lobe and lateral mesencephalic surface (Figs. 5, 106D, 107D).

The transverse fissure contains vessels running towards the subiculum, the hippocampus (see Chap. 5), and the geniculate bodies. The posterior cerebral artery, usually in the ambient cistern (Fig. 104B,D), sometimes curves into the transverse fissure (Fig. 50; Lecaque et al. 1978; Yasargil 1984).

The ambient cistern contains numerous vessels which curve round the mesencephalon. These are, in descending order, the posterior cerebral artery (P2 segment), with the adjacent basal vein, and the posteromedial choroidal, collicular, and superior cerebellar arteries (Khan 1969; Duvernoy 1999; Lang 1981). The free edge of the tentorium cerebelli is far from the hippocampal body, since it usually follows the inferior surface of the parahippocampal gyrus (Fig. 45). Finally, the cerebellum limits the ambient cistern below via the tentorial opening (Fig. 107D).

4.3 Hippocampal Head

The hippocampal head includes an intraventricular part, the digitationes hippocampi, and an extraventricular or uncal part.

4.3.1 Intraventricular Part

The intraventricular part is the anterior part of the arc of the hippocampus. It features the *digitationes hippocampi*, or internal digitations (Figs. 3, 24). There are usually three of four digitations, sagittally oriented and separated by small but definite sulci (Klinger 1948). A *vertical digitation* sometimes joins them, corresponding to the intraventricular part of the medial surface of the uncus (Figs. 21, 104B, C). There are two opposing theories on the origin of digitations. Some consider them due to a cortical atrophy (Zuckerkandl 1887), whereas others (Giacomini 1884; Testut and Latarjet 1948) believe that their characteristic folding is due to some obstacle to forward development of the hippocampus, which is the more likely theory.

In frontal sections, the digitations are seen to be transverse foldings of the cornu Ammonis (Figs. 26, 68). The folding is also visible on the extraventricular surface of the head, as will be seen later; for this reason Retzius (1896) referred to the intraventricular digitations as *internal digitations* and to the extraventricular ones as *external digitations*. Each digitation is cored by a digital extension of the gyrus dentatus (Fig. 22).

When the hippocampal digitations appear at the junction of the body and head, the fimbria gives way to a thick alveus which covers them. The taeniae of the fimbria and stria terminalis unite, forming the velum terminale (see p. 40; Fig. 29). As the tela choroidea is absent from anterior part of the temporal horn, the hippocampal head is free of choroid plexuses and is visible in intraventricular views (38, 53). Anterior to the hippocampus, the ventricular cavity is often prolonged into the deep part of the uncus, as the *uncal recess* of the temporal horn (Figs. 3, 116B; Klinger 1948). The intraventricular surface of the amygdala, composed of basal and lateral nuclei, overhangs the hippocampal head along almost its entire surface (Figs. 113–116). The hippocampal digitations and amygdala are often joined together across the ventricular cavity (Fig. 24).

4.3.2 Extraventricular or Uncal Part

Understanding this complex region requires a general description of the uncus, based on the observations made by Retzius (1896).

The uncus, or anterior segment of the parahippocampal gyrus, curls posteriorly to rest on the parahippocampal gyrus itself, separated from the latter by the uncal sulcus (Figs. 27, 28). This posterior curving of the uncus may be due to obstruction by the amygdala to anterior development of the parahippocampal gyrus (Stephan and Manolescu 1980). Others consider that the fimbria, fixed to the uncal apex (Figs. 27, 28), holds the uncus back during anterior development of the parahippocampal gyrus (Giacomini 1884; Mutel 1923; Anthony 1947; Grassé 1972). Note that the uncus is especially well developed in humans and primates (Tilney 1939).

The uncus is structurally divided into an anterior segment, belonging to the piriform lobe (see p. 5), and a posterior segment, belonging to the hippocampus (Giacomini 1884; Mutel 1923).

Anterior Segment

Two distinct protrusions can be discerned in the anterior segment, the semilunar gyrus and the ambient gyrus, separated by the semianular or amygdaloid sulcus (Figs. 28, 29; B.H. Turner 1981). The *semilunar gyrus* covers the cortical nucleus of the amygdala (Fig. 14) and is separated from the anterior perforated substance by a deep fold, the endorhinal sulcus (Figs. 29, 31). The *ambient gyrus* shows a marked uncal notch, produced by the free edge of the tentorium cerebelli (Figs. 28, 45). The ambient gyrus continues into the anterior extremity of the parahippocampal gyrus, which is limited by the rhinal sulcus (Fig. 4). The anterior part of the parahippocampal gyrus has an irregular surface formed of small protrusions named by Retzius (1896) and Klinger (1948) as the *verruccae gyri hippocampi* (Fig. 28); the significance of these protrusions is explained on p. 28.

Posterior Segment

The posterior segment is part of the hippocampus and the subiculum and is separated from the parahippocampal gyrus by the uncal sulcus. It has an inferior surface, hidden in the uncal sulcus, and a medial surface, exposed on the medial aspect of the temporal lobe.

Inferior surface. This surface, visible only after ablation of the subjacent parahippocampal gyrus, is divided into the band of Giacomini, the external digitations, and the inferior surface of the uncal apex (Figs. 25, 57).

In the hippocampal body (Fig. 22), the gyrus dentatus is a medially concave cellular layer whose superficial, visible segment forms the margo denticulatus, which is flanked by the superficial hippocampal sulcus. In the hippocampal head, the gyrus dentatus has the same appearance, but the cellular layer is caudally concave (Figs. 22, 27). The segment of the gyrus dentatus visible here is the *band of Giacomini*, and it is also flanked by the superficial hippocampal sulcus. This change in terminology complicates the description, and the term "margo denticulatus" could well be reserved for the visible segment of the gyrus dentatus, both in the body and in the head of the hippocampus.

On the inferior uncal surface (Fig. 25), the margo denticulatus turns into the band of Giacomini at a right angle. The band crosses the inferior uncal surface to appear on its medial surface (Figs. 27, 28). The flattened surface of the band often makes it difficult to identify. Rostrally, it is well defined by the superficial hippocampal sulcus, which can always be distinguished.

The *external digitations*, anterior to the band of Giacomini, form two or three small, convex lobules separated by sagittal sulci (Fig. 25). These digitations are inverse images of the internal digitations (digitationes hippocampi), visible on the intraventricular aspect of the hippocampal head (Figs. 26, 68, 104B). The external and internal digitations are due to folding of the cornu Ammonis. These folds vary in thickness, as is frequent in cortical gyri in general. The cortex of the cornu Ammonis is thick in the external and thin in the internal digitations. Digitations are principally formed by the CA1 field of the cornu Ammonis.

The *inferior surface of the uncal apex* (Fig. 25) is posterior to the band of Giacomini (the term "uncal apex" is prefered to "intralimbic gyrus," which is sometimes used, as the latter may be confused with the intralimbic gyrus proper). The uncal apex is the caudal end of the uncus; the fimbria is attached to its extremity. Its inferior surface is like a cone, and its base is separated from the band of Giacomini by a discrete sulcus. Retzius (1896) likened this surface to a helmet, with the band of Giacomini forming its edge. The uncal apex is made up of CA3 and CA4 covered by alveus (Fig. 27). In the hippocampal body, all these structures are deep and hidden by the fimbria (Fig. 7). In the uncus, the fimbria has having disappeared, and CA3 and CA4, covered by alveus, appear on the surface as the uncal apex. Because of this inversion, Elliot Smith (1896) named the uncal apex the hippocampus inversus, a term later used by numerous workers (Gastaut and Lammers 1961).

Medial Surface. This surface, visible on the medial aspect of the temporal lobe (Figs. 4, 27–29) is divided into the terminal segment of the band of Giacomini, the medial surface of the uncal apex, and the uncinate gyrus.

The *terminal segment of the band of Giacomini* appears on the upper lip of the uncal sulcus; it follows a vertical route on the medial surface of the uncus and is flanked by the terminal segment of the superficial hippocampal sulcus. In toto, the band has an initial, hidden segment on the inferior uncal surface (pars occulta, Fig. 25) and a visible terminal segment on the medial uncal surface (pars aperta, Fig. 28) (Villiger and Ludwig 1946; Klinger 1948). As described earlier, the band is the equivalent of the margo denticulatus, i.e., the superficial segment of the gyrus dentatus. The deep segment of the gyrus dentatus is a vertical and caudally concave cellular layer of the uncal apex (Figs. 22, 27). The band of Giacomini and the gyrus dentatus diminish superiorly and disappear at the superior edge of the uncus.

The *medial surface of the uncal apex* resembles the inferior surface described above. It is also composed of CA4 and CA3, is covered by alveus, and forms the hippocampus inversus (Fig. 27). The junction of the fimbria to the apex of the uncus is clearly distinguishable.

The *uncinate gyrus*, anterior to the band of Giacomini, joins up with the ambient gyrus. Its structure is uncertain, but it seems to be composed of a strip of the CA1 field, overflowing from the hippocampal sulcus, and of the subiculum as far as the ambient gyrus (Figs. 27, 122, 123; Vogt and Vogt 1937; Braak 1980).

4.3.3 Relations of the Uncus with Adjacent Structures

The anterior and posterior uncal segments have different relations. The *anterior segment* is the lateral limit of the anterior perforated substance, the interpeduncular region, and the chiasmatic and interpeduncular cisterns. It is related to the oculomotor nerve, the first segment of the middle cerebral artery, the posterior communicating artery, the tuber, and the hypophysial stalk (Figs. 30, 31, 40). The *posterior segment* is situated near the crus cerebri, but is separated from it by the narrow crural cistern (Figs. 30, 31, 41, 122D, 123D).

Numerous vessels cross the uncal surface (Yasargil 1984). On the superior uncal surface, the anterior choroidal artery follows the semianular sulcus, separating the semilunar gyrus from the ambient gyrus (Figs. 44, 59). The anterior choroidal artery reaches the uncal apex and choroid plexuses of the temporal horn; here, it supplies an uncal branch (Carpenter et al. 1954), which descends with the band of Giacomini and reaches the uncal sulcus (Fig. 56).

The posterior cerebral artery (P2 segment) runs along the medial uncal surface, hiding the uncal sulcus (Fig. 44). It is often accompanied by the basal vein (Fig. 43). At the uncal apex, the basal vein receives an important collateral, the inferior ventricular vein (vein of the temporal horn). Below the posterior cerebral artery, the free edge of the tentorium cerebelli is situated, with which the trochlear nerve is associated (Fig. 44).

Relations between the tentorial edge and uncus have been studied by Yates (1976) and Noël et al. (1977), among others. These relations depend on the size of the tentorial opening (Fig. 42), which greatly varies (Corsellis 1958). Often, however, the tentorial edge is close to the uncus, where it frequently marks the ambient gyrus (uncal notch) (Lang 1985; Fig. 28). In herniation of the temporal lobe, the uncus may slip between the tentorial edge and the crus cerebri. In addition to lesions due to compression of the mesencephalon, uncal herniation may also compress the P2 segment of the cerebral artery against the tentorial edge, causing marked hemodynamic disturbances (incisural sclerosis, see p. 32).

Crossing the uncus is not the only critical point in passage of the posterior cerebral artery. At the posterior extremity of the parahippocampal gyrus, the beginning of the P3 segment of the artery has to cross a narrow cleft between the parahippocampal gyrus and tentorial edge. It is likely that temporal herniation may compress the artery here (Fig. 40).

4.4 Hippocampal Tail

The tail is the posterior part of hippocampal arc (Fig. 3). As with the body and the head, the tail can be divided into intraventricular and extraventricular parts.

4.4.1 Intraventricular Part

The intraventricular part is a transverse bulge, oriented like the intraventricular part of the head, but smaller. Although digitations do not appear on the surface of the tail, its internal structure is similar to that of the head and is composed of a vast layer of the cornu Ammonis centered by digital extensions of the gyrus dentatus (Figs. 22, 108). The intraventricular surface of the tail is thickly covered by the alveus and subependymal veins. The intraventricular part is flanked medially by the fimbria and laterally by the collateral trigone; the flat surface of the collateral trigone and the intraventricular part of the tail together form the floor of the atrium (Fig. 3). Caudally, the convexity of the hippocampus reaches a marked protrusion, the calcar avis (Figs. 3, 39, 42). The atrial roof overhanging the tail is composed of the caudate nucleus with the stria terminalis alongside. A strip of white matter, chiefly visual (optic radiations), separates the cerebral cortex from the ventricular cavity (Fig. 120D). The choroid plexuses here are even more voluminous than near the hippocampal body, forming the *choroid glomus*, which hides the ventricular floor completely (Figs. 37, 53).

4.4.2 Extraventricular Part

Full discussion of the controversy in studies of this region will be avoided here, since this would only further complicate the problems; the description will thus be simplified to correlate the hippocampal surface with its internal structure.

The extraventricular part of the hippocampal tail may be divided into an initial segment (a continuation of the body), a middle segment, and a terminal segment inferior to the splenium (Fig. 32).

The *initial segment* of the tail resembles the body. The margo denticulatus is divided into dentes which successively decrease in size (Fig. 23). In its deep part, the gyrus dentatus has many extensions penetrating deeply into the hippocampus (Fig. 22). The margo denticulatus is partly hidden by the fimbria and is separated from the subiculum by the superficial hippocampal sulcus.

In the *middle segment,* three modifications appear (Fig. 32):

1. The *margo denticulatus* becomes smooth and narrow, forming the fasciola cinerea, which is limited below by the superficial hippocampal sul-

cus. The *fasciola cinerea* thus prolongs the margo denticulatus and, like it, forms the visible part of the gyrus dentatus (Giacomini 1884; Klinger 1948).

2. The *fimbria*, which in the initial segment hides the margo denticulatus, separates from it, ascending to join the crus of fornix. Thus the fimbriodentate sulcus widens progressively. Hence a whitish band appears, the *gyrus fasciolaris*, which is composed of CA3 and covered by a thin layer of alveus (Fig. 32). The CA3 field of the cornu Ammonis is deep and hidden in the hippocampal body, but in this segment it is superficial. Hence the gyrus fasciolaris is referred to as the hippocampus inversus, as is the uncal apex (Elliot Smith 1898; Gastaut and Lammers 1961). Sometimes, a hippocampus inversus is prolonged anteriorly in the hippocampal body, in which case the fimbria and the margo denticulatus remain separate (Fig. 35). This arrangement is rare in humans, but is frequent in many macrosmatic mammals. The gyrus fasciolaris is separated from the fasciola cinerea by the sulcus dentatofasciolaris (Retzius 1896; Fig. 32).
3. *CA1* is deep in the hippocampal body and hidden by the subiculum. In the tail, on the other hand, CA1 appears progressively at the surface of the parahippocampal gyrus (Fig. 32). The CA1 layer, which is here heavily folded, sometimes raises the surface of the parahippocampal gyrus, producing rounded bulges, the so-called gyri of Andreas Retzius (Retzius 1896; Fig. 89). The terms "gyri retrospleniales" (Riley 1960; Naidich et al. 1987) or "eminentiae subcallosae" (Zuckerkandl 1887) can lead to confusion with other cortical regions.

The gyri of Andreas Retzius are separated from the fasciola cinerea by the superficial hippocampal sulcus; Figs. 32 and 33 show well-developed gyri of Andreas Retzius, whereas they are absent in Fig. 23.

In summary, the middle segment of the hippocampal tail consists, in descending order, of the gyrus fasciolaris, the fasciola cinerea, and the gyri of Andreas Retzius.

The *terminal segment of the hippocampal tail* (see Figs. 32, 90) covers the inferior splenial surface and,alone, merits the name subsplenial gyrus (Riley 1960; Gastaut and Lammers 1961), a term sometimes applied to the entire tail.

The results of this study provide support for the view (Elliot Smith 1898; Macchi 1951; Stephan 1975) that the fasciola cinerea, which is an extension of the gyrus dentatus, has disappeared in the terminal segment of the hippocampal tail, although some (Giacomini 1884; Ariëns Kappers et al. 1967) regard it as extending to dorsal surface of the corpus callosum. The subsplenial gyrus, which prolongs the gyrus fasciolaris, is thus a thin layer of cornu Ammonis that surrounds the splenium and is continued by the indusium griseum on the dorsum of the corpus callosum (Klinger 1948; Tryhubczak 1975). It appears that the CA3 neuronal type forms the medial edge, while most of the subsplenial gyrus consists of CA1 (Schwerdtfeger 1984), although identification of neuronal types is difficult in this region (Ramon y Cajal 1911, 1968; Klinger 1948). In the callosal sulcus, the lateral edge of the subsplenial gyrus joins with the cortex of the isthmus of the cingulate gyrus (Fig. 109; Jacobs et al. 1979).

The origin and structure of longitudinal striae could not be elucidated by the methods used in this study. The medial and lateral longitudinal striae are currently considered to be aberrant fibers of the fornix which, on leaving the fimbria, reach the dorsum of the corpus callosum on the indusium griseum to join the fornix again rostrally (Williams 1995; Nieuwenhuys et al. 1988) The origin of these small fasciculi in the hippocampus (Fig. 32) is uncertain. The medial stria may stem from the fasciola cinerea, and the lateral stria from the gyrus fasciolaris (Giacomini 1884; Elliot Smith 1897; Ramon y Cajal 1911, 1968; Dejerine 1980), but Duval (1881) and Macchi (1951) deny any connection between the indusium griseum and longitudinal striae on the one hand and the hippocampus on the other.

4.4.3 Relations with Adjacent Structures

The extraventricular, superficial part of the hippocampal tail has relations similar to those of the body. The tail forms the depths of the lateral part of the transverse fissure (Fig. 119B). Among the vessels in this fissure, the trunk of the medial atrial vein is noteworthy (Salamon and Huang 1976; Lang 1981). As shown in Fig. 33, the trunk of the medial atrial vein is the junction of subependymal branches which cross the calcar avis and then perforate the fimbria. The longitudinal hippocampal veins join these branches (see p. 75). The trunk of the medial atrial vein is situated in a triangular zone, the subcallosal trigone, formed by the separation between the crus of fornix and the hippocampal tail (Fig. 32).

The transverse fissure leads into the ambient cistern medially (Figs. 5, 107D) and, more caudally, the quadrigeminal cistern (Fig. 108D). The latter is situated beneath the splenium and adjoined by the pineal gland, colliculi, and cerebellum through the tentorial opening. The quadrigeminal cistern contains numerous vessels, i.e., posterior cerebral and posteromedial choroidal arteries, terminal branches of collicular arteries, and terminal segments of basal and internal cerebral veins flowing into the vein of Galen (Duvernoy 1975, 1978; Wolfram-Gabel 1983).

4.5 General Features

At the end of this study of a particularly complex region, several practical points should be noted:

- The structure of the hippocampus is the same in its different segments, as Giacomini (1884) and Mutel (1923) have shown. The cornu Ammonis has in fact an analogous structure in the head, body, and tail of the hippocampus (Fig. 21), as does the gyrus dentatus, which forms a continuous U-shaped lamina into which the cornu Ammonis penetrates. The visible segment of the gyrus dentatus is known as the margo denticulatus in the body, the band of Giacomini in the uncus, and the fasciola cinerea in the tail. However, it is in fact the same structure and the same term could be used for its whole length. Note that the visible part of the gyrus dentatus is bordered by the superficial hippocampal sulcus along its entire length.
- Because of the arched form of the hippocampus, coronal sections of the body and sagittal sections of the head and tail have similar appearances, which may lead to confusion (Figs. 101, 111).
- Also because of the hippocampal curve, coronal sections are often difficult to interpret. Whereas coronal sections of the hippocampal body correspond to classic views of the hippocampus (Fig. 106), coronal sections of the hippocampal head (Figs. 103 – 105 and of the hippocampal tail (Figs. 107, 108) cut through these formations tangentially. In particular, a section of the body and a section of the uncus can be found in the same figure (Fig. 105).

The anatomical study presented here is designed to make it easier to understand sections of the hippocampus in different planes, which are becoming increasingly clear in medical and academic imaging (see Chap. 7).

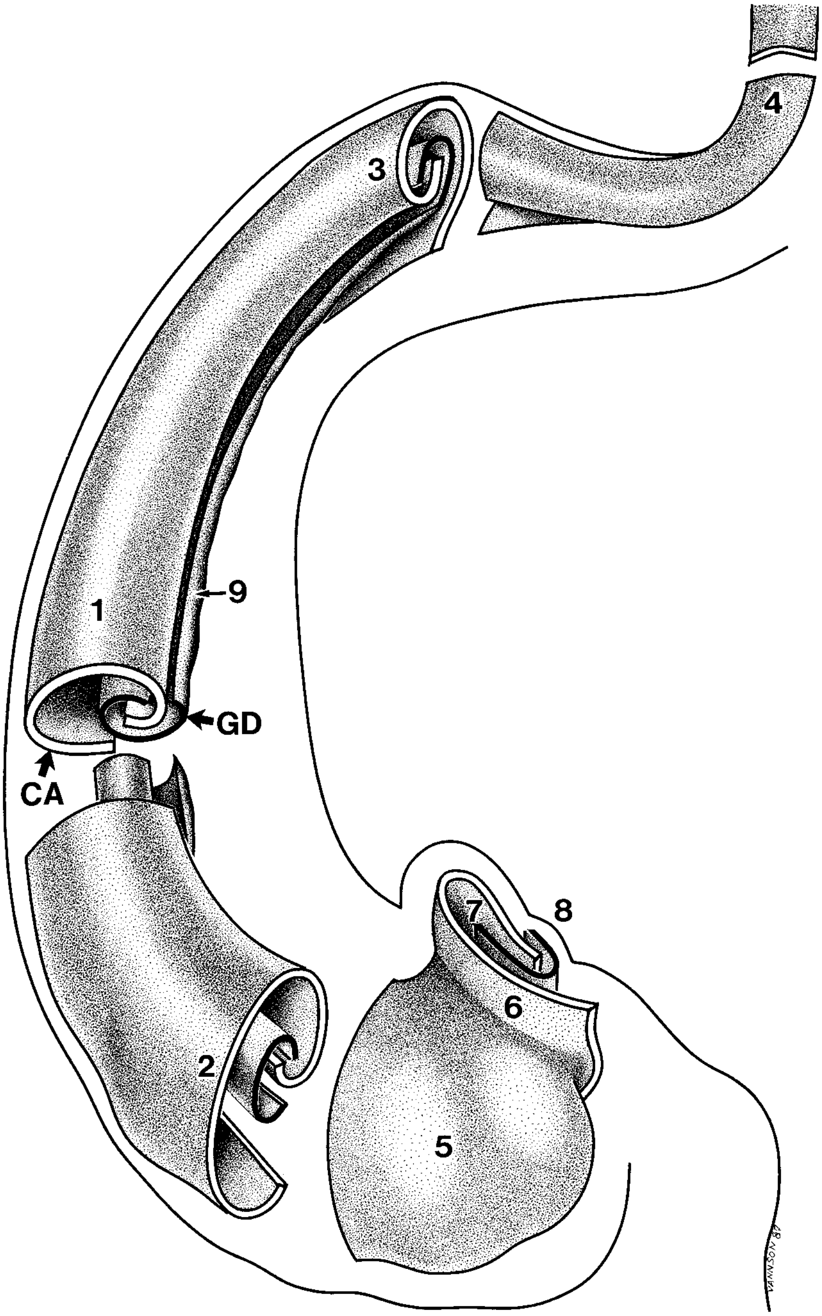

Fig. 21. General view of the internal structure of the hippocampus. The cornu Ammonis (**CA**) and gyrus dentatus (**GD**) form two interlocking, U-shaped laminae
1, hippocampal body; **2**, hippocampal head; **3**, hippocampal tail; **4**, terminal segment of the tail; **5**, digitationes hippocampi; **6**, vertical digitation; **7**, cornu Ammonis and gyrus dentatus in the medial surface of the uncus; **8**, band of Giacomini; **9**, margo denticulatus

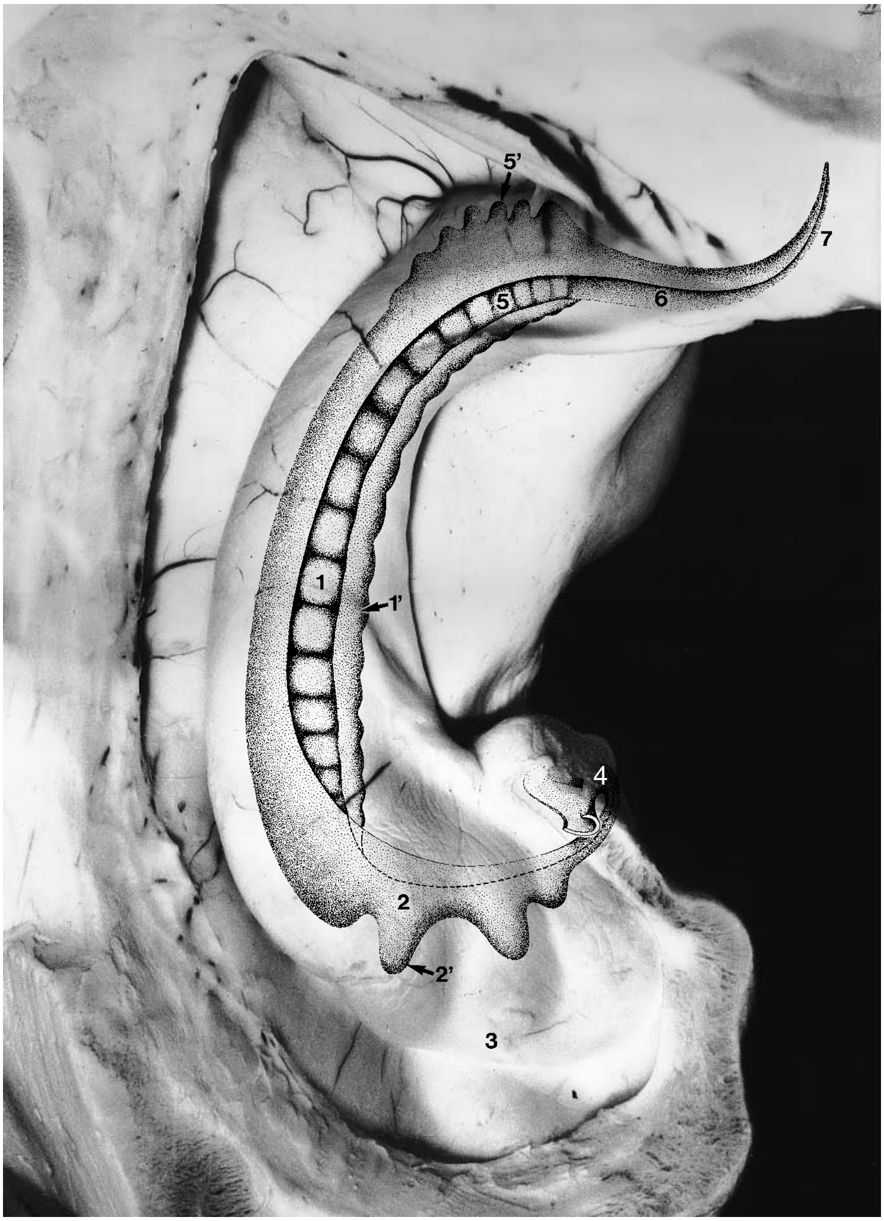

Fig. 22. Gyrus dentatus seen through the hippocampus (transparent)
1, gyrus dentatus in the hippocampal body; **1′**, margo denticulatus; **2**, gyrus dentatus in the hippocampal head; **2′**, digital extensions of the gyrus dentatus; **3**, digitationes hippocampi; **4**, band of Giacomini and terminal part of gyrus dentatus in the medial surface of the uncus; **5**, gyrus dentatus in the hippocampal tail; **5′**, digital extensions of the gyrus dentatus; **6**, fasciola cinerea; **7**, terminal part of the fasciola cinerea

▷

Fig. 23. Aspect of hippocampus after opening of the temporal horn of the lateral ventricle. **Bar**, 3.6 mm
1, intraventricular aspect of hippocampal body; **2**, fimbria; **3**, taenia fimbriae; **4**, dentes of margo denticulatus; **5**, superficial hippocampal sulcus; **6**, subiculum and parahippocampal gyrus; **7**, hippocampal tail; **8**, calcar avis; **9**, collateral trigone; **10**, collateral eminence

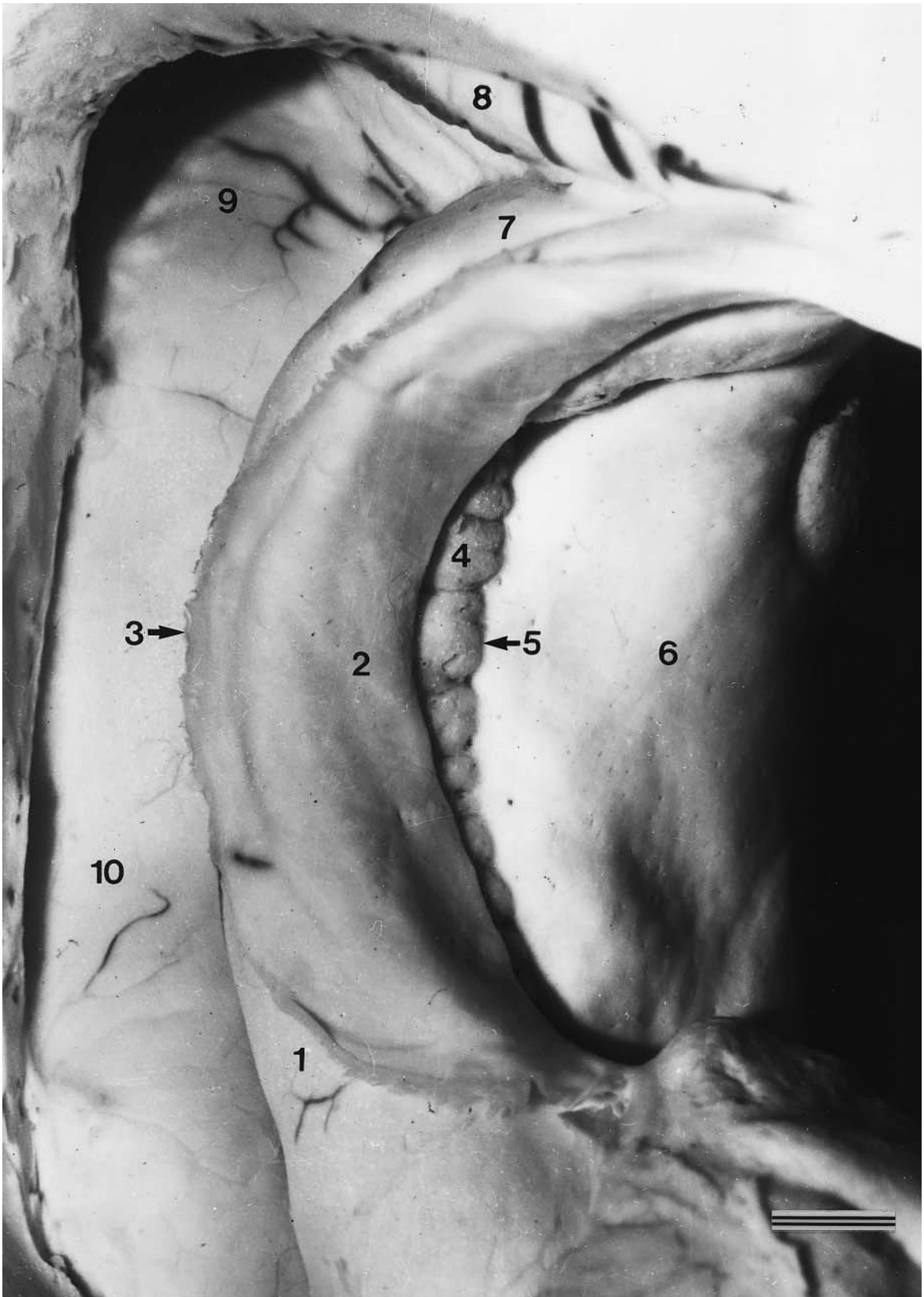
8
9
7
4
3
5
2
6
10
1

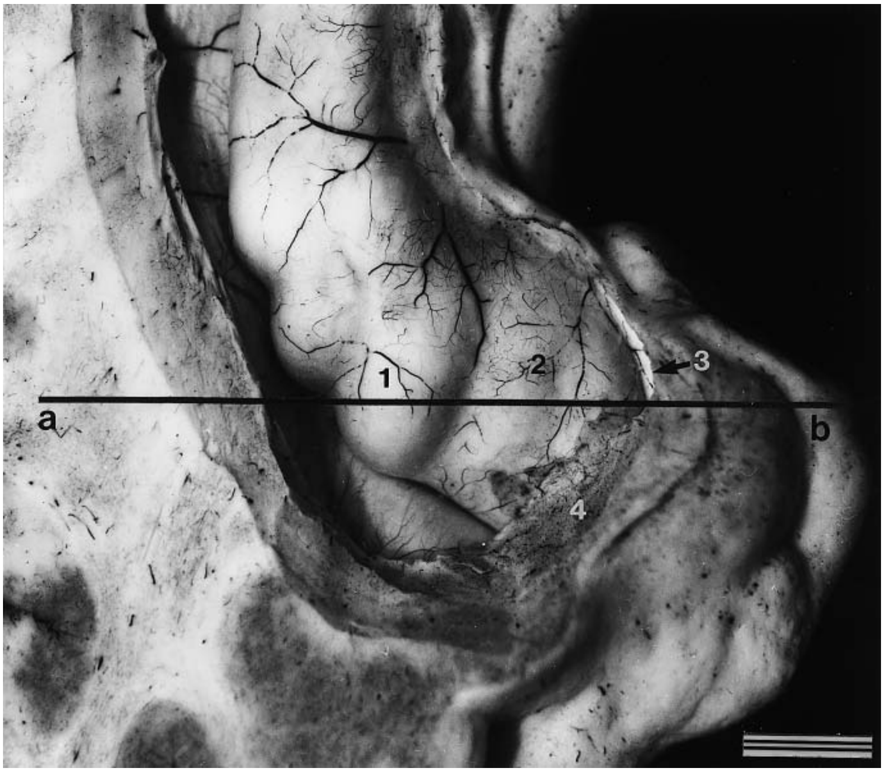

Fig. 24. Intraventricular aspect of the hippocampal head (seen from the direction of arrow A in Fig. 26). **a–b**, plane of the section in Fig. 26. **Bar**, 6.6 mm
1, **2**, digitationes hippocampi (internal digitations); **3**, vertical digitation; **4**, cut section of the adhesion between digitationes hippocampi and amygdala through the ventricular cavity

Fig. 25. Inferior aspect of the hippocampal head (seen from the direction of arrow B in Fig. 26). The parahippocampal gyrus has been removed. **a–b**, plane of section in Fig. 26. **Arrows** indicate the superficial hippocampal sulcus. **Bar**, 5 mm
1, band of Giacomini; **2**, margo denticulatus; **3**, insertion of the fimbria on the uncal apex; **4**, inferior surface of the uncal apex covered with alveus (hippocampus inversus); **5**, prelimbic sulcus; **6**, **7**, external digitations; **8**, **9**, sulci between the external digitations

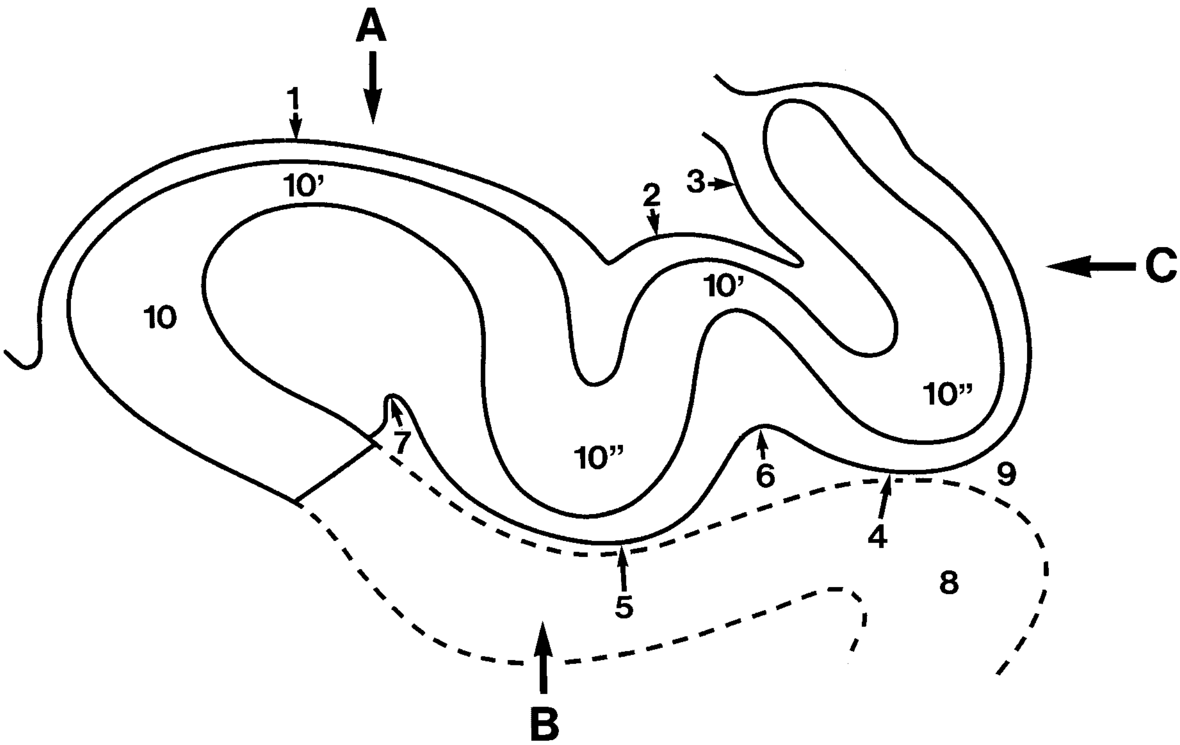

Fig. 26. Transverse section of the hippocampal head
A, intraventricular aspect of hippocampal head; **B**, inferior aspect of the hippocampal head; **C**, medial aspect of uncus (see Fig. 28). **1**, **2**, internal digitations (digitationes hippocampi); **3**, vertical digitation; **4**, **5**, external digitations; **6**, **7**, sulci between the external digitations; **8**, the parahippocampal gyrus has been removed; **9**, uncal sulcus; **10**, cornu Ammonis, thin in the internal digitations (**10′**), but thick in the external digitations (**10″**)

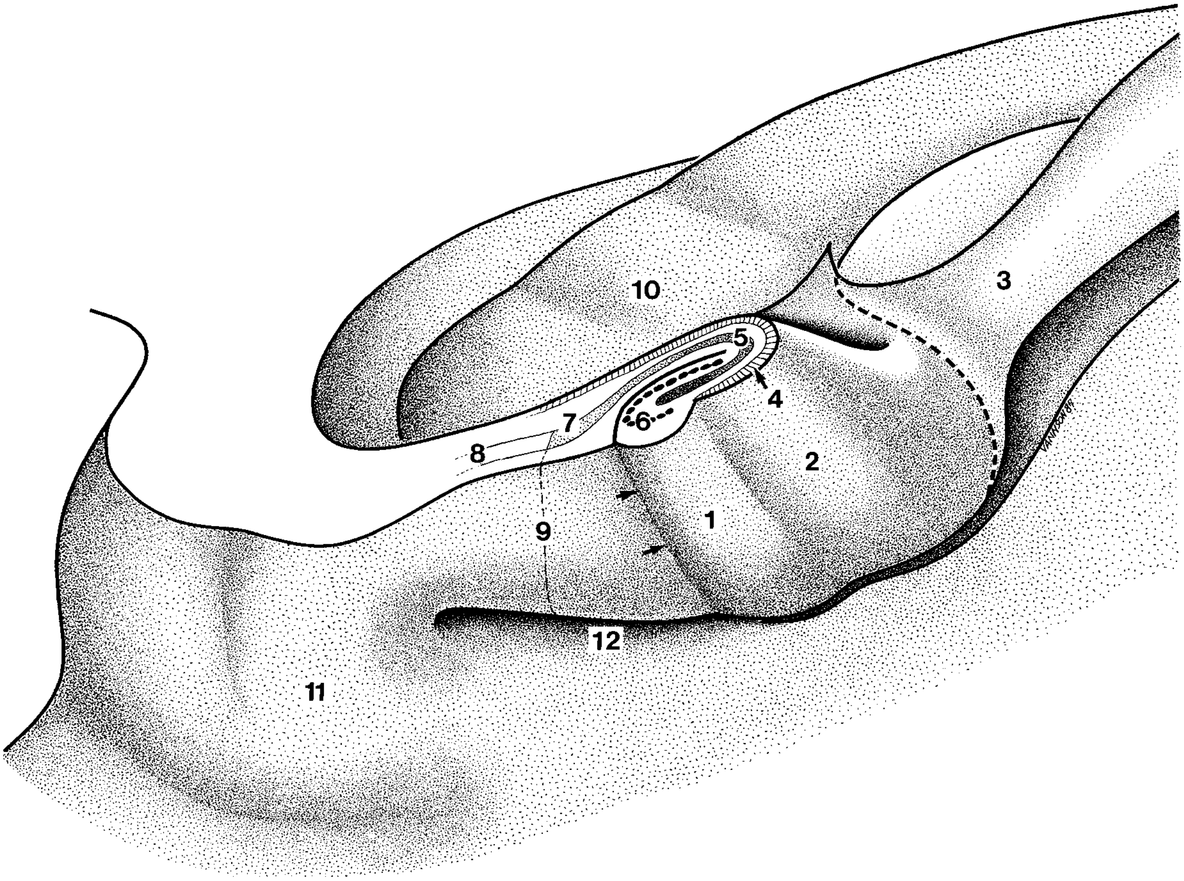

Fig. 27. Possible structure of the posterior uncal segment **1**, band of Giacomini (**arrows** along the superficial hippocampal sulcus); **2**, uncal apex; **3**, fimbria. Structure of posterior uncal segment: **4**, alveus covering the uncal apex (hippocampus inversus); **5**, CA3 field; **6**, gyrus dentatus; **7**, CA1 field; **8**, subiculum; **9**, uncinate gyrus; **10**, intraventricular aspect of hippocampal head after opening of the ventricular cavity; **11**, ambient gyrus; **12**, uncal sulcus

Fig. 28. Medial aspect of the uncus (see arrow C in Fig. 26). **Bar**, 4 mm
Posterior segment of medial uncal surface belonging to the hippocampus: **1**, band of Giacomini (**arrows** along the superficial hippocampal sulcus); **2**, medial surface of uncal apex; **3**, fimbria; **4**, choroid fissure (the choroid plexuses have been removed); **5**, uncinate gyrus; **6**, uncal sulcus. Anterior segment of medial uncal surface belonging to the piriform lobe: **7**, endorhinal sulcus; **8**, semilunar gyrus; **9**, semianular sulcus; **10**, ambient gyrus; **11**, uncal notch produced by the free edge of the tentorium cerebelli; **12**, entorhinal area and verrucae gyri hippocampi; **13**, rhinal sulcus; **14**, parahippocampal gyrus

Fig. 29. Superior aspect of the uncus. **Arrows** indicate the superficial hippocampal sulcus. **Bar:** 3.8 mm
1, choroid fissure (the choroid plexuses have been removed); **2**, taenia fimbriae; **3**, fimbria; **4**, stria terminalis; **5**, optic tract; **6**, taenia of stria terminalis; **7**, velum terminale (Aeby) or inferior choroidal point; **8**, endorhinal sulcus; **9**, semilunar gyrus; **10**, semianular sulcus; **11**, uncinate gyrus; **12**, ambient gyrus; **13**, uncal sulcus; **14**, band of Giacomini; **15**, uncal apex covered with alveus (hippocampus inversus); **16**, parahippocampal gyrus

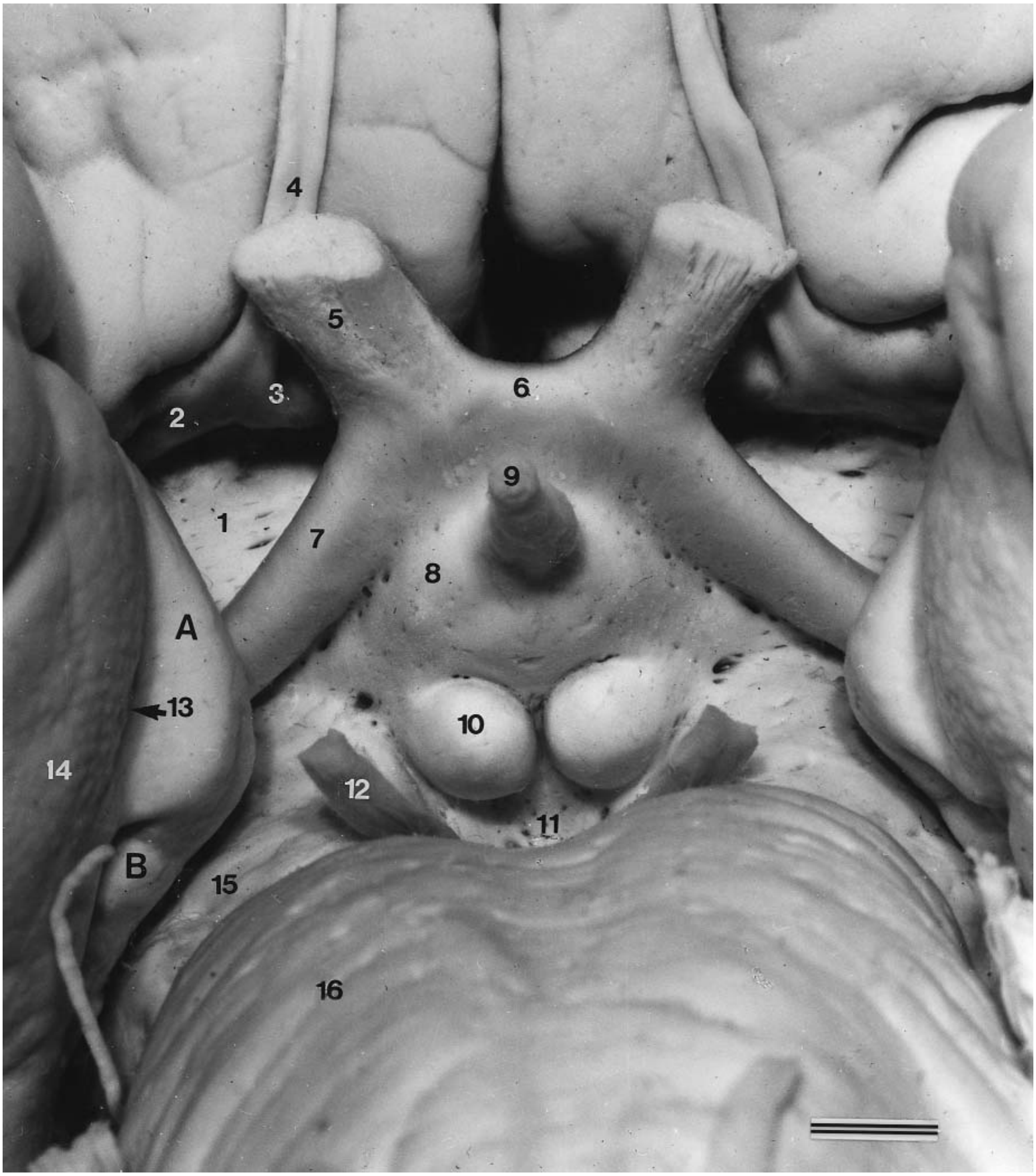

Fig. 30. Inferior cerebral aspect to show relation of the uncus to adjacent structures. Note the small protrusions of the entorhinal area (**14**), the verrucae gyri hippocampi, due to neuronal clusters in the entorhinal cortex (see Fig. 15). **Bar**, 4.8 mm **A**, Relation of the anterior segment of the uncus: **1**, anterior perforated substance; **2**, lateral olfactory stria; **3**, medial olfactory stria; **4**, olfactory tract; **5**, optic nerve; **6**, optic chiasma; **7**, optic tract; **8**, tuber; **9**, cut surface of the hypophysial stalk; **10**, mamillary body; **11**, interpeduncular fossa; **12**, oculomotor nerve; **13**, uncal notch produced by the free edge of the tentorium cerebelli; **14**, entorhinal area. **B**, Relation of the posterior segment of the uncus: **15**, crus cerebri; **16**, pons

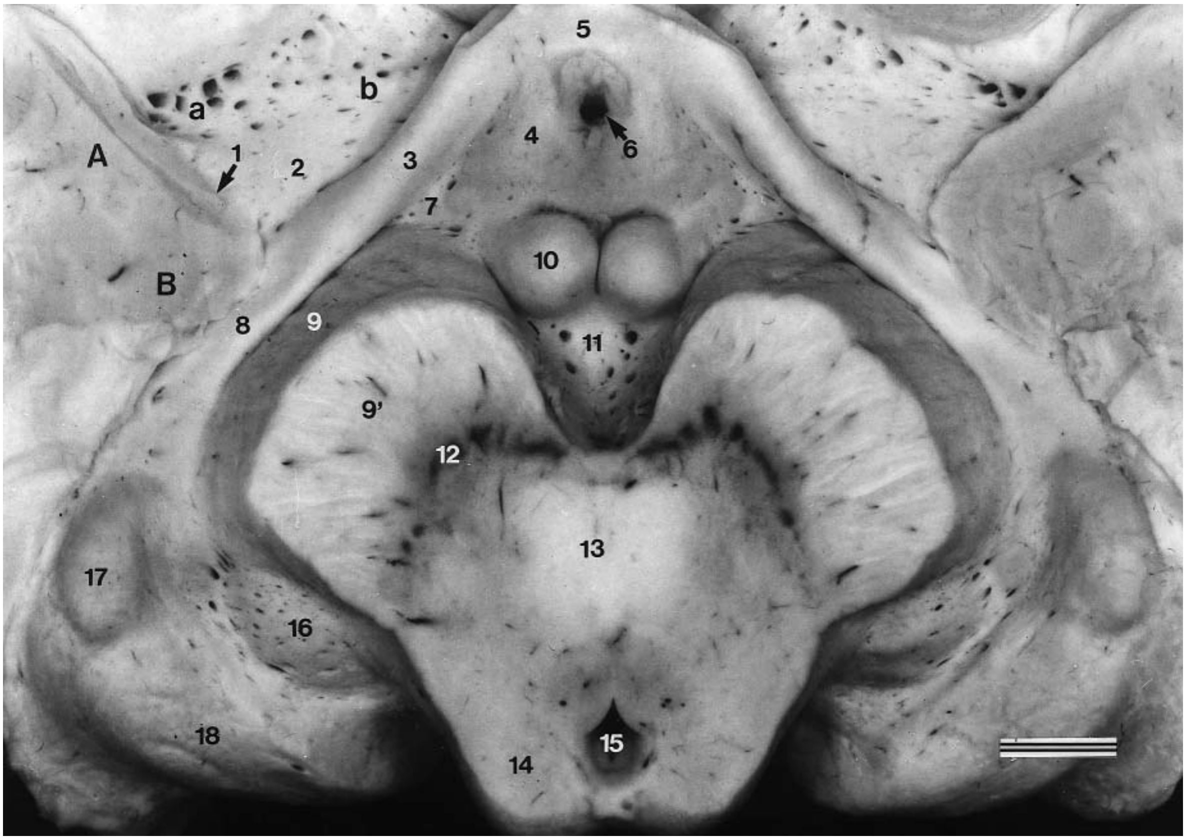

Fig. 31. Inferior cerebral aspect to show relation of the uncus to basal structures. The uncus and the mesencephalon have been partly cut off. **Bar**, 5.5 mm
A, Relation of the anterior segment of the uncus: **1**, endorhinal sulcus; **2**, anterior perforated substance (**a**, penetration point of lateral lenticulostriate arteries; **b**, penetration point of medial lenticulostriate arteries); **3**, optic tract; **4**, lateral tuber; **5**, optic chiasma; **6**, infundibulum of the third ventricle (opened); **7**, lateral perforated substance. **B**, Relation to the posterior segment of the uncus: **8**, optic tract; **9**, crus cerebri; **9′**, cut surface of the crus cerebri; **10**, mamillary body; **11**, posterior perforated substance and penetration point of thalamoperforating arteries; **12**, substantia nigra; **13**, brachium conjunctivum; **14**, inferior colliculus; **15**, cerebral aqueduct; **16**, medial geniculate body and penetration point of thalamogeniculate arteries; **17**, lateral geniculate body; **18**, pulvinar

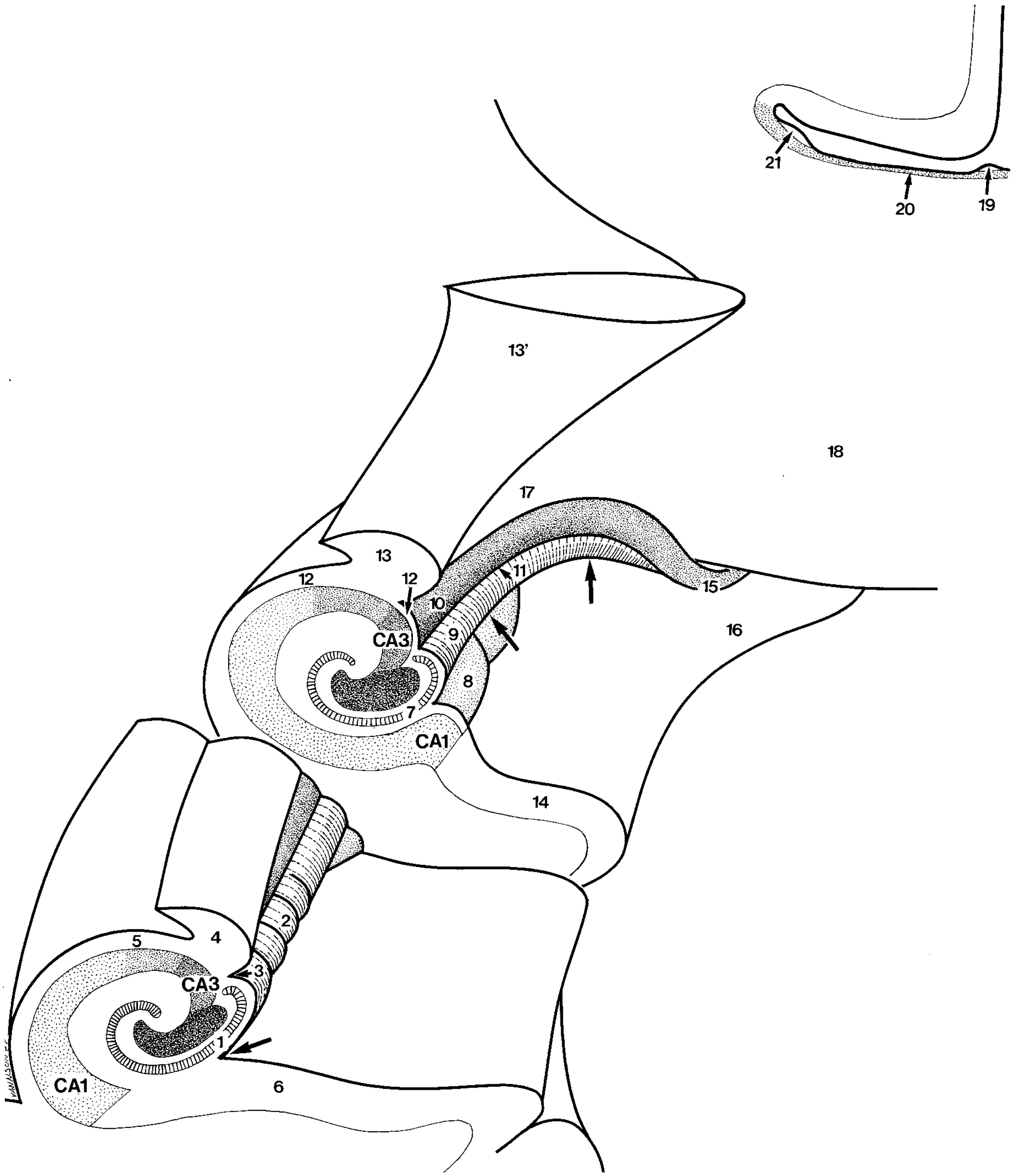

Fig. 32. A Drawing and **B** dissection showing the structure of the three segments of the extraventricular part of hippocampal tail (the fimbria is partly removed). **Arrows** indicate the superficial hippocampal sulcus. Note the whitish appearance of the hippocampus inversus in B (**10**). **Bar**, 4.4 mm
Initial segment of the tail: **CA1**, **CA3**, fields of cornu Ammonis; **1**, gyrus dentatus; **2**, last dentes of margo denticulatus; **3**, fimbriodentate sulcus; **4**, fimbria; **5**, alveus; **6**, subiculum. Middle segment of the tail: **7**, gyrus dentatus; **8**, gyri of Andreas Retzius composed of CA1; **9**, the fasciola cinerea, an extension of the margo denticulatus; **10**, gyrus fasciolaris composed of CA3 covered with alveus (hippocampus inversus); **11**, sulcus dentatofasciolaris; **12**, alveus; **13**, fimbria; **13′**, crus of fornix; **14**, subiculum. Terminal segment of the tail: **15**, the subsplenial gyrus, an extension of the gyrus fasciolaris; **16**, isthmus; **17**, subcallosal trigone; **18**, splenium; **19**, medial longitudinal stria; **20**, indusium griseum; **21**, lateral longitudinal stria

Fig. 32 B

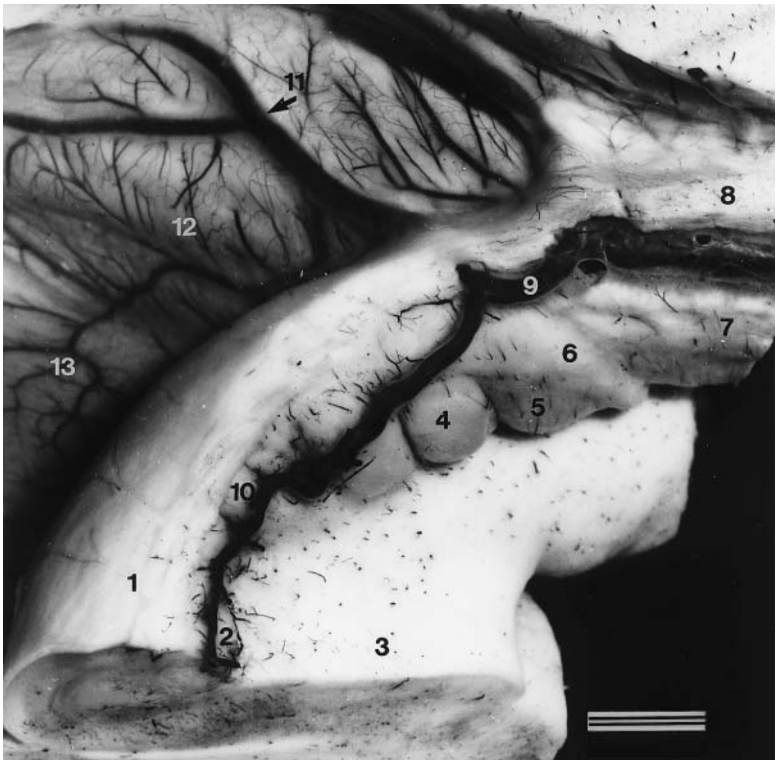

Fig. 33. Hippocampal tail. **Bar,** 3.7 mm
1, ventricular cavity opened and fimbria partly removed; **2**, margo denticulatus; **3**, subiculum; **4**, gyri of Andreas Retzius; **5**, fasciola cinerea; **6**, gyrus fasciolaris; **7**, splenium of the corpus callosum; **8**, corpus callosum; **9**, trunk of the medial atrial vein situated in the subcallosal trigone; **10**, venous arch of the fimbriodentate sulcus draining into the medial atrial vein; **11**, subependymal atrial veins passing through the crus of fornix to reach the trunk of the medial atrial vein; **12**, calcar avis; **13**, collateral trigone

Fig. 34. Posterior aspect of a cerebral section. **Bar,** 4,6 mm
1, corpus callosum; **2**, splenium; **3**, crus of fornix; **4**, subcallosal trigone; **5**, gyrus fasciolaris; **6**, fasciola cinerea; **7**, the subsplenial gyrus, an extension of the gyrus fasciolaris; **8**, isthmus; **9**, parahippocampal gyrus

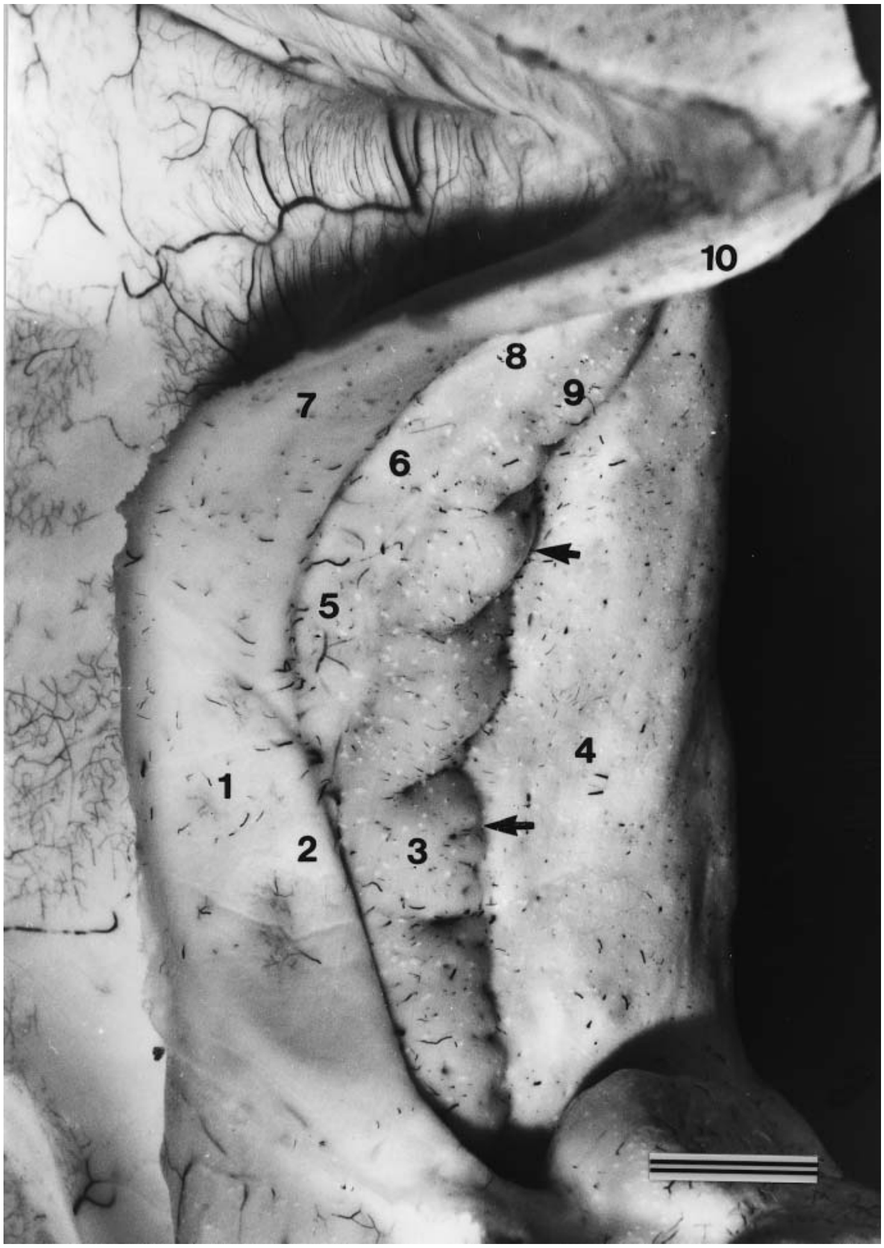

Fig. 35. Extraventricular part of hippocampal body and tail. In this case, the fimbriodentate sulcus is large and hence CA3, covered with alveus, is visible, forming the hippocampus inversus (**6**). **Arrows** indicate the superficial hippocampal sulcus. **Bar**, 4.6 mm

1, hippocampal body; **2**, fimbria; **3**, margo denticulatus; **4**, parahippocampal gyrus; **5**, fimbriodentate sulcus; **6**, hippocampus inversus; **7**, hippocampal tail; **8**, gyrus fasciolaris; **9**, fasciola cinerea; **10**, crus of fornix

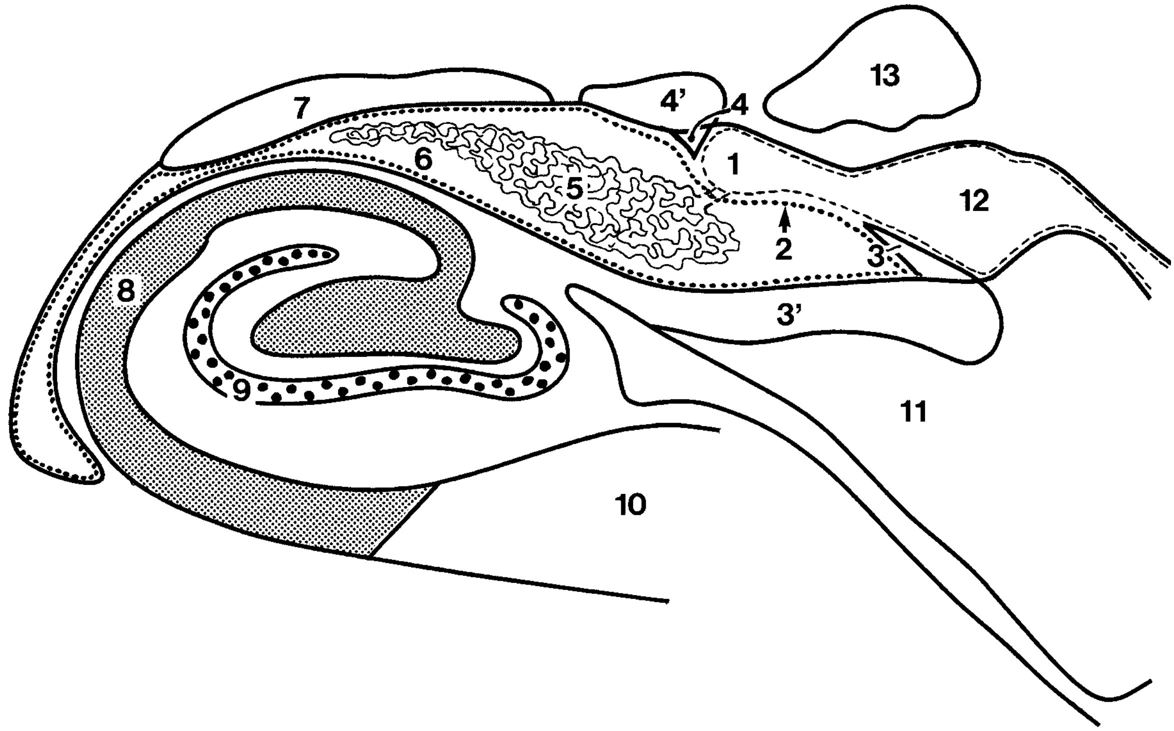

Fig 36. A, B Coronal section of hippocampus and temporal horn of lateral ventricle. **A** Explanatory diagram. **B** Intravascular India ink injection. The tela choroidea (**2**) is composed of an ependymal layer (**large dots**) and a pial layer (**small dots**), as described on p. 40. **Bar**, 1.4 mm

1, choroid fissure; **2**, tela choroidea; **3**, taenia of fimbria; **3′**, fimbria; **4**, taenia of stria terminalis; **4′**, stria terminalis; **5**, choroid plexuses; **6**, ventricular cavity of the temporal (inferior) horn; **7**, caudate nucleus; **8**, cornu Ammonis; **9**, gyrus dentatus; **10**, subiculum; **11**, uncal apex (see Fig. 105); **12**, lateral part of the transverse fissure (wing of ambient cistern); **13**, lateral geniculate body

Fig. 36 B

Figures 37–42 are dissections at descending levels in the diencephalon and brain stem showing the relation of these median structures to the hippocampus.


13
12
14
15
2
7
1
3
6
4
10
9
5
5'
11'
11
8

Fig. 38. Horizontal section of thalamus and third ventricle. The choroid plexuses of the temporal horn hide the hippocampal body and tail, but the head (digitationes hippocampi) is free of choroid plexuses and is visible. **Bar**, 11 mm
1, thalamus, **2**, third ventricle; **3**, choroid plexuses of temporal horn; **4**, head (digitationes hippocampi); **5**, collateral eminence; **6**, olfactory tract; **7**, lesser wing of sphenoid; **8**, temporal pole; **9**, optic nerve; **10**, lamina terminalis; **11**, anterior commissure, median part; **11′**, anterior commissure, lateral part; **12**, column of fornix; **13**, posterior commissure; **14**, pineal gland; **15**, superior colliculus

◁
Fig. 37. The superior cerebral structures (frontal and parietal lobes, corpus callosum, and fornix) have been removed to show the superior aspect of the thalamus and caudate nucleus. The choroid plexuses of the prosencephalon are seen along their whole length in **3–6. Arrow**, interventricular foramen. **Bar**, 11.8 mm

1, thalamus; **2**, caudate nucleus; **3**, roof of the third ventricle; **4**, body of the lateral ventricle; **5**, atrium; **5′**, choroid glomus; **6**, temporal or ventricular horn; **7**, hippocampal head (free of choroid plexuses); **8**, occipital horn; **9**, superior colliculus; **10**, pineal gland; **11**, anterior calcarine sulcus; **11′**, calcar avis; **12**, olfactory tract; **13**, olfactory bulb; **14**, lesser wing of sphenoid; **15**, temporal pole

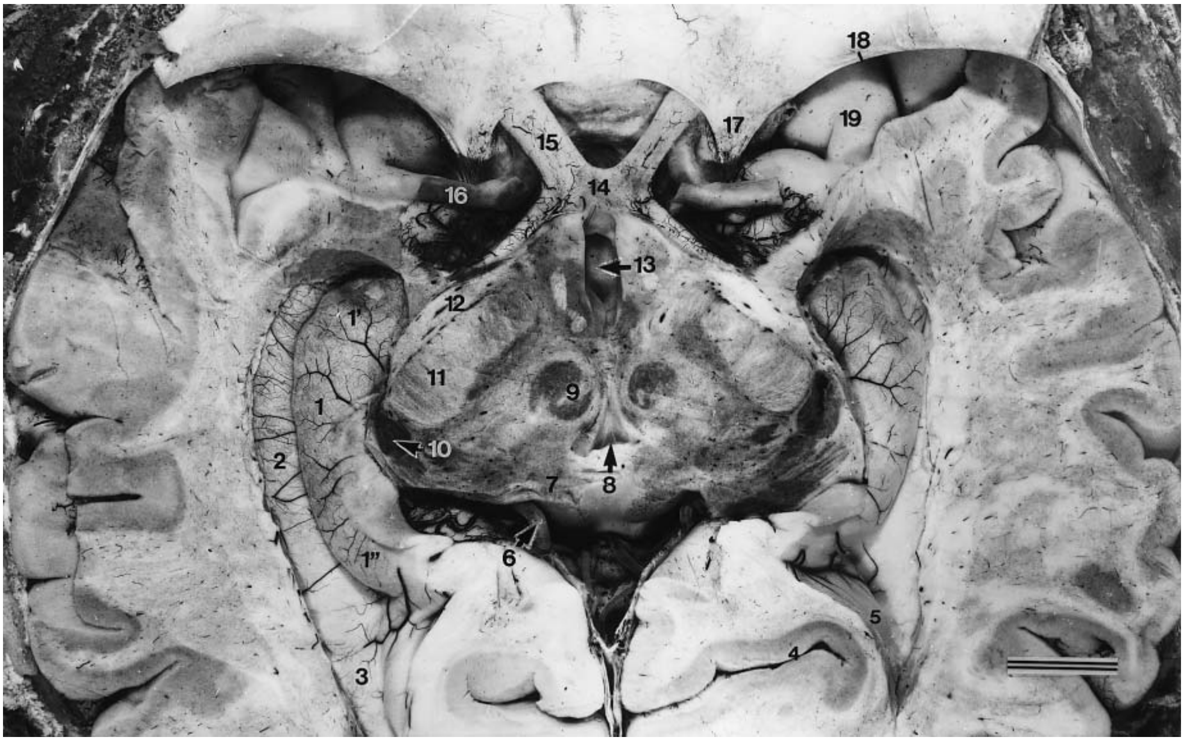

Fig. 39. Horizontal section at the junction of diencephalon and mesencephalon. The temporal horns have been opened and the choroid plexuses removed. **Bar**, 13.8 mm
1, hippocampal body; **1′**, hippocampal head; **1″**, hippocampal tail; **2**, collateral eminence; **3**, occipital horn; **4**, anterior calcarine sulcus; **5**, calcar avis; **6**, P3 segment of the posterior cerebral artery; **7**, superior colliculus; **8**, cerebral aqueduct; **9**, red nucleus; **10**, lateral geniculate body; **11**, crus cerebri; **12**, optic tract; **13**, floor of the third ventricle; **14**, optic chiasma; **15**, optic nerve; **16**, middle cerebral artery; **17**, anterior clinoid process; **18**, lesser wing of sphenoid; **19**, temporal pole

Fig. 40. Horizontal section of upper mesencephalon. The temporal horns have been opened and the choroid plexuses removed. Note the radial disposition of subependymal veins. The right and left hippocampi encircle the mesencephalon. The posterior cerebral artery may be divided into three segments (P1, P2 and P3): P1 segment in the interpeduncular fossa (**a**); the P2 segment may be subdivided into two parts, the first (**b**) in close relationship to the uncus in the crural cistern and the second (**c**) lining the margin of the parahippocampal gyrus in the ambient cistern; beginning of P3 segment (**d**) reaching the occipital lobe through a narrow cleft between posterior part of parahippocampal gyrus and free edge of tentorium cerebelli. **Bar,** 8.7 mm

1, hippocampal body; **1′**, hippocampal head; **1″**, hippocampal tail; **2**, fimbria; **3**, crus of fornix; **4**, collateral eminence; **5**, superior colliculus; **6**, medial geniculate body; **7**, cerebral aqueduct; **8**, oculomotor nucleus; **9**, red nucleus; **10**, substantia nigra; **11**, crus cerebri; **12**, posterior segment of uncus in close relationship with the crus cerebri; **13**, semilunar gyrus; **14**, ambient gyrus; **15**, anterior choroidal artery in the semianular sulcus; **16**, oculomotor nerve; **17**, pons; **18**, basilar artery; **19**, posterior communicating artery; **20**, internal carotid artery; **21**, hypophysial stalk; **22**, optic nerve; **23**, anterior clinoid process; **24**, lesser wing of sphenoid; **25**, temporal pole; **26**, parahippocampal gyrus; **27**, tentorium cerebelli

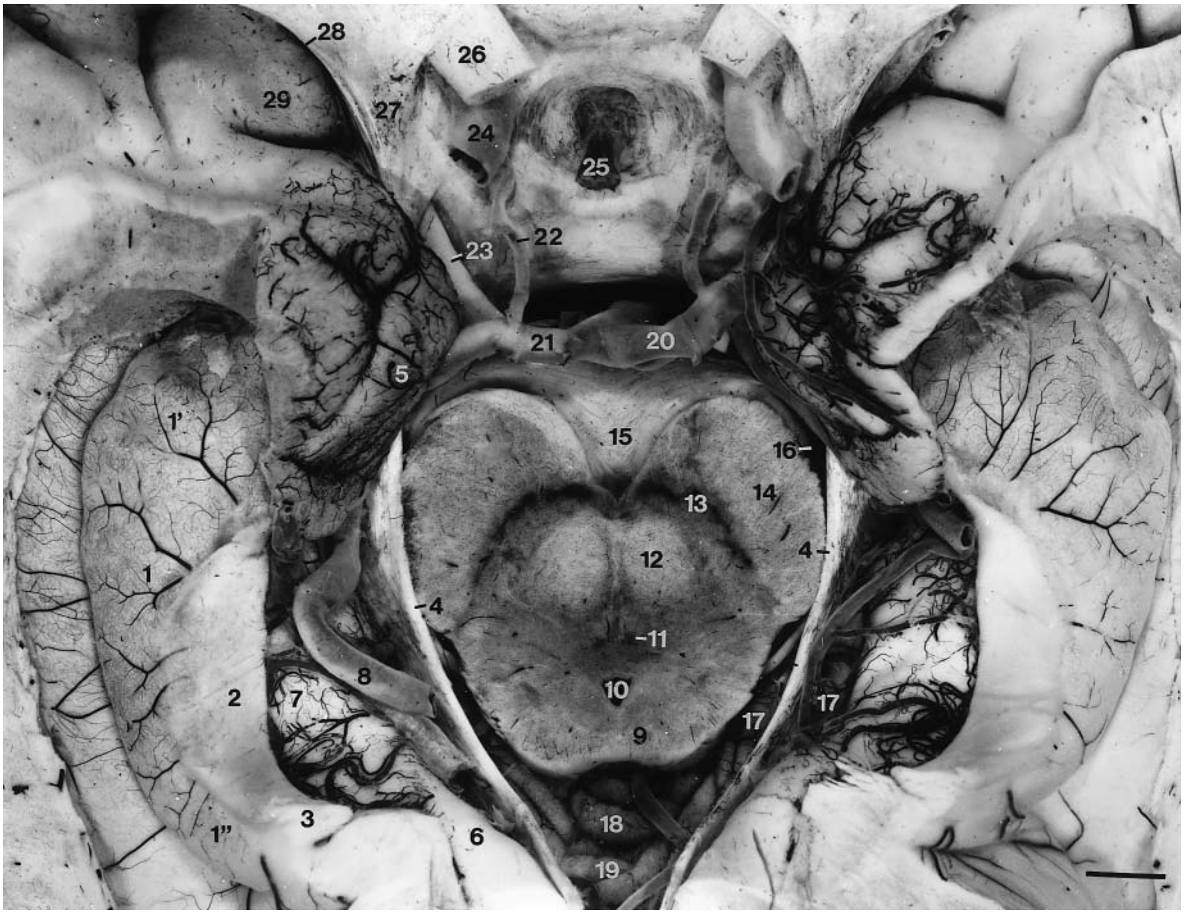

Fig. 41. Horizontal section of lower mesencephalon. This preparation shows the cisterns around the mesencephalon. The tentorium cerebelli (**4**) is in contact with the anterior (uncus, ambient gyrus, **5**) and posterior parts (isthmus, **6**) of the parahippocampal gyrus, whose middle part (subiculum, **7**) is far from the free edge. **Bar.** 10.5 mm
1, hippocampal body; **1′**, hippocampal head; **1″**, hippocampal tail; **2**, fimbria; **3**, crus of fornix; **4**, free edge and opening of the tentorium cerebelli; **5**, uncus, ambient gyrus; **6**, isthmus; **7**, subiculum; **8**, P2 segment of the posterior cerebral artery, following a curved path on the superior surface of the subiculum; **9**, inferior colliculus; **10**, cerebral aqueduct; **11**, trochlear nucleus; **12**, brachium conjunctivum (superior cerebellar peduncle); **13**, substantia nigra; **14**, crus cerebri; **15**, interpeduncular (intercrural) cistern; **16**, crural cistern; **17**, ambient cistern (over and below the free edge); **18**, quadrigeminal cistern; **19**, superior vermis of cerebellum; **20**, basilar artery; **21**, P1 segment of the posterior cerebral artery; **22**, posterior communicating artery; **23**, oculomotor nerve; **24**, internal carotid artery; **25**, hypophysial stalk; **26**, optic nerve; **27**, anterior clinoid process; **28**, lesser wing of sphenoid; **29**, temporal pole

▷
Fig. 42. Horizontal section at the junction of mesencephalon with pons. **Right**, the temporal lobe has been removed to show the tentorium cerebelli and the free edge (**arrows**) of the tentorial opening. **Left**, the parahippocampal gyrus and the hippocampus have been left intact. **Bar**, 9.2 mm
1, junction between pons and mesencephalon; **2**, tentorium cerebelli; **3**, anterior clinoid process; **4**, optic nerve; **5**, hypophysial stalk; **6**, internal carotid artery; **7**, posterior communicating artery; **8**, oculomotor nerve; **9**, superior vermis; **10**, hippocampal body; **10′**, hippocampal head; **10″**, hippocampal tail; **11**, calcar avis; **12**, collateral eminence; **13**, uncal recess of the temporal horn; **14**, cut surface of amygdala; **15**, margo denticulatus; **16**, the subiculum (parahippocampal gyrus) forming the floor of the transverse fissure; **17**, posterior cerebral artery in the ambient cistern (P_2 segment) **arrowheads** show its branches to the hippocampus (see p. 74); **18**, uncus

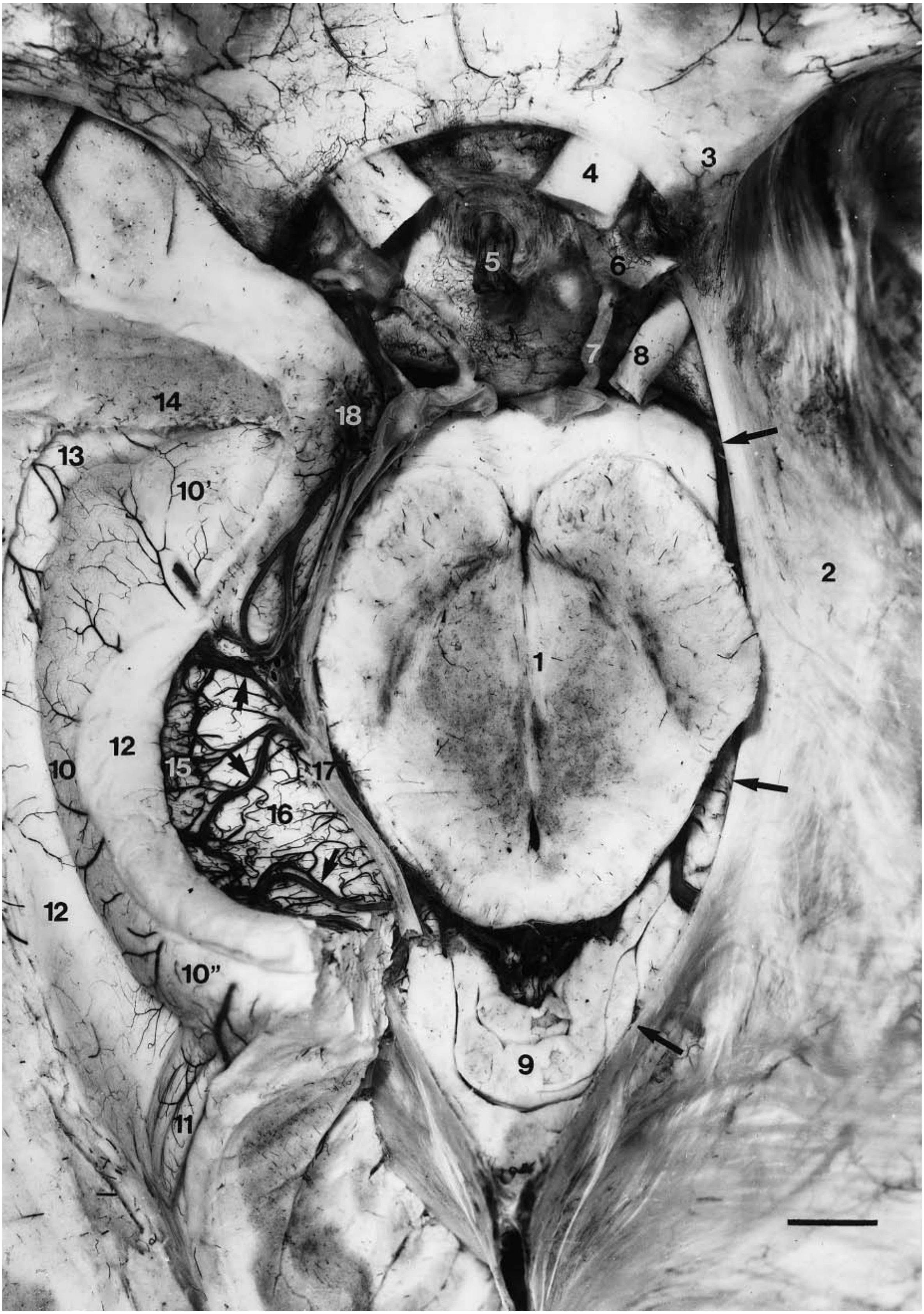
3
4
5
6
7
8
18
14
13
10'
2
1
12
10
15
17
16
12
10"
9
11

Fig. 43. Sagittal section (cerebellum and brain stem removed). The lower part of the medial surface of the uncus is hidden by the oculomotor nerve (**2**), the posterior cerebral artery (**3**), and the basal vein (**4**). **Bar**, 7 mm

1, medial surface of the uncus; **2**, oculomotor nerve; **3**, posterior cerebral artery (P2 segment); **4**, basal vein; **5**, inferior ventricular vein (vein of temporal horn); **6**, free edge of tentorium cerebelli; **7**, trochlear nerve; **8**, ambient gyrus; **9**, trigeminal nerve; **10**, posterior cranial fossa; **11**, internal acoustic meatus and vestibulocochlear nerve

Figures 43–45 show sagittal sections in which cerebellum and brain stem have been removed. These sections show, in succession, the relationships of the uncus and parahippocampal gyrus with the basal vein and posterior cerebral artery (Fig. 43), the posterior cerebral artery only (Fig. 44), and the free edge of the tentorium cerebelli (Fig. 45).

Fig. 44. Sagittal section (cerebellum and brain stem removed). The anterior choroidal artery (**1**) is situated in the semianular sulcus, which separates the semilunar gyrus (**2**) and the ambient gyrus **3**. Note that P2 segment of the posterior cerebral artery (**8**) is divided into two parts, the first (**8′**) along the uncus in the crural cistern and the second (**8″**) along the parahippocampal gyrus in the ambient cistern. **Bar,** 6.5 mm

1, anterior choroidal artery; **2**, semilunar gyrus; **3**, ambient gyrus; **4**, uncinate gyrus; **5**, uncal apex; **6**, uncal branch of the anterior choroidal artery crossing the medial surface of the uncus (see Figs. 58, 59); **7**, fimbria; **8**, P2 segment of the posterior cerebral artery; **9**, parahippocampal gyrus; **10**, free edge of tentorium cerebelli; **11**, trochlear nerve; **12**, oculomotor nerve; **13**, posterior communicating artery; **14**, middle cerebral artery; **15**, optic nerve; **16**, anterior cerebral artery; **17**, hypophysis

Fig. 45. Sagittal section (cerebellum and brain stem removed). **Bar**, 7 mm
1, medial surface of uncus; **2**, semilunar gyrus; **2′**, semianular sulcus; **3**, uncinate gyrus; **4**, uncal apex; **5**, ambient gyrus overlying the free edge of the tentorium cerebelli (**arrow a**); **6**, middle part of the parahippocampal gyrus far from the free edg (**arrow b**); **7**, posterior part of the parahippocampal gyrus (isthmus) in close contact with the free edge (**arrow c**); **8**, posterior cranial fossa; **9**, corpus callosum; **9′**, splenium; **10**, margo denticulatus; **11**, fimbria

Vascularization

Two steps have characterized the study of the hippocampal vessels during the last few decades. In a first step, the special aspect of blood vessels was used to explain the particular vulnerability of the hippocampus to anoxia (Uchimura 1928; Scharrer 1940). In a second step, the knowledge of the vascular anatomy paralleled new progress in surgery of the hippocampus (Wieser and Yasargil 1982; Olivier 1996).

The superficial (leptomeningeal) vessels and the intrahippocampal (deep) vessels will be successively studied (Figs. 46 – 79).

5.1 Superficial (Leptomeningeal) Blood Vessels

5.1.1 Superficial Hippocampal Arteries

General Remarks

The hippocampal arteries arise mainly from the posterior cerebral artery and to a lesser degree from the anterior choroidal artery (Stephens and Stilwell 1969).

The *posterior cerebral artery* can be divided, during its perimesencephalic path, into two segments: P1 segment, which is located in the intercrural (or interpeduncular) cistern, and P2 segment, which is situated in the crural (along the uncus) and ambient cisterns (Fig. 40). In the ambient cistern, the posterior cerebral artery is usually situated along the margin of the parahippocampal gyrus (Figs. 46, 48), but may cover the subiculum by occasional loops (Fig. 50) in the wing of the ambient cistern (laterally closed by the choroid fissure). In its P2 segment, the posterior cerebral artery gives rise to numerous important branches, which render the surgical approach to the medial temporal lobe particularly difficult (Gaffan and Lim 1991). These branches are the inferior temporal arteries (Fig. 60), which are usually divided into the anterior, middle, and posterior inferior temporal arteries, the posterolateral choroidal artery (Fig. 53), and the splenial artery (Figs. 47 – 49) (Stephens and Stilwell 1969; Margolis et al. 1974; Lecaque et al. 1978; Milisavljevic et al. 1986).

The anterior choroidal artery, a branch of the internal carotid artery, reaches the choroid fissure and the choroid plexuses of the temporal (or inferior) horn. During its course in the semianular sulcus of the uncus (Figs. 44, 58, 59), the anterior choroidal artery give rise to an uncal branch, which crosses by a descending path the medial surface of the uncus and disappears into the uncal sulcus (Fig. 56; Carpenter et al. 1954; Stephens and Stillwell 1969; Goldberg 1974; Rhoton et al. 1979; Fujii et al. 1980; Hussein et al. 1988; Morandi et al. 1996).

Origin (Figs. 46 – 52, 56)

General Arrangement. Three arteries (or group of arteries) usually vascularize the hippocampus: the anterior, middle, and posterior hippocampal arteries. The anterior and middle arteries arise either from the trunk of the posterior cerebral artery or from its inferior temporal branches, whereas the posterior hippocampal artery frequently arises from the splenial artery, a branch of the posterior cerebral artery.

Variations. Numerous variations have been described concerning the origin of the hippocampal arteries (this is true of the whole superficial arterial network of the brain). As the number of hemispheres observed in this study concerning the superficial vessels was insufficient ($n = 16$), the reader is referred to the work of Lang (1981) and Marinkovic et al. (1992) and to the more recent, exhaustive studies carried out by Erdem et al. (1993). In these later studies, the origins of the hippocampal arteries were divided into five groups of decreasing frequency:

Group A. This is most frequent type (57%) and is characterized by mixed origins of the hippocampal arteries; it corresponds to the type of description presented here (Figs. 46, 50). Origins from the anterior and posterolateral choroidal arteries may be included in this group.

Group B. In this group, the hippocampal arteries mainly arise from all the inferior temporal arteries (27%).

Group C. In this group, the hippocampal arteries only arise from the anterior inferior temporal artery (10%).

Group D. The trunk of the posterior cerebral artery was the principal supply of the hippocampal arteries (3%) in this group. Uchimura's artery may belong to group D.

Group E. The anterior choroidal artery was the main supply to the hippocampus (3%) in this group.

Course and Branches. The hippocampal arteries can be divided into two groups according to their territories: the middle and posterior hippocampal arteries supply the hippocampal body and tail, whereas the anterior hippocampal artery vascularizes the hippocampal head and uncus.

Middle and Posterior Hippocampal Arteries (Figs. 46–52)

The middle (the largest) and the posterior hippocampal arteries have a straight or slighty curved path on the flat surface of the subiculum, supplying this structure by small and scattered branches. When they reach the hippocampus, the hippocampal arteries curve to follow a sinuous, longitudinal course parallel to the superficial hippocampal sulcus and the margo denticulatus (Muller and Shaw 1965; Sasaki et al. 1993). Along their *longitudinal terminal segment,* the hippocampal arteries give rise to numerous branches, which can be divided into large and small branches (their intrahippocampal path is described on p. 75). The large branches directly penetrate the hippocampus in the deep sulci between the dentes of the margodenticulatus (Figs. 51, 52). These dentes, which are only present in primates, have an unknown origin. It is possible that the penetration of the large arteries at a right angle, which produces depressions on the surface of the margo denticulatus, may contribute to the formation of the dentes. The small arteries penetrate the whole surface of the margo denticulatus. Some small, parallel arteries have a rectilinear course on the margo denticulatus and penetrate the hippocampus in the fimbriodentate sulcus (Figs. 46, 51). Because of their appearance, they may be called "straight arteries." It should be noted that, contrary to the observations made by Marinkovic et al. (1992), the straight arteries are not important in size or number and have a reduced intrahippocampal territory (see p. 76). Moreover, it appears that this aspect is not specific to the fimbriodentate sulcus, but may be found in other encephalic sulci, e.g., in the bottom of cerebellar sulci (Duvernoy et al. 1983).

The middle and posterior hippocampal arteries are richly anastomosed (Fig. 46). In some cases, anastomoses between their longitudinal terminal segments form a continuous arterial arcade along the superficial hippocampal sulcus. According to observations by Scharrer (1940), a continuous arcade and its branches arising at right angles in a rake-like appearance may explain the particular vulnerability of hippocampal tissue to anoxia due to a sudden fall in blood pressure. In fact, this continuous arcade, previously described by Heiman (1938), Nilges (1944), and Lindenberg (1957), is rarely found in humans (Muller and Shaw 1965).

Anterior Hippocampal Artery (Figs. 56, 57)

The anterior hippocampal artery contributes to the dense hippocampo-parahippocampal arterial complex (Fig. 61), together with ramifications of the anterior inferior temporal artery (Marinkovic et al. 1992). This complex, in relation to the uncal apex, is partly hidden by the voluminous trunks of the posterior cerebral artery and basal vein in a medial view. The anterior hippocampal artery usually arises from the anterior inferior temporal artery (Muller and Shaw 1965). It disappears into the uncal sulcus and often reappears on the surface of the piriform lobe, participating in the vascularization of the subjacent entorhinal area (Fig. 62). During its hidden course in the uncal sulcus, it gives rise to branches which mainly penetrate the longitudinal sulci between the external digitations and vascularize the hippocampal head (Figs. 57, 68). The uncal branch of the anterior choroidal artery (Figs. 56, 58, 59) is frequently anastomosed with the anterior hippocampal artery within the uncal sulcus (Fig. 57). The contribution of the anterior choroidal artery to the vascular supply of the hippocampal head is highly variable and may be preponderant in some cases (Gastaut and Lammers 1961).

5.1.2 Superficial Hippocampal Veins

The hippocampal veins are branches of the basal vein (Huang and Wolf 1974). The origin of the *basal vein* is situated on the anterior perforated substance. Its first ventral segment extends until it receives the inferior ventricular vein (vein of the temporal horn). During its course, the basal vein is in close contact with the medial surface of the uncus and hides the uncal sulcus together with the posterior cerebral artery (Fig. 43). Its second laterodorsal segment crosses the midbrain lateral surface to reach the vein of Galen (Duvernoy 1975). During its laterodorsal segment in the ambient cistern, the basal vein is situated just above the P2 segment of the posterior cerebral artery (Fig. 46B) and receives the venous drainage of the hippocampus.

The superficial hippocampal veins have a simpler, more typical aspect than the arteries. They form two longitudinal superficial venous arches covering the fimbriodentate and the superficial hippocampal sulci (as a general rule, the superficial cerebral veins often follow the sulci on the nervous tissue surface). On account of their position, these two arches may be called the venous arch of fimbriodentate sulcus and the venous arch of superficial hippocampal sulcus.

The *venous arch of the fimbriodentate sulcus* (Figs. 46, 47, 53) is often hidden by the fimbria (Fig. 48). This continuous arcade receives the subependymal intrahippocampal veins at a right angle, and these are visible on the intraventricular aspect of the hippocampus.

The *venous arch of the superficial hippocampal sulcus* (Figs. 46, 48, 53) is often discontinuous. It receives the deep or sulcal intrahippocampal veins (see p. 76) emerging either from the hippocampal sulcus or from the sulci between the dentes of the margo denticulatus. Theses two arches join together at their anterior and posterior extremities. The anterior extremity of these arches flows into the inferior ventricular vein (often called the vein of the temporal horn), and the posterior extremity reaches the medial atrial vein. Both the inferior ventricular and the medial atrial veins are tributaries of the basal vein: the inferior ventricular vein (vein of the temporal horn) reaches the basal vein near the uncal apex (Fig. 46), and the medial atrial vein crosses the subcallosal trigone to join the basal vein (Figs. 33, 46).

5.2 Intrahippocampal (Deep) Blood Vessels

In the following, the intrahippocampal arteries and veins and the hippocampal capillary network will be studied. Our description represents the results of observations of blocks several millimeters thick that were cleared using the Spalteholz technique (see p. 3). In these blocks, it is possible to follow arteries and veins along their whole course.

5.2.1 Intrahippocampal Arteries

As described on p. 74, the branches of the longitudinal terminal segment of superficial hippocampal arteries are divided into large and small arteries. According to their intrahippocampal aspect and situation, these two groups may be subdivided into large ventral, large dorsal, small ventral, and small dorsal intrahippocampal arteries. This description correlates well with the observations made by Marinkovic et al. (1992). The intrahippocampal arteries are characterized by their curved path following the rolling up of the cornu Ammonis and the gyrus dentatus.

Large Ventral Intrahippocampal Arteries (Fig. 63)
The large ventral intrahippocampal arteries penetrate the hippocampus between the dentes of the margo denticulatus. They cross the proximal part of the gyrus dentatus, briefly follow the vestigial hippocampal sulcus, and course in the stratum lacunosum and sometimes in the stratum pyramidale of CA1 (Altschul 1939; Hens and Van den Bergh 1977; Sasaki et al. 1993). The large ventral arteries vascularize CA1 (the *Sektorgefässe* of Uchimura 1928) and, by their terminal ramifications, CA2. Arterial branches arising from the large ventral arteries often have a long and oblique course through CA1. The collaterals of these branches often arise in a curiously recurrent aspect (Fig. 71). These long branches of the large ventral arteries, specific to CA1, vascularize the pyramidal neurons, whereas the short branches reach the molecular layer of the cornu Ammonis (Fig. 63).

Large Dorsal Intrahippocampal Arteries (Figs. 63, 65, 69)
The large dorsal intrahippocampal arteries have a shorter, curved route in comparison to the large ventral arteries. They penetrate between the dentes of the gyrus dentatus and are then situated inside CA4 along the gyrus dentatus. Their terminal segment reaches CA3, and sometimes CA2, via a sharp curve. Along their route, the large dorsal arteries also vascularize CA4 and the distal part of the gyrus dentatus. The branches to the gyrus dentatus have a long, typically rectilinear course. Fine ramifications arise at right angles from these branches and reach the molecular layer of the gyrus dentatus across its granular layer (Figs. 63, 73, 74). Some branches supplying the terminal curved part of the gyrus dentatus have a brush-like appearance (Figs. 63, 75).

Small Ventral Intrahippocampal Arteries (Fig. 63)
The small ventral intrahippocampal arteries penetrate the surface of the margo denticulatus. They vascularize the proximal part of the gyrus dentatus (Uchimura 1928) with the same rectilinear course as those previously described in its distal part.

Small Dorsal Intrahippocampal Arteries (Figs. 63, 66)
The small dorsal intrahippocampal arteries cross the surface of the margo denticulatus and reach the fimbriodentate sulcus. On account of their rectilinear and parallel superficial path (see p. 74), they are often referred to as "straight arteries." This denomination may thus be restricted to the small dorsal arteries (although, in the description by Marinkovic et al. (1992), all the intrahippocampal arteries were called straight arteries). The few, fine straight arteries have a small intrahippocampal territory limited to CA3 and the adjacent part of CA4.

Variations
The intrahippocampal territories of these four arterials groups are the subject of variations. For example, an artery belonging to the large ventral or the large dorsal (Fig. 66) group may have a territory extending to almost the whole hippocampal tissue visible on a section. In most cases, however (Fig. 63), CA1 is only vascularized by the large ventral arteries, whereas CA2 – CA4 and the gyrus dentatus have several supplies coming from different arterial groups (Uchimura 1928; Scharrer 1940). This specific arterial supply of CA1 and the long course of its arterial branches have been the support to the vascular theory explaining the selective vulnerability of CA1 to anoxia. However, the vascular theory has now been abandoned, as described on p. 32. Against this explanation it may be noted that the gyrus dentatus, like CA1, is vascularized by long, fine arteries, whereas it is generally considered as a sector resistant to anoxia.

5.2.2 Intrahippocampal Veins (Fig. 64)

The intrahippocampal veins have been poorly studied, probably due to technical difficulties (see p. 3). In the hippocampus, two types of veins may be distinguished: the sulcal and subependymal intrahippocampal veins.

Sulcal Intrahippocampal Veins (Figs. 64, 65)
The sulcal intrahippocampal veins have their whole course in the vestigial hippocampal sulcus and are thus situated between the strata molecularia of the cornu Ammonis and the gyrus dentatus. Originating from the distal part of CA1 and from the adjacent CA2 field, they follow a curved path and reach the venous arch of the superficial hippocampal sulcus. On their concave side, the sulcal veins receive fine branches from the stratum moleculare of the gyrus dentatus (Figs. 64, 76).Their convex side receives branches from the stratum moleculare of the cornu Ammonis and large venous branches draining CA1 and the adjacent subiculum (Fig. 64).

Subependymal Intrahippocampal Veins (Figs. 54, 55, 64)
The subependymal intrahippocampal veins have a long, arched path that can be observed in endoventricular views of the hippocampus (Wolf and Huang 1964; Lazorthes et al. 1976). They have a regular and radial aspect, and reach the venous arch of the fimbriodentate sulcus through the fimbria. The subependymal intrahippocampal veins drain the blood of the deep layers (Fig. 72) of CA2, CA1, and the adjacent subiculum. In addition to the sulcal and subependymal veins, small intrahippocampal veins may partially drain CA2, CA3, and CA4 directly into the vein of the fimbriodentate sulcus (Fig. 64).

5.2.3 Hippocampal Head

The above description of the intrahippocampal arteries and veins concerns the body and tail of the hippocampus. The hippocampal head is vascularized by arterial and venous axes situated within each digitation (Fig. 68). These vascular axes stem from the superficial network situated in the sulci between the external digitations observed in the uncal sulcus (Fig. 57).

5.2.4 Vascular Network

In the hippocampus, it is possible to recognize the layers of the cornu Ammonis and the gyrus dentatus according to their different vascular densities (Figs. 65 – 67, 69); in the cornu Ammonis, the strata pyramidale and oriens have a marked vascular density (Cobb 1929). Vessels in the stratum radiatum are arranged in parallel, like the apical dendrites of its pyramidal neurons. The vascular network of the stratum radiatum is generally poor and appears in sections as a light band whose end indicates the limit of the hippocampus and the beginning of the subiculum (Figs. 8, 65, 85B; Uchimura 1928). The stratum lacunosum is the least vascularized layer of the cornu Ammonis. Among the fields in the stratum pyramidale, the remarkable vascular density of CA2 is notable (Fig. 65), followed in intensity by CA3, whereas CA1 is poorly vascularized; however, the most intense vascular density in the cornu Ammonis is in the stratum moleculare (Figs. 65–67). In the gyrus dentatus, it is also the stratum moleculare that is the most densely vascularized (Figs. 66, 67, 69), whereas the stratum granulosum is almost devoid of capillaries (Figs. 10, 73). Thus the vascular networks of the strata molecularia of the cornu Ammonis and the gyrus dentatus are especially dense and separated by a clear lamina without capillaries, the vestigial hippocampal sulcus.

Numerous researchers have studied the differences in density of capillary networks in many regions of the grey matter. A relation generally exists between the density of neuronal somata and capillary networks, but many exceptions have been recorded. In the hippocampus, for example, the stratum granulosum, although extremely rich in neurons, is only poorly vascularized, while the strata molecularia of the cornu Ammonis and the gyrus dentatus, both poor in neurons, show the highest vascular density in the hippocampus. The intensity of capillary networks may thus be due more to the density of synapses than to the number of neuronal somata (Lorente de No 1928; Dunning and Wolff 1937; Wolff 1938; Craigie 1945; Duvernoy et al. 1981).

The intrahippocampal vascularization, like that of the isocortex, is of a network vascular type, composed of a continuous capillary network (a loop vascular type composed of independant vascular trees is found in some mammals, e.g., opossums; Scharrer 1944). Despite this continuous capillary network, the capillary anastomoses are inefficient to correct a local insufficiency in blood supply (Klosovski 1963).

In the hippocampus, as in the isocortex (Ravens 1974), large arterial, venous, or arteriovenous anastomoses have never been found. However, precapillary arterial and arteriovenous shunts may be present in the vascular network of the hippocampus resembling those described in the isocortex (Hasegawa et al. 1967; Kennady and Taplin 1967; Duvernoy 1999a; Duvernoy et al. 1981).

The presence of vascular units, each with a vein at the center and surrounded by an arterial ring, has been described in the isocortex (Wolff 1976; Bär 1980; Duvernoy et al. 1981). The folded aspect of the hippocampal allocortex makes this research difficult. However, some features suggest that such vascular units may exist; the succession of penetrations or emergences of the hippocampal arteries and veins between the dentes of the margo denticulatus (Figs. 51, 52; Nilges 1944; Lierse 1963), the position of the subependymal intrahippocampal veins at regular intervals, and the bush-like aspect of the hippocampal capillary network are particularly noteworthy (Figs. 54, 70).

The vascular network of the hippocampus does in fact have some features in common with that of the isocortex. For example, as in the isocortex (Pfeifer 1930; Saunders and Bell 1971; Duvernoy et al. 1981), each arterial branch is surrounded by a circular zone of nervous tissue devoid of capillaries (Fig. 71). The significance of this capillary-free space is unknown. However, it is possible that the nervous tissue in the capillary-free space may be supplied by the arterial branch itself, whose wall characteristics allow an exchange with the adjacent tissue (Cervos-Navarro and Rozas 1978).

As in the vascular isocortical network, arterial coilings and capillary deformations are often found in the hippocampus, especially in the pyramidal layer of CA2. These special features (visible in Figs. 77–79) have not yet been explained (Hassler 1967; Saunders and Bell 1971; Duvernoy et al. 1981).

However, the vascular hippocampal network differs in many points from that of the isocortex. For example, the long tangential course of arteries and veins (Figs. 63, 64) contrasts with the isocortical blood vessels, whose course is perpendicular to the surface with a palisade aspect. Curiously, the vascular organisation of the allocortical hippocampus is in many points similar to that of the cerebellar cortex (Spielmeyer 1930; Duvernoy et al. 1983).

This study of the hippocampal vessels completes previous research on the vascularization of the isocortex, cerebellar cortex, brain stem, and circumventricular organs, which together offers a general view of the vascular architecture of the brain (Duvernoy 1972, 1975, 1995a, 1999a,b; Duvernoy and Koritke 1964 1965; Duvernoy et al. 1969, 1971, 1972, 1981, 1983, 2000).

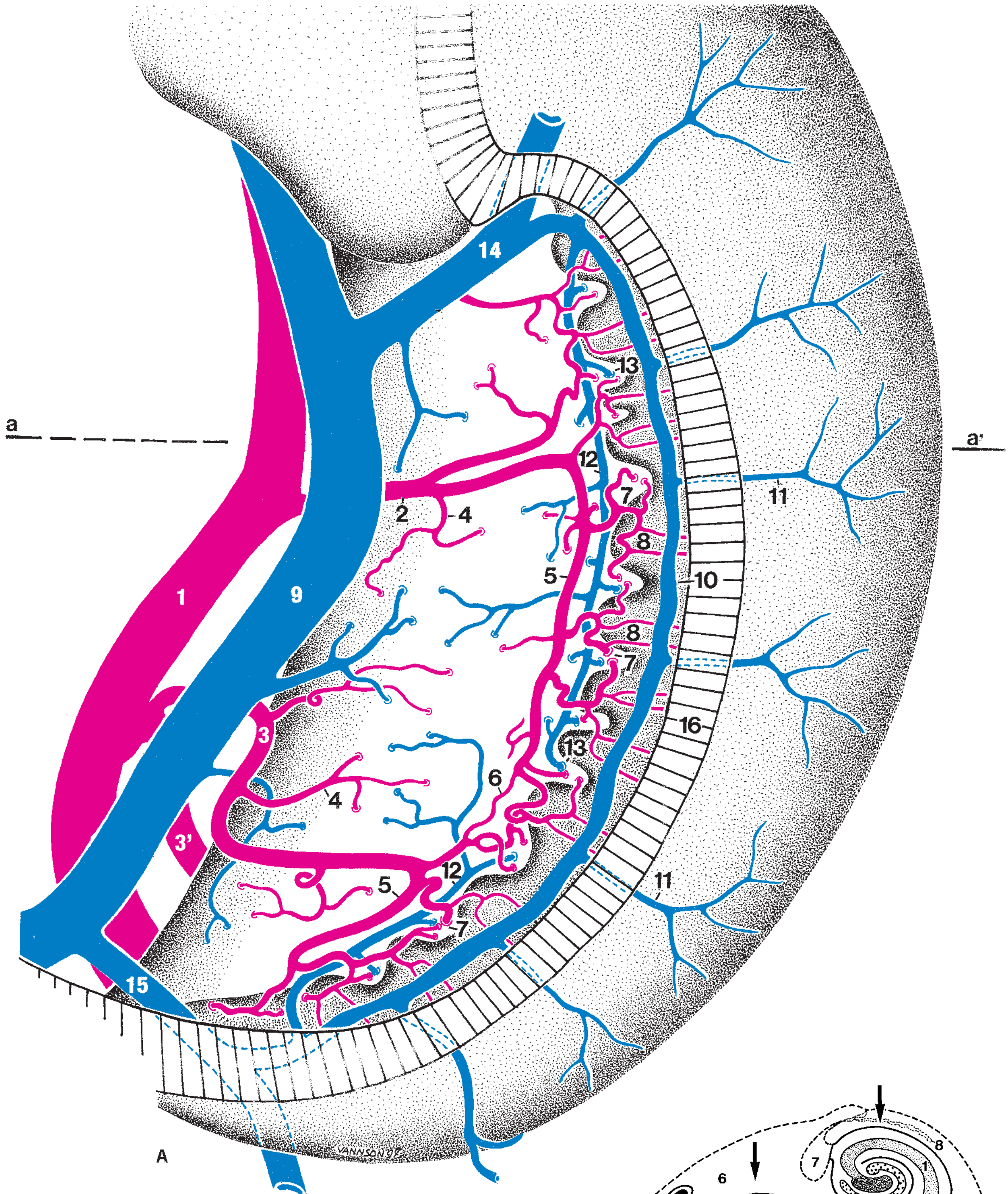

A

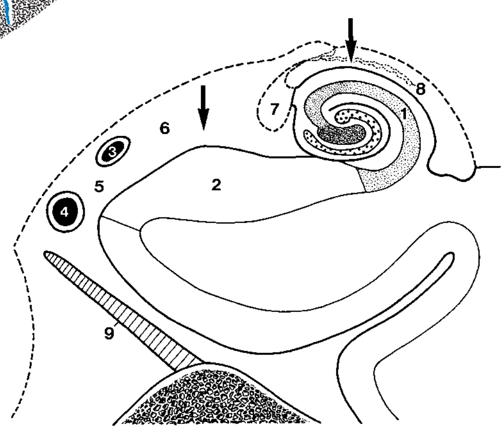

B

Fig. 46. A Superficial arteries and veins of hippocampal body and tail. The temporal horn has been opened and the fimbria removed, as seen in **B**

Superficial arteries: **1**, posterior cerebral artery; **2**, middle hippocampal artery arising from the trunk of the posterior cerebral artery; **3**, posterior hippocampal artery arising from an inferior temporal artery (**3′**); **4**, arterial branches to the

Fig. 47. Intravascular India ink injection. **Bar**, 2.8 mm
1, superior surface of subiculum; **2**, margo denticulatus; **3**, fimbria (removed); **4**, middle hippocampal arteries; **5**, posterior hippocampal artery arising from a splenial artery (**5′**); **6**, longitudinal terminal segments of the hippocampal arteries; **7**, arterial branches to the subiculum; **8**, large arterial branches penetrating the hippocampus between the dentes (**9**) of margo denticulatus; **10**, venous arch of the fimbriodentate sulcus receiving the subependymal intrahippocampal veins (**11**); **12**, venous arch of the superficial hippocampal sulcus; **13**, superficial hippocampal sulcus

◁
subiculum; **5**, longitudinal terminal segment of the hippocampal arteries running along the superficial hippocampal sulcus; **6**, anastomosis between the longitudinal terminal segments of hippocampal arteries; **7**, large arterial branches penetrating in the sulci between the dentes of the margo denticulatus; **8**, small arterial branches (straight arteries). Superficial veins: **9**, basal vein. The longitudinal hippocampal veins may be divided into two venous arches: **10**, venous arch of the fimbriodentate sulcus receiving the subependymal intrahippocampal veins (**11**), visible in an endoventricular view; **12**, venous arch of the superficial hippocampal sulcus receiving the sulcal intrahippocampal veins (**13**) emerging between the dentes of margo denticulatus. These two arches are drained into the basal vein by the inferior ventricular vein (vein of the temporal horn, **14**) and by the medial atrial vein (**15**). **16**, cut surface of fimbria
B Transverse section of the hippocampus according to the plane **a–a′** shown in **A**, showing the superior aspects of subiculum and hippocampus (**arrows**) after removal of central structures (**dotted lines**)
1, cornu Ammonis; **2**, subiculum; **3**, basal vein; **4**, posterior cerebral artery; **5**, ambient cistern; **6**, wing of ambient cistern; **7**, fimbria (removed); **8**, choroid plexuses (removed)

Fig. 48. Same preparation as in Fig. 47 (the fimbria is left intact). The temporal (inferior) horn has been opened and the choroid plexuses removed. Note on the surface of the fimbria (**1**) the imprints left by branches of choroidal arteries (**arrowheads**). **Bar**, 3 mm

1, fimbria; **2**, margo denticulatus (partly hidden by the fimbria); **3**, posterior cerebral artery lining the margin of the parahippocampal gyrus (**4**); **5**, middle hippocampal arteries; **6**, splenial artery; **7**, venous arch of the superficial hippocampal sulcus (the venous arch of the fimbriodentate sulcus is hidden by the fimbria); **8**, endoventricular view of the hippocampus

Fig. 49. Intravascular India ink injection. **Bar**, 2.6 mm
1, fimbria; **2**, margo denticulatus (largely hidden by the fimbria); **3**, subiculum; **4**, posterior cerebral artery; **5**, middle hippocampal arteries arising from the posterior cerebral artery; **6**, group of posterior hippocampal arteries arising from a curved splenial artery (**7**), which is a branch of the posterior cerebral artery; **8**, large arterial branches penetrating the hippocampus between the dentes of the margo denticulatus (**9**)

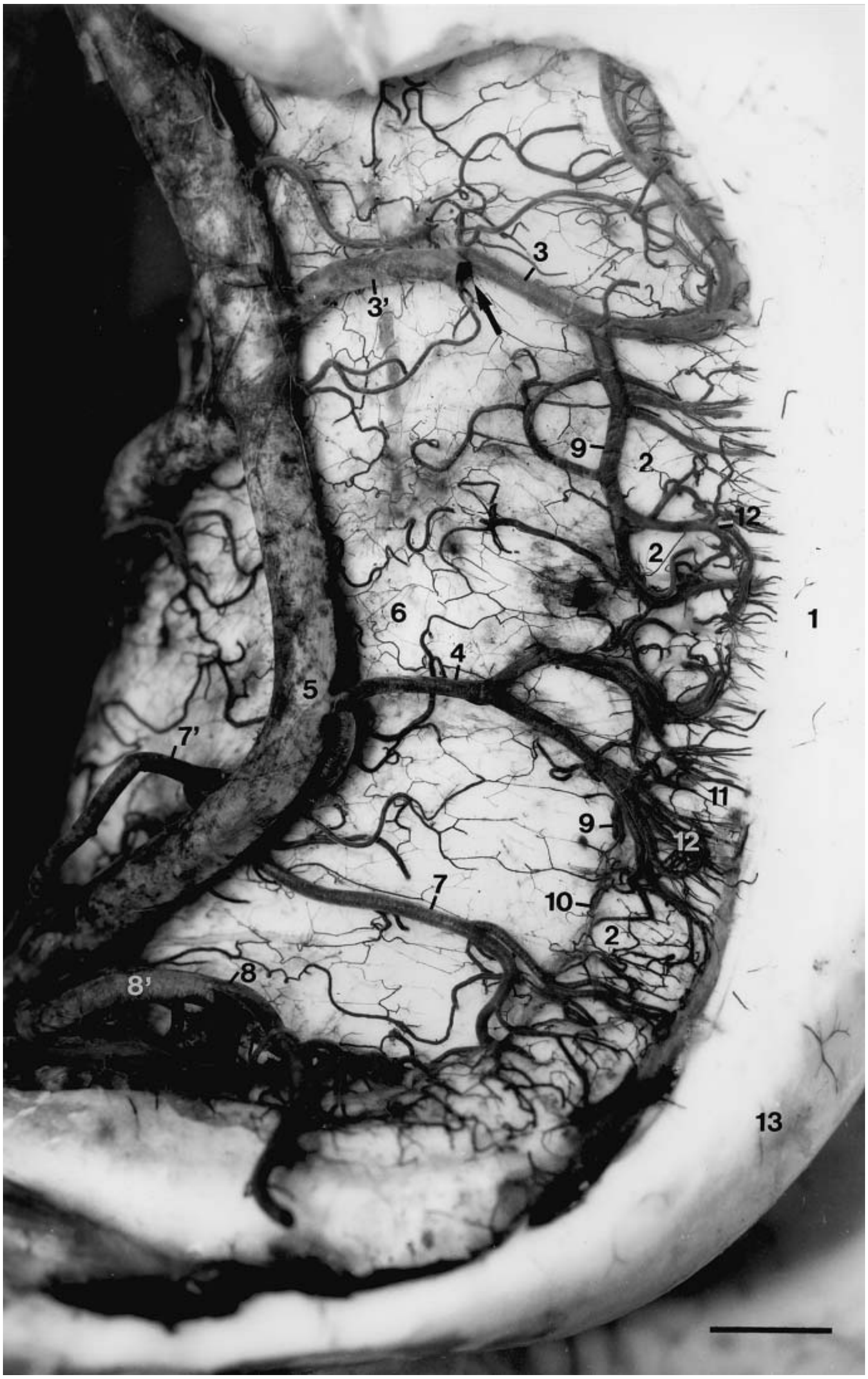

Fig. 50. Vascular India ink injection. The fimbria has been removed (**1**) to show the margo denticulatus (**2**). This preparation shows several superficial hippocampal arteries with various origins. **Bar**, 2.9 mm

1, fimbria (removed); **2**, margo denticulatus; **3**, middle hippocampal artery arising from a posterolateral choroidal artery (**3′**), whose course towards the temporal horn has been cut off (**arrow**); **4**, middle hippocampal artery arising directly from the posterior cerebral artery (**5**), which curves on the subicular surface (**6**); **7**, posterior hippocampal artery arising from a small inferior temporal artery (**7′**); **8**, posterior hippocampal artery arising from the splenial artery (**8′**); **9**, longitudinal terminal segment of the hippocampal arteries situated along the superficial hippocampal sulcus (**10**); **11**, small "straight" arteries; **12**, large arterial branches penetrating between the dentes of margo denticulatus; **13**, endoventricular aspect of the hippocampal tail

Fig. 51. Enlargement of Fig. 50 to show with more details the large arterial branches (**1**) penetrating in the sulci between the dentes of margo denticulatus (**2**). **3**, straight arteries; **4**, subiculum. The temporal horn has been opened and the choroid plexuses removed to show the endoventricular aspect of hippocampus (**5**). **Bar**, 1.6 mm

Fig. 52. Intravascular India ink injection. On this preparation, the middle group of hippocampal arteries (**1**), arising from an inferior temporal artery (**1′**), are the main arterial supply to the hippocampal body. **Bar**, 2.5 mm

1, middle group of hippocampal arteries; **1′**, inferior temporal artery; **2**, the posterior hippocampal artery with a territory restricted to the terminal segment of the tail; **3**, large arterial branches penetrating in the sulci between the dentes of margo denticulatus (**4**); **5**, venous arch of the fimbriodentate sulcus; **6**, subiculum; **7**, posterior cerebral artery

Fig. 53. Intravascular India ink injection. The temporal (inferior) horn of the lateral ventricle has been opened. **Bar,** 5.3 mm

1, choroid plexuses of the temporal horn covering and hiding the hippocampal body and tail; **2**, the hippocampal head, devoid of choroid plexuses, is clearly visible; **3**, choroid glomus; **4**, anterior choroidal artery; **5**, posterolateral choroidal artery arising from the posterior cerebral artery (**6**); **7**, fimbria; **8**, the margo denticulatus, large in this preparation, is free from the fimbria; **9**, venous arch of the fimbriodentate sulcus; **10**, venous arch of the hippocampal sulcus; **11**, subiculum; **12**, crus of fornix

Fig. 54. Intravascular India ink injection. The temporal (inferior) horn of the lateral ventricle has been opened and the choroid plexuses removed. **Bar,** 5.2 mm
1 hippocampal head and digitationes hippocampi;
2, hippocampal body; **3**, hippocampal tail; **4**, fimbria;
5, collateral eminence; **6**, collateral trigone; **7**, calcar avis;
8, occipital horn; **9**, subependymal intrahippocampal veins (note the regular and radial arrangement); **10**, subiculum

Fig. 55. Intravascular India ink injection. The temporal (inferior) horn of the lateral ventricle has been opened and the choroid plexuses removed. **Bar**, 2.8 mm

1, hippocampal head; **2**, hippocampal body; **3**, fimbria; **4**, subependymal intrahippocampal veins (note the fine arborizations)

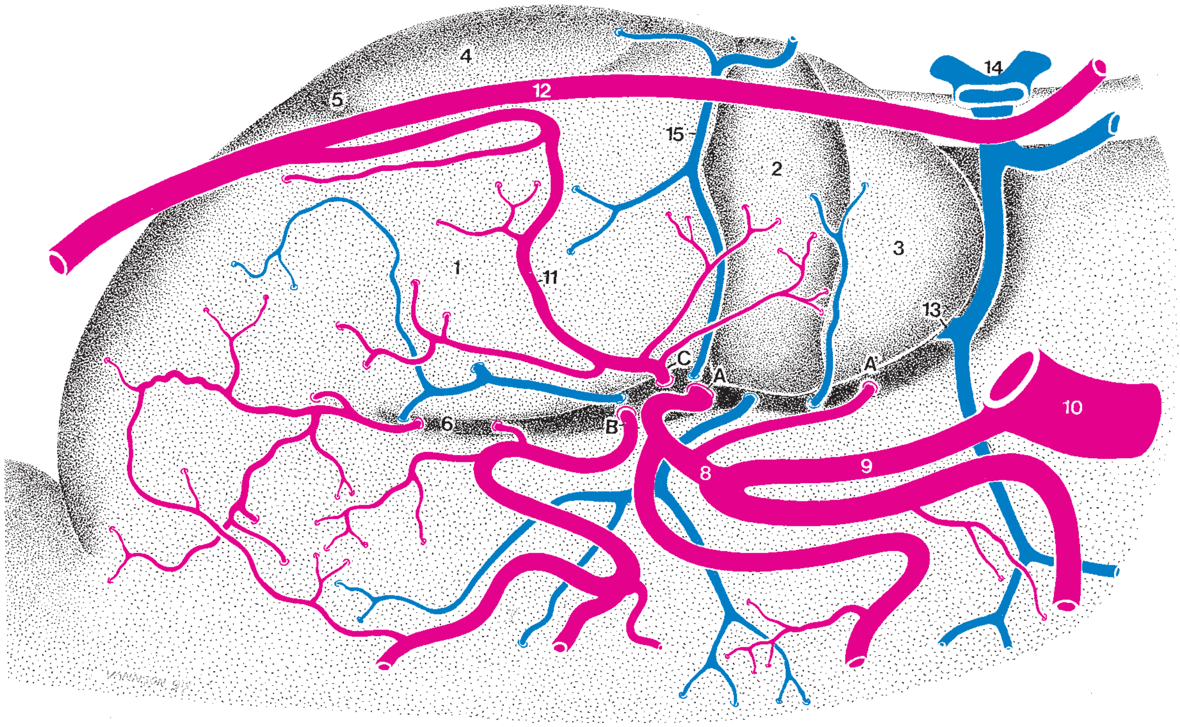

Fig. 56 A, B. Medial aspect of the piriform lobe (uncus and entorhinal area). **A** Drawing. **B** India ink injection. The anterior hippocampal artery (**8**) penetrates (**A**) into the uncal sulcus (see Fig. 57A) and often reappears (**B**) to vascularize the entorhinal area (**7**). The uncal branch of the anterior choroidal artery (**11**) penetrates into the uncal sulcus (**C**). **A'**, Collateral branch of the anterior hippocampal artery. The venous network of the hippocampal head emerging from the uncal sulcus (**13**) is drained towards the inferior ventricular vein (**14**). **Bar**, 2.5 mm

1, medial aspect of the uncus; **2**, band of Giacomini; **3**, uncal apex; **4**, semilunar gyrus; **5**, semianular sulcus; **6**, uncal sulcus; **7**, entorhinal area; **8**, anterior hippocampal artery arising from an anterior inferior temporal artery (**9**); **10**, posterior cerebral artery; **11**, uncal branch of the anterior choroidal artery; **12**, anterior choroidal artery; **13**, venous drainage of the hippocampal head; **14**, vein of the temporal horn (inferior ventricular vein); **15**, vein of the superficial hippocampal sulcus bordering the band of Giacomini

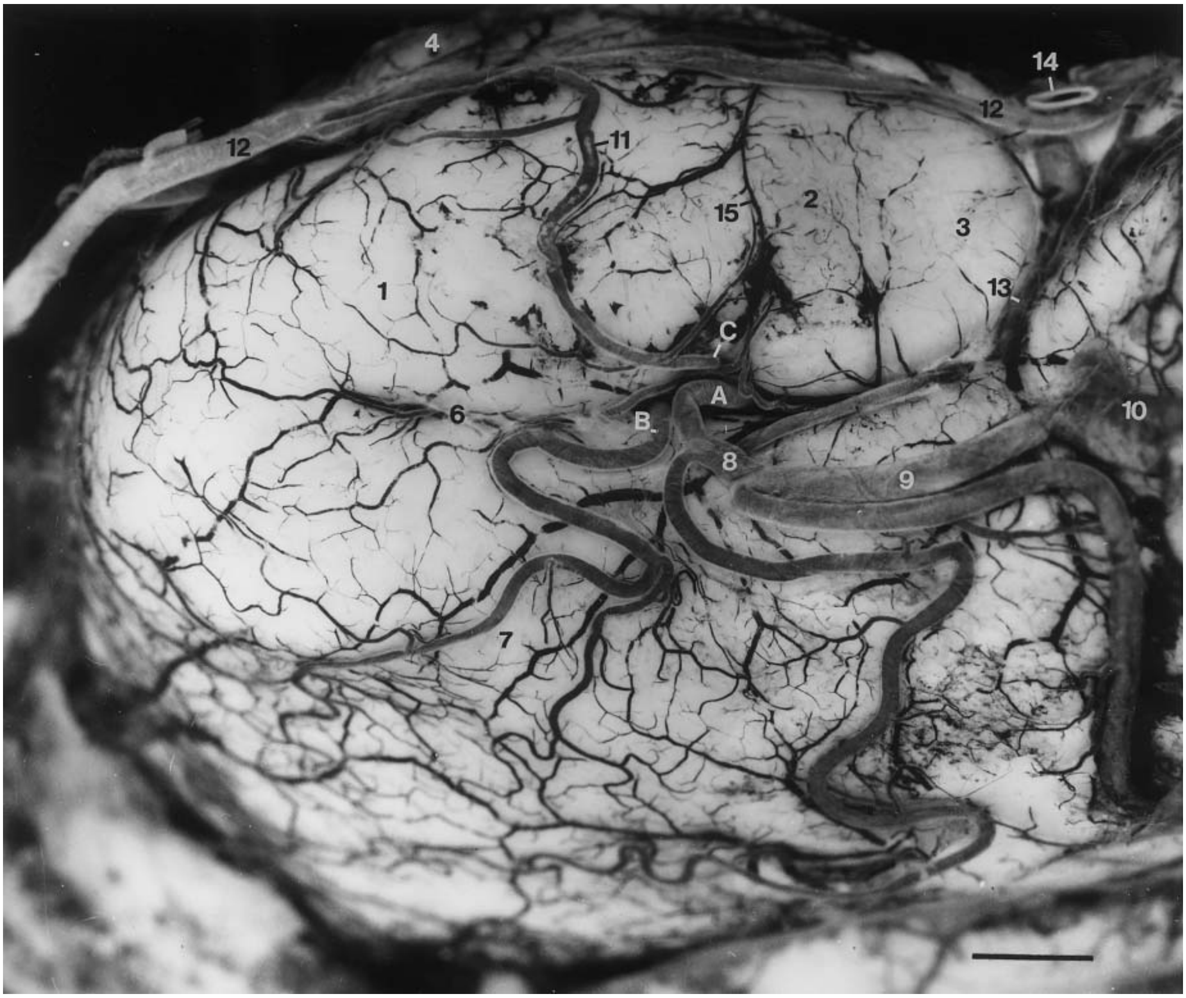

Fig. 56 B

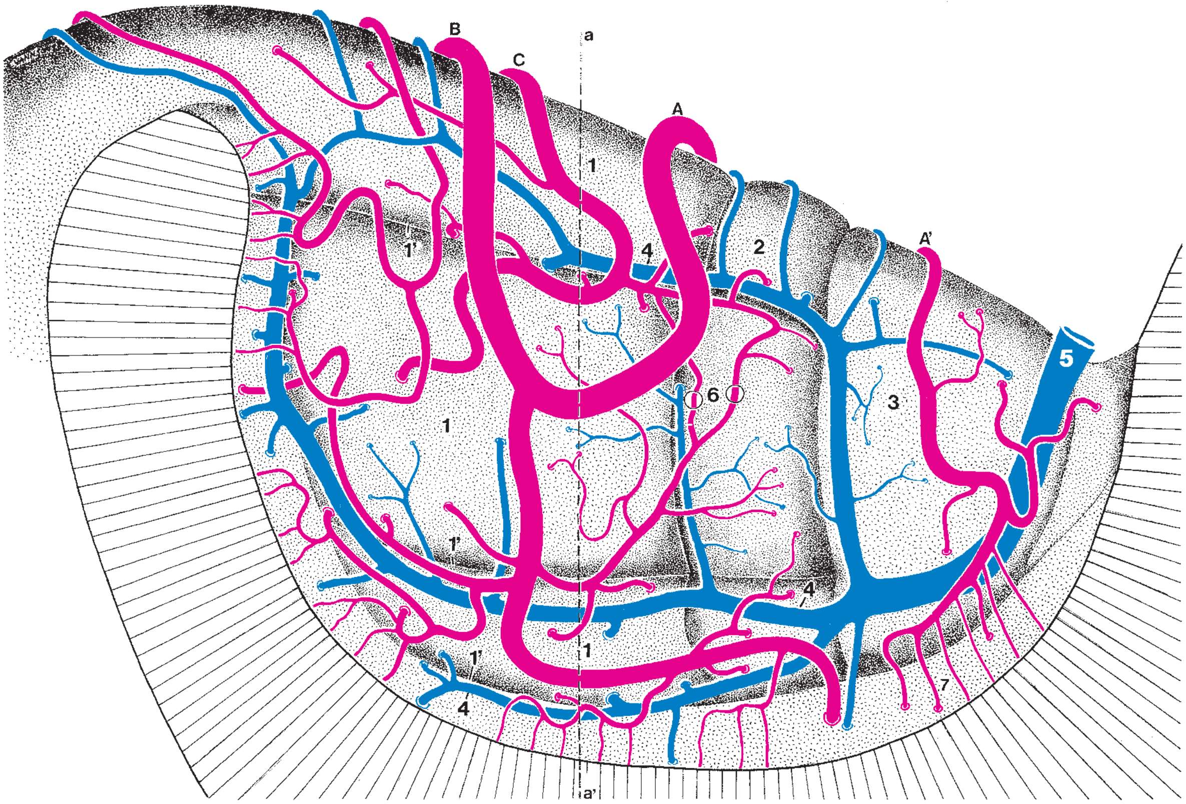

Fig. 57. A Drawing and **B** intravascular injection showing the superior side of the uncal sulcus after ablation of its inferior side, as shown in C. By this method, the inferior surface of the hippocampal head may be seen. **Bar**, 2.2 mm
1, external digitations; **1′**, sulci between these digitations. The parts of the band of Giacomini (**2**) and of the uncal apex (**3**) normally hidden in the uncal sulcus are visible by this dissection. The arterial branches vascularizing the hippocampal head mainly penetrate into the sulci between the external digitations. The venous network is also mainly situated in these sulci (**4**). **5**, venous drainage towards the inferior ventricular vein (corresponds to **13** in Fig. 56); **6**, arterial anastomoses between branches of anterior hippocampal and anterior choroidal arteries; **7**, straight arteries. **A**, anterior hippocampal artery penetrating into the uncal sulcus and emerging from it (**B**); **C**, uncal branch of the anterior choroidal artery penetrating into the uncal sulcus (see corresponding lettering in Fig. 56); **A′**, collateral of anterior hippocampal artery

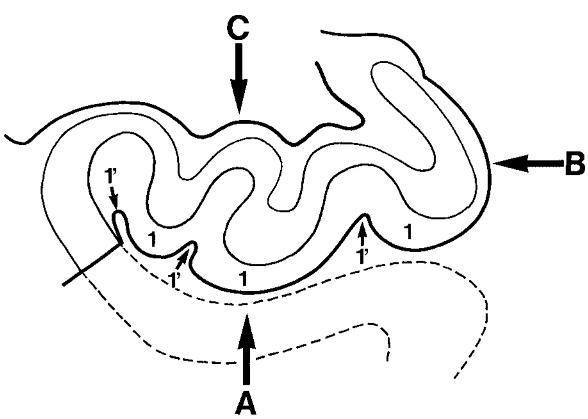

C Tranverse coronal section of the hippocampus according to the plane a–a' shown in Fig. 57A. The inferior side of the uncal sulcus has been removed (**dotted line**)
A, inferior aspect of the uncus; **B**, medial aspect of the uncus; **C**, superior (endoventricular) aspect of the uncus: internal digitations (digitationes hippocampi) in relation to the temporal horn of the lateral ventricle. **1**, external digitations; **1′**, sulci between external digitations

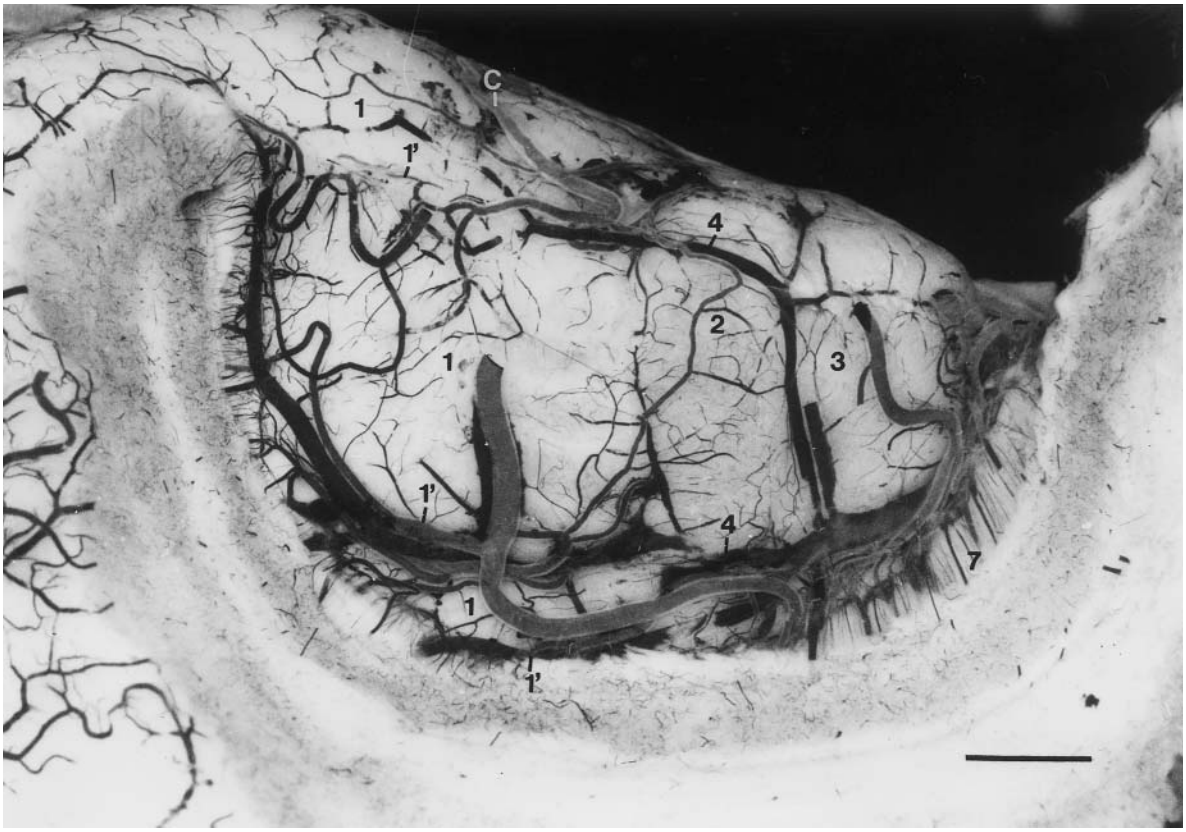

Fig. 57 B

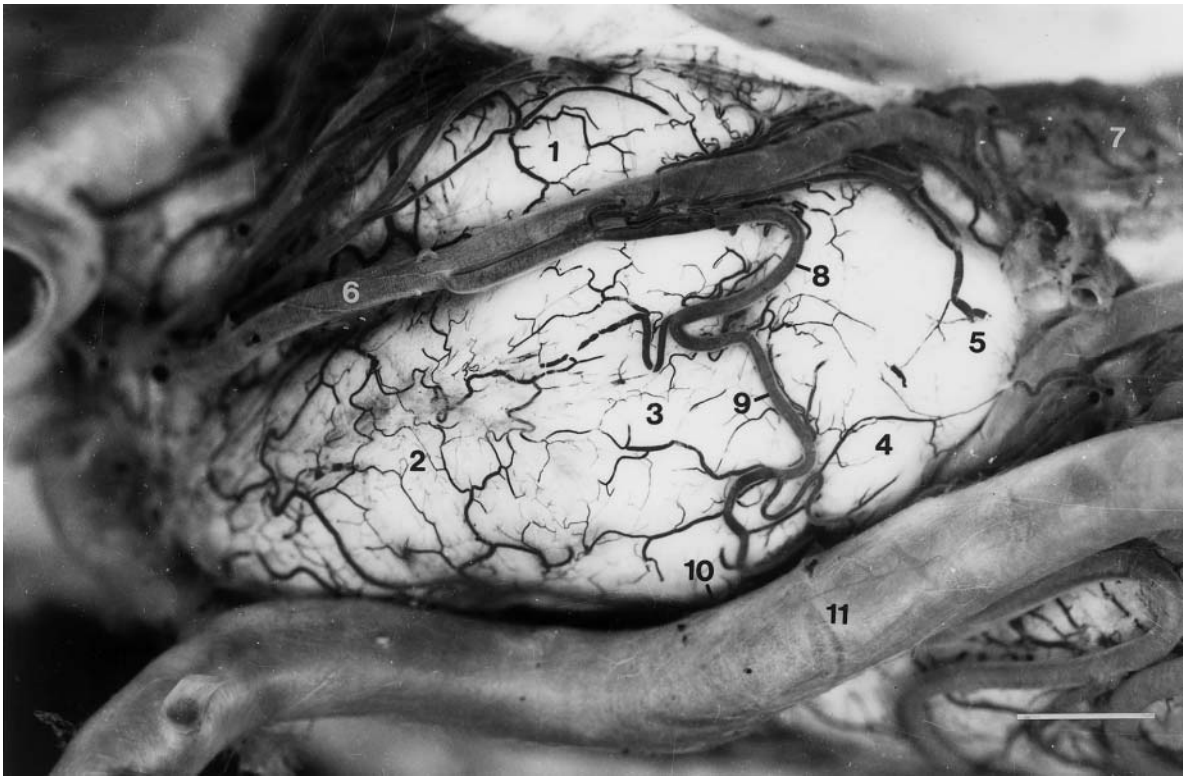

Fig. 58. Superior aspect of the uncus. Intravascular India ink injection. **Bar**, 2.7 mm
1, semilunar gyrus; **2**, ambient gyrus; **3**, uncinate gyrus; **4**, band of Giacomini; **5**, uncal apex; **6**, the anterior choroidal artery courses in the semianular sulcus to reach the choroid plexuses of the temporal horn (**7**); **8**, uncal branch of the anterior choroidal artery running along the uncal part of the superficial hippocampal sulcus (**9**) to reach the uncal sulcus (**10**); **11**, posterior cerebral artery

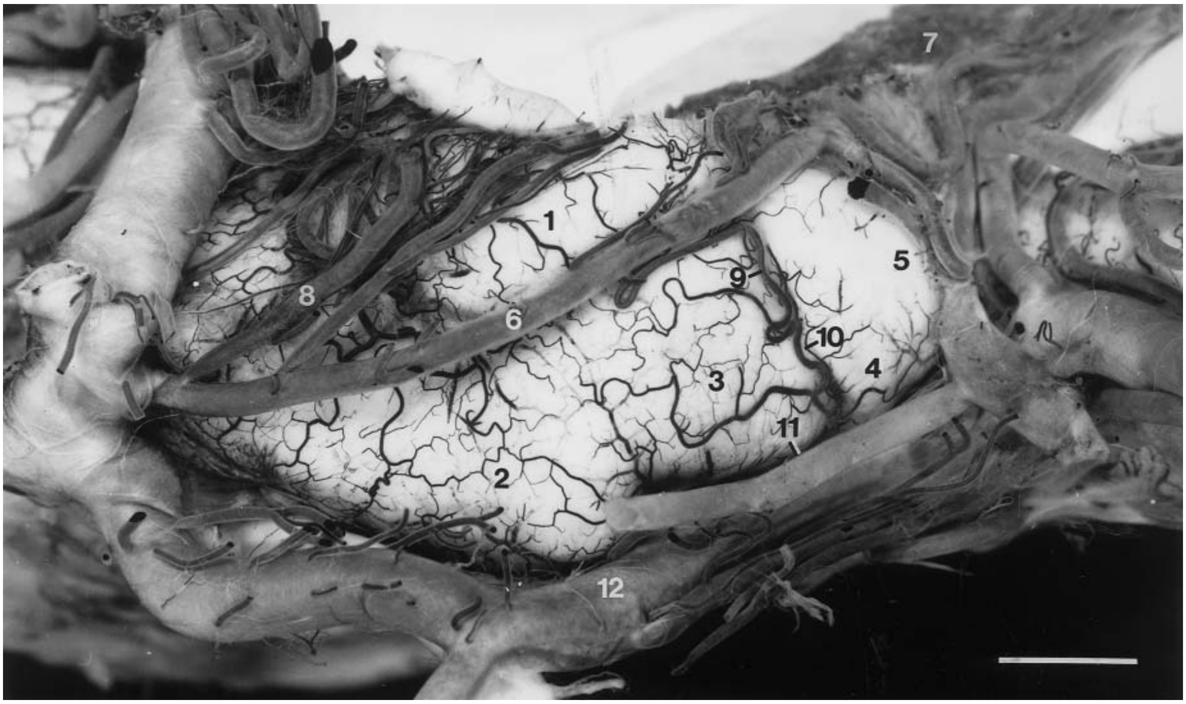

Fig. 59. Superior aspect of the uncus. Intravascular India ink injection. **Bar**, 3.3 mm
1, semilunar gyrus; **2**, ambient gyrus; **3**, uncinate gyrus; **4**, band of Giacomini; **5**, uncal apex; **6**, anterior choroidal artery situated in the semianular sulcus and reaching the choroid plexuses of the temporal horn (**7**); **8**, deep perforating branches of the anterior choroidal artery; **9**, the uncal branch of the anterior choroidal artery courses along the superficial hippocampal sulcus (**10**) to reach the uncal sulcus (**11**); **12**, posterior cerebral artery

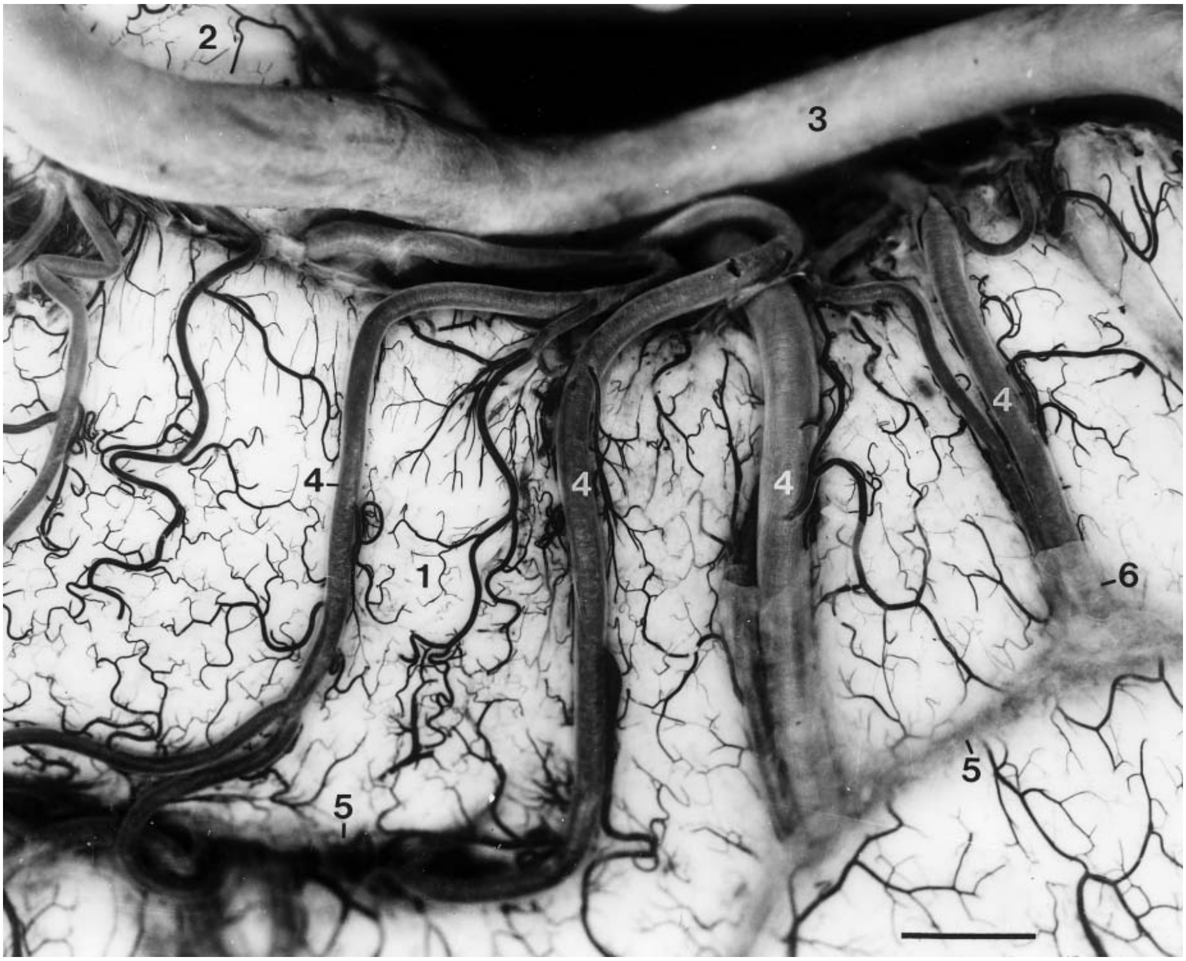

Fig. 60. Inferior view of the temporal lobe. Intravascular India ink injection. **Bar**, 2.5 mm
1, parahippocampal gyrus; **2**, uncal apex; **3**, posterior cerebral artery (P2 segment) located along the margin of the parahippocampal gyrus; **4**, group of inferior temporal arteries crossing the parahippocampal gyrus to reach the collateral sulcus (**5**); **6**, the arachnoid has been left partly intact

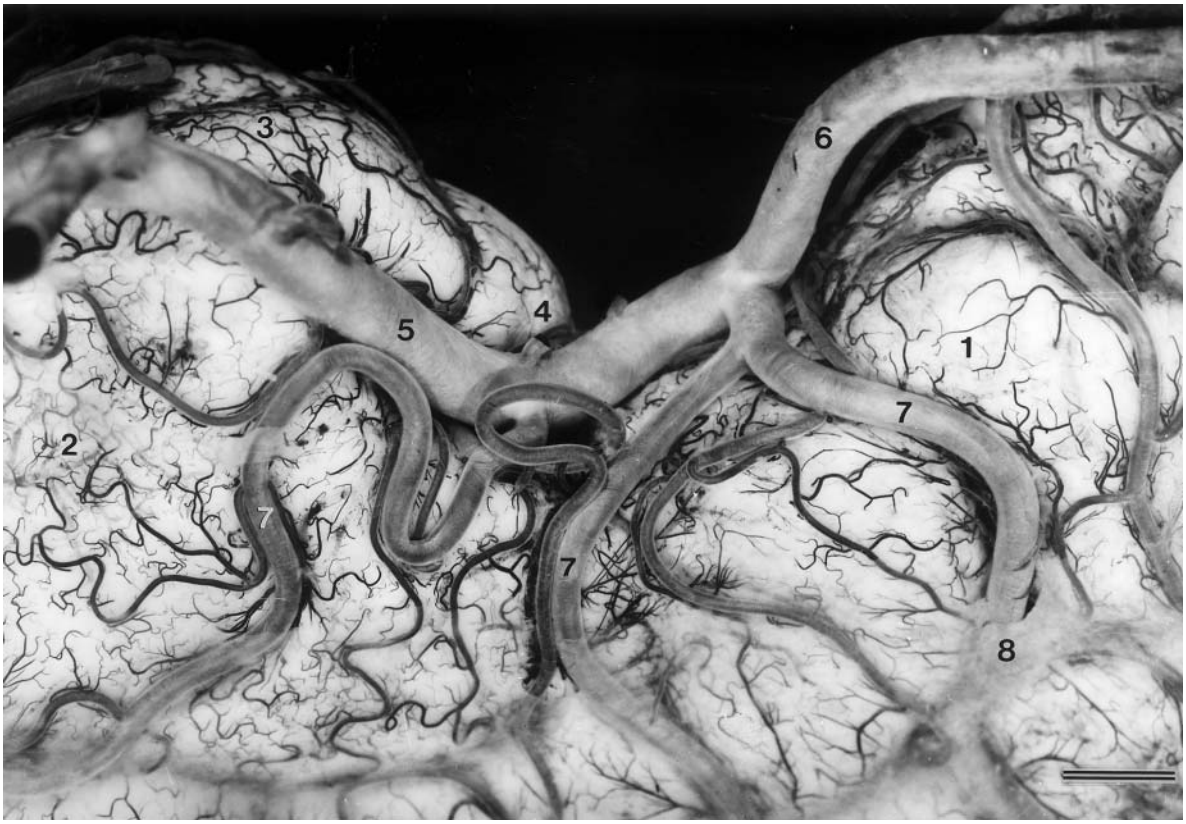

Fig. 61. Inferior view of the temporal lobe. Intravascular India ink injection. **Bar**, 4 mm
1, parahippocampal gyrus; **2**, entorhinal area; **3**, uncus, ambient gyrus; **4**, uncal apex. The P2 segment of the posterior cerebral artery may be divided into two parts: the first part (**5**) crosses the uncus and hiddes the uncal sulcus; the second part (**6**) follows the margin of the parahippocampal gyrus. Note the high density of the hippocampal parahippocampal arterial complex situated at the level of the uncal apex and composed of the trunk of the posterior cerebral artery and its numerous collaterals, in particular the group of anterior inferior temporal arteries (**7**); **8**, the arachnoid has been left partly intact

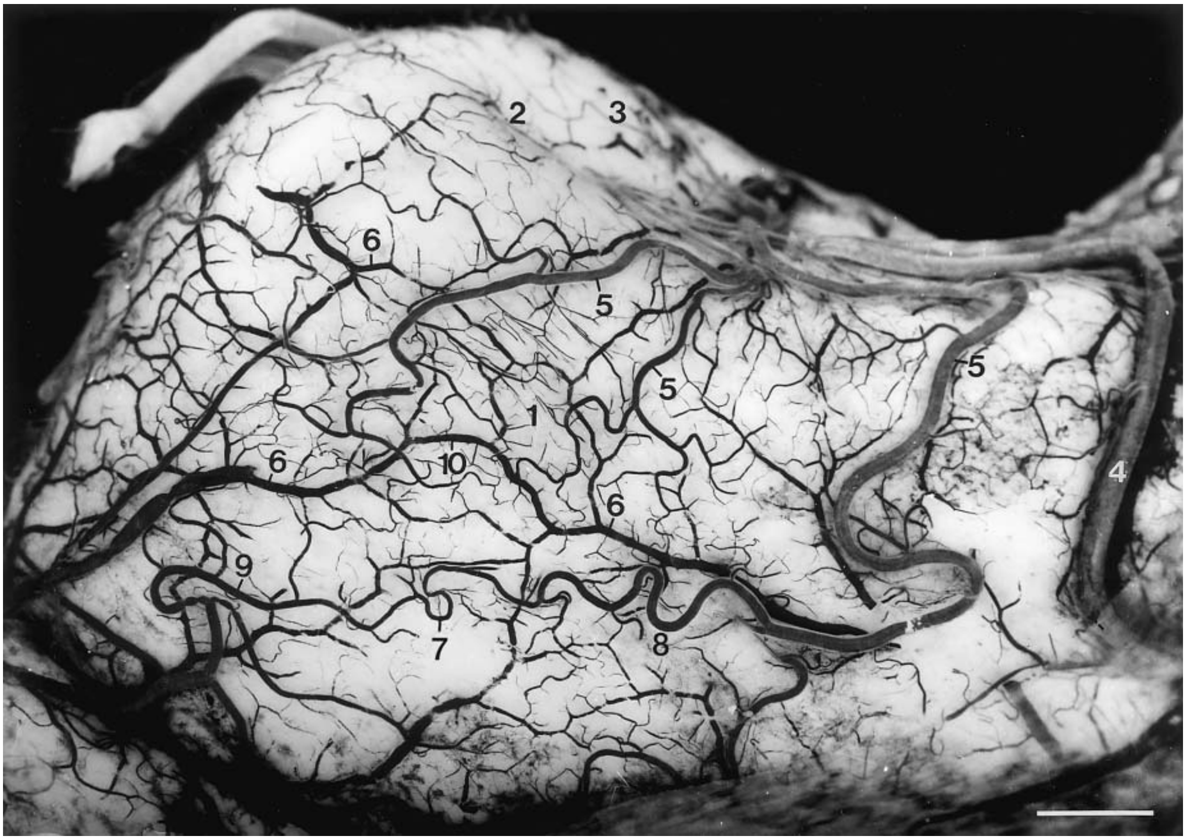

Fig. 62. Inferior aspect of the piriform lobe whose medial aspect is seen in Fig. 56B. Note the dense arterial and venous networks covering the entorhinal area. **Bar**, 5 mm
1, entorhinal area; **2**, uncal sulcus; **3**, uncus; **4**, anterior inferior temporal artery; **5**, branches of the anterior hippocampal artery supplying the entorhinal area; **6**, arterial and venous networks; **7**, arterial anastomosis between a branch of the anterior hippocampal artery (**8**) and a branch of the middle cerebral artery (**9**); **10**, venous anastomoses

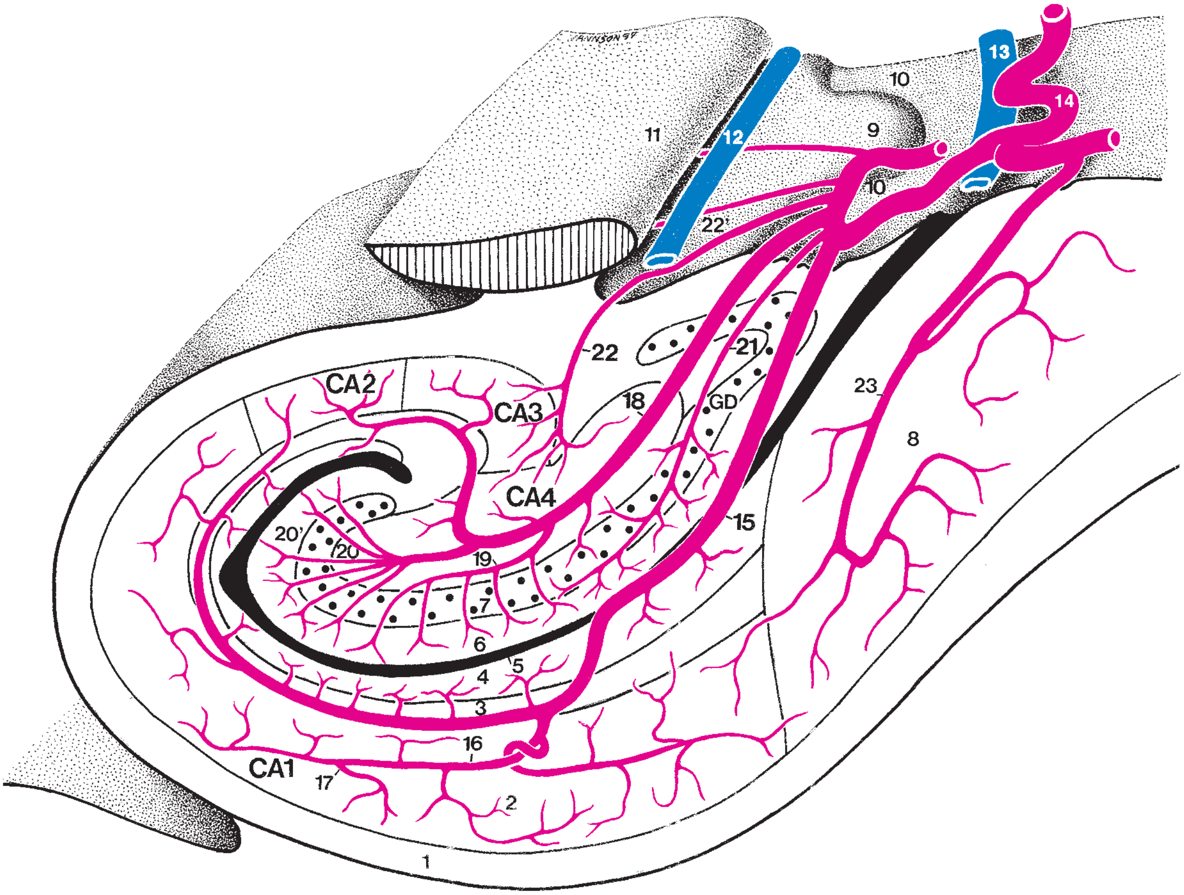

Fig. 63. Coronal section showing the arterial supply of the hippocampal body
Cornu Ammonis: **CA1–CA4**, fields of the cornu Ammonis. **1**, alveus; **2**, stratum pyramidale and stratum radiatum; **3**, stratum lacunosum; **4**, stratum moleculare; **5**, vestigial hippocampal sulcus. Gyrus dentatus (**GD**): **6**, stratum moleculare; **7**, stratum granulosum; **8**, subiculum; **9**, dentes of margo denticulatus; **10**, sulci between dentes; **11**, fimbria; **12**, venous arch of the fimbriodentate sulcus; **13**, venous arch of the superficial hippocampal sulcus; **14**, longitudinal terminal segment of the superficial hippocampal arteries. The intrahippocampal arteries may be divided into the large dorsal, large ventral, small ventral, and small dorsal group: **15**, large ventral intrahippocampal arteries, with a long course in CA1 reaching CA2; **16**, collaterals with a long path in the pyramidal layer of CA1; **17**, note their branches often steming in a counterflow way; **18**, large dorsal intrahippocampal arteries situated in CA4 along the gyrus dentatus and reaching CA3 and CA2; **19**, branches with a rectilinear path supplying the molecular layer of the gyrus dentatus; **20**, branches with a brushlike appearance supplying the genu of the gyrus dentatus (**20′**); **21**, small ventral intrahippocampal arteries reaching the proximal part of the gyrus dentatus with a rectilinear course; **22**, small dorsal intrahippocampal arteries (straight arteries, **22′**) with a territory restricted to part of CA3 and CA4; **23**, the arteries of the subiculum have a long course similar to that of CA1

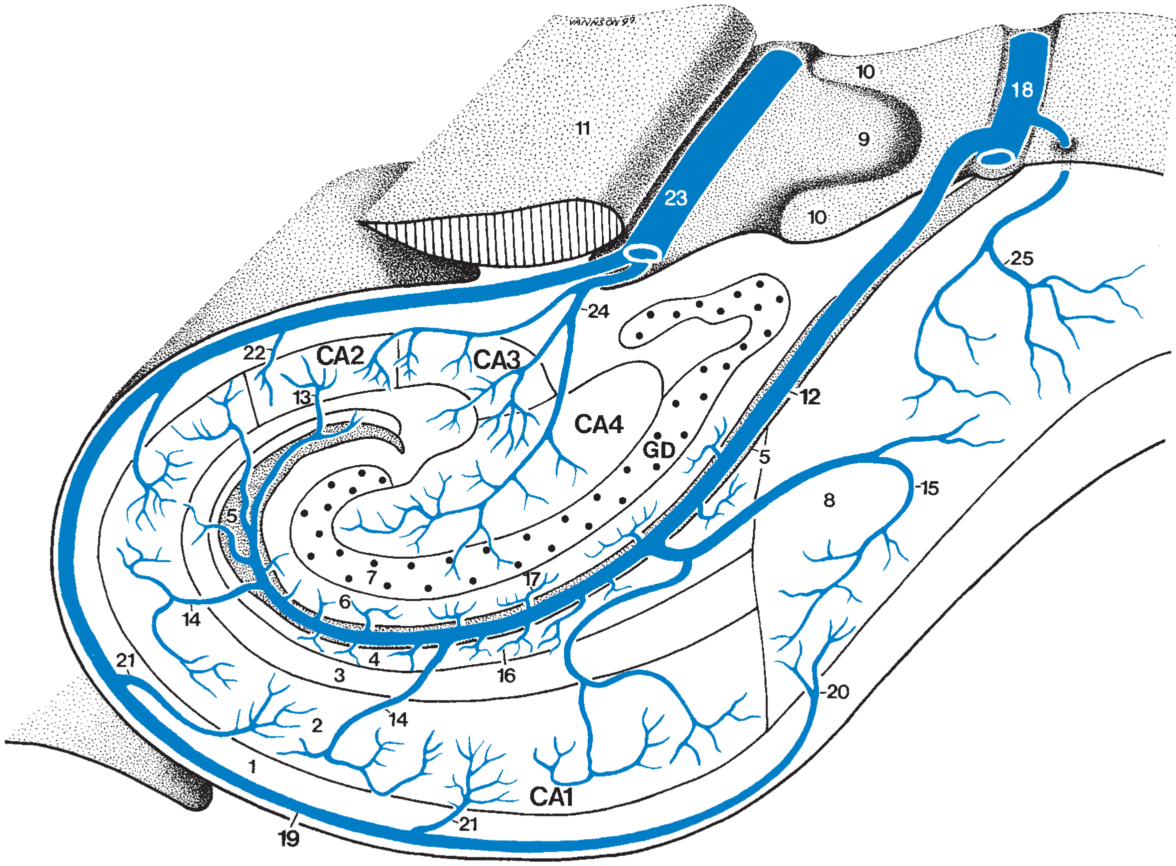

Fig. 64. Coronal section showing the venous supply of the hippocampal body
Cornu Ammonis: **CA1–CA4**, fields of the cornu Ammonis. **1**, alveus; **2**, stratum pyramidale and stratum radiatum; **3**, stratum lacunosum; **4**, stratum moleculare; **5**, vestigial hippocampal sulcus. Gyrus dentatus (**GD**): **6**, stratum moleculare; **7**, stratum granulosum; **8**, subiculum; **9**, dentes of margo denticulatus; **10**, sulci between dentes; **11**, fimbria. The main venous drainage of the hippocampus depends on two groups of intrahippocampal veins: the sulcal intrahippocampal veins (**12**) and the subependymal intrahippocampal veins (**19**). **12**, The whole course of the sulcal intrahippocampal veins is situated in the vestigial hippocampal sulcus (**5**); they drain by long branches parts of CA2 (**13**), CA1 (**14**), and the subiculum (**15**) and by small branches of the molecular layers of the cornu Ammonis (**16**) and the gyrus dentatus (**17**); the sulcal veins flow into the venous arch of the superficial hippocampal sulcus (**18**); **19**, the subependymal intrahippocampal veins (**19**) have a long course in the alveus draining parts of the subiculum (**20**), CA1 (**21**), and CA2 (**22**); they flow into the vein of the fimbriodentate sulcus (**23**); some small veins (**24**) draining parts of CA3 and CA4 may directly reach the vein of the fimbriodentate sulcus; **25**, veins of the subiculum

Fig. 65. Coronal section of the hippocampal body. Intravascular India ink injection. **Bar**, 1.2 mm

1, large dorsal intrahippocampal artery; **2**, sulcal intrahippocampal vein; **3**, long oblique path of an arterial branch in CA1 (see Fig. 71). The poor capillary network of CA1 (**4**) in comparison with that of the subiculum (**5**) allows these two structures to be distinguished. Note the dense capillary network of CA2 (**6**) and CA3 (**7**). The stratum lacunosum (**8**) is the less vascularized layer in the cornu Ammonis, whereas the strata molecularia of the cornu Ammonis (**9**) and the gyrus dentatus (**10**) are characterized by their high vascular density. **11**, fimbria; **12**, temporal (inferior horn) of the lateral ventricle; **13**, tail of caudate nucleus; **14**, lateral geniculate body

1, large dorsal intrahippocampal artery with a preponderant territory; **2**, small dorsal intrahippocampal arteries (straight arteries, **2′**) with a territory restricted to part of CA3 (**4**). In the pyramidal layer of the cornu Ammonis, the highest capillary network is found in CA2 (**3**) and CA3 (**4**), whereas CA1 (**5**) is poorly vascularized. Note the parallel aspect of the vessels in the stratum radiatum (**6**) of CA1 and the highest capillary density in the strata molecularia of the cornu Ammonis (**7**) and the gyrus dentatus (**8**) separated by the vestigial hippocampal sulcus (**9**). **10**, small ventral intrahippocampal arteries

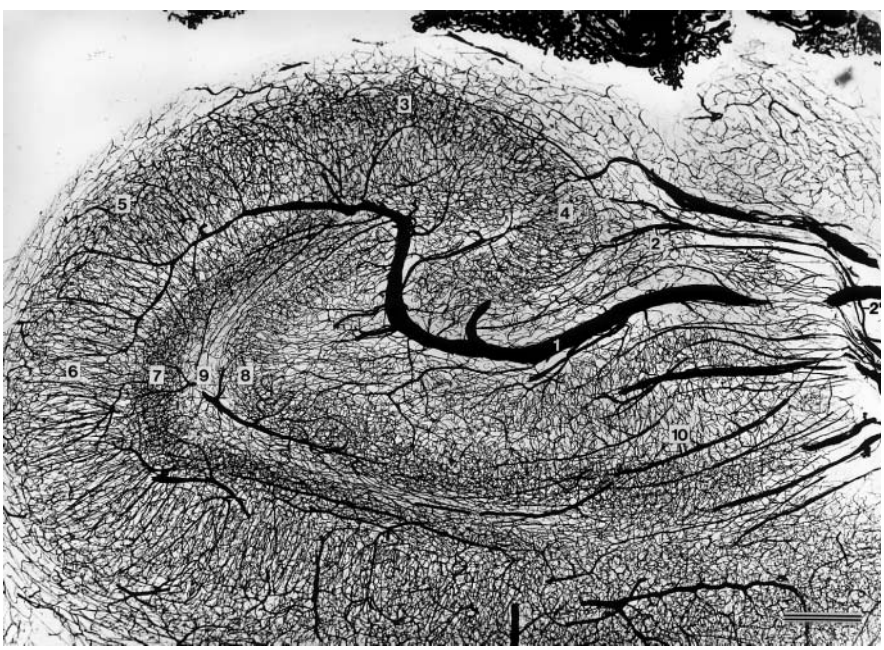

Fig. 66. Coronal section of hippocampal body. Intravascular India ink injection. **Bar**, 770 µm

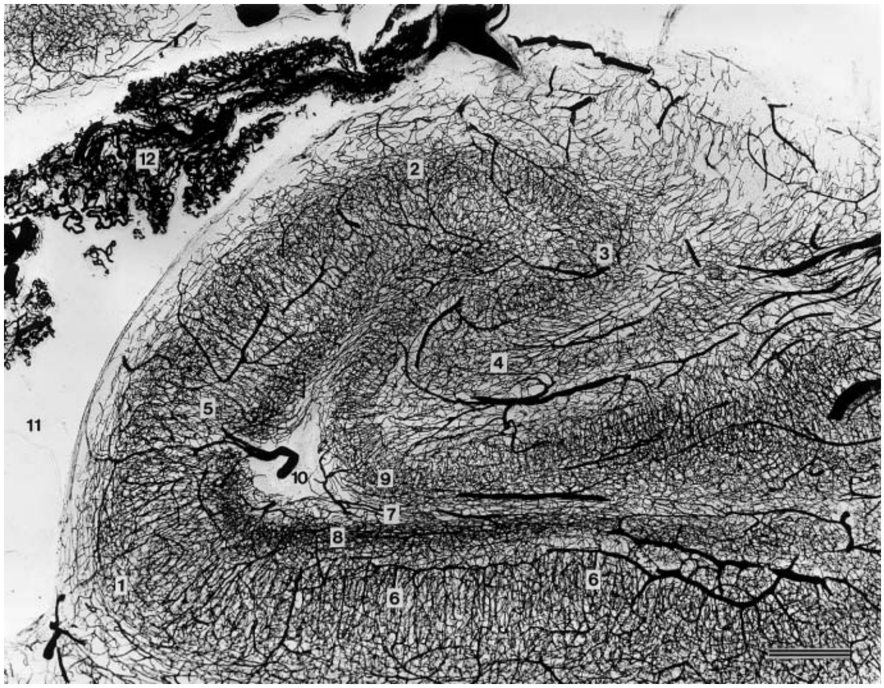

Fig. 67. Coronal section of the hippocampal body. Intravascular India ink injection (**Bar**: 1 mm). The stratum pyramidale of CA1 (**1**) is less vascularized than those of CA2–CA4 (**2**, **3**, **4**). Note the clear aspect of the stratum radiatum (**5**) due to the poor density of its vessels and the long arterials branches situated in the stratum lacunosum of CA1 (**6**). The vestigial hippocampal sulcus (**7**) separates the highly vascularized strata molecularia of the cornu Ammonis (**8**) and gyrus dentatus (**9**). Note a residual cavity which contains a sulcal intrahippocampal vein (**10**). **11**, temporal horn of the lateral ventricle; **12**, choroid plexuses

1, digitationes hippocampi (internal digitations); **2**, external digitations; **3**, uncal sulcus (**arrow**), **4**, the intrahippocampal arteries and veins form a vascular axis at the center of each digitation; **5**, the blood vessels penetrate in the sulci between the external digitations; **6**, stratum pyramidale of the cornu Ammonis; **7**, strata radiatum and lacunosum; **8**, stratum moleculare, highly vascularized; **9**, band of Giacomini; **10**, temporal horn of the lateral ventricle; **11**, subiculum

Fig. 68. Coronal section of hippocampal head. Intravascular India ink injection. **Bar**, 2.6 mm

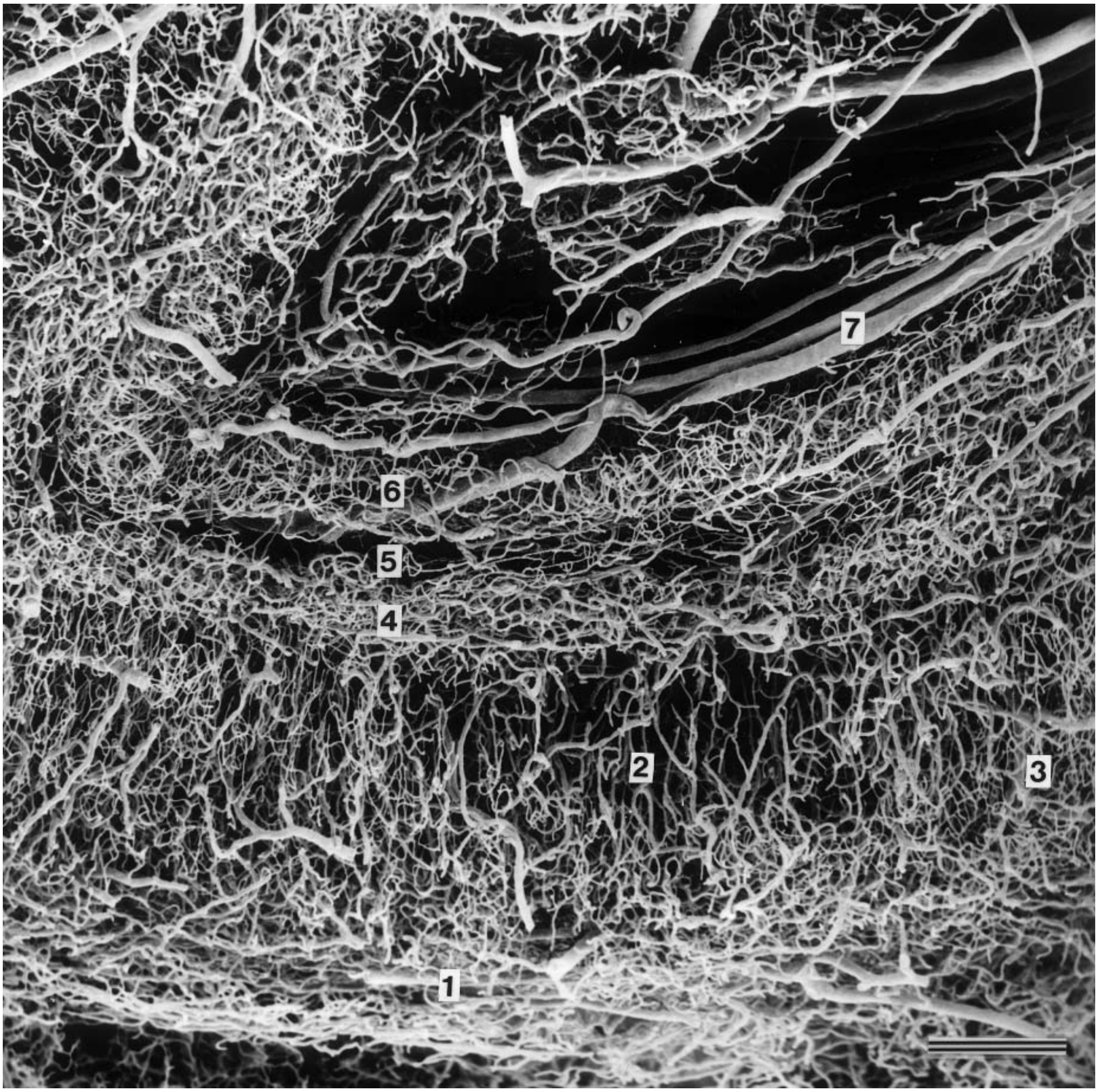

Fig. 69. Coronal section of the hippocampal body. Intravascular resin injection (Mercox) and scanning electron microscope view after corrosion. The layers of the cornu Ammonis and the gyrus dentatus can be distinguished according to their specific capillary network densities. The poor vascular network of the strata radiatum and lacunosum (**2**), in comparison to that of the adjacent subiculum (**3**), permits the hippocampal boundary to be delineated. **Bar**, 500 μm
1, stratum pyramidale of CA1; **2**, strata radiatum and lacunosum; **3**, subiculum; **4**, stratum moleculare of CA1; **5**, vestigial hippocampal sulcus; **6**, stratum moleculare of the gyrus dentatus; **7**, large dorsal intrahippocampal arteries

▷
Fig. 70. Dorsal view of the hippocampus after intravascular resin injection (Mercox) and corrosion of the hippocampal tissue. This overall view of the intrahippocampal vascularization shows the bushlike aspect of the capillary network (**arrows**) and its possible division into vascular units. Note the dense ramifications of the middle and posterior superficial hippocampal arteries (**2, 3**) at the hippocampal sulcus level (**4**). Note also the regular intervals between the subependymal intrahippocampal veins (**6**). **Bar**, 3 mm
1, posterior cerebral artery; **2**, middle superficial hippocampal artery; **3**, posterior superficial hippocampal artery; **4**, hippocampal sulcus; **5**, vein of the fimbriodentate sulcus; **6**, subependymal intrahippocampal veins


6
6
2
4
1
6
3
4
6
5

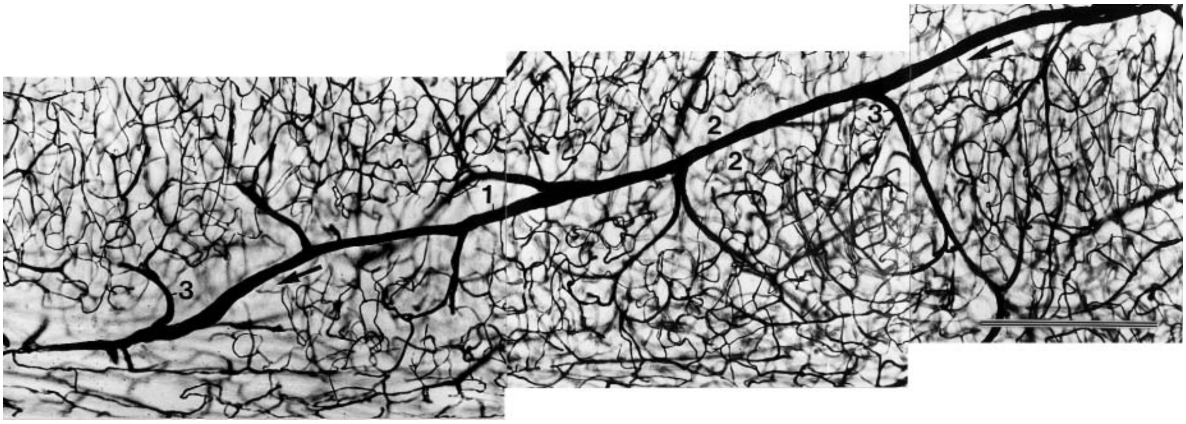

Fig. 71. Intravascular India ink injection. Typical aspect of an arterial branch (1) in CA1 (see its position in Fig. 65). Note its long oblique path, the important periarterial capillary free space (2), and the frequent recurrent branching of their collaterals (3) (**arrows** indicate the direction of the bloodstream). **Bar,** 600 μm

Fig. 72. Intravascular India ink injection. The capillary network of the stratum pyramidale (1) is supplied by deep arteries (2) and drained towards subependymal intrahippocampal veins (3). **Bar,** 160 μm

Fig. 73. Intravascular India ink injection. Vascularization of the gyrus dentatus. Fine arterial branches (**1**) reach the dense vascular network of the stratum moleculare (**2**) through the poorly vascularized stratum granulosum (**3**). Note the rectilinear aspect of some arteries (**4**) in the gyrus dentatus. **5**, vestigial hippocampal sulcus. **Bar**, 200 µm

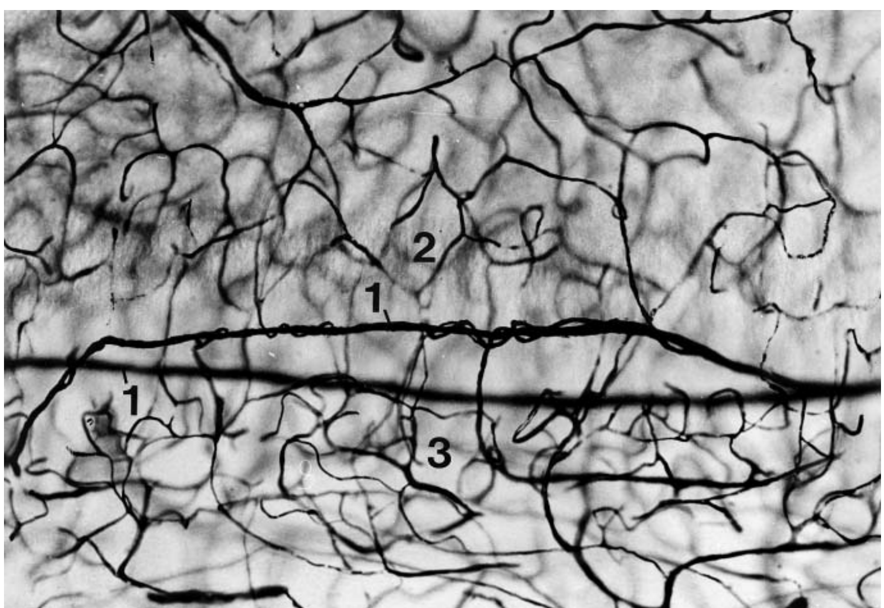

Fig. 74. Intravascular India ink injection. The arteries of the gyrus dentatus frequently have a rectilinear aspect. **Bar**, 200 µm
1, arteries of the gyrus dentatus; **2**, stratum granulosum; **3**, stratum moleculare

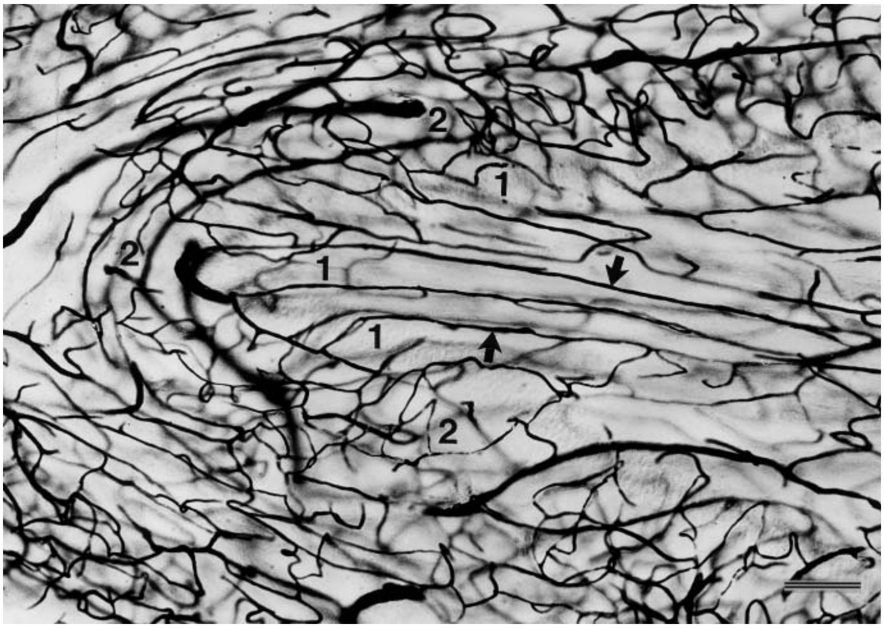

Fig. 75. Intravascular India ink injection. The arterial branches (**arrows**) supplying the genu of the gyrus dentatus have a brushlike appearance. **Bar**, 160 µm
1, stratum granulosum;
2, stratum moleculare of the gyrus dentatus

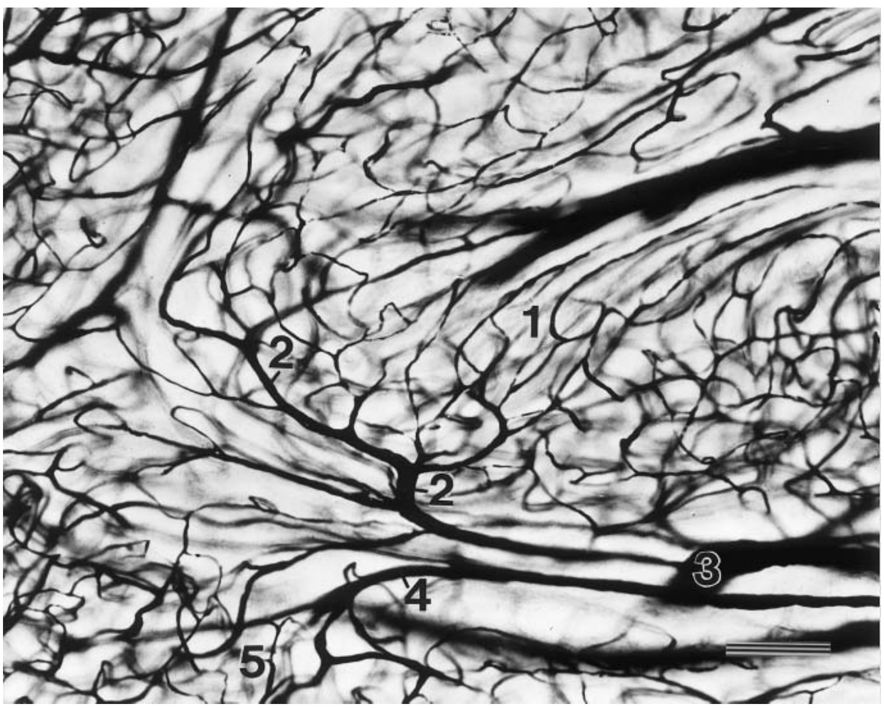

Fig. 76. Intravascular India ink injection. **Bar**, 240 µm
1, arterial supply of the stratum moleculare of the gyrus dentatus; **2**, venous drainage towards the sulcal intrahippocampal veins (**3**) situated in the vestigial hippocampal sulcus; **4**, venous drainage of the stratum moleculare of the cornu Ammonis (**5**)

Fig. 77. Intravascular India ink injection. Note numerous arterial and capillary deformations (1) within the stratum pyramidale of CA2. **Bar**, 135 μm

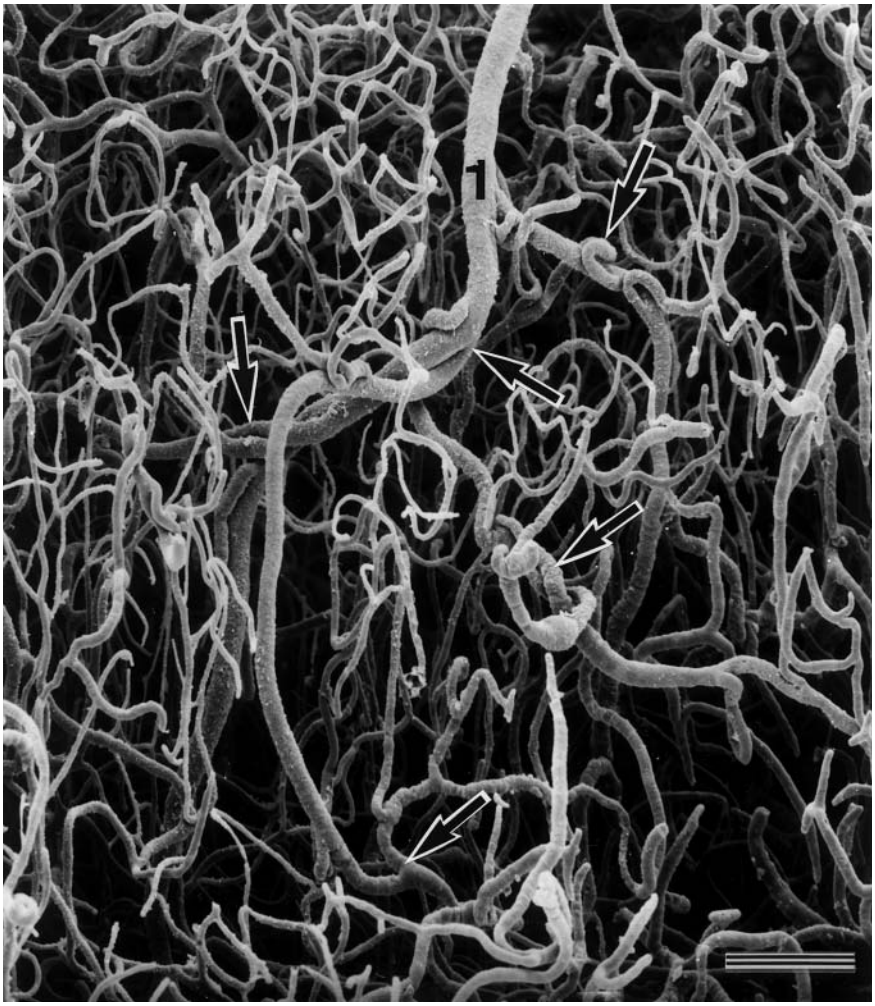

Fig. 78. Intravascular resin injection (Mercox) and scanning electron microscope view after corrosion. Note the tortuous aspect (**arrows**) of branches of an artery (1) in the stratum radiatum of CA1. **Bar,** 100 μm

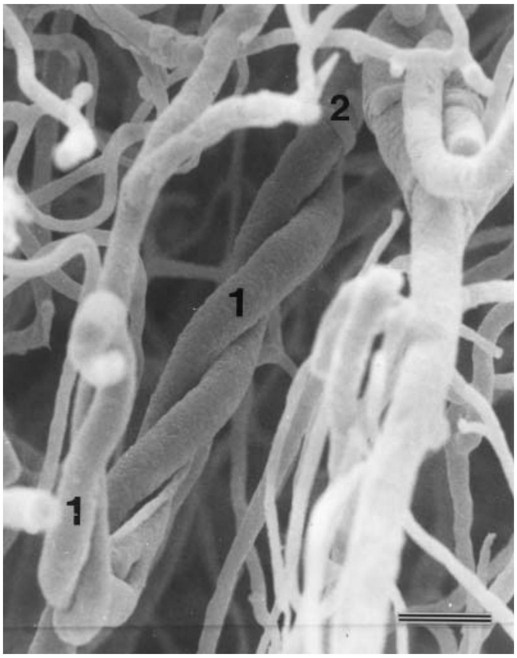

Fig. 79. Intravascular resin injection (Mercox) and scanning electron microscope view after corrosion. Coiling of branches (1) of an intrahippocampal artery (2). **Bar,** 38 μm

CHAPTER 6

Coronal, Sagittal and Axial Sections of the Hippocampus Showing its Relationships with the Surrounding Structures

(after intravascukar India ink injection)

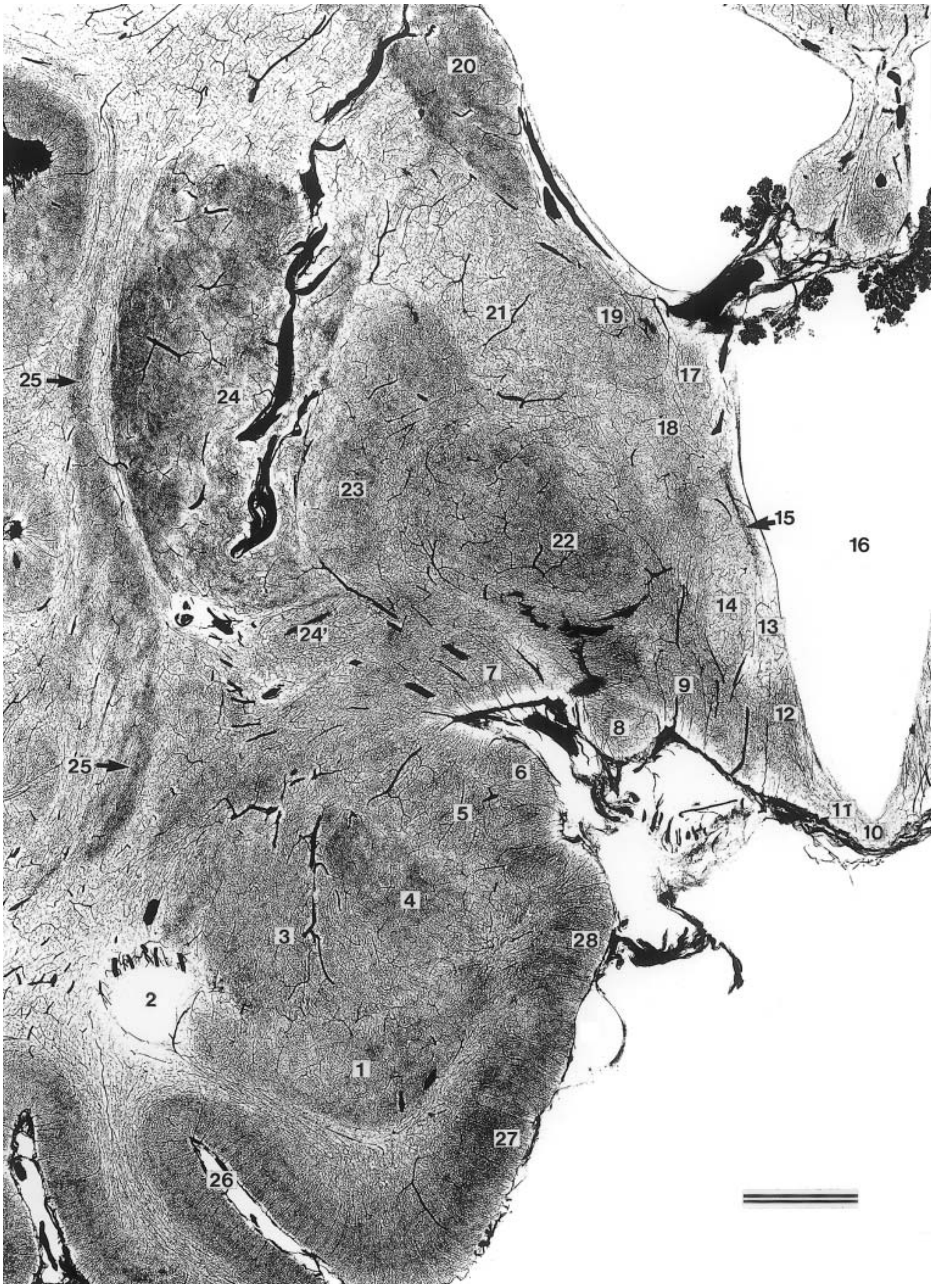

Fig 80. Coronal section of the brain. Vascular injection. Tentorium cerebelli removed. **Bar,** 4.3 mm. See Fig. 102 for precise description of the Hippocampus and MRI
1, hippocampal head; **2**, temporal horn;
Amygdala:
- **3** lateral nucleus,
- **4** basal nucleus,
- **5** accessory basal nucleus,
- **6** cortical nucleus;

7, anterior perforated substance; **8**, optic tract; **9**, lateral hypothalamus; **10**, posterior tuber; **11**, arcuate hypothalamic nucleus; **12**, ventromedial hypothalamic nucleus; **13**, dorsomedial hypothalamic nucleus; **14**, column of fornix; **15**, paraventricular hypothalamic nucleus; **16**, third ventricle; **17**, anterior thalamic nucleus; **18**, ventral anterior thalamic nucleus; **19**, thalamic reticular nucleus; **20**, caudate nucleus; **21**, genu of internal capsule; **22**, globus pallidus, medial part; **23**, globus pallidus lateral part; **24**, putamen; **24'**, anterior commissure; **25**, claustrum; **26**, collateral sulcus; **27**, parahippocampal gyrus; **28**, ambient gyrus

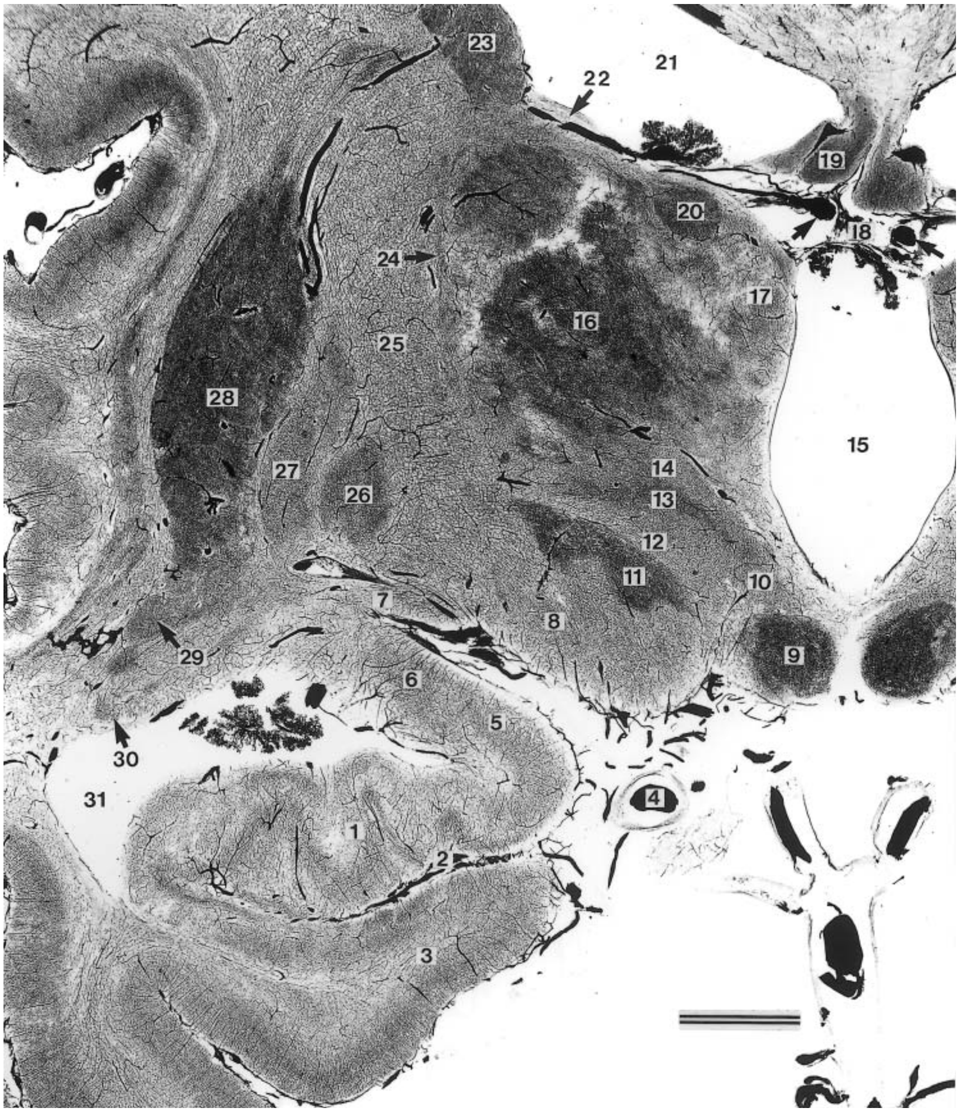

Fig. 81. Coronal section of the brain. Vascular injection. Tentorium cerebelli removed. **Bar,** 5.2 mm. See Fig. 103 for precise description of the Hippocampus and MRI
1, hippocampal head (digitationes hippocampi); **2**, uncal sulcus; **3**, parahippocampal gyrus; **4**, posterior cerebral artery; **5**, uncinate gyrus; **6**, amygdala (cortical nucleus); **7**, optic tract; **8**, crus cerebri; **9**, mamillary body; **10**, posterior hypothalamus; **11**, substantia nigra; **12**, H2 field of Forel; **13**, zona incerta; **14**, H1 field of Forel; **15**, third ventricle; **16**, ventral lateral thalamic nucleus; **17**, dorsomedial thalamic nucleus; **18**, median part of the transverse fissure (velum interpositum; arrows indicate the internal cerebral veins; **19**, fornix; **20**, anterior thalamic nucleus; **21**, body of lateral ventricle; **22**, lamina affixa; **23**, caudate nucleus; **24**, thalamic reticular nucleus; **25**, posterior limb of internal capsule; **26**, globus pallidus, medial part; **27**, globus pallidus, lateral part; **28**, putamen; **29**, peduncle of lentiform nucleus; **30**, tail of caudate nucleus; **31**, temporal horn of lateral ventricle

Fig. 82. Coronal section o the brain. Vascular injection. Tentorium cerebelli removed. **Bar,** 4.6 mm. See Fig. 104 for precise description of the Hippocampus and MRI
1, hippocampal head (digitationes hippocampi); **2**, uncal sulcus; **3**, parahippocampal gyrus; **4**, crural cistern; **5**, optic tract; **6**, crus cerebri; **7**, ventral part of pons; **8**, interpeduncular fossa (interpeduncular cistern); **9**, substantia nigra; **10**, red nucleus; **11**, subthalamic nucleus; **12**, third ventricle; **13**, dorsomedial thalamic nucleus; **14**, ventral lateral thalamic nucleus; **15**, anterior thalamic nucleus; **16**, median part of the transverse fissure (velum interpositum); **17**, fornix; **18**, corpus callosum; **19**, medial longitudinal stria; **20**, indusium griseum; **21**, lateral longitudinal stria; **22**, lateral ventricle; **23**, caudate nucleus; **24**, thalamic reticular nucleus; **25**, posterior limb of internal capsule; **26**, globus pallidus, medial part; **27**, globus pallidus, lateral part; **28**, putamen; **29**, peduncle of lentiform nucleus; **30**, tail of caudate nucleus

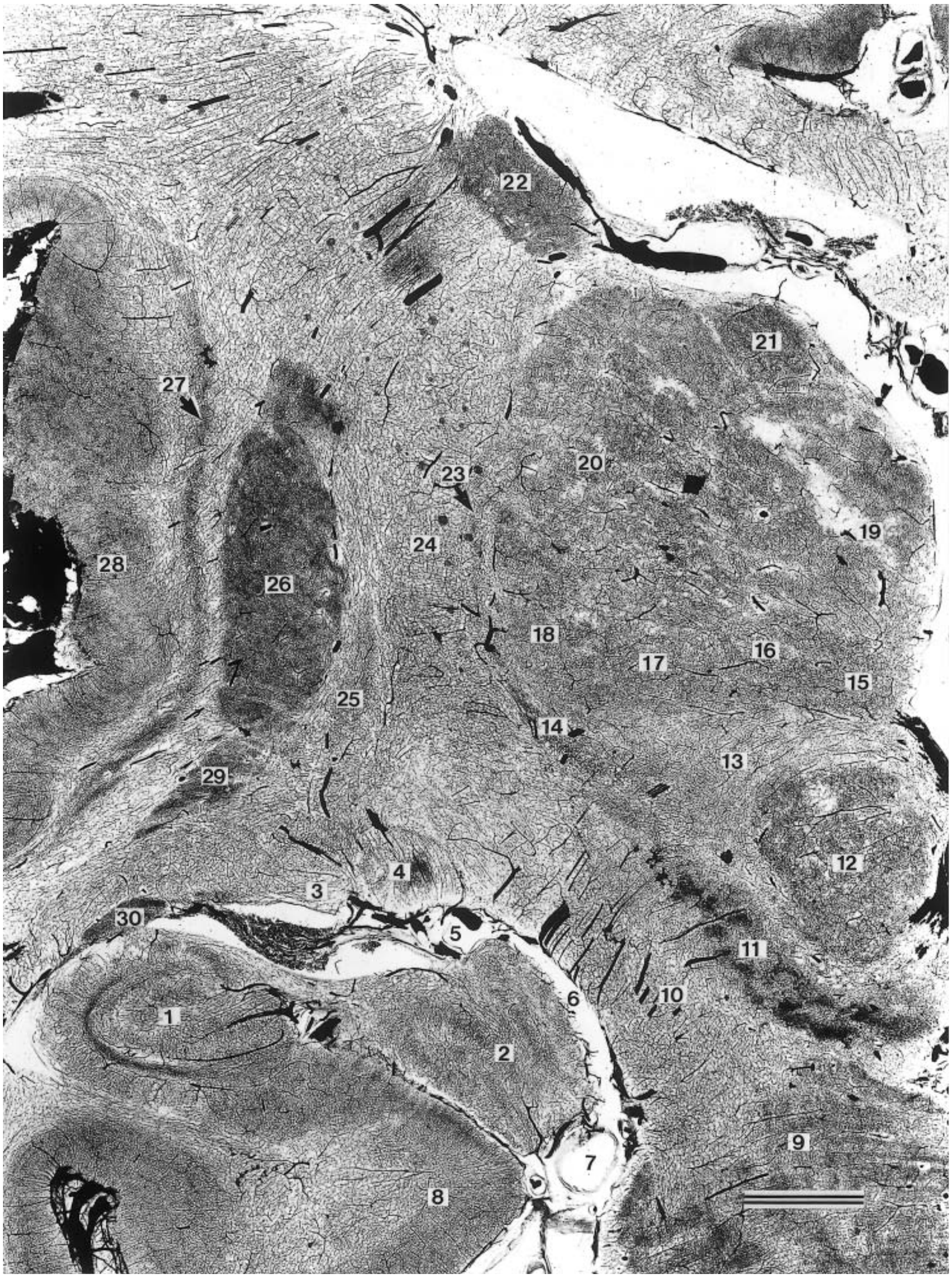

Fig. 83. Coronal section of the brain. Vascular injection. Tentorium cerebelli removed. **Bar,** 4.8 mm. See Fig. 105 for precise description of the Hippocampus and MRI
1, hippocampal body; **2**, uncal apex; **3**, stria terminalis; **4**, lateral geniculate body; **5**, transverse fissure; **6**, crural cistern; **7**, posterior cerebral artery; **8**, parahippocampal gyrus; **9**, ventral part of pons; **10**, crus cerebri; **11**, substantia nigra; **12**, red nucleus; **13**, medial lemniscus; **14**, zona incerta; **15**, Parafascicular nucleus; **16**, centromedian thalamic nucleus; **17**, ventral posteromedial thalamic nucleus; **18**, ventral posterolateral thalamic nucleus; **19**, dorsomedial thalamic nucleus; **20**, ventral lateral thalamic nucleus; **21**, lateral dorsal thalamic nucleus; **22**, caudate nucleus; **23**, thalamic reticular nucleus; **24**, posterior limb of internal capsule; **25**, globus pallidus, lateral part; **26**, putamen; **27**, claustrum; **28**, insula; **29**, peduncle of lentiform nucleus; **30**, tail of caudate nucleus

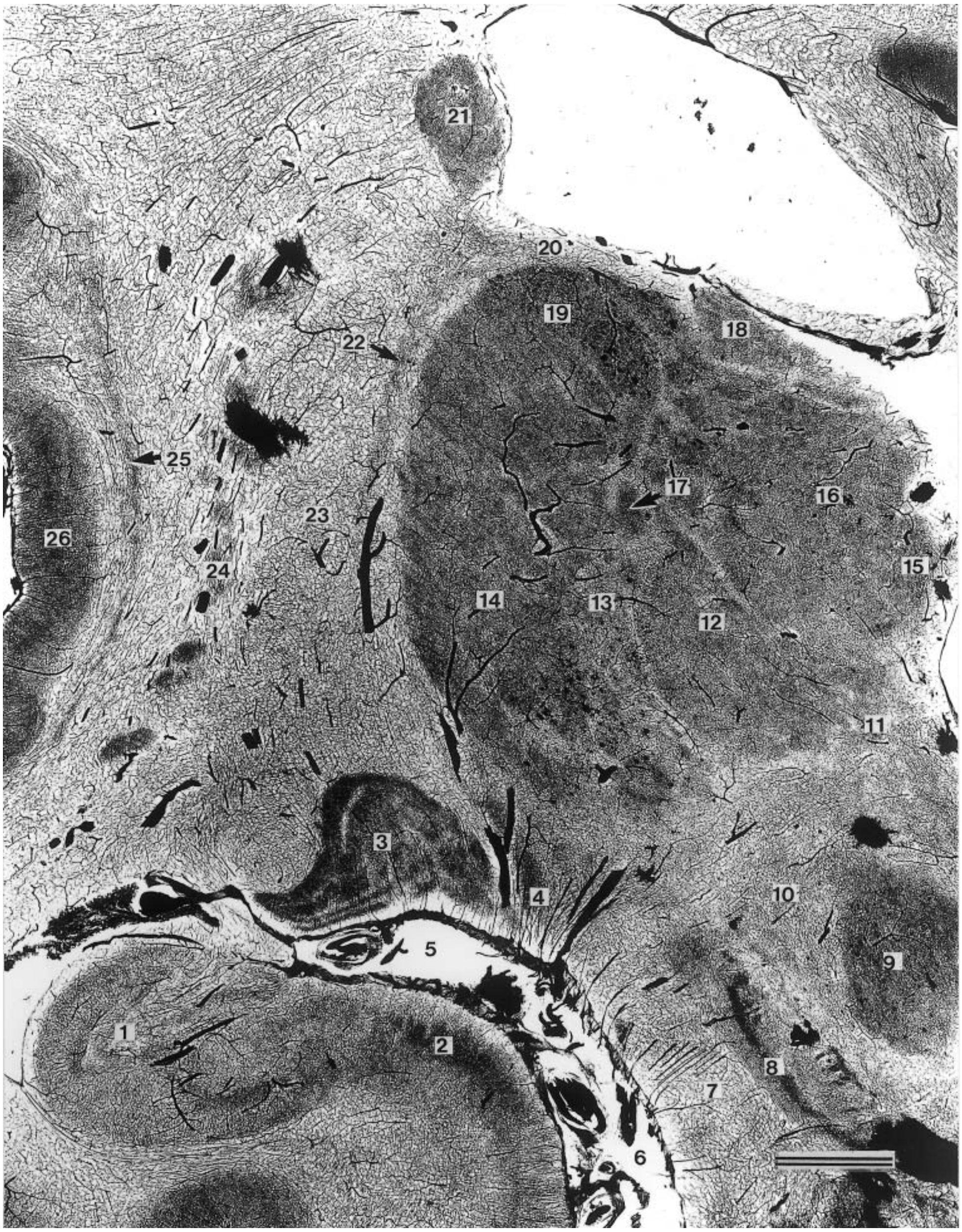

Fig. 84. Coronal section of the brain. Vascular injection. Tentorium cerebelli removed. **Bar,** 3.8 mm. See Fig. 106 for precise description of the Hippocampus and MRI
1, hippocampal body; **2**, parahippocampal gyrus (subiculum); **3**, lateral geniculate body; **4**, medial geniculate body; **5**, transverse fissure (lateral part); **6**, ambient cistern; **7**, crus cerebri; **8**, substantia nigra; **9**, red nucleus; **10**, medial lemniscus; **11**, parafascicular nucleus; **12**, centromedian thalamic nucleus; **13**, ventral posteromedial thalamic nucleus; **14**, ventral posterolateral thalamic nucleus; **15**, habenular nucleus; **16**, dorsomedial thalamic nucleus; **17**, intralaminar thalamic nuclei; **18**, lateral dorsal thalamic nucleus; **19**, lateral posterior thalamic nucleus; **20**, lamina affixa; **21**, caudate nucleus; **22**, thalamic reticular nucleus; **23**, posterior limb of internal capsule; **24**, pontes grisei caudatolenticulares; **25**, claustrum; **26**, insula

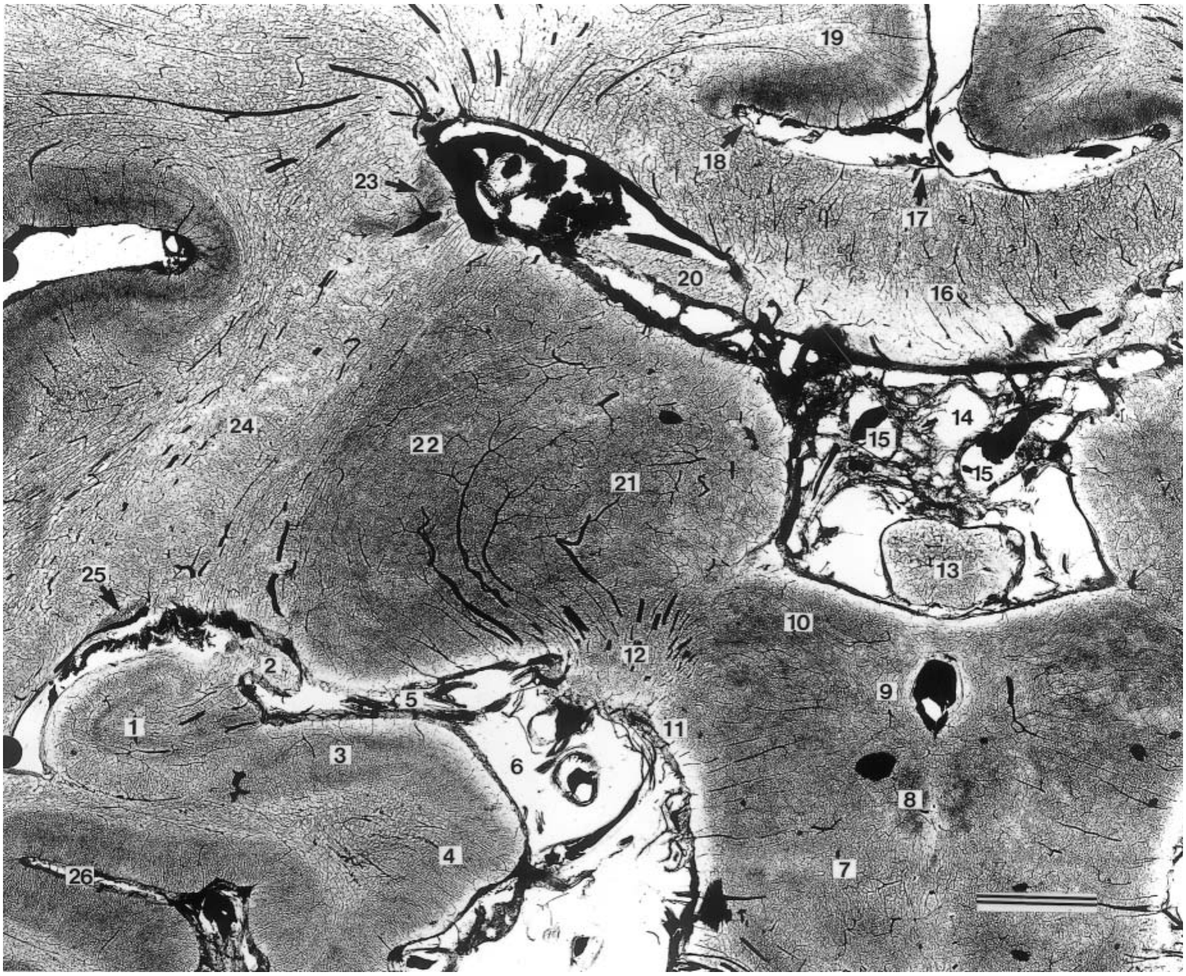

Fig. 85. Coronal section of the brain. Vascular injection. Tentorium cerebelli removed. **Bar,** 4.4 mm. See Fig. 107 for precise description of the Hippocampus and MRI
1, hippocampal body; **2**, fimbria; **3**, subiculum; **4**, parahippocampal gyrus; **5**, transverse fissure (lateral part); **6**, ambient cistern; **7**, brachium conjunctivum; **8**, oculomotor nucleus; **9**, periaqueductal grey matter; **10**, superior colliculus and pretectal area; **11**, inferior collicular brachium; **12**, superior collicular brachium; **13**, pineal gland; **14**, quadrigeminal cistern; **15**, internal cerebral veins; **16**, splenium; **17**, medial longitudinal stria; **18**, lateral longitudinal stria; **19**, cingulate gyrus; **20**, fornix; **21**, medial pulvinar; **22**, lateral pulvinar; **23**, caudate nucleus; **24**, retrolentiform part of internal capsule; **25**, tail of caudate nucleus; **26**, collateral sulcus

Fig. 86. Coronal section of the brain. Vascular injection. Tentorium cerebelli removed. **Bar,** 5.7 mm. See Fig. 108 for precise description of the Hippocampus and MRI
1, hippocampal tail; **2**, isthmus; **3**, anterior calcarine sulcus; **4**, parahippocampal gyrus (posterior part); **5**, cerebellar hemisphere; **6**, locus coeruleus; **7**, brachium conjunctivum; **8**, inferior colliculus; **9**, quadrigeminal cistern; **10**, internal cerebral veins; **11**, splenium; **12**, medial longitudinal stria; **13**, indusium griseum; **14**, lateral longitudinal stria; **15**, cingulate gyrus; **16**, atrium of lateral ventricle; **17**, optic radiations; **18**, caudate nucleus

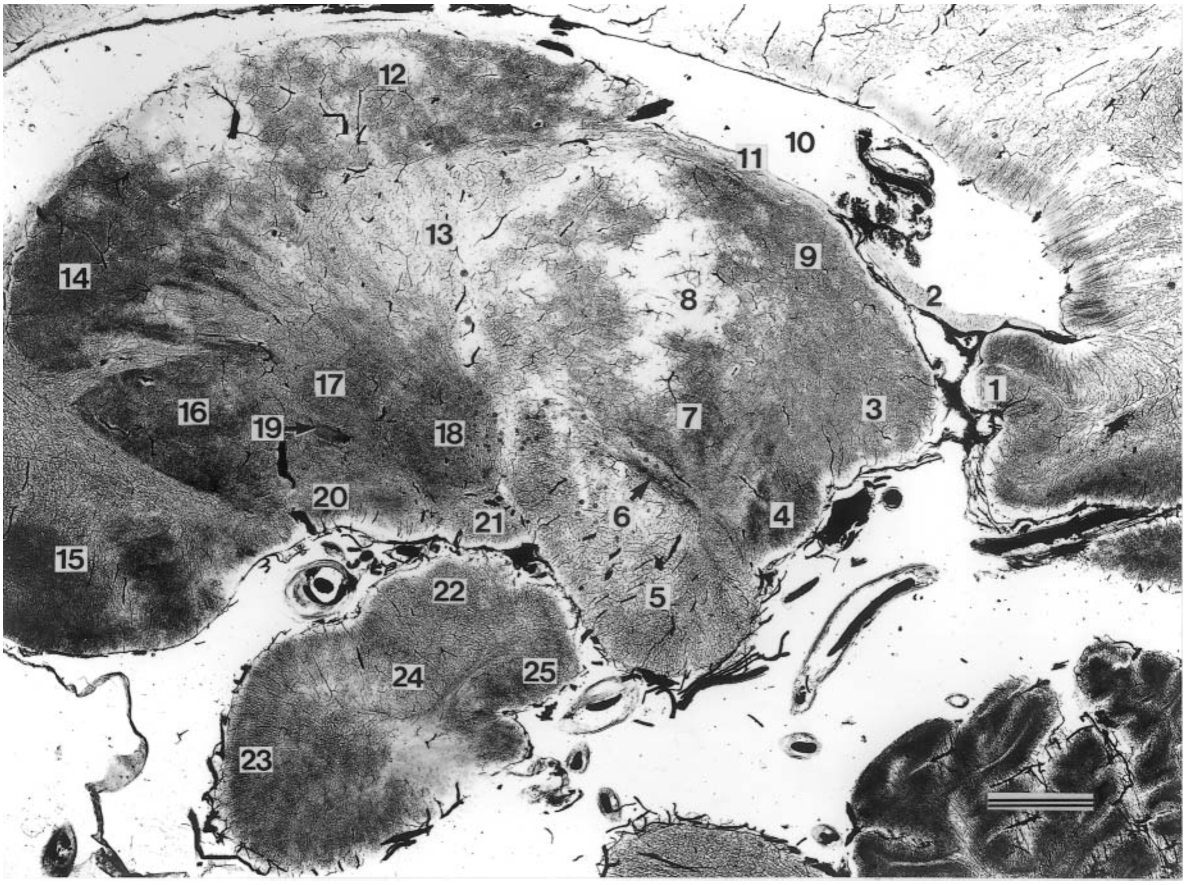

Fig. 87. Sagittal section of the brain. Vascular injection. Tentorium cerebelli removed. **Bar,** 4.8 mm. See Fig. 112 for precise description of the Hippocampus and MRI
1, hippocampal tail; **2**, crus of fornix; **3**, pulvinar; **4**, medial geniculate body; **5**, crus cerebri; **6**, zona incerta; **7**, ventral posterolateral thalamic nucleus; **8**, ventral lateral thalamic nucleus; **9**, lateral posterior thalamic nucleus; **10**, lateral ventricle; **11**, lamina affixa; **12**, caudate nucleus; **13**, internal capsule; **14**, head of caudate nucleus; **15**, medial orbital gyrus; **16**, putamen; **17**, globus pallidus, lateral part; **18**, globus pallidus, medial part; **19**, anterior commissure; **20**, anterior perforated substance; **21**, optic tract; **22**, cortical nucleus of amygdala; **23**, ambient gyrus; **24**, accessory basal nucleus of amygdala; **25**, uncinate gyrus (head of Hippocampus)

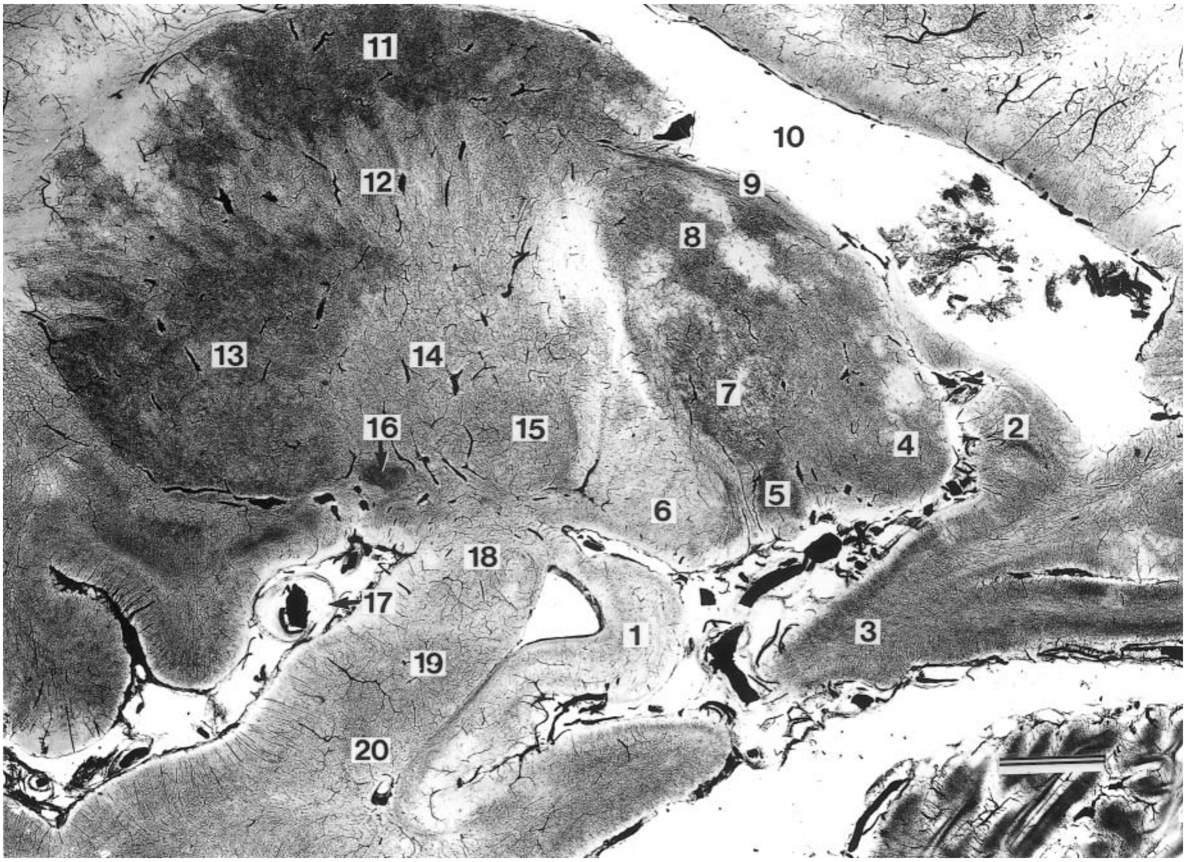

Fig. 88. Sagittal section of the brain. Vascular injection. Tentorium cerebelli removed. **Bar,** 4.8 mm. See Fig. 113 for precise description of the Hippocampus and MRI
1, hippocampal head; **2**, hippocampal tail; **3**, parahippocampal gyrus; **4**, pulvinar; **5**, medial geniculate body; **6**, crus cerebri; **7**, ventral posterolateral thalamic nucleus; **8**, lateral posterior thalamic nucleus; **9**, lamina affixa; **10**, lateral ventricle; **11**, caudate nucleus; **12**, anterior limb of internal capsule; **13**, putamen; **14**, globus pallidus, lateral part; **15**, globus pallidus, medial part; **16**, anterior commissure; **17**, middle cerebral artery; **18**, medial nucleus of amygdala; **19**, accessory basal nucleus of amygdala; **20**, basal nucleus of amygdala

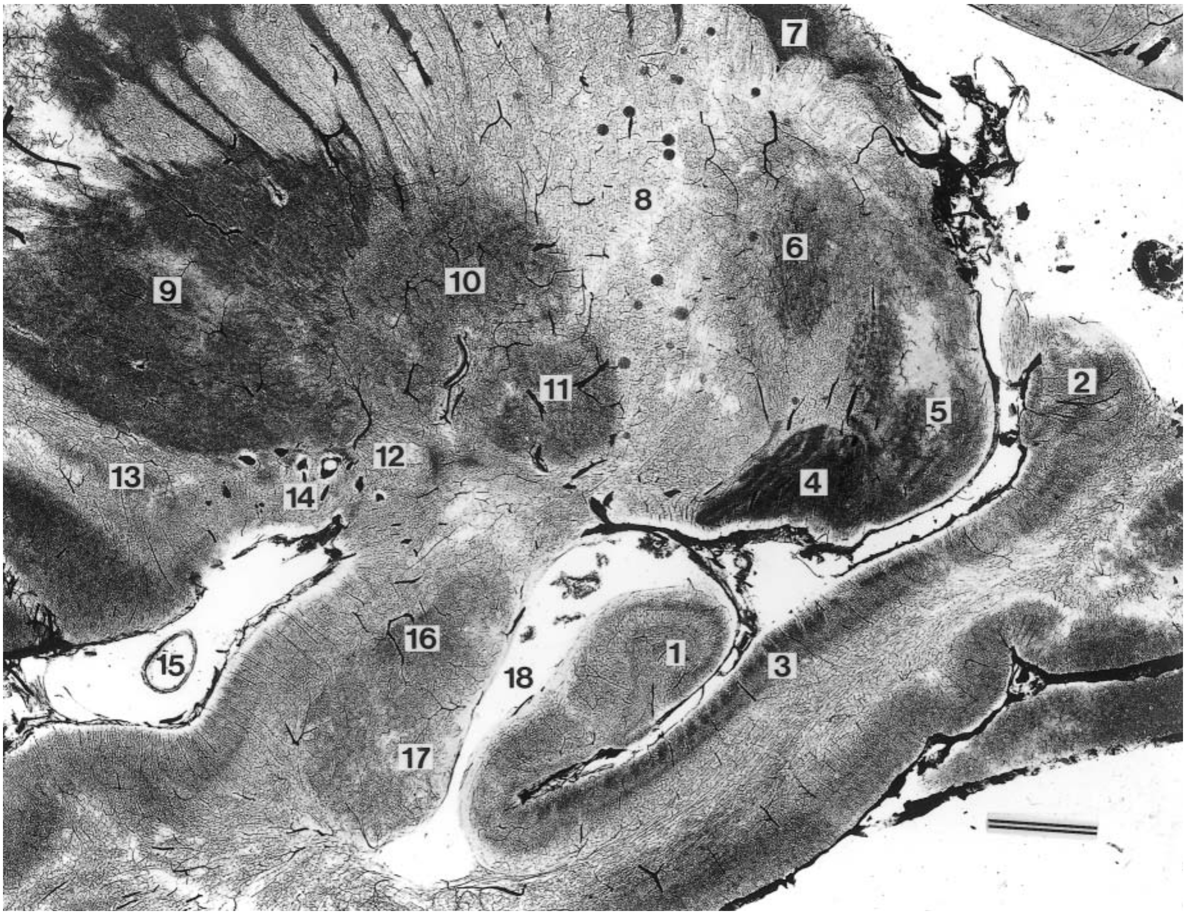

Fig. 89. Sagittal section of the brain. Vascular injection. Tentorium cerebelli removed. **Bar,** 4.8 mm. See Fig. 114 for precise description of the Hippocampus and MRI
1, hippocampal head; **2**, hippocampal tail; **3**, presubiculum (note the maculate aspect of the capillary network); **4**, lateral geniculate body; **5**, pulvinar; **6**, lateral posterior thalamic nucleus; **7**, caudate nucleus; **8**, posterior limb of internal capsule; **9**, putamen; **10**, globus pallidus, lateral part; **11**, globus pallidus, medial part; **12**, anterior commissure; **13**, claustrum; **14**, anterior perforated substance; **15**, middle cerebral artery; **16**, basal nucleus of amygdala; **17**, lateral nucleus of amygdala; **18**, temporal horn of lateral ventricle

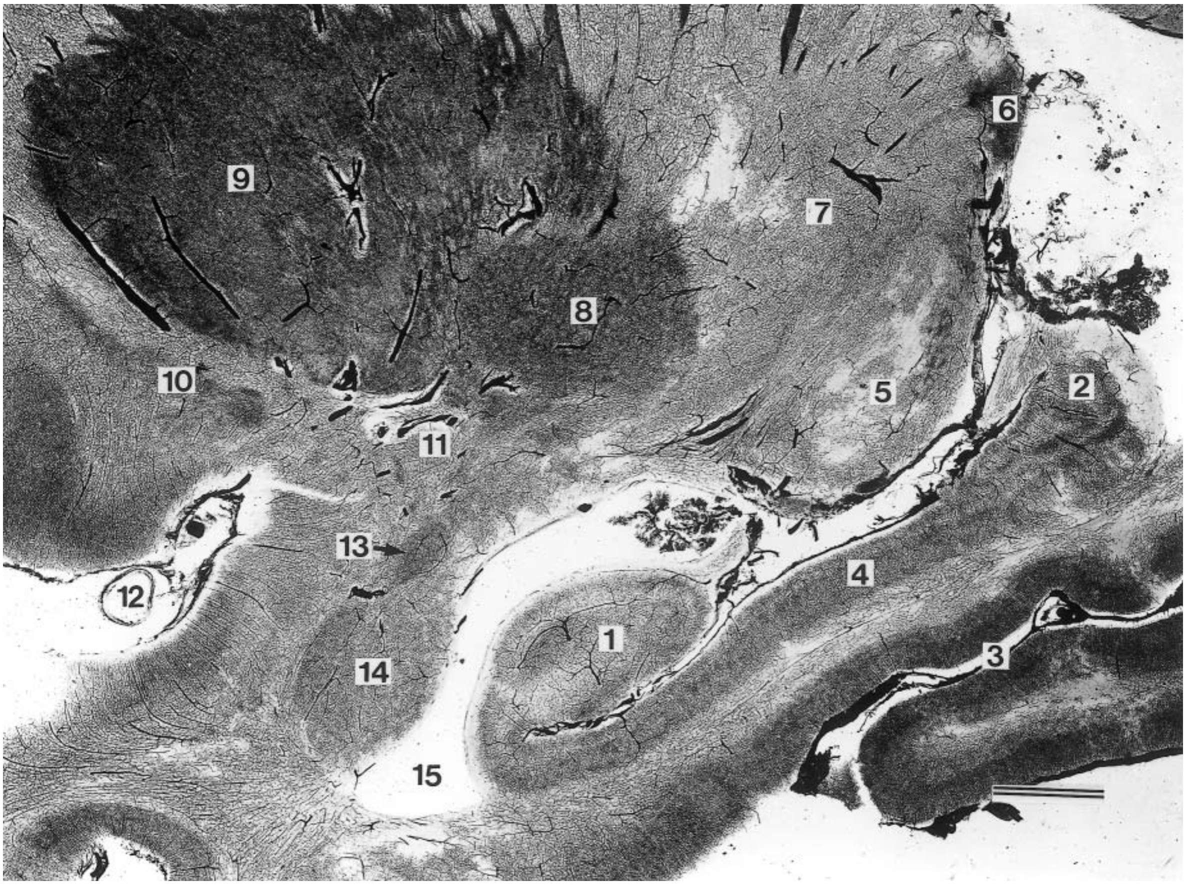

Fig. 90. Sagittal section of the brain. Vascular injection. Tentorium cerebelli removed. **Bar,** 5 mm. See Fig. 115 for precise description of the Hippocampus and MRI
1, hippocampal head; **2**, hippocampal tail; **3**, collateral sulcus; **4**, subiculum; **5**, pulvinar; **6**, caudate nucleus; **7**, retrolentiform part of internal capsule; **8**, globus pallidus, lateral part; **9**, putamen; **10**, claustrum; **11**, anterior commissure; **12**, middle cerebral artery; **13**, basal nucleus of amygdala; **14**, lateral nucleus of amygdala; **15**, temporal horn of lateral ventricle (uncal recess)

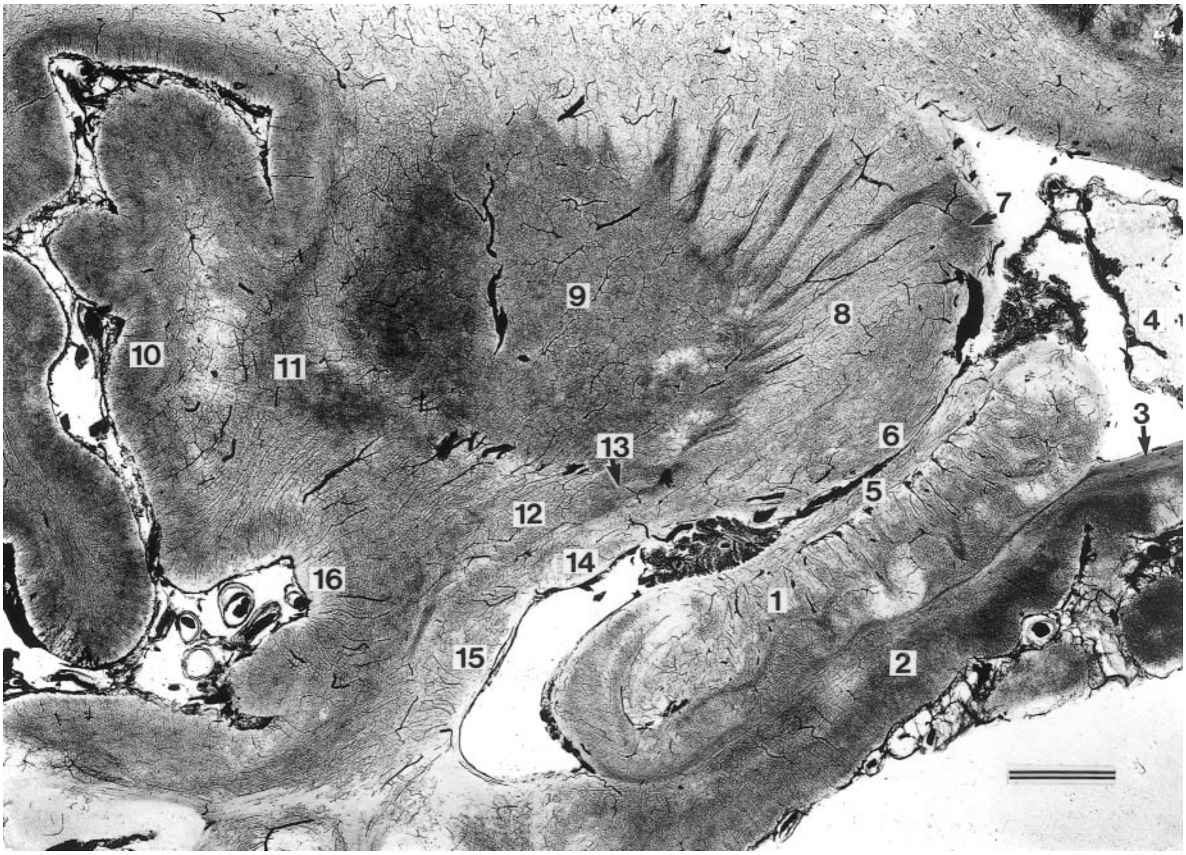

Fig. 91. Sagittal section of the brain. Vascular injection. Tentorium cerebelli removed. **Bar,** 5 mm. See Fig. 116 for precise description of the Hippocampus and MRI
1, hippocampus; **2**, parahippocampal gyrus; **3**, collateral trigone; **4**, atrium; **5**, fimbria; **6**, stria termalis; **7**, Caudate nucleus; **8**, retrolentiform part of internal capsule; **9**, putamen; **10**, insula; **11**, claustrum; **12**, anterior commissure, **13**, peduncle of lentiform nucleus; **14**, tail of caudate nucleus; **15**, lateral nucleus of amygdala; **16**, limen insulae

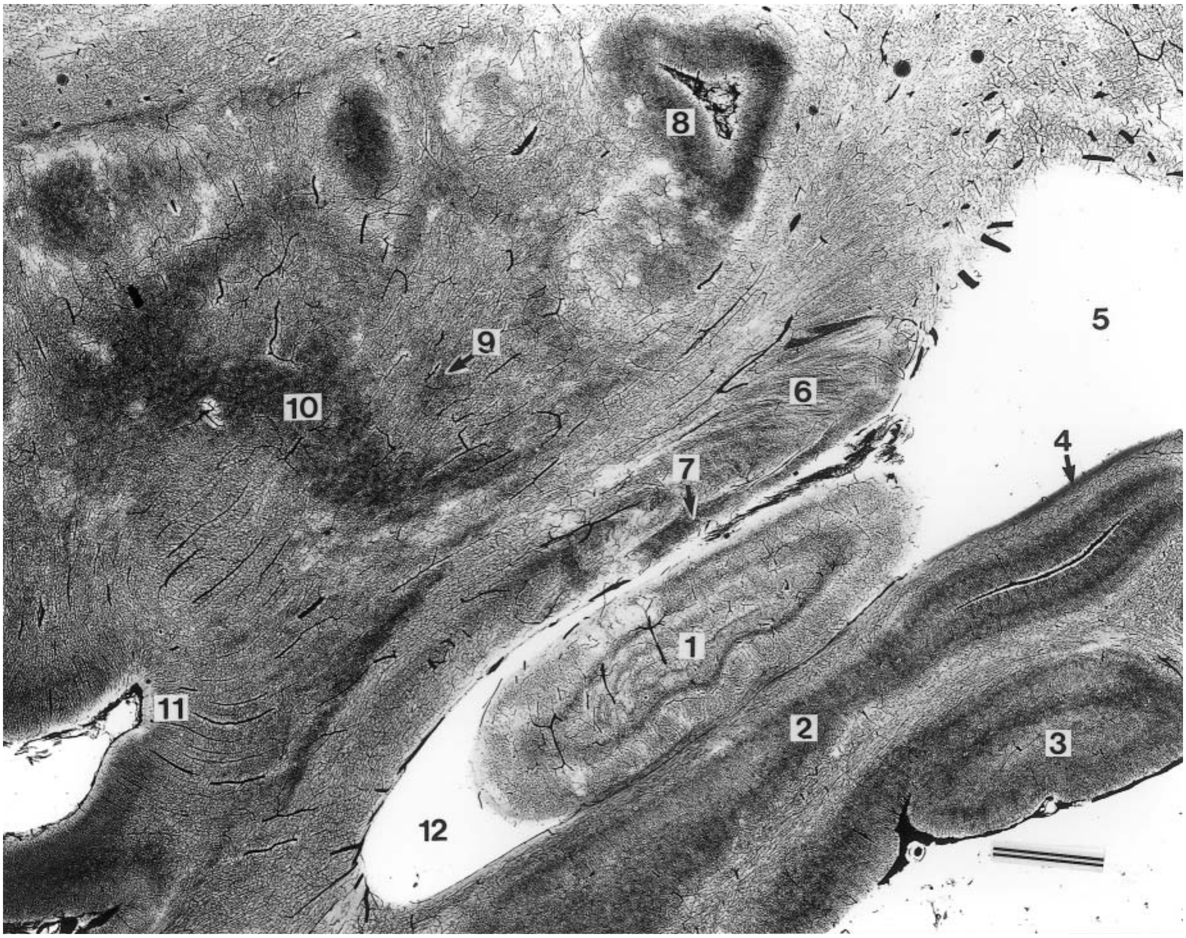

Fig. 92. Sagittal section of the brain. Vascular injection. Tentorium cerebelli removed. **Bar,** 4.3 mm. See Fig. 117 for precise description of the Hippocampus and MRI

1, hippocampal body; **2**, parahippocampal gyrus; **3**, fusiform gyrus; **4**, collateral trigone; **5**, atrium; **6**, optic radiations; **7**, caudate nucleus; **8**, insula; **9**, putamen; **10**, claustrum; **11**, limen insulae; **12**, temporal horn of the lateral ventricle

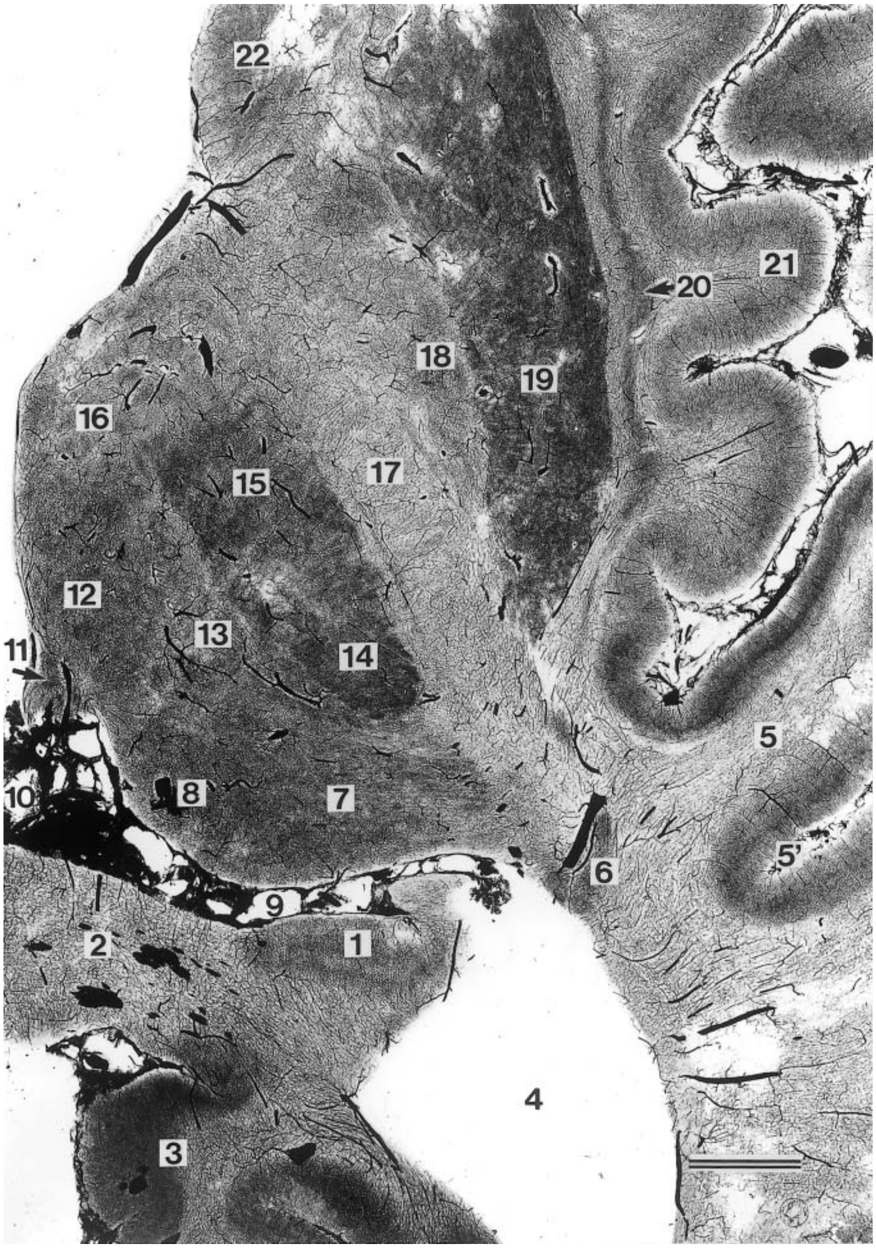

Fig. 93. Axial section of the brain. Vascular injection. **Bar,** 4.6 mm. See Fig. 119 for precise description of the Hippocampus and MRI
1, hippocampal tail; **2**, splenium; **3**, cingulate gyrus; **4**, occipital horn of lateral ventricle; **5**, superior temporal gyrus; **5′**, superior temporal sulcus; **6**, tail of caudate nucleus; **7**, lateral pulvinar; **8**, medial pulvinar; **9**, transverse fissure, lateral part; **10**, quadrigeminal cistern; **11**, habenular nucleus; **12**, dorsomedial thalamic nucleus; **13**, centromedian thalamic nucleus, **14**, ventral posterolateral thalamic nucleus, **15**, ventral lateral thalamic nucleus; **16**, anterior thalamic nucleus; **17**, internal capsule, posterior limb; **18**, globus pallidus, lateral part; **19**, putamen; **20**, claustrum; **21**, insula; **22**, head of the caudate nucleus

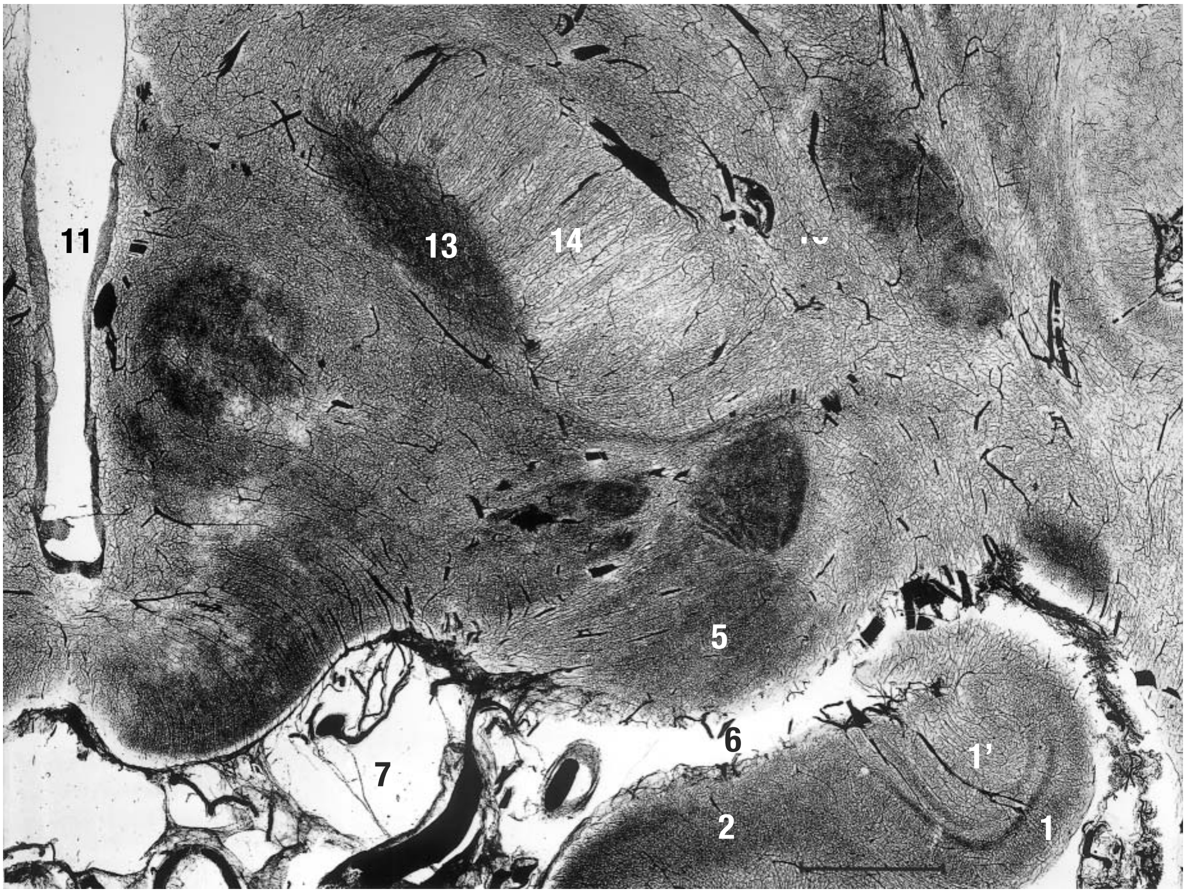

Fig. 94. Axial section of the brain. Vascular injection. **Bar,** 4.7 mm. See Fig. 120 for precise description of Hippocampus and MRI
1, hippocampal body, cornu ammonis; **1′**, hippocampal body, gyrus dentatus; **2**, parahippocampal gyrus; **3**, tail of caudate nucleus; **4**, stria terminalis; **5**, pulvinar; **6**, transverse fissure, lateral part; **7**, quadrigeminal cistern; **8**, superior colliculus; **9**, medial geniculate body; **10**, lateral geniculate body; **11**, third ventricle; **12**, red nucleus; **13**, subthalamic nucleus; **14**, internal capsule, posterior limb; **15**, globus pallidus, medial part; **16**, globus pallidus, lateral part; **17**, putamen; **18**, claustrum

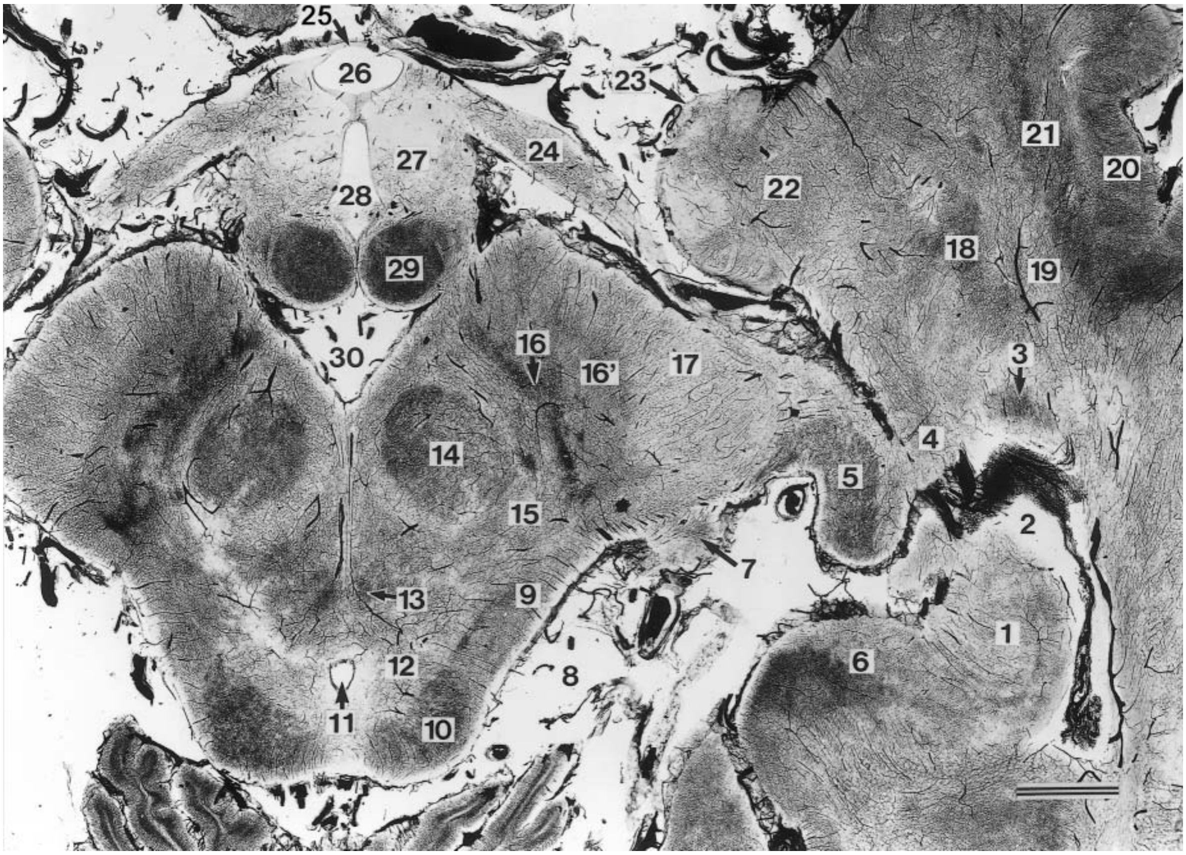

Fig. 95. Axial section of the brain. Vascular injection. **Bar,** 4.8 mm. See Fig. 121 for precise description of Hippocampus and MRI
1, hippocampal body; **2**, temporal horn of lateral ventricle; **3**, tail of caudate nucleus; **4**, stria terminalis; **5**, lateral geniculate body; **6**, parahippocampal gyrus; **7**, medial geniculate body; **8**, ambient cistern; **9**, lemniscal trigone; **10**, superior colliculus, **11**, cerebral aqueduct; **12**, periaqueductal grey matter; **13**, oculomotor nucleus; **14**, red nucleus; **15**, medial lemniscus; **16**, substantia nigra, pars compacta; **16'**, substantia nigra, pars reticulata; **17**, crus cerebri; **18**, putamen; **19**, external capsule; **20**, insula; **21**, claustrum; **22**, central nucleus of amygdala; **23**, semilunar gyrus; **24**, optic tract; **25**, lamina terminalis; **26**, Suprachiasmatic recess; **27**, tuber; **28**, third ventricle; **29**, mamillary body; **30**, interpeduncular cistern

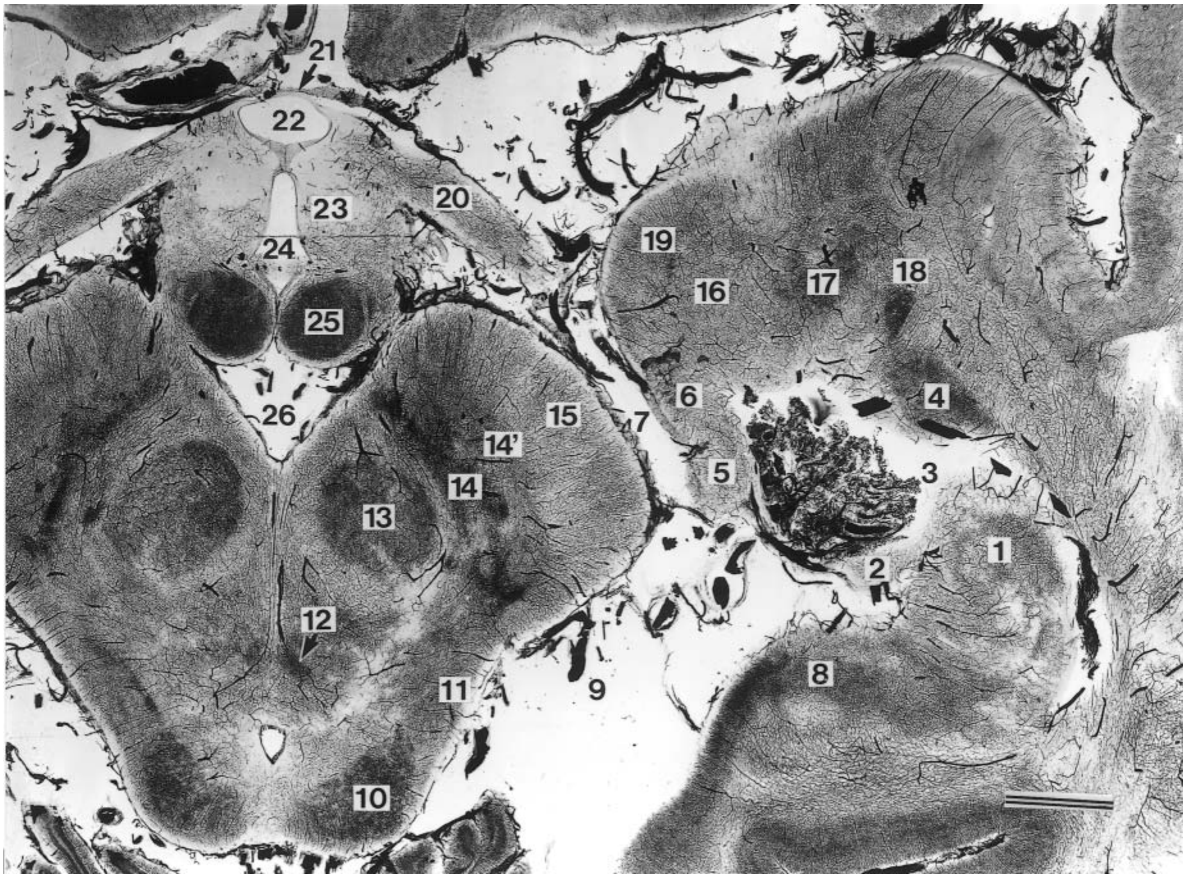

Fig. 96. Axial section of the brain. Vascular injection. **Bar,** 5 mm. See Fig. 122 for precise description of Hippocampus and MRI
1, hippocampal body and head (digitationes hippocampi); **2**, fimbria; **3**, temporal horn; **4**, tail of caudate nucleus; **5**, uncal apex; **6**, uncinate gyrus; **7**, crural cistern (artificially enlarged); **8**, parahippocampal gyrus; **9**, ambient cistern; **10**, superior colliculus; **11**, lemniscal trigone; **12**, oculomotor nucleus; **13**, red nucleus; **14**, substantia nigra, pars compacta; **14′**, substantia nigra, pars reticulata; **15**, crus cerebri; **16**, accessory basal nucleus of amygdala; **17**, basal nucleus of amygdala; **18**, lateral nucleus of amygdala; **19**, cortical nucleus of amygdala; **20**, optic tract; **21**, lamina terminalis; **22**, suprachiasmatic recess; **23**, tuber; **24**, third ventricle; **25**, mamillary body; **26**, interpeduncular cistern

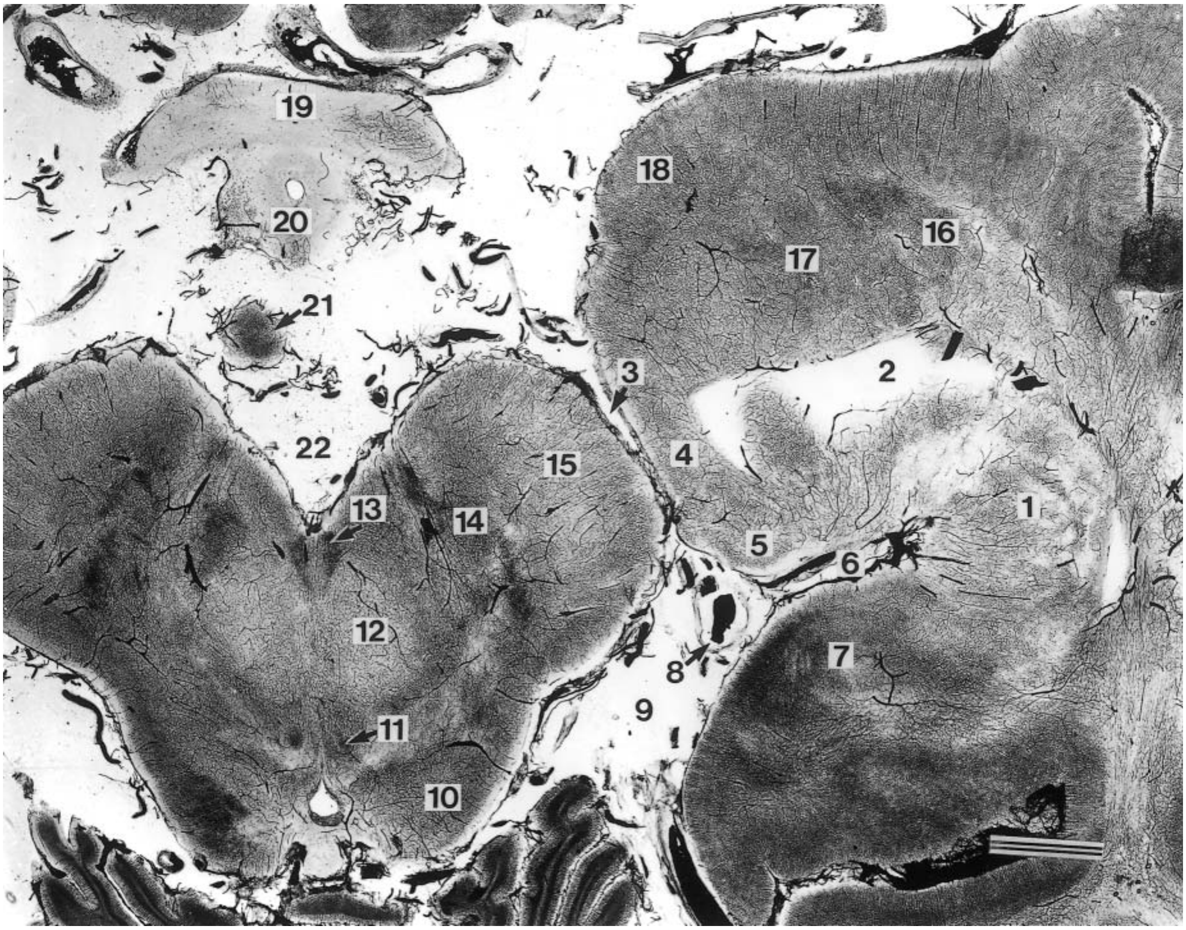

Fig. 97. Axial section of the brain. Vascular injection. **Bar,** 4.7 mm. See Fig. 123 for precise description of Hippocampus and MRI
1, hippocampal head (digitationes hippocampi); **2**, temporal horn (uncal recess); **3**, crural cistern; **4**, uncinate gyrus; **5**, uncal apex; **6**, uncal sulcus; **7**, parahippocampal gyrus; **8**, posterior cerebral artery; **9**, ambient cistern; **10**, inferior colliculus; **11**, trochlear nucleus; **12**, brachium conjunctivum; **13**, interpeduncular nucleus; **14**, substantia nigra; **15**, crus cerebri; **16**, lateral nucleus of amygdala; **17**, basal nucleus of amygdala; **18**, ambient gyrus; **19**, optic chiasma; **20**, infundibulum; **21**, mamillary body; **22**, interpeduncular cistern

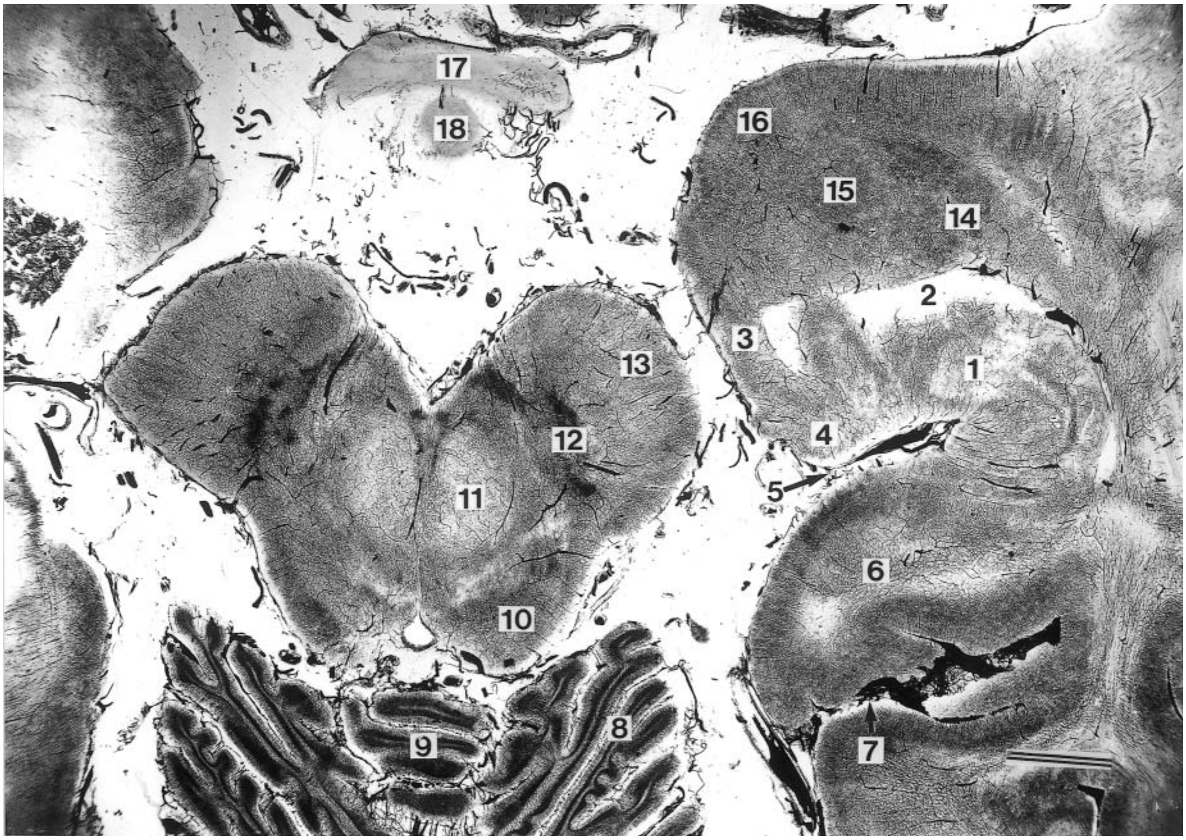

Fig. 98. Axial section of the brain. Vascular injection. **Bar**, 5.6 mm. See Fig. 124 for precise description of Hippocampus and MRI
1, hippocampal head (digitationes hippocampi); **2**, temporal horn of the lateral ventricle (uncal recess); **3**, uncinate gyrus; **4**, uncal apex; **5**, uncal sulcus; **6**, parahippocampal gyrus; **7**, collateral sulcus; **8**, cerebellar hemisphere; **9**, vermis; **10**, inferior colliculus; **11**, brachium conjunctivum; **12**, substantia nigra; **13**, crus cerebri; **14**, lateral nucleus of amygdala; **15**, basal nucleus of amygdala; **16**, ambient gyrus; **17**, optic chiasma; **18**, infundibulum

Sectional Anatomy and Magnetic Resonance Imaging

Coronal, sagittal, and axial sections according to the bicommissural plane, will be successively studied in 20 plates each composed of 4 pages, showing the plane of the section, details about structures, MRI views, and head section.

The following publications have aided identification of structures visible in the section: Sheps 1945; Olszewski 1952; Kuhlenbeck 1954; Riley 1960, Singer and Yakovlev 1964; Talairach and Szikla 1967; Andrew and Watkins 1969; Roberts and Hanaway 1970; Van Buren and Borke 1972; De Armond et al. 1974; Miller and Burack 1977; Duvernoy 1995a,b, 1999a,b; Dejerine 1980; Gluhbegovic and Williams 1980; Salamon and Huang 1980; Koritké and Sick 1982; Unsöld et al. 1982; Braak and Braak 1983; Haines 1987; Naidich et al. 1987; Talairach and Tournoux 1988; Mark et al. 1993.

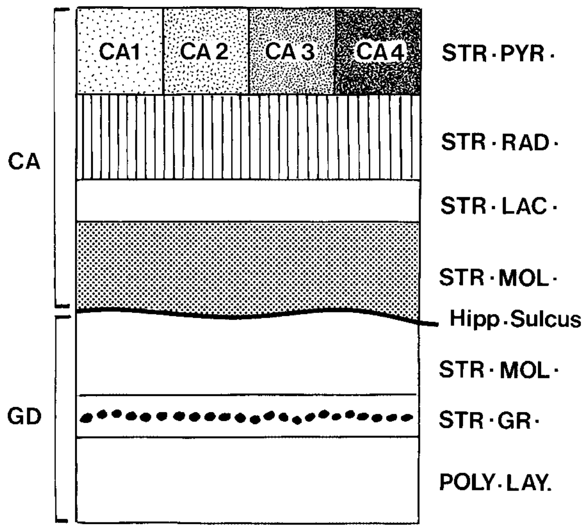

Fig. 99. Structure of the hippocampus
CA, cornu Ammonis; **STR. PYR.**, stratum pyramidale; **STR. RAD.**, stratum radiatum; **STR. LAC.**, stratum lacunosum; **STR. MOL.**, stratum moleculare; **Hipp. Sulcus**, vestigial intrahippocampal sulcus; **GD**, gyrus dentatus; **STR. MOL.**, stratum moleculare; **STR. GR.**, stratum granulosum; **POLY. LAY.**, polymorphic layer

7.1 Coronal Sections

Figures 102 – 109 show sections of the hippocampus from anterior to posterior levels.

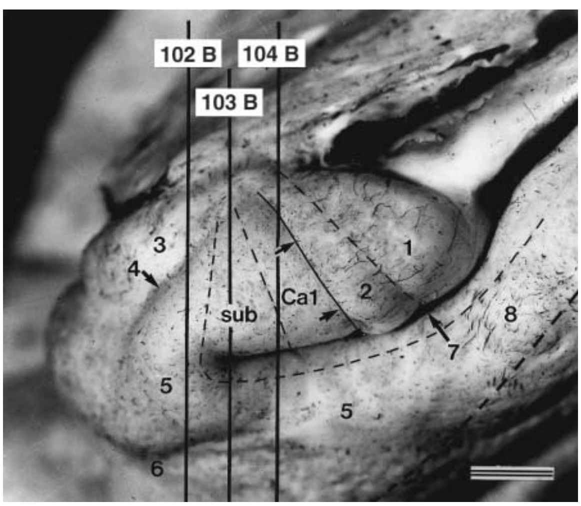

Fig. 100. Medial surface of the uncus. This preparation is an indication of the position of CA1 and the subiculum (**sub**), visible in Figs. 102B, 103B, and 104B. **Arrows** show the superficial hippocampal sulcus. **Bar**, 4.4 mm
1, uncal apex; **2**, band of Giacomini; **3**, semilunar gyrus; **4**, semianular sulcus; **5**, possible situation of the entorhinal area; **6**, uncal notch; **7**, uncal sulcus; **8**, parahippocampal gyrus

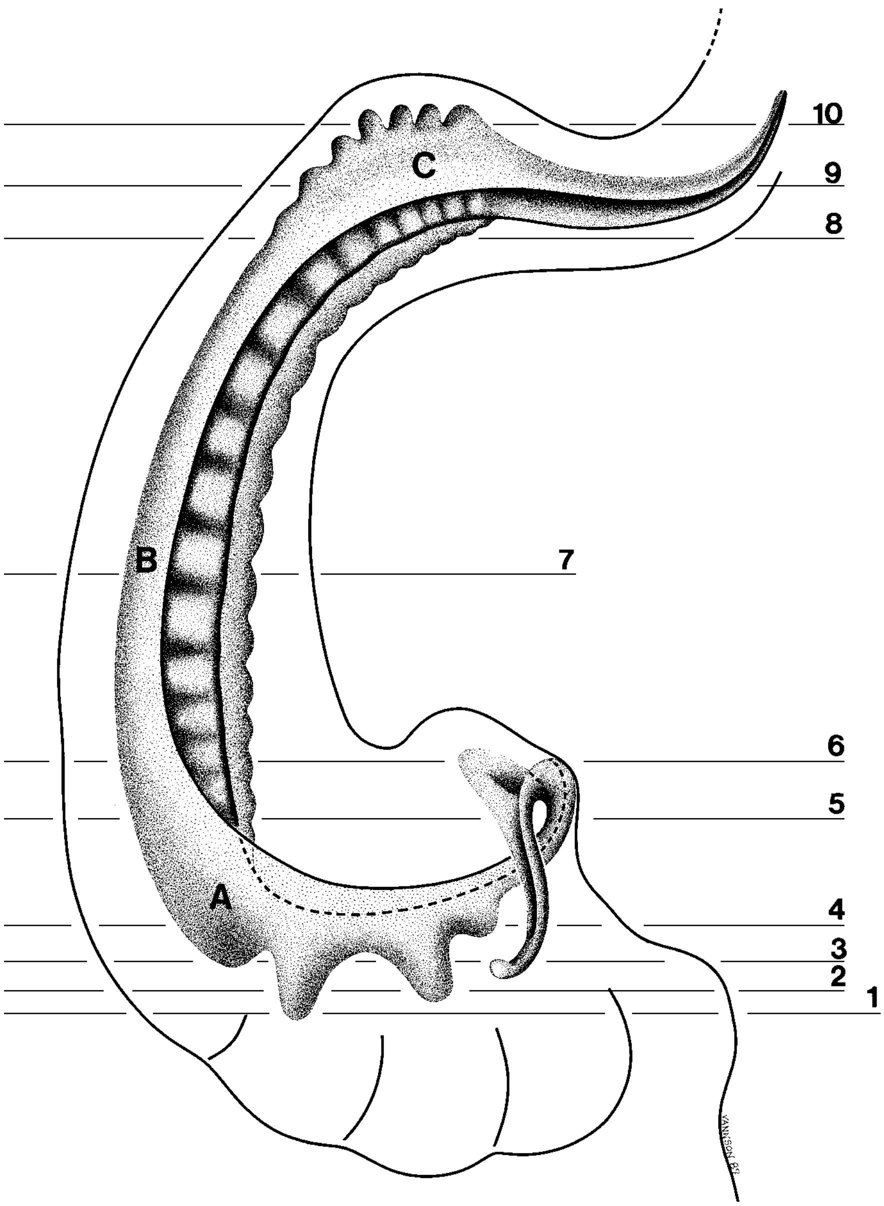

Fig. 101. A, B General position of the gyrus dentatus in the head (**A**), body (**B**), and tail (**C**) of the hippocampus **1–10**, Successive planes of coronal sections are shown in **B**

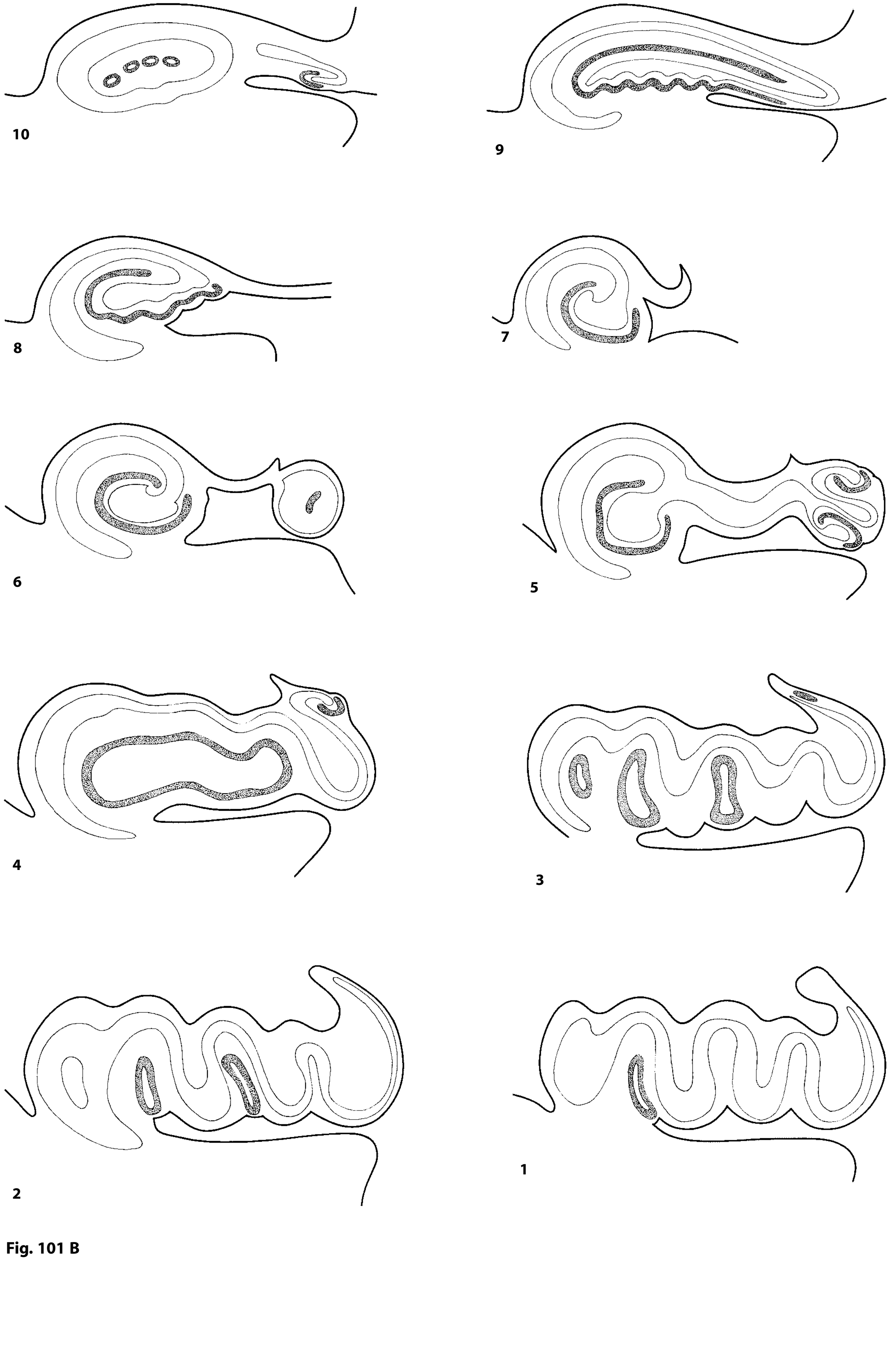

Fig. 101 B

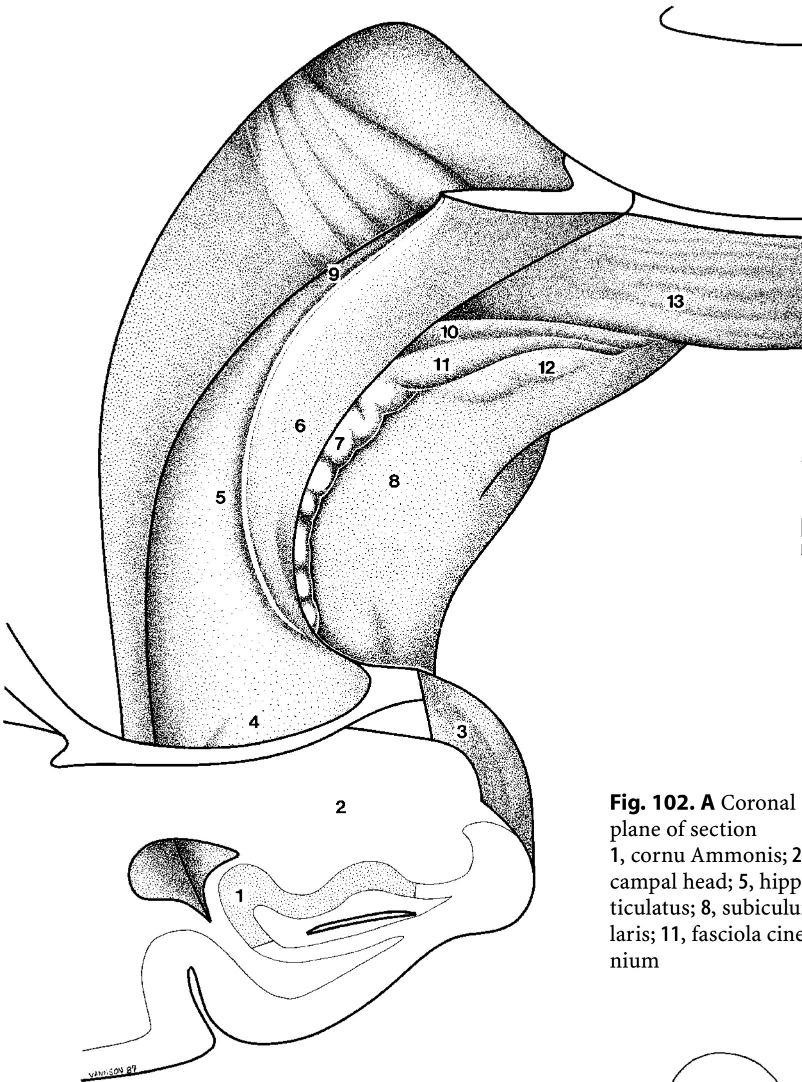

Fig. 102. A Coronal section of hippocampal head, showing plane of section
1, cornu Ammonis; **2**, amygdala; **3**, semilunar gyrus; **4**, hippocampal head; **5**, hippocampal body; **6**, fimbria; **7**, margo denticulatus; **8**, subiculum; **9**, hippocampal tail; **10**, gyrus fasciolaris; **11**, fasciola cinerea; **12**, gyri of Andreas Retzius; **13**, splenium

Fig. 102. Coronal section of hippocampal head
B explanatory diagram
B′ intravascular india ink injection
B″ 9.4T MRI view
1, cornu Ammonis (CA1); **2**, subiculum; **3**, uncal sulcus; **4**, parahippocampal gyrus; **5**, uncal notch; **6**, ambient gyrus and entorhinal area (see Fig. 100); **7**, cortical nucleus of amygdala; **7′**, semilunar gyrus; **7″**, semianular sulcus; **8**, endorhinal sulcus; **9**, medial nucleus of amygdala; **10**, central nucleus of amygdala; **11**, accessory basal nucleus of amygdala; **12**, basal nucleus of amygdala; **13**, lateral nucleus of amygdala; **14**, temporal horn of lateral ventricle

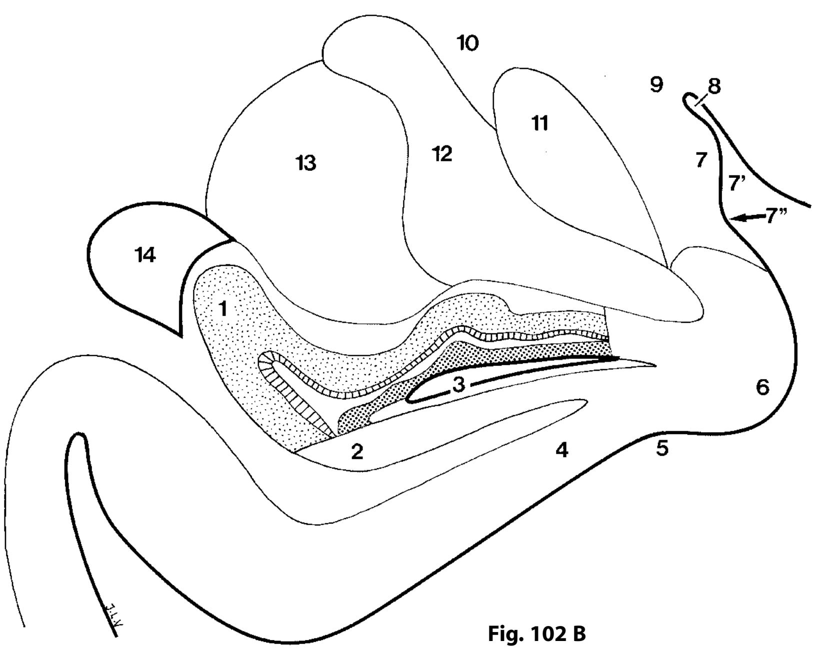

Fig. 102 B

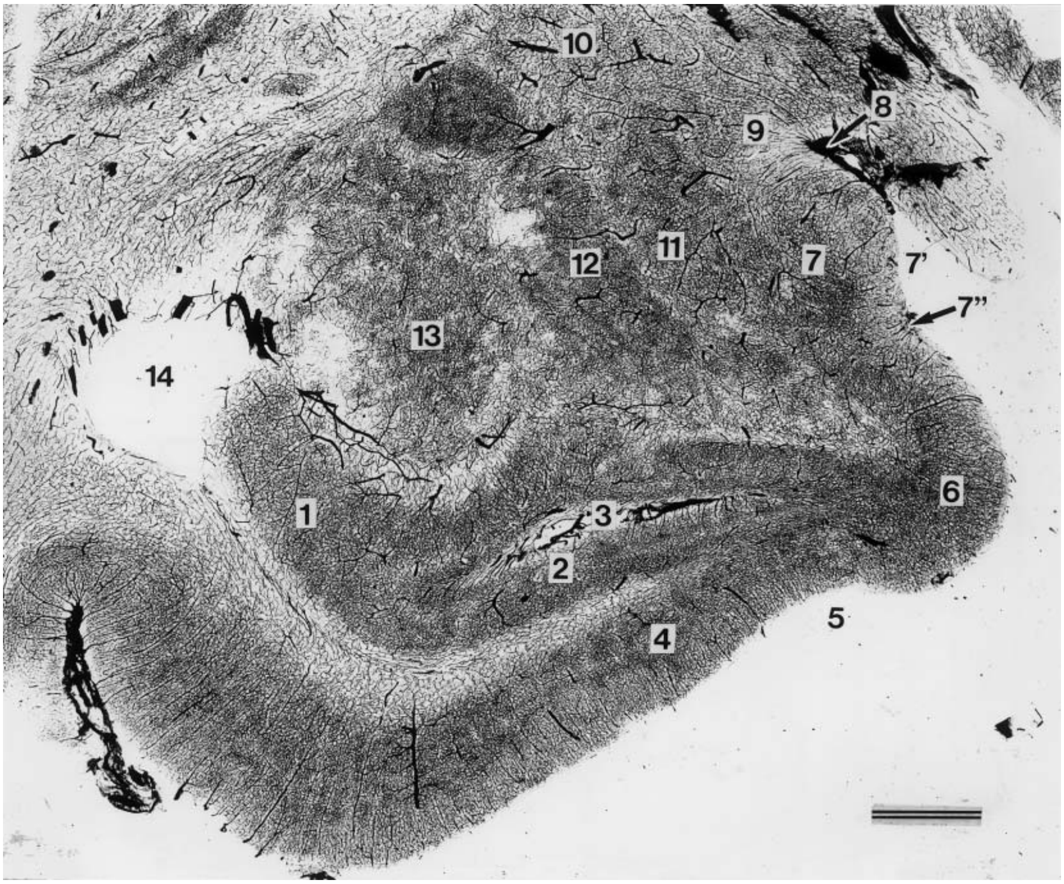

Fig. 102 B′. Bar, 2,2 mm

Fig. 102. B″ 9.4T MRI view

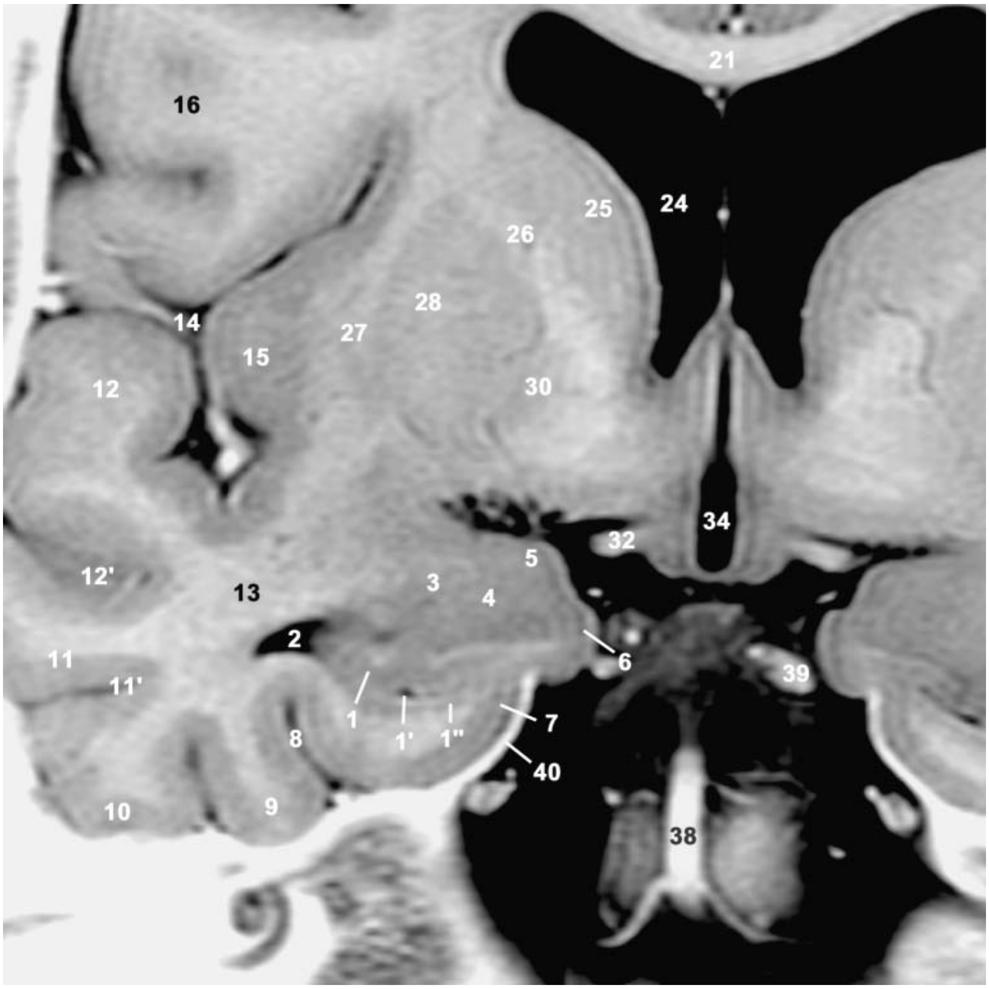

Fig. 102. C 3T MRI view

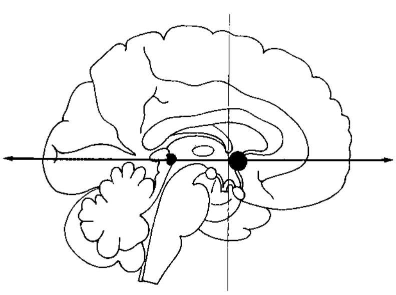

1, hippocampal head; **1′**, uncal sulcus; **1″**, subiculum; **2**, temporal (inferior) horn of the lateral ventricle; **3**, lateral nucleus of amygdala; **4**, basal nucleus of amygdala; **5**, cortical nucleus of amygdala; **6**, ambient gyrus; **7**, parahippocampal gyrus; **8**, collateral sulcus; **9**, fusiform gyrus; **10**, inferior temporal gyrus; **11**, middle temporal gyrus; **11′**, inferior temporal sulcus; **12**, superior temporal gyrus; **12′**, superior temporal sulcus; **13**, temporal stem; **14**, lateral fissure; **15**, insula; **16**, precentral gyrus; **17**, middle frontal gyrus; **18**, superior frontal gyrus; **19**, cingulate sulcus; **20**, cingulate gyrus; **21**, corpus callosum; **22**, fornix; **23**, anterior commissure, median part; **24**, frontal horn of the lateral ventricle; **25**, caudate nucleus; **26**, internal capsule, genu; **27**, claustrum; **28**, putamen; **29**, globus pallidus, lateral part; **30**, globus pallidus, medial part; **31**, anterior commisure, lateral part; **32**, optic tract; **33**, column of fornix; **34**, third ventricle; **35**, internal carotid artery; **36**, articular disc of the temporomandibular joint; **37**, mandibular condyle; **38**, basilar artery; **39**, posterior cerebral artery; **40**, tentorium cerebelli

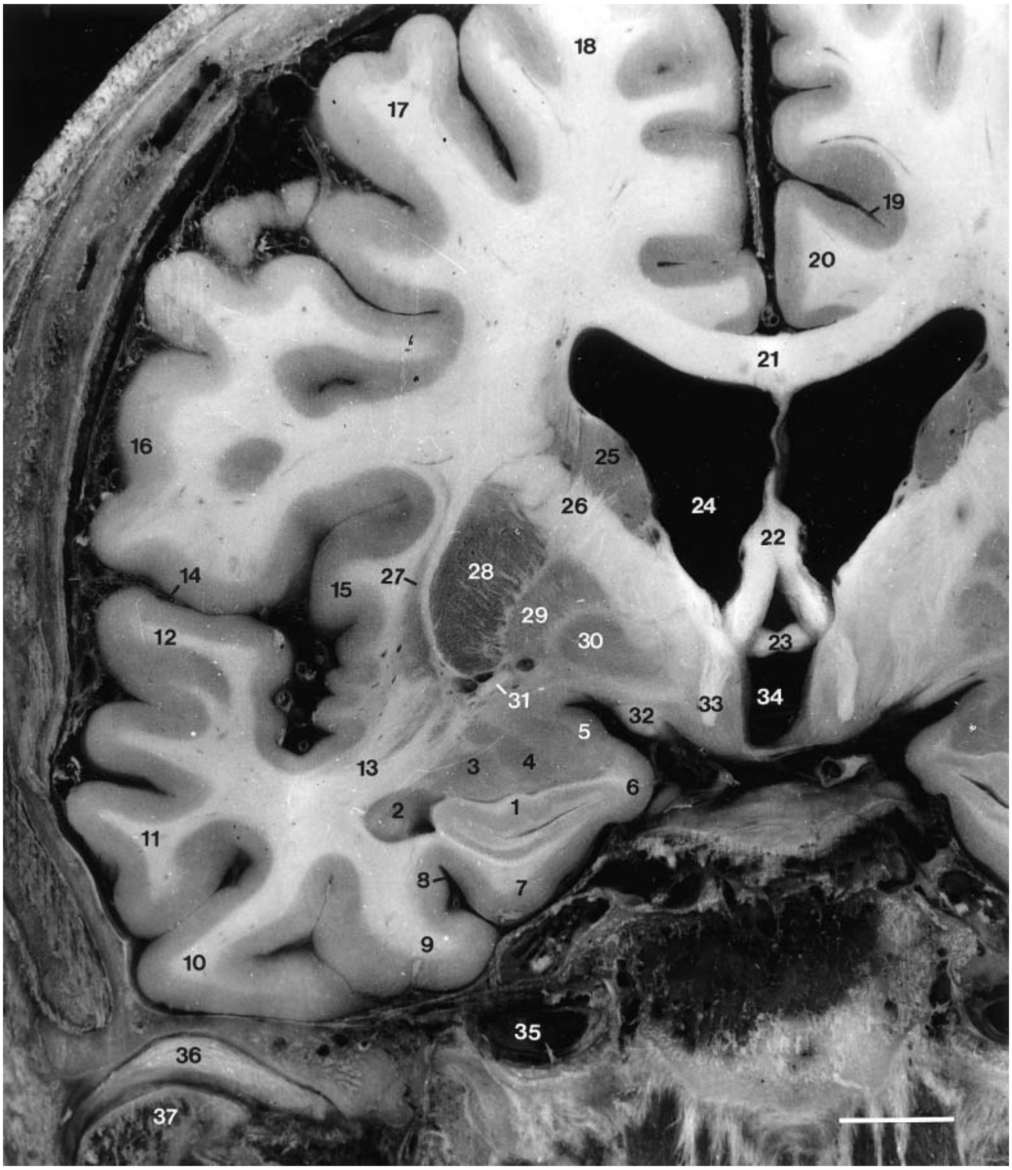

Fig. 102. D Coronal head section (posterior view of the section). **Bar**, 10 mm

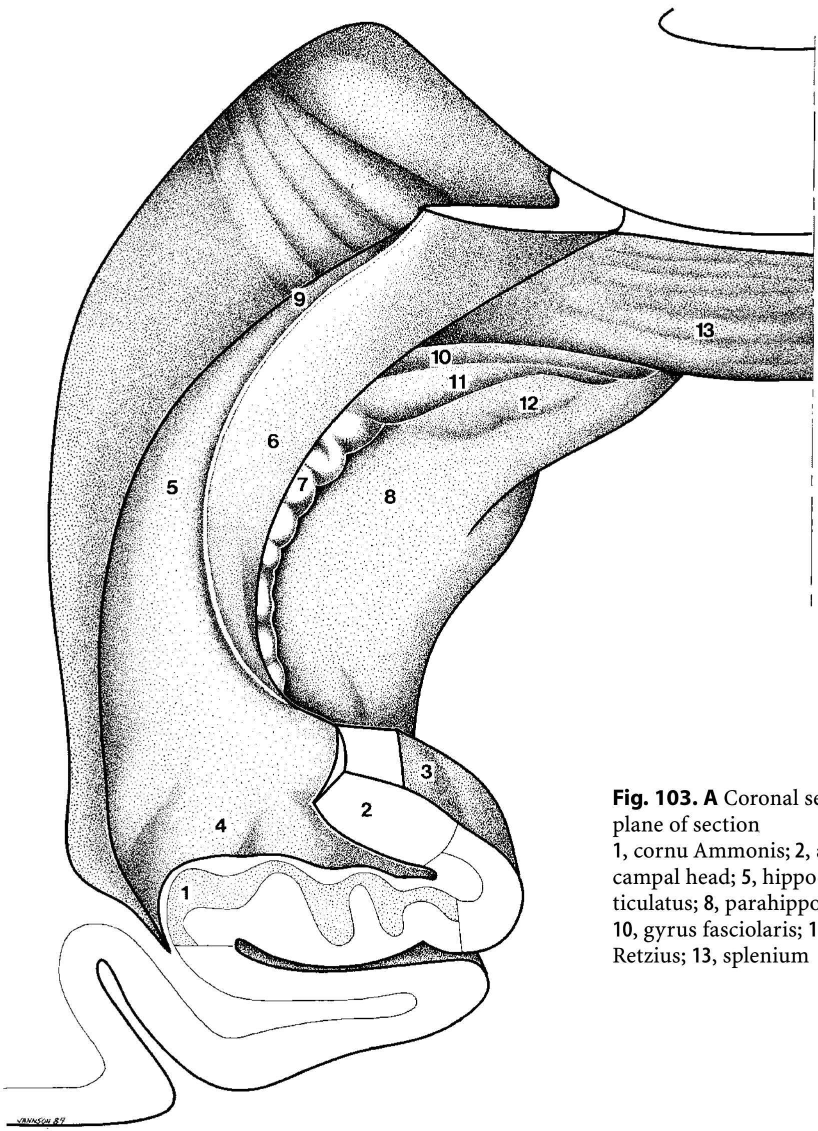

Fig. 103. A Coronal section of hippocampal head, showing plane of section
1, cornu Ammonis; 2, amygdala; 3, semilunar gyrus; 4, hippocampal head; 5, hippocampal body; 6, fimbria; 7, margo denticulatus; 8, parahippocampal gyrus; 9, hippocampal tail; 10, gyrus fasciolaris; 11, fasciola cinerea; 12, gyri of Andreas Retzius; 13, splenium

Fig. 103. Coronal section of hippocampal head
B explanatory diagram
B′ intravascular india ink injection
B″ 9.4T MRI view
1, cornu Ammonis (CA1); 1′, internal digitations (digitationes hippocampi); 2, subiculum; 3, parahippocampal gyrus; 4, uncal sulcus; 5, subiculum in uncinate gyrus (see Fig. 100); 6, accessory basal nucleus of amygdala; 7, cortical nucleus of amygdala; 8, temporal horn; 9, tail of caudate nucleus; 10, lateral nucleus of amygdala; 11, basal nucleus of amygdala; 12, cortical nucleus of amygdala

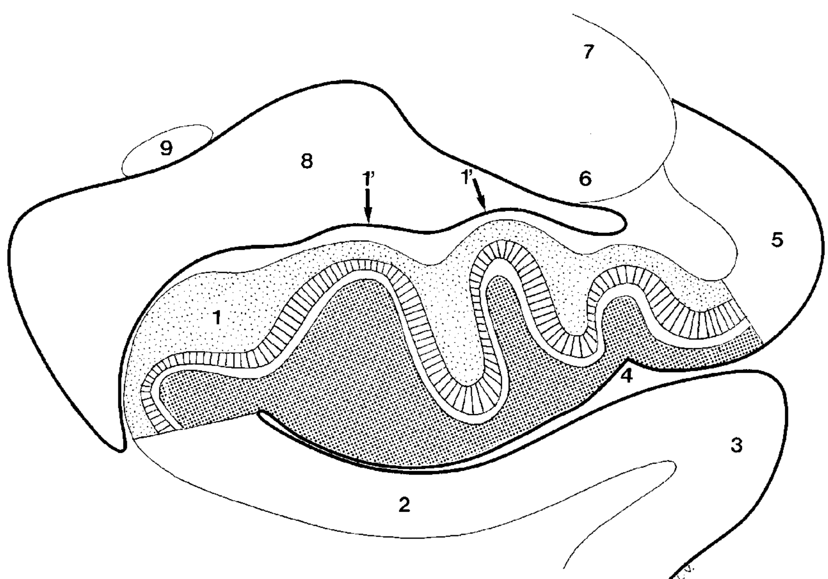

Fig. 103 B

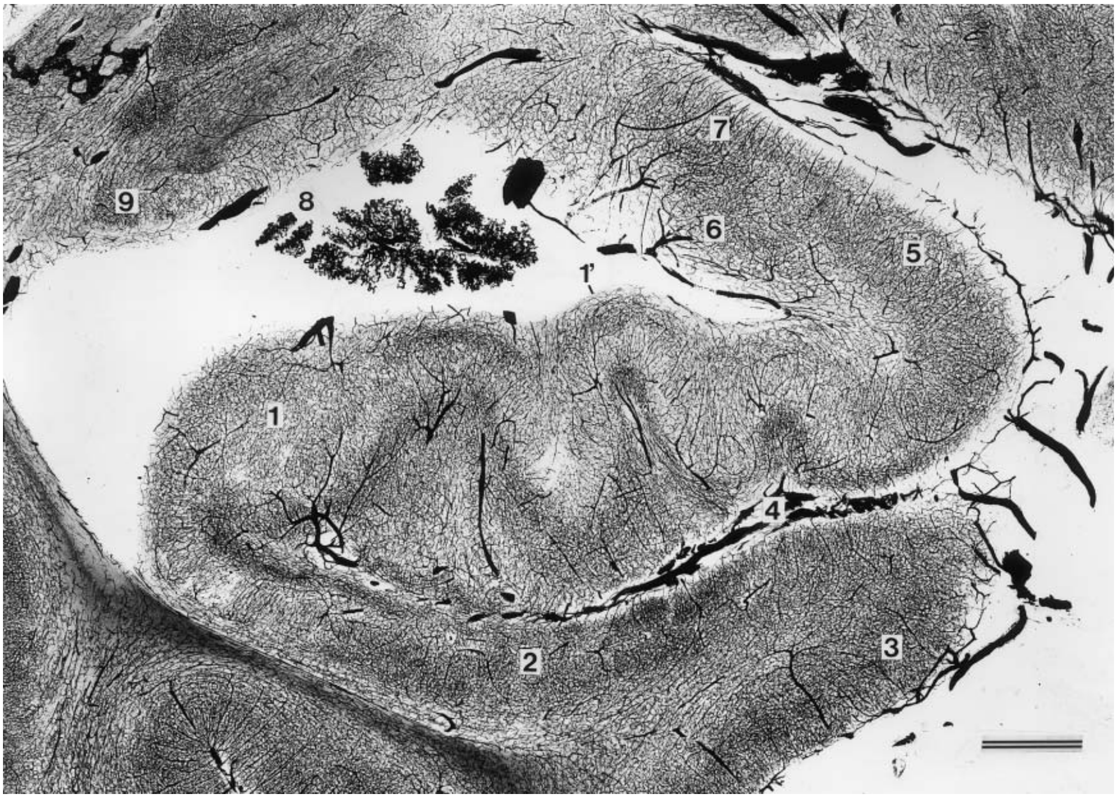

Fig. 103. B′ Bar, 2mm

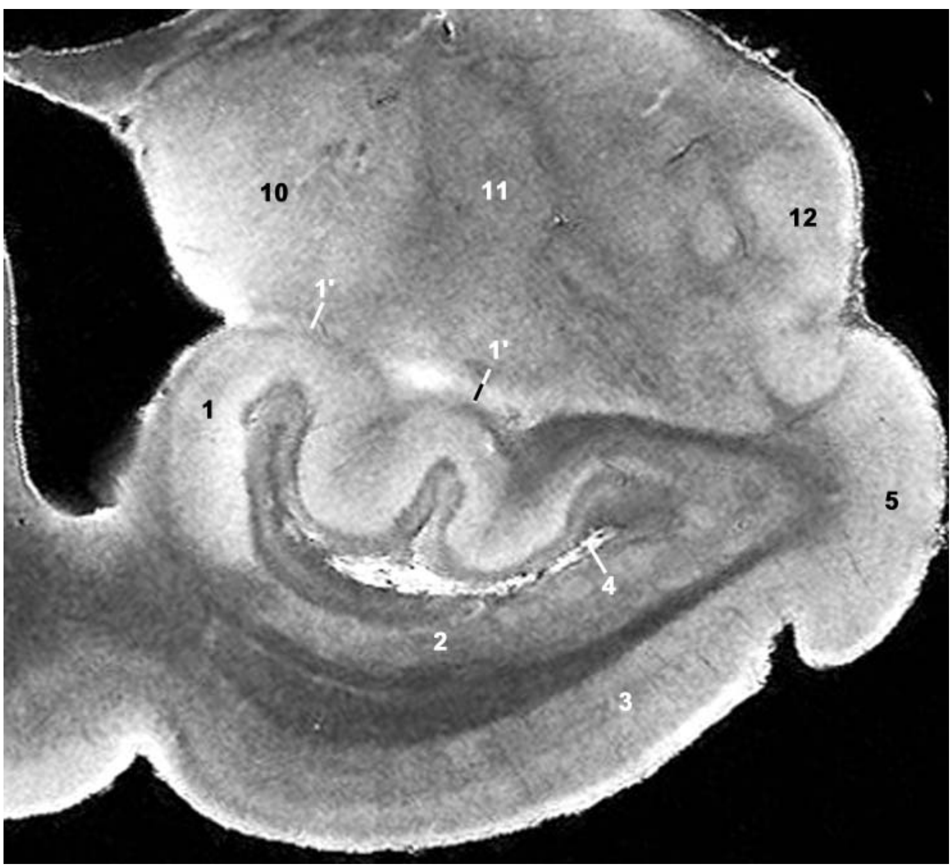

Fig. 103. B″ 9.4T MRI view

Fig. 103. C 3T MRI view

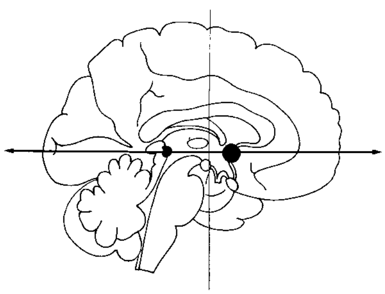

1, hippocampal head, cornu Ammonis; **1′**, internal digitations (digitationes hippocampi); **2**, temporal (inferior) horn of the lateral ventricle; **3**, amygdala; **4**, uncal sulcus; **4′**, uncinate gyrus; **5**, parahippocampal gyrus; **6**, collateral sulcus; **7**, fusiform gyrus; **8**, inferior temporal gyrus; **9**, middle temporal gyrus; **10**, superior temporal sulcus; **11**, superior temporal gyrus; **12**, temporal stem; **13**, lateral fissure; **14**, insula; **15**, postcentral gyrus; **16**, precentral gyrus; **17**, middle frontal gyrus; **18**, superior frontal gyrus; **19**, cingulate sulcus; **20**, cingulate gyrus; **21**, corpus callosum; **22**, fornix; **23**, lateral ventricle; **24**, caudate nucleus; **25**, claustrum; **26**, tail of caudate nucleus; **27**, putamen; **28**, globus pallidus, lateral part; **29**, globus pallidus, medial part; **29′**, striate vessels; **30**, internal capsule, posterior limb; **31**, ventral anterior thalamic nucleus; **32**, third ventricle; **33**, optic tract; **34**, mamillary body; **35**, basilar artery; **36**, pons; **37**, internal carotid artery; **38**, temporomandibular joint; **39**, posterior cerebral artery; **40**, tentorium cerebelli

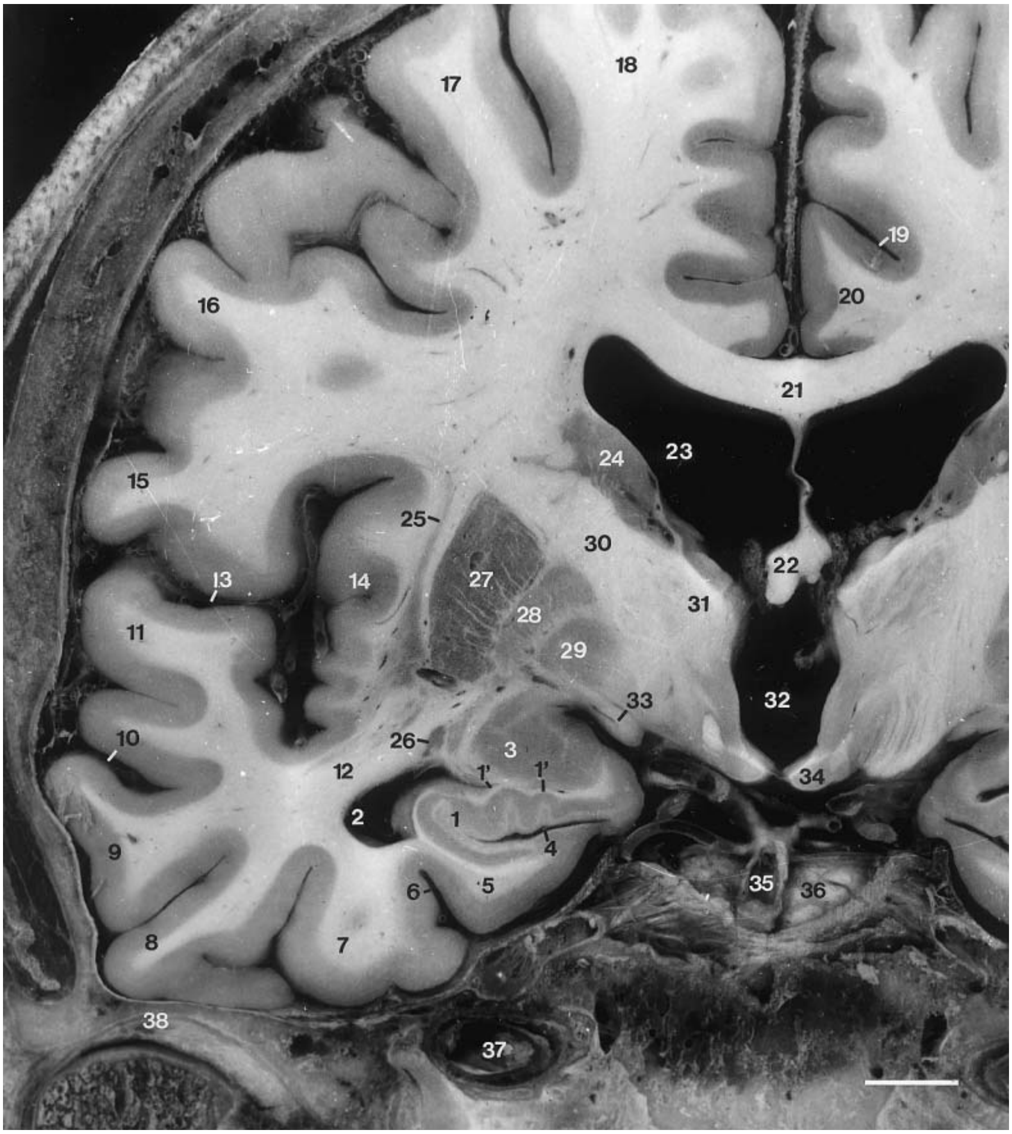

Fig. 103. D Coronal head section. Anterior view of the section. **Bar,** 10 mm

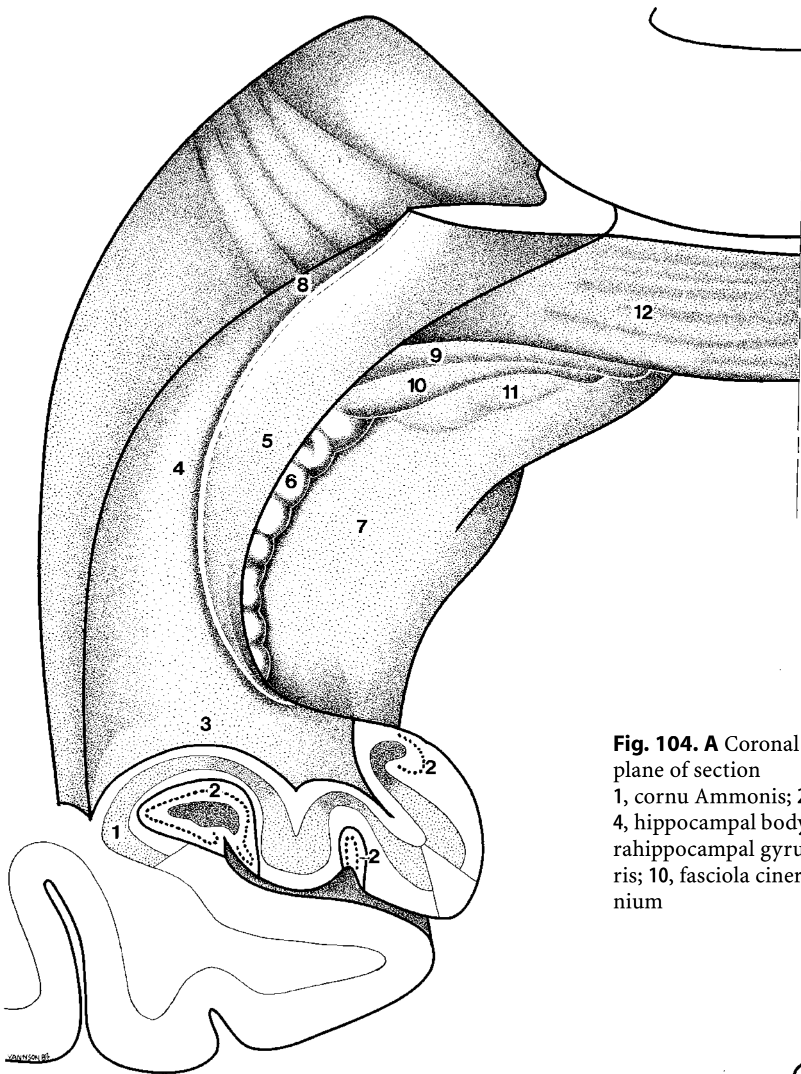

Fig. 104. A Coronal section of hippocampal head, showing plane of section
1, cornu Ammonis; **2**, gyrus dentatus; **3**, hippocampal head; **4**, hippocampal body; **5**, fimbria; **6**, margo denticulatus; **7**, parahippocampal gyrus; **8**, hippocampal tail; **9**, gyrus fasciolaris; **10**, fasciola cinerea; **11**, gyri of Andreas Retzius; **12**, splenium

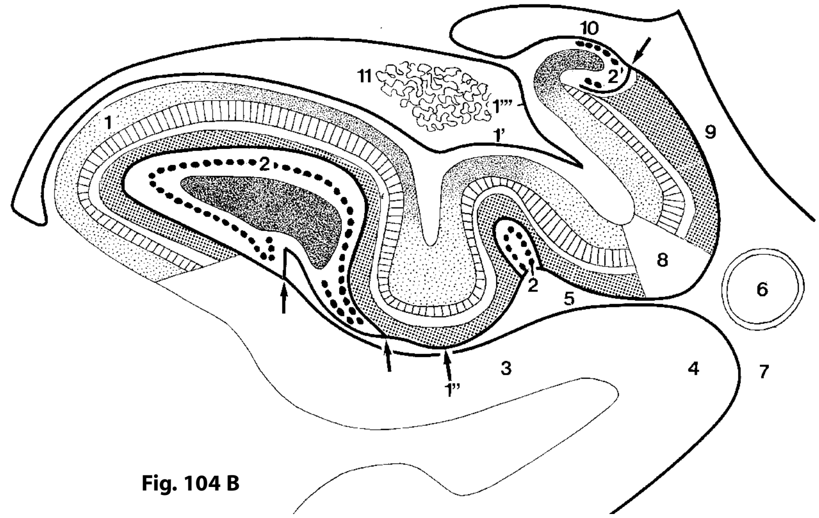

Fig. 104 B

Fig. 104. Coronal section of hippocampal head
B explanatory diagram
B′ intravascular india ink injection
B″ 9.4T MRI view
Note the end of stratum radiatum (**asterisk**) and the beginning of subiculum. **Arrows** indicate the superficial hippocampal sulcus.

1, cornu Ammonis (CA1 – CA4), **1′**, internal digitations (digitationes hippocampi); **1″**, external digitations; **1‴**, vertical digitation; **2**, gyrus dentatus; **3**, subiculum; **4**, parahippocampal gyrus; **5**, uncal sulcus; **6**, posterior cerebral artery (P2 segment); **7**, crural cistern; **8**, subiculum in the medial surface of uncus (see Fig. 100); **9**, transverse fissure (lateral part); **10**, band of Giacomini; **11**, temporal horn of the lateral ventricle; **12**, lateral nucleus of amygdala; **13**, basal nucleus of amygdala; **14**, cortical nucleus of amygdala

Fig. 104. B′ Bar 2 mm

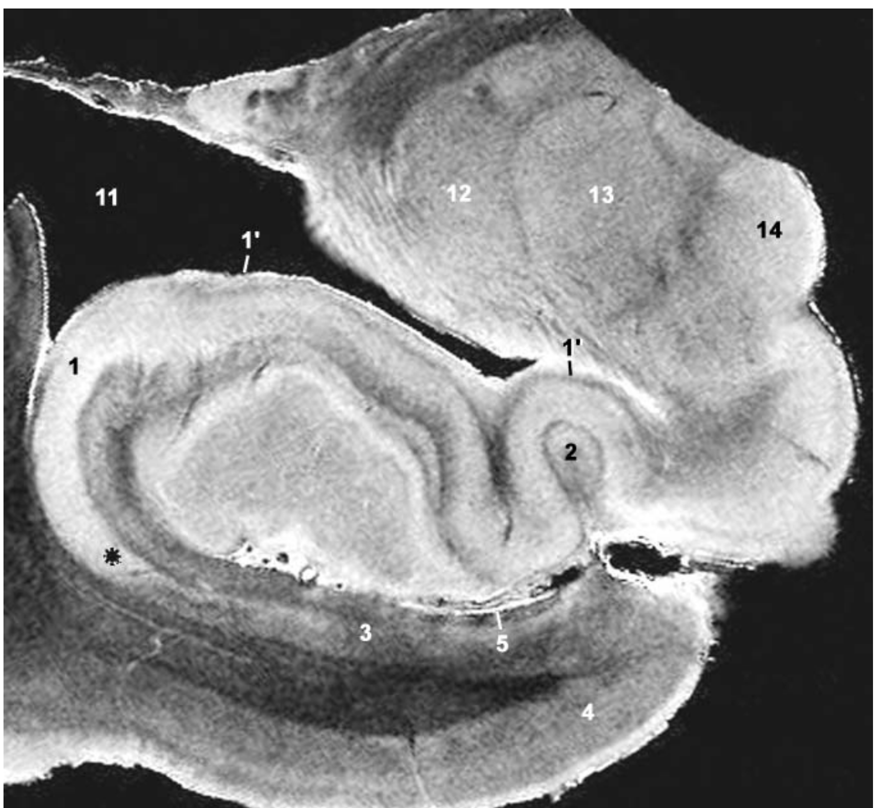

Fig. 104. B″ 9.4T MRI view

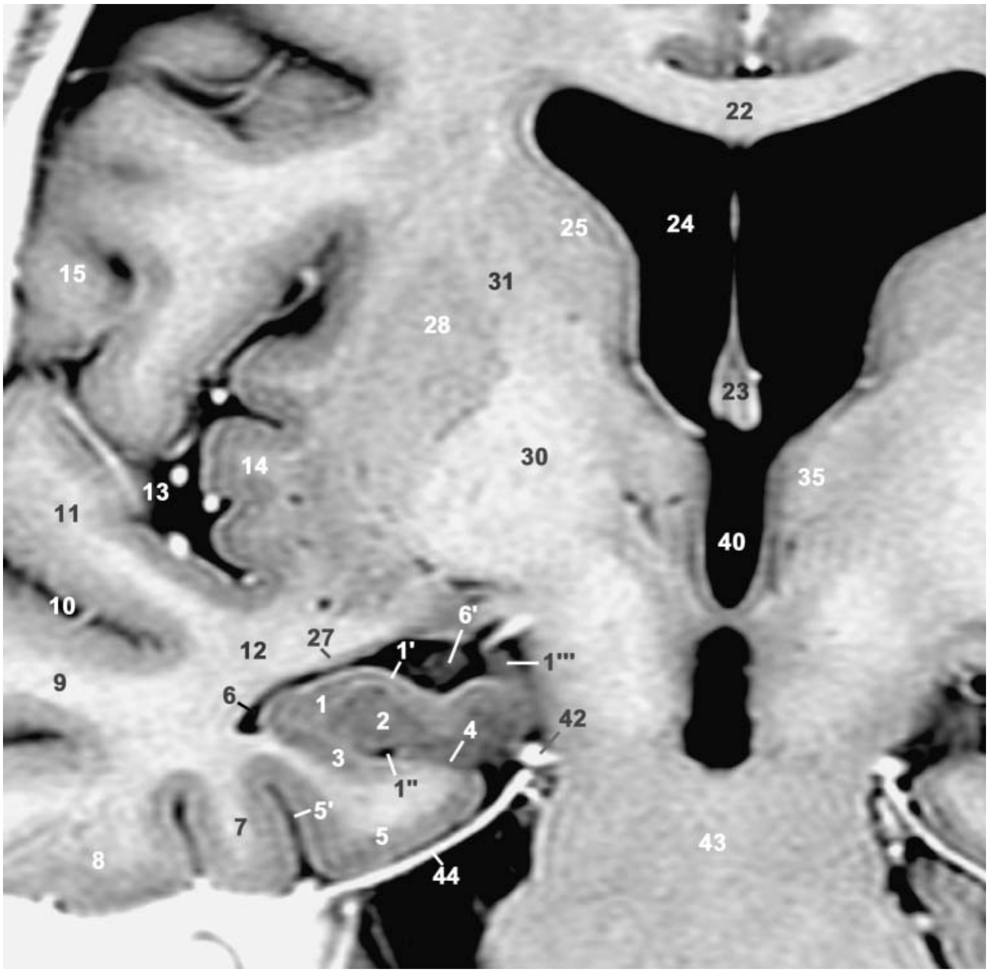

Fig. 104. C 3T MRI view

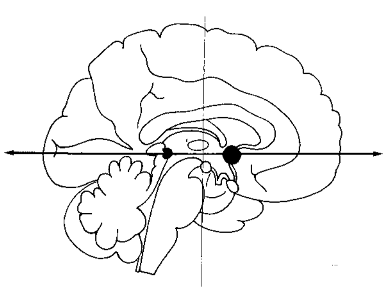

1, hippocampal head, cornu Ammonis; **1′**, internal digitations (digitationes hippocampi); **1″**, external digitations; **1‴**, vertical digitation; **2**, hippocampal head, gyrus dentatus; **3** subiculum; **4**, uncal sulcus; **5**, parahippocampal gyrus; **5′**, collateral sulcus; **6**, temporal (inferior) horn of the lateral ventricle; **6′** choroid plexuses; **7**, fusiform gyrus; **8**, inferior temporal gyrus; **9**, middle temporal gyrus; **10**, superior temporal sulcus; **11**, superior temporal gyrus; **12**, temporal stem; **13**, lateral fissure; **14**, insula; **15**, postcentral gyrus; **16**, central sulcus; **17**, precentral gyrus; **18**, middle frontal gyrus; **19**, superior frontal gyrus; **20**, cingulate sulcus; **21**, cingulate gyrus; **22**, corpus callosum; **23**, fornix; **24**, lateral ventricle; **25**, caudate nucleus; **26**, claustrum; **27**, tail of caudate nucleus; **28**, putamen; **29**, globus pallidus, lateral part; **30**, globus pallidus, medial part; **31**, internal capsule, posterior limb; **32**, optic tract; **33**, anterior thalamic nucleus; **34**, ventral lateral thalamic nucleus; **35**, dorsomedial thalamic nucleus; **36**, mamillothalamic tract; **37**, subthalamic nucleus; **38**, substantia nigra; **39**, crus cerebri; **40**, third ventricle; **41**, mamillary body; **42**, posterior cerebral artery; **43**, pons; **44**, tentorium cerebelli; **45**, internal carotid artery; **46**, temporomandibular joint

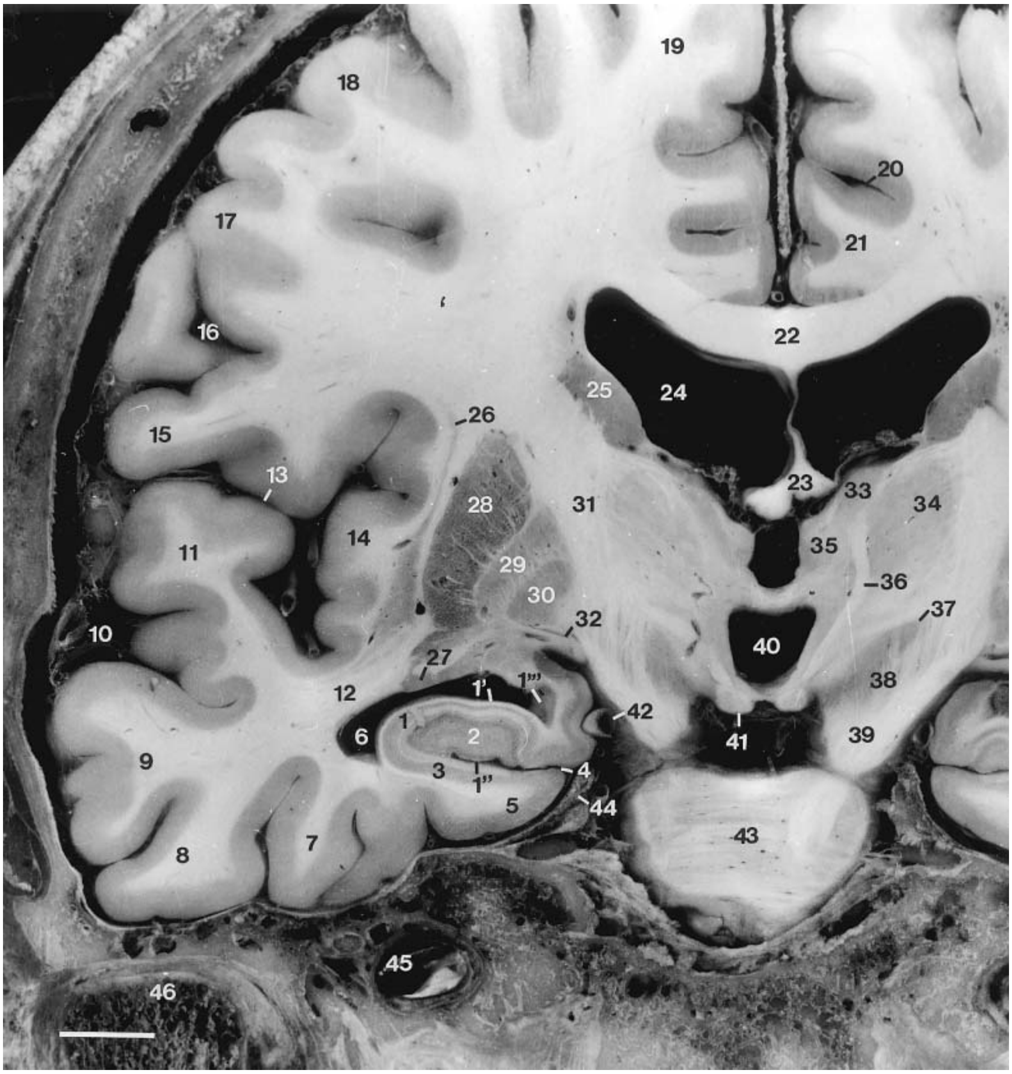

Fig. 104. D Coronal head section. Anterior view of the section. **Bar,** 10 mm

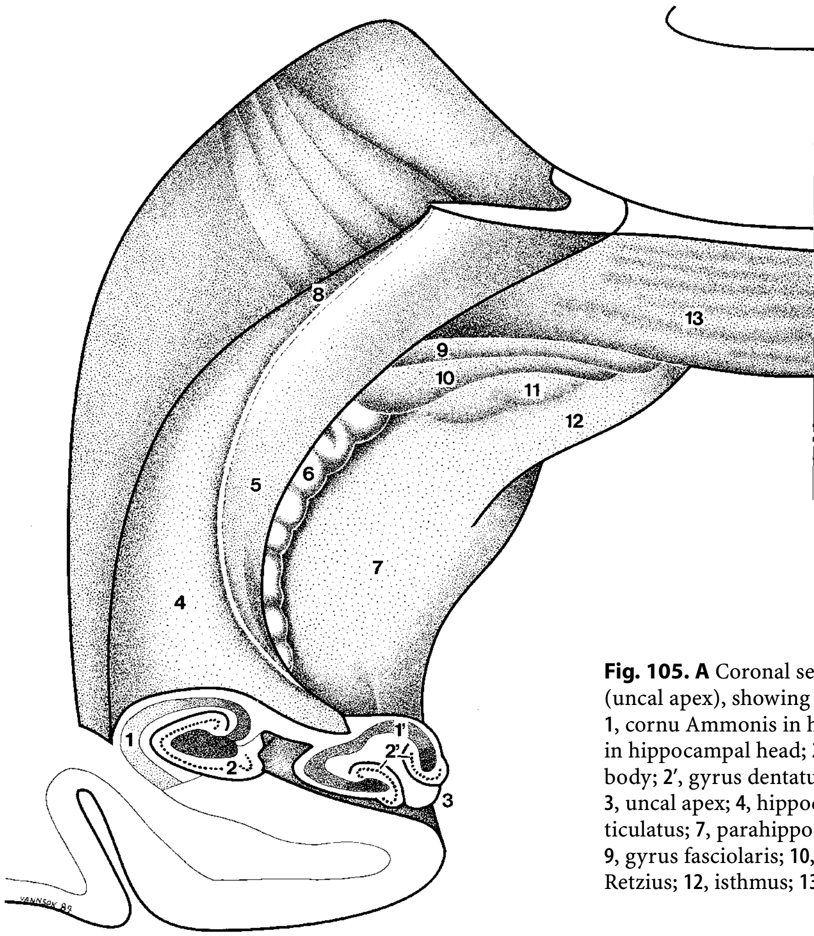

Fig. 105. A Coronal section of hippocampal body and head (uncal apex), showing plane of section
1, cornu Ammonis in hippocampal body; **1′**, cornu Ammonis in hippocampal head; **2**, gyrus dentatus in hippocampal body; **2′**, gyrus dentatus in hippocampal head (uncal apex); **3**, uncal apex; **4**, hippocampal body; **5**, fimbria; **6**, margo denticulatus; **7**, parahippocampal gyrus; **8**, hippocampal tail; **9**, gyrus fasciolaris; **10**, fasciola cinerea; **11**, gyri of Andreas Retzius; **12**, isthmus; **13**, splenium

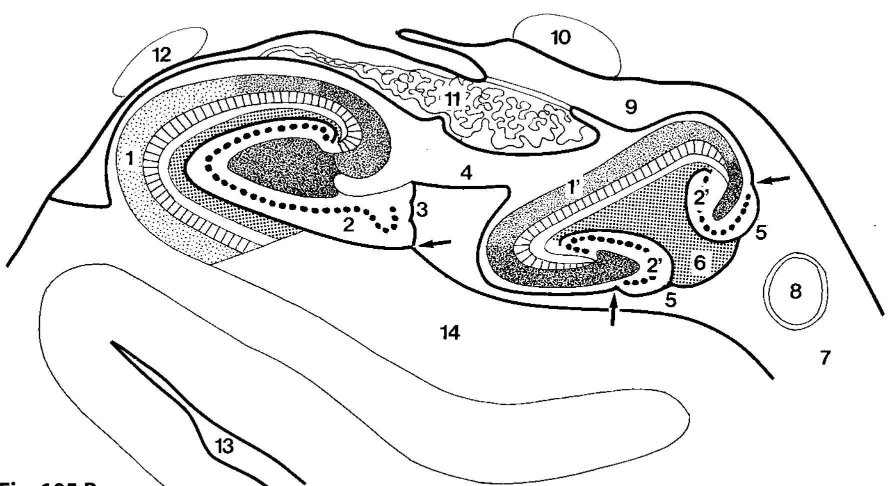

Fig. 105 B

Fig. 105. Coronal section of hippocampal body and head
B explanatory diagram
B′ intravascular india ink injection
B″ 9.4T MRI view
Arrows indicate the superficial hippocampal sulcus.
1, cornu Ammonis (CA1–CA4) in hippocampal body; **1′**, cornu Ammonis (CA3, CA4) in hippocampal head; **2**, gyrus dentatus in hippocampal body; **2′**, gyrus dentatus in hippocampal head; **3**, margo denticulatus; **4**, fimbria; **5**, band of Giacomini; **6**, uncal apex; **7**, crural cistern; **8**, posterior cerebral artery; **9**, transverse fissure (lateral part); **10**, optic tract and lateral geniculate body; **11**, choroid plexuses and temporal horn; **12**, caudate nucleus; **13**, collateral sulcus; **14**, subiculum

Fig. 105. B'
Bar 2 mm

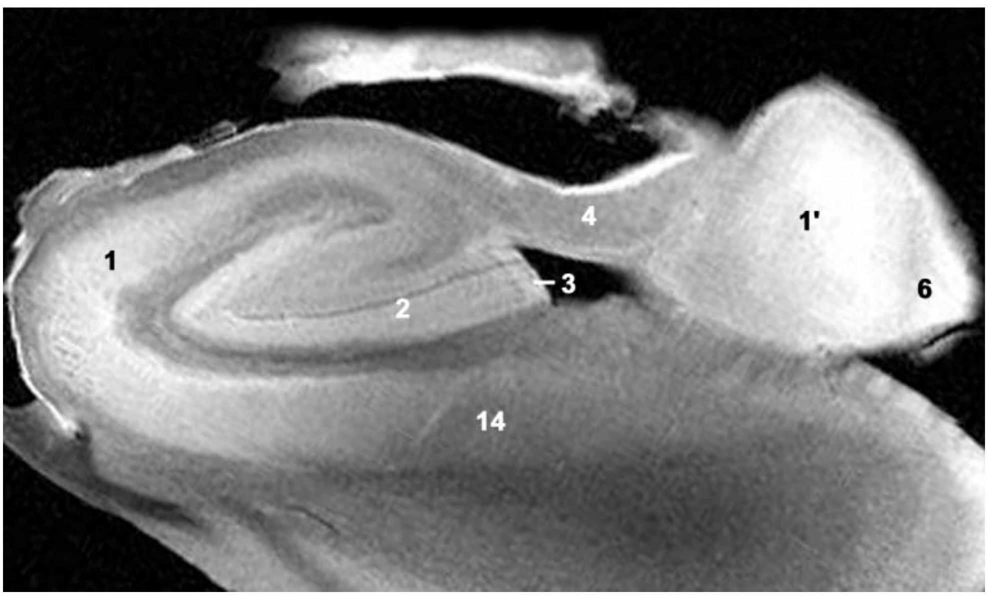

Fig. 105. B" 9.4T MRI view

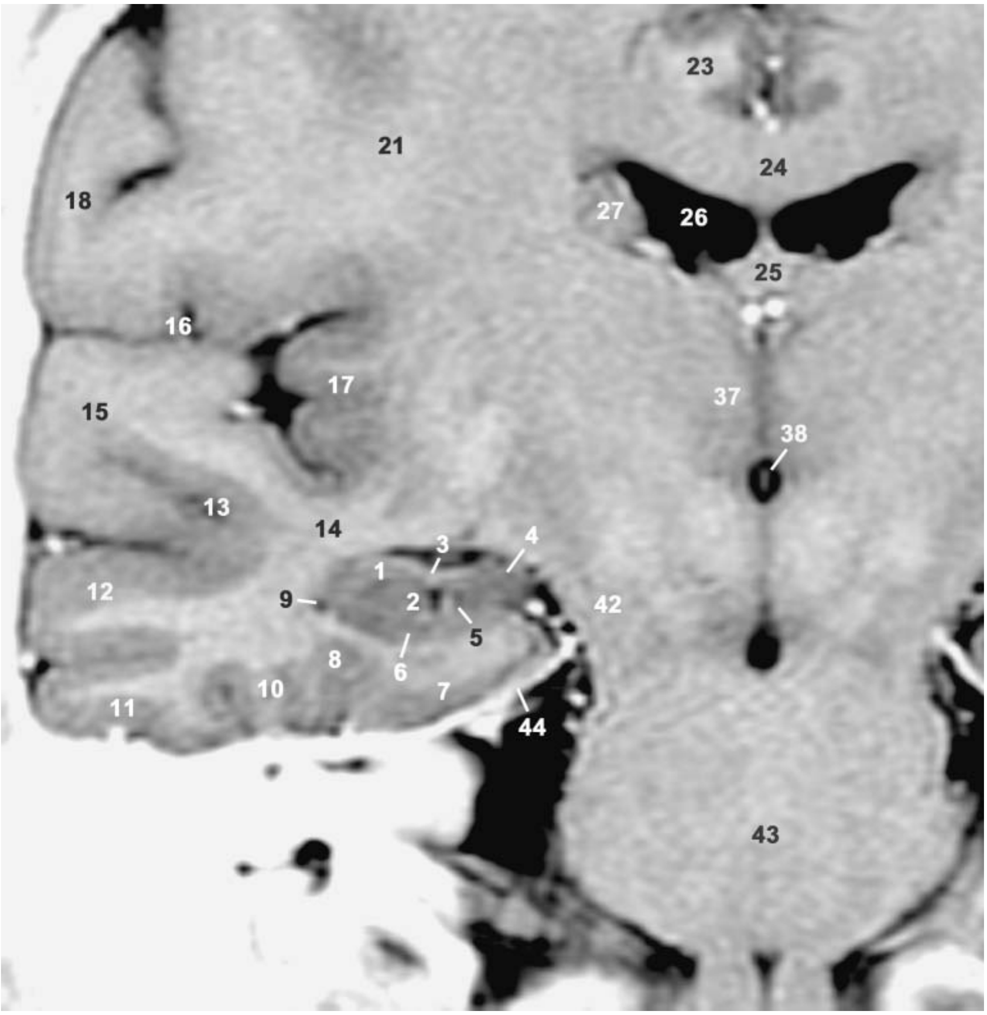

Fig. 105. C 3T MRI view

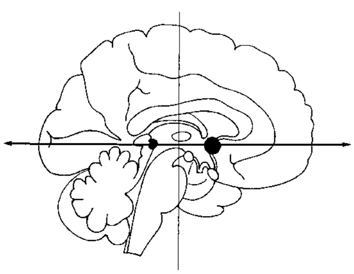

1, hippocampal body, cornu Ammonis; **2**, hippocampal body, gyrus dentatus; **3**, fimbria; **4**, hippocampal head, uncal apex; **5**, uncal sulcus; **6**, subiculum; **7**, parahippocampal gyrus; **8**, collateral sulcus; **9**, temporal (inferior) horn of the lateral ventricle; **10**, fusiform gyrus; **11**, inferior temporal gyrus; **12**, middle temporal gyrus; **13**, superior temporal sulcus; **14**, temporal stem; **15**, superior temporal gyrus; **16**, lateral fissure; **17**, insula; **18**, postcentral gyrus; **19**, central sulcus; **20**, precentral gyrus; **21**, centrum ovale; **22**, cingulate sulcus; **23**, cingulate gyrus; **24**, corpus callosum; **25**, fornix; **26**, lateral ventricle; **27**, caudate nucleus; **28**, internal capsule, posterior limb; **29**, putamen; **30**, claustrum; **31**, tail of caudate nucleus; **32**, optic tract; **33**, globus pallidus, lateral part; **34**, globus pallidus, medial part; **35**, ventral lateral thalamic nucleus; **36**, anterior thalamic nucleus; **37**, dorsomedial thalamic nucleus; **38**, third ventricle; **39**, red nucleus; **40**, subthalamic nucleus; **41**, substantia nigra; **42**, crus cerebri; **43**, pons; **44**, tentorium cerebelli; **45**, internal carotid artery

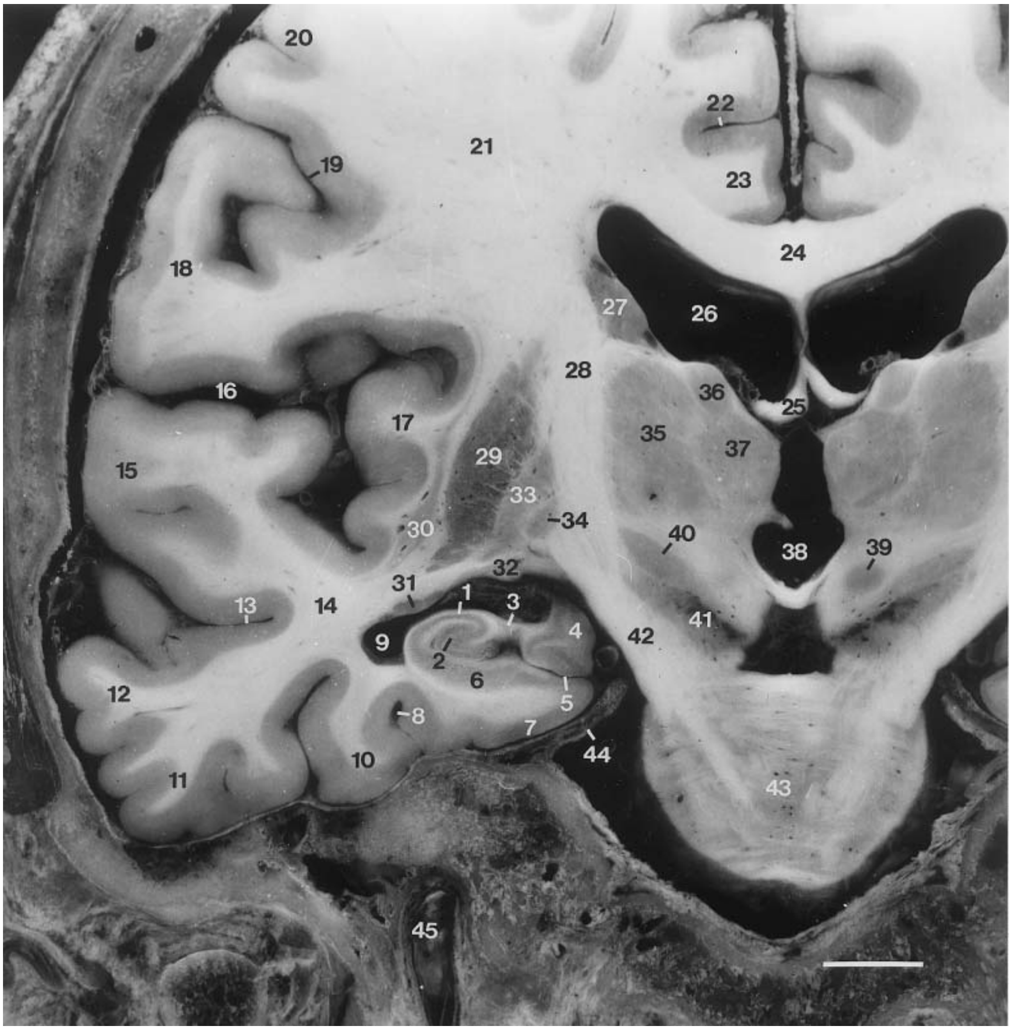

Fig. 105. D Head section, anterior view of the section. **Bar**, 10 mm

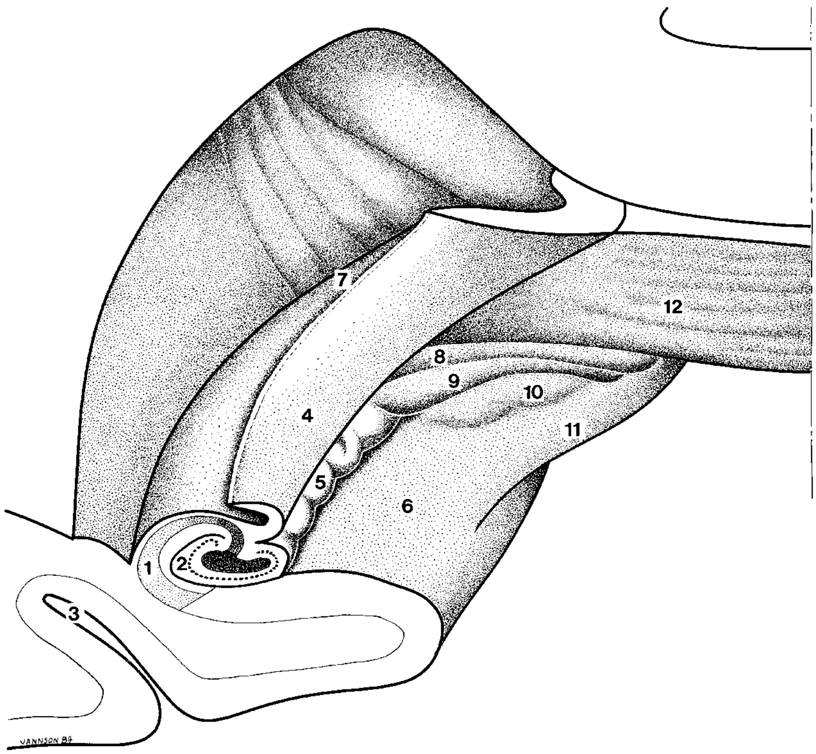

Fig. 106. A Coronal section of hippocampal body, showing plane of section
1, cornu Ammonis; **2**, gyrus dentatus; **3**, collateral sulcus; **4**, fimbria; **5**, margo denticulatus; **6**, parahippocampal gyrus; **7**, hippocampal tail; **8**, gyrus fasciolaris; **9**, fasciola cinerea; **10**, gyri of Andreas Retzius; **11**, isthmus; **12**, splenium

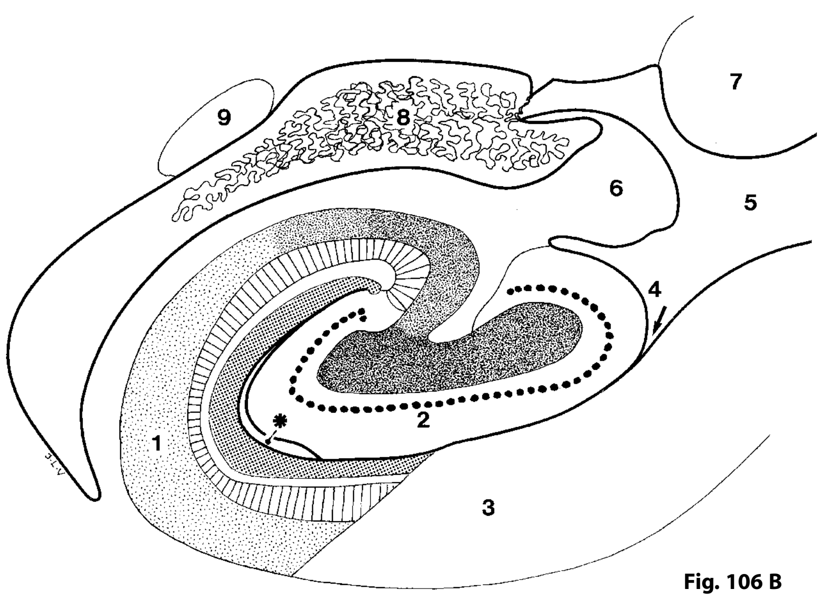

Fig. 106 B

Fig. 106. Coronal section of the hippocampal body
B explanatory diagram,
B′ intravascular india ink injection,
B″ 9.4T MRI view
Arrow indicates the superficial hippocampal sulcus and **asterisk** shows a residual cavity in the vestigial hippocampal sulcus.
1, cornu Ammonis (CA1 – CA4); **2**, gyrus dentatus; **3**, subiculum; **4**, margo denticulatus; **5**, lateral part of the transverse fissure; **6**, fimbria; **7**, lateral geniculate body; **8**, choroid plexuses and temporal horn of lateral ventricle; **9**, caudate nucleus

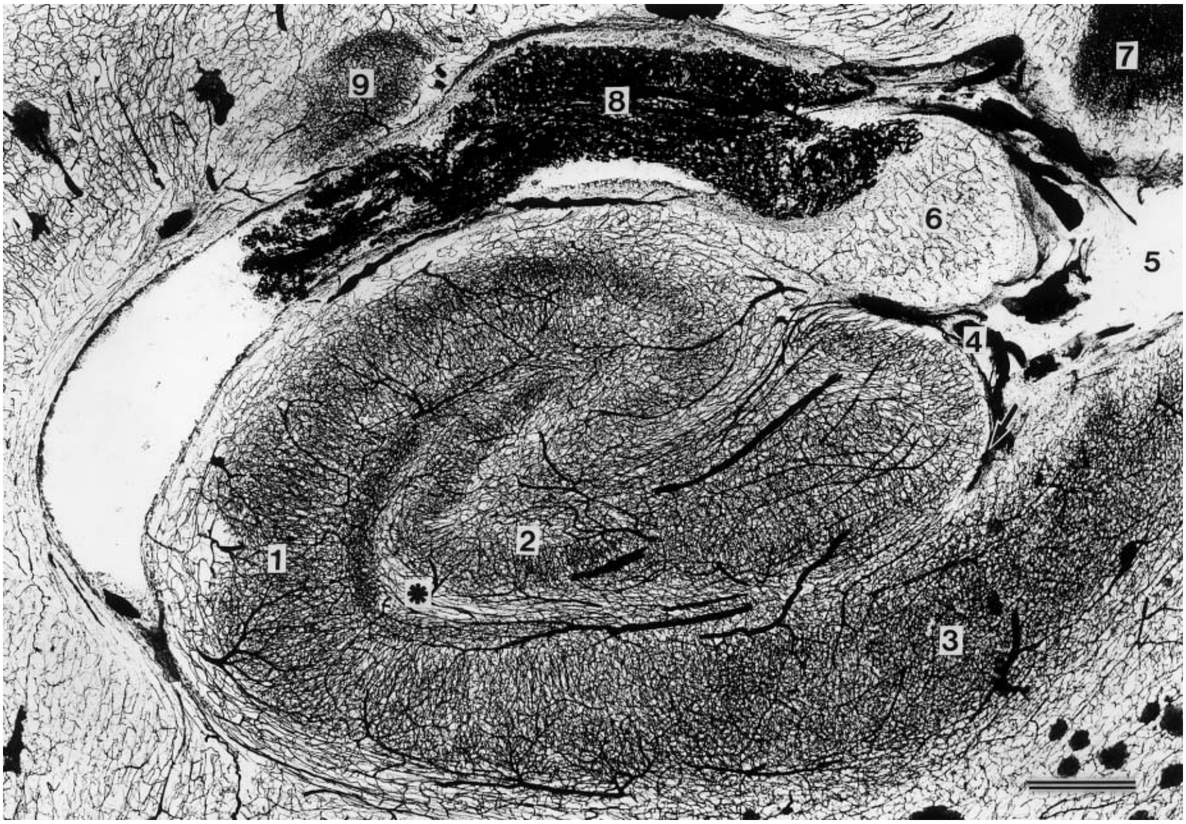

Fig. 106. B′
Bar 1.2 mm

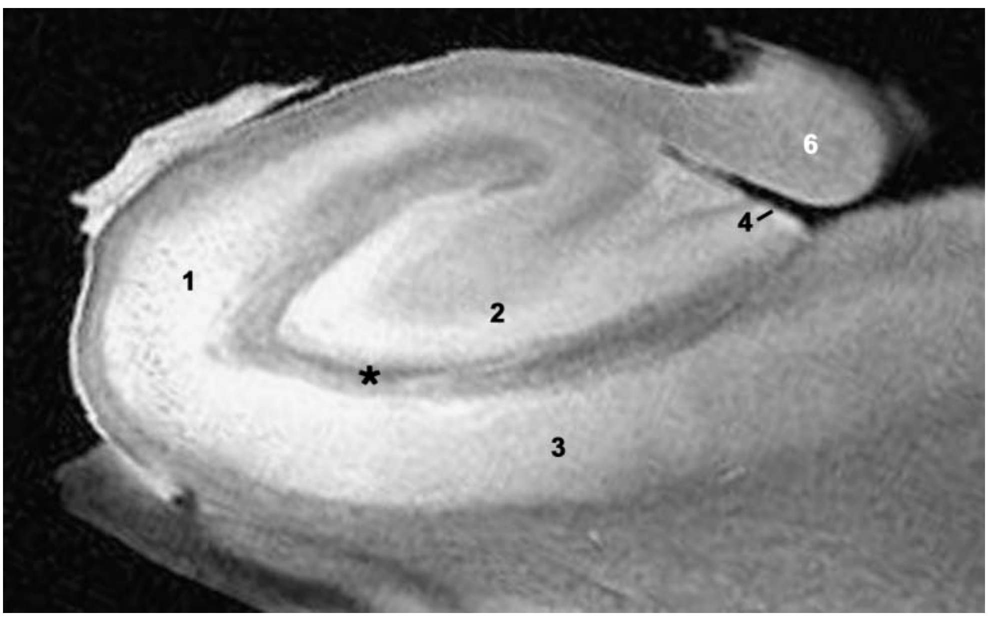

Fig. 106. B″ 9.4T MRI view

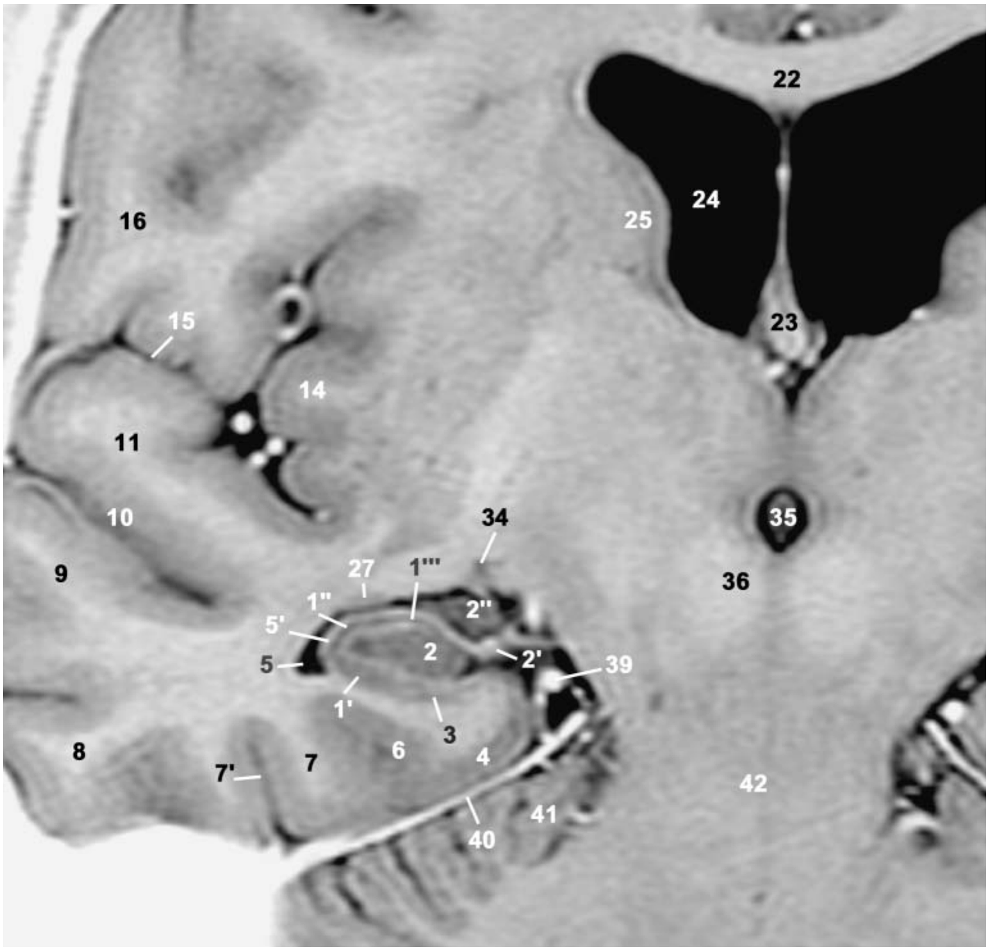

Fig. 106. C 3T MRI view

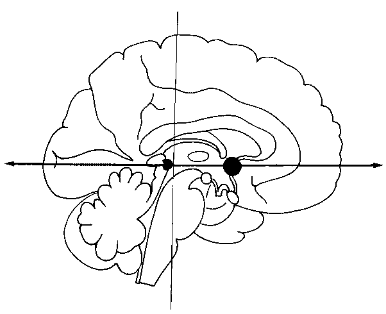

1, hippocampal body, cornu Ammonis: **1′**, CA1; **1″**, CA2; **1‴**, CA3; **2**, hippocampal body, gyrus dentatus, and CA4; **2′**, fimbria; **2″**, choroid plexuses; **3**, subiculum; **4**, parahippocampal gyrus; **5**, temporal (inferior) horn of the lateral ventricle; **5′**, alveus; **6**, collateral sulcus; **7**, fusiform gyrus; **7′**, lateral occipitotemporal sulcus; **8**, inferior temporal gyrus; **9**, middle temporal gyrus; **10**, superior temporal sulcus; **11**, superior temporal gyrus; **12**, transverse temporal gyrus; **13**, temporal stem; **14**, insula; **15**, lateral fissure; **16**, postcentral gyrus; **17**, central sulcus; **18**, precentral gyrus; **19**, superior frontal gyrus; **20**, cingulate sulcus; **21**, cingulate gyrus; **22**, corpus callosum; **23**, fornix; **24**, lateral ventricle; **25**, caudate nucleus; **26**, pontes grisei caudatolenticulares; **27**, tail of caudate nucleus; **28**, internal capsule, retrolentiform part; **29**, lateral posterior thalamic nucleus; **30**, lateral dorsal thalamic nucleus; **31**, dorsomedial thalamic nucleus; **32**, centromedian thalamic nucleus; **33**, ventral posterolateral thalamic nucleus; **34**, lateral geniculate body; **35**, third ventricle; **36**, decussation of superior cerebellar peduncles; **37**, substantia nigra; **38**, crus cerebri; **39**, ambient cistern and posterior cerebral artery; **40**, tentorium cerebelli; **41**, cerebellum; **42**, pons; **43**, medulla, pyramid; **44**, internal ear; **45**, middle ear; **46**, external acoustic meatus

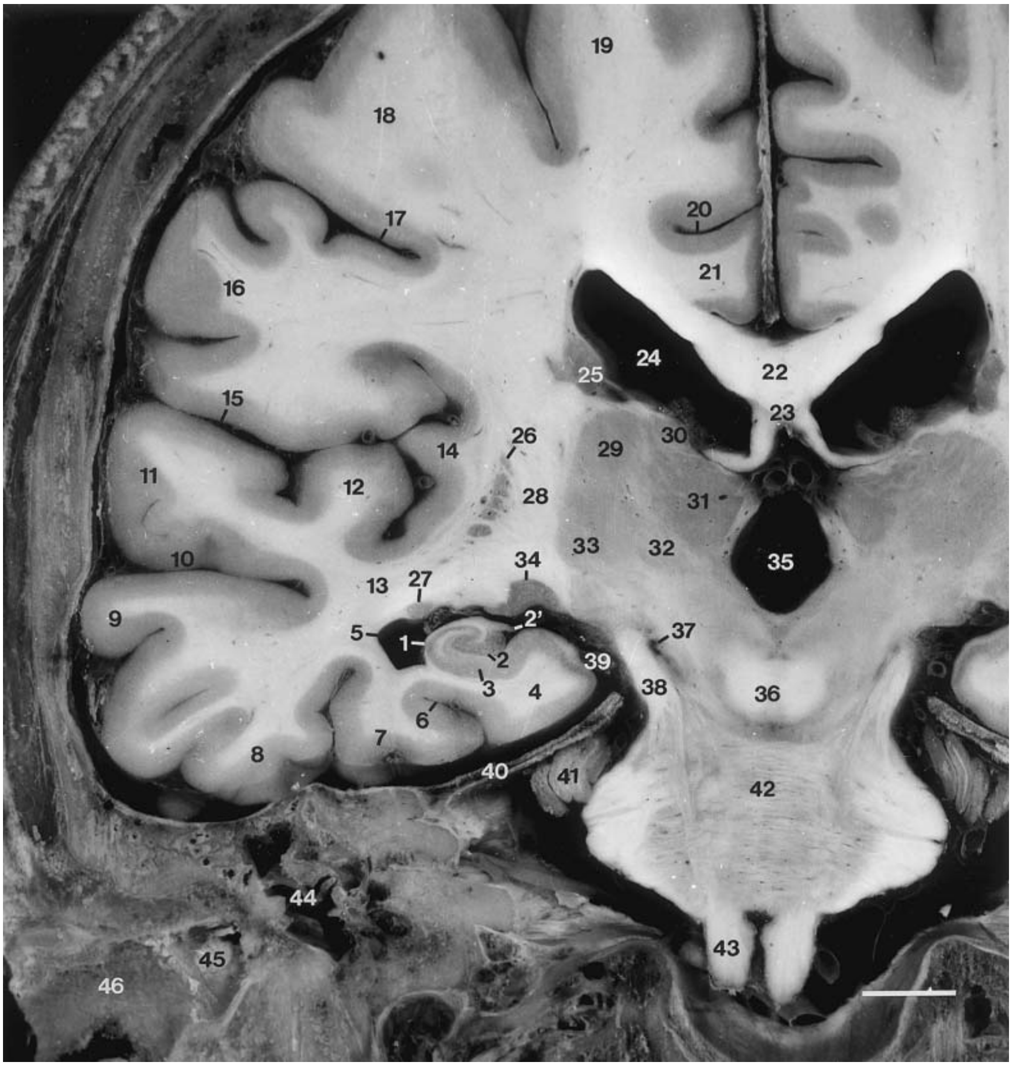

Fig. 106. D Head section, posterior view of the section. **Bar,** 10 mm

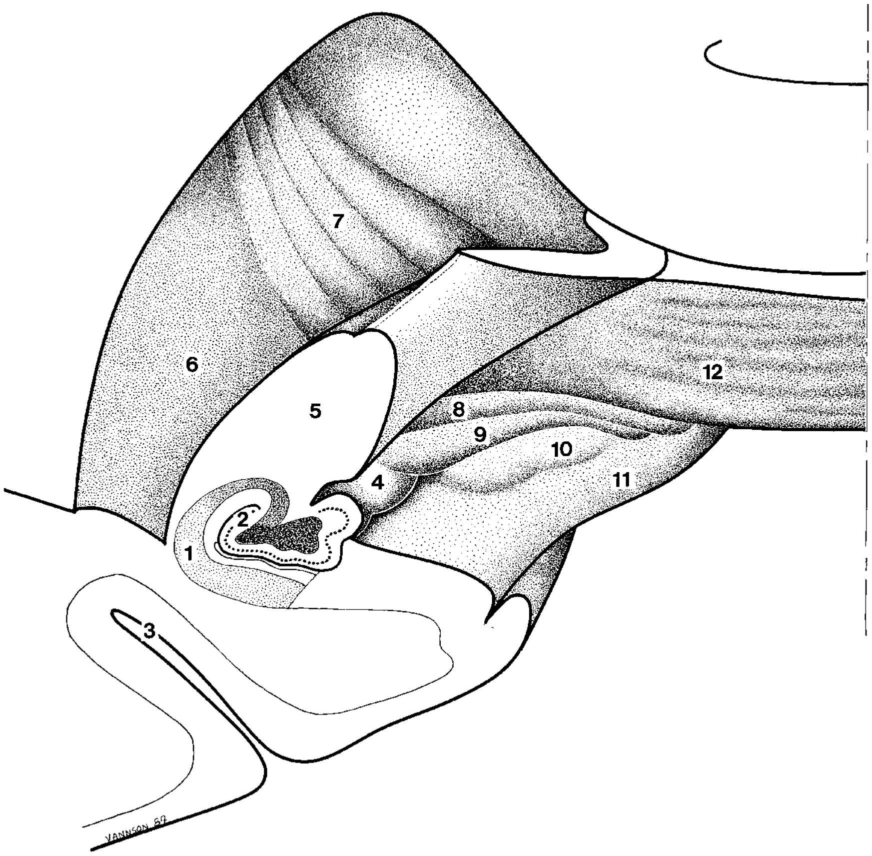

Fig. 107. A Coronal section of initial segment of the hippocampal tail, showing plane of section 1, cornu Ammonis; 2, gyrus dentatus; 3, collateral sulcus; 4, margo denticulatus; 5, crus of fornix; 6, collateral trigone; 7, calcar avis; 8, gyrus fasciolaris; 9, fasciola cinerea; 10, gyrus of Andreas Retzius; 11, isthmus; 12, splenium

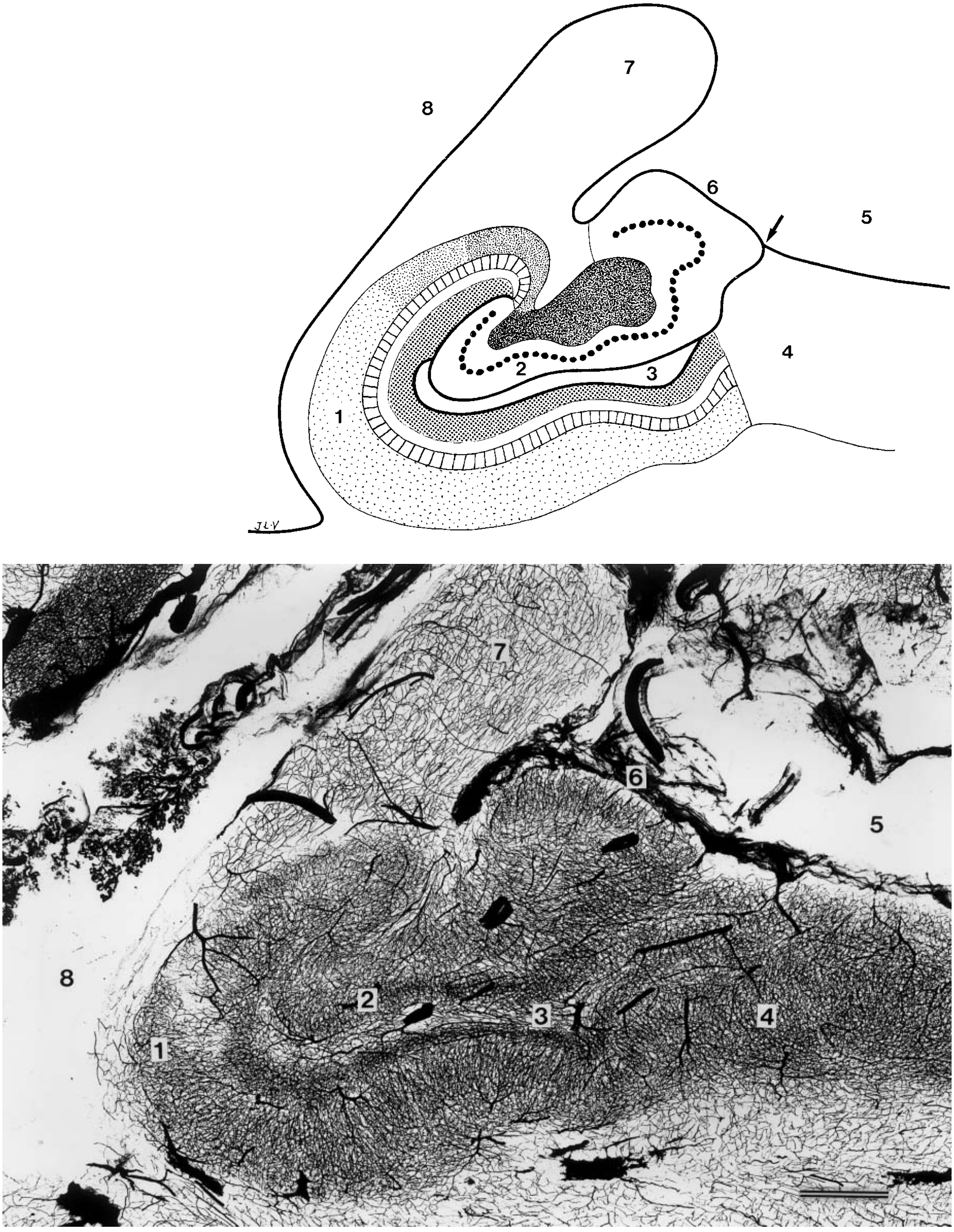

Fig. 107. B Coronal section of the hippocampal tail. Intravascular India ink injection with explanatory diagram. **Arrow** indicates the superficial hippocampal sulcus. **Bar,** 1.3 mm

1, cornu Ammonis (CA1 – CA4); **2**, gyrus dentatus; **3**, vestigial hippocampal sulcus; **4**, subiculum; **5**, lateral part of the transverse fissure; **6**, margo denticulatus; **7**, crus of fornix; **8**, temporal horn of lateral ventricle

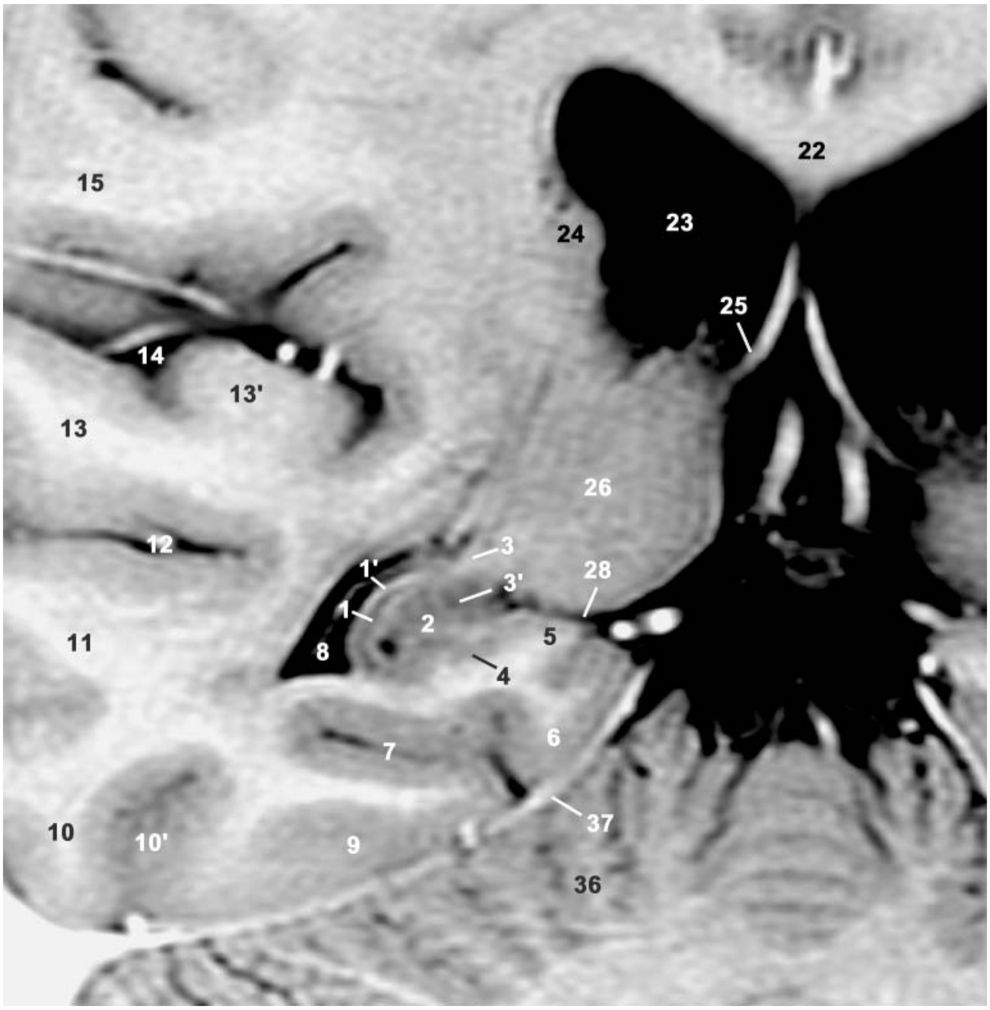

Fig. 107. C 3T MRI view

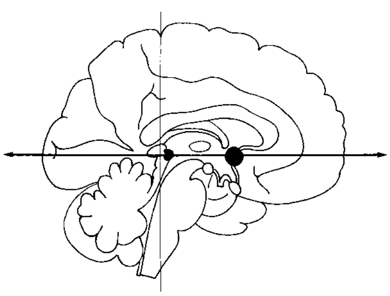

1, hippocampal tail, cornu Ammonis; **1′**, alveus; **2**, hippocampal tail, gyrus dentatus; **3**, fimbria; **3′**, margo denticulatus; **4**, gyrus of Andreas Retzius; **5**, subiculum; **6**, parahippocampal gyrus; **7**, collateral sulcus; **8**, temporal (inferior) horn of the lateral ventricle; **9**, fusiform gyrus; **10**, inferior temporal gyrus; **10′**, lateral occipitotemporal sulcus; **11**, middle temporal gyrus; **12**, superior temporal sulcus; **13**, superior temporal gyrus; **13′**, transverse temporal gyrus; **14**, lateral fissure; **15**, supramarginal gyrus; **16**, postcentral gyrus; **17**, central sulcus; **18**, precentral gyrus; **19**, superior frontal gyrus; **20**, cingulate sulcus; **21**, cingulate gyrus; **22**, splenium of corpus callosum; **23**, lateral ventricle; **24**, caudate nucleus; **25**, crus of fornix; **26**, pulvinar; **27**, tail of caudate nucleus; **28**, wing of ambient cistern (lateral part of the transverse fissure); **29**, ambient cistern; **30**, pineal gland and quadrigeminal cistern; **31**, superior colliculus; **32**, inferior colliculus; **33**, cerebral aqueduct; **34**, brachium conjunctivum (superior cerebellar peduncle); **35**, brachium pontis; **36**, quadrangular lobule; **37**, tentorium cerebelli; **38**, flocculus; **39**, medulla; **40**, vertebral artery; **41**, sigmoid sinus; **42**, mastoid process; **43**, mastoid air cells

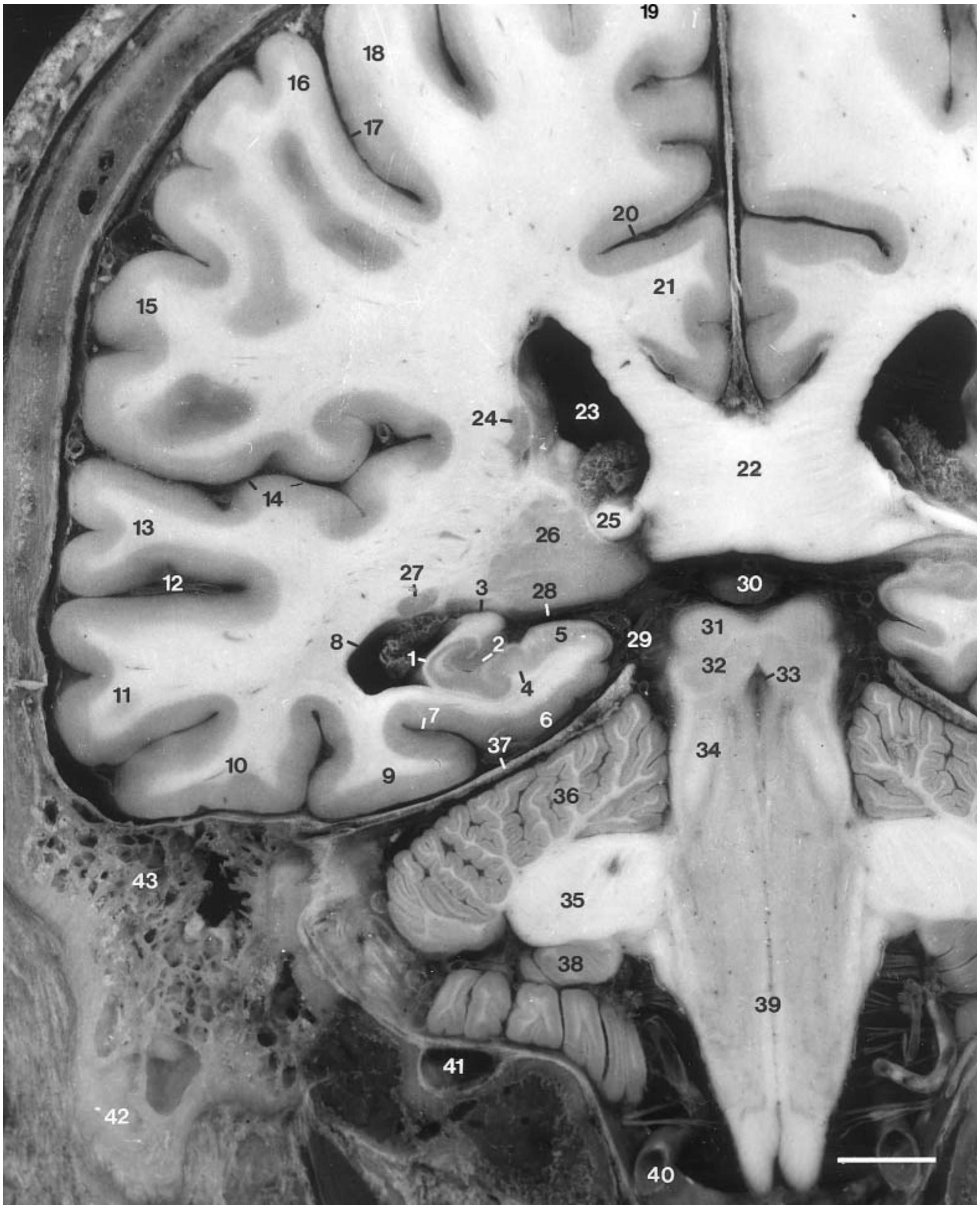

Fig. 107. D Head section, posterior view of the section. **Bar**, 10 mm

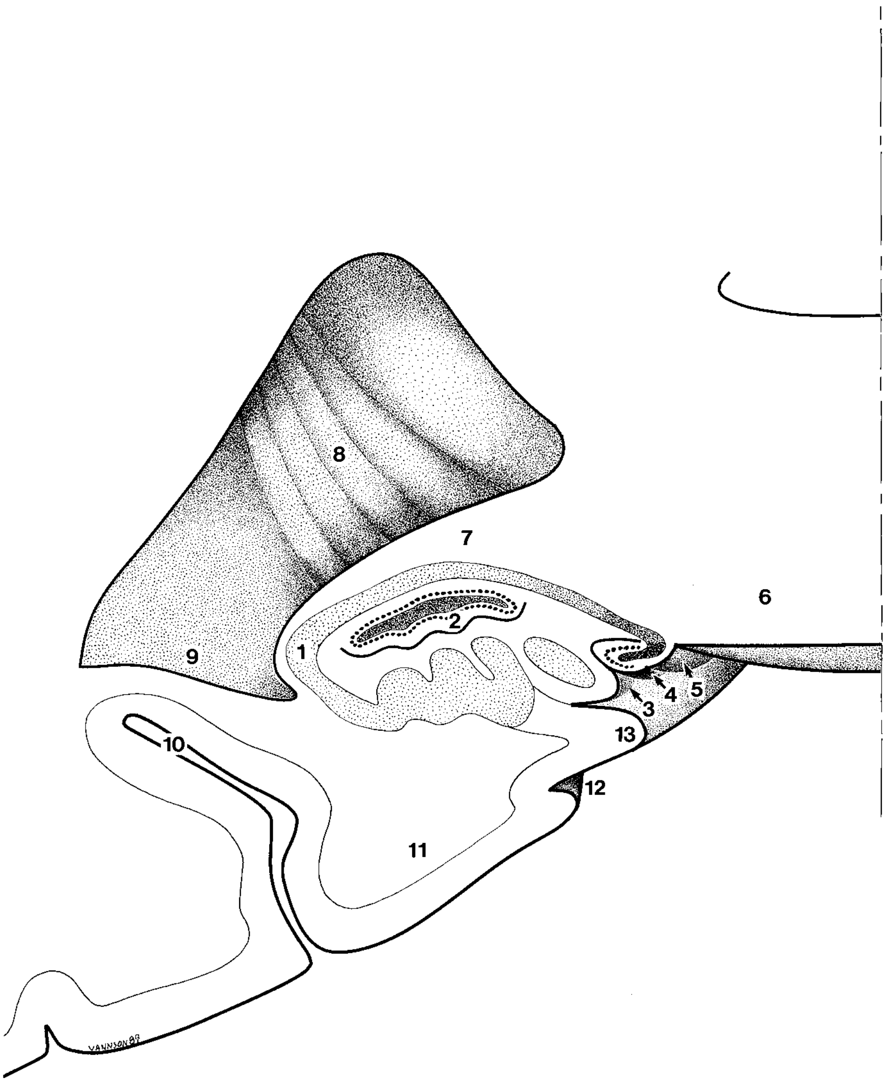

Fig. 108. A Coronal section of middle segment of the hippocampal tail, showing plane of section **1**, cornu Ammonis; **2**, gyrus dentatus; **3**, gyrus of Andreas Retzius; **4**, fasciola cinerea; **5**, gyrus fasciolaris; **6**, splenium; **7**, crus of fornix; **8**, calcar avis; **9**, collateral trigone; **10**, collateral sulcus; **11**, parahippocampal gyrus; **12**, anterior calcarine sulcus; **13**, isthmus

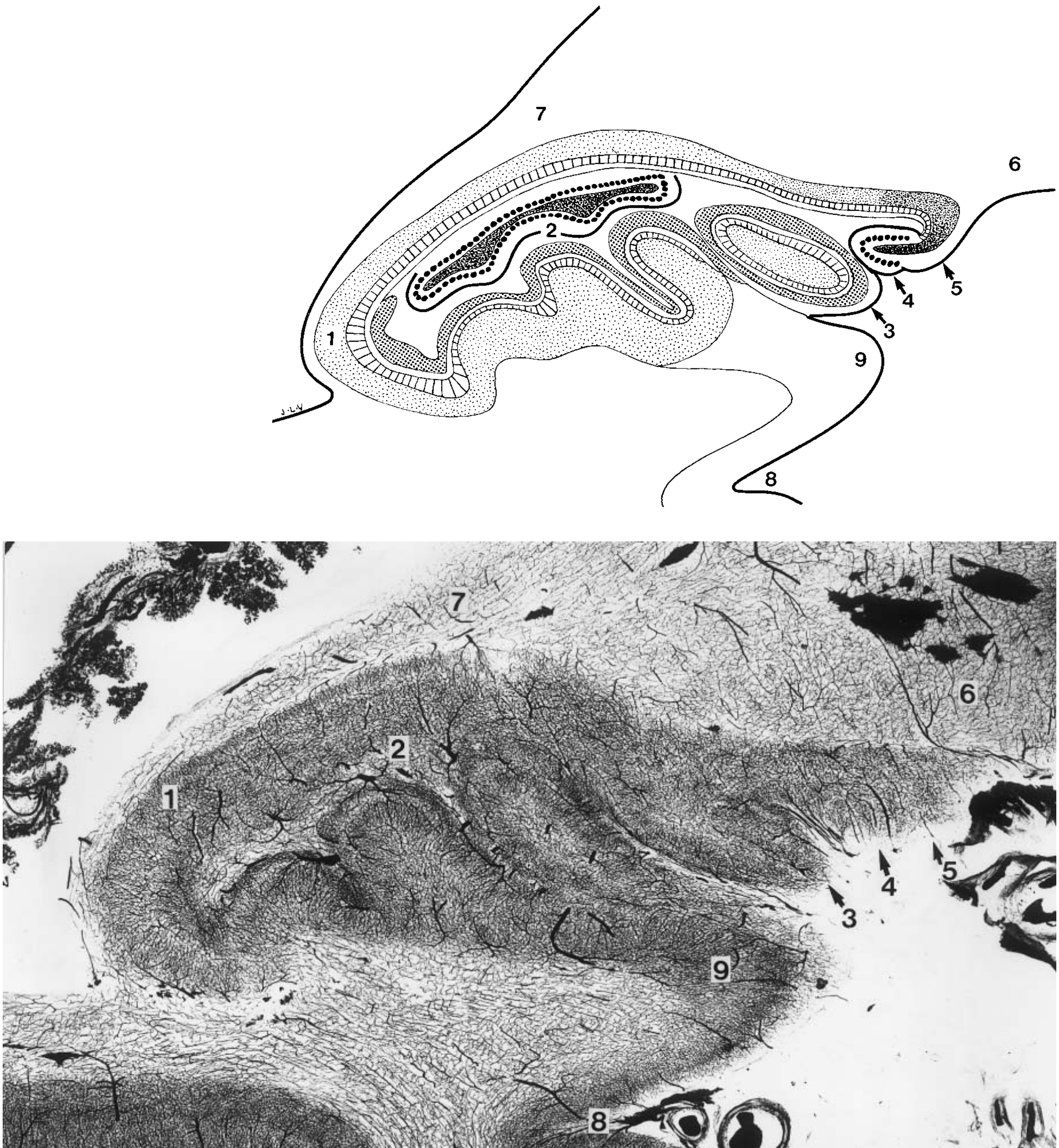

Fig. 108. B Coronal section of the hippocampal tail. Intravascular India ink injection with explanatory diagram. **Bar**, 2.2 mm

1, cornu Ammonis (CA1 – CA4); **2**, gyrus dentatus; **3**, gyri of Andreas Retzius; **4**, fasciola cinerea; **5**, gyrus fasciolaris; **6**, splenium; **7**, crus of fornix; **8**, anterior calcarine sulcus; **9**, isthmus

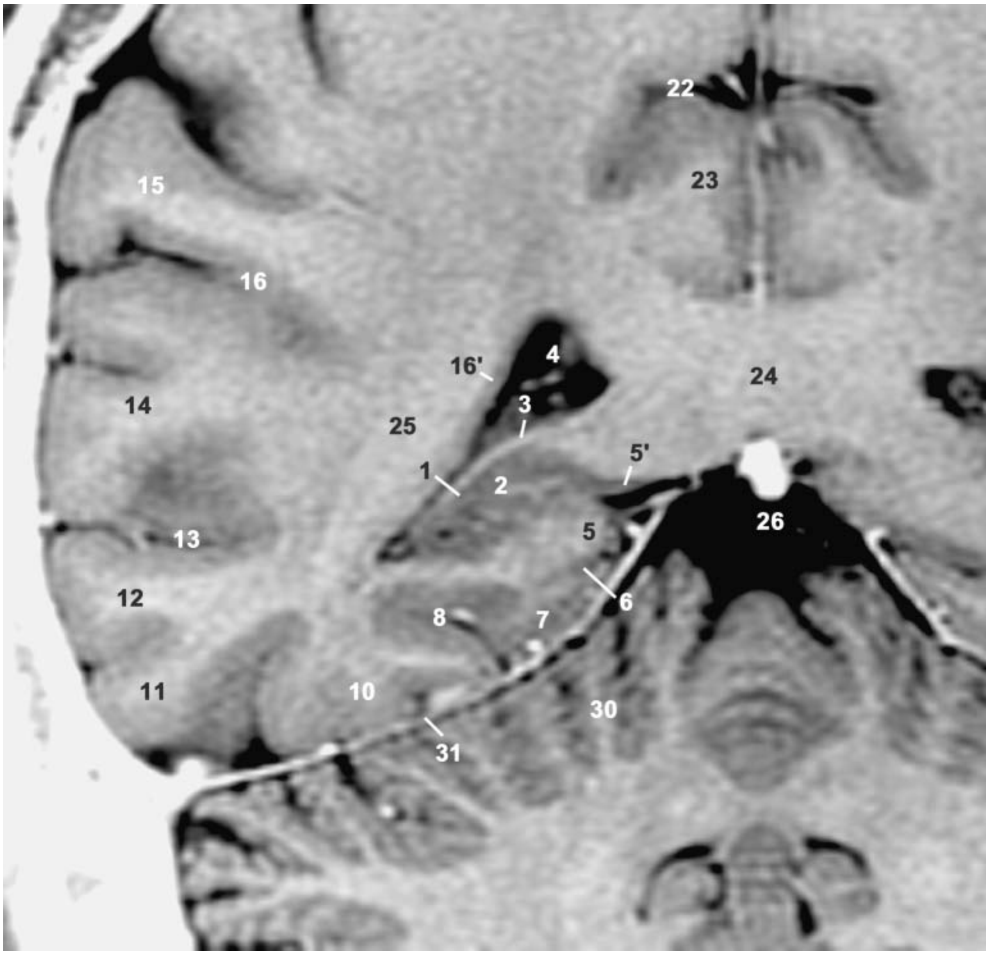

Fig. 108. C 3T MRI view

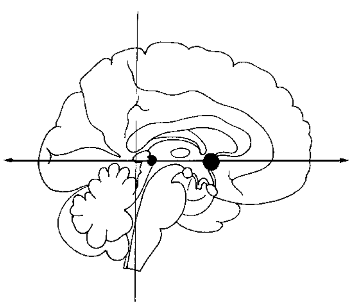

1, hippocampal tail, cornu Ammonis; **2**, hippocampal tail, gyrus dentatus; **3**, crus of fornix; **4**, atrium of the lateral ventricle; **5**, isthmus; **5′**, gyrus fasciolaris; **6**, anterior calcarine sulcus; **7**, parahippocampal gyrus; **8**, collateral sulcus; **9**, collateral trigone; **10**, fusiform gyrus; **11**, inferior temporal gyrus; **12**, middle temporal gyrus; **13**, superior temporal sulcus; **14**, superior temporal gyrus; **15**, supramarginal gyrus; **16**, lateral fissure, posterior ascending segment; **16′**, caudate nucleus; **17**, intraparietal sulcus; **18**, postcentral gyrus; **19**, central sulcus; **20**, precentral gyrus; **21**, superior frontal gyrus; **22**, cingulate sulcus; **23**, cingulate gyrus; **24**, splenium; **25**, optic radiations; **26**, pineal gland and quadrigeminal cistern; **27**, superior colliculus; **28**, cerebral aqueduct; **29**, brachium conjunctivum; **30**, quadrangular lobule; **31**, tentorium cerebelli; **32**, brachium pontis; **33**, flocculus; **34**, medulla; **35**, vertebral artery; **36**, sigmoid sinus; **37**, mastoid air cells; **38**, mastoid process

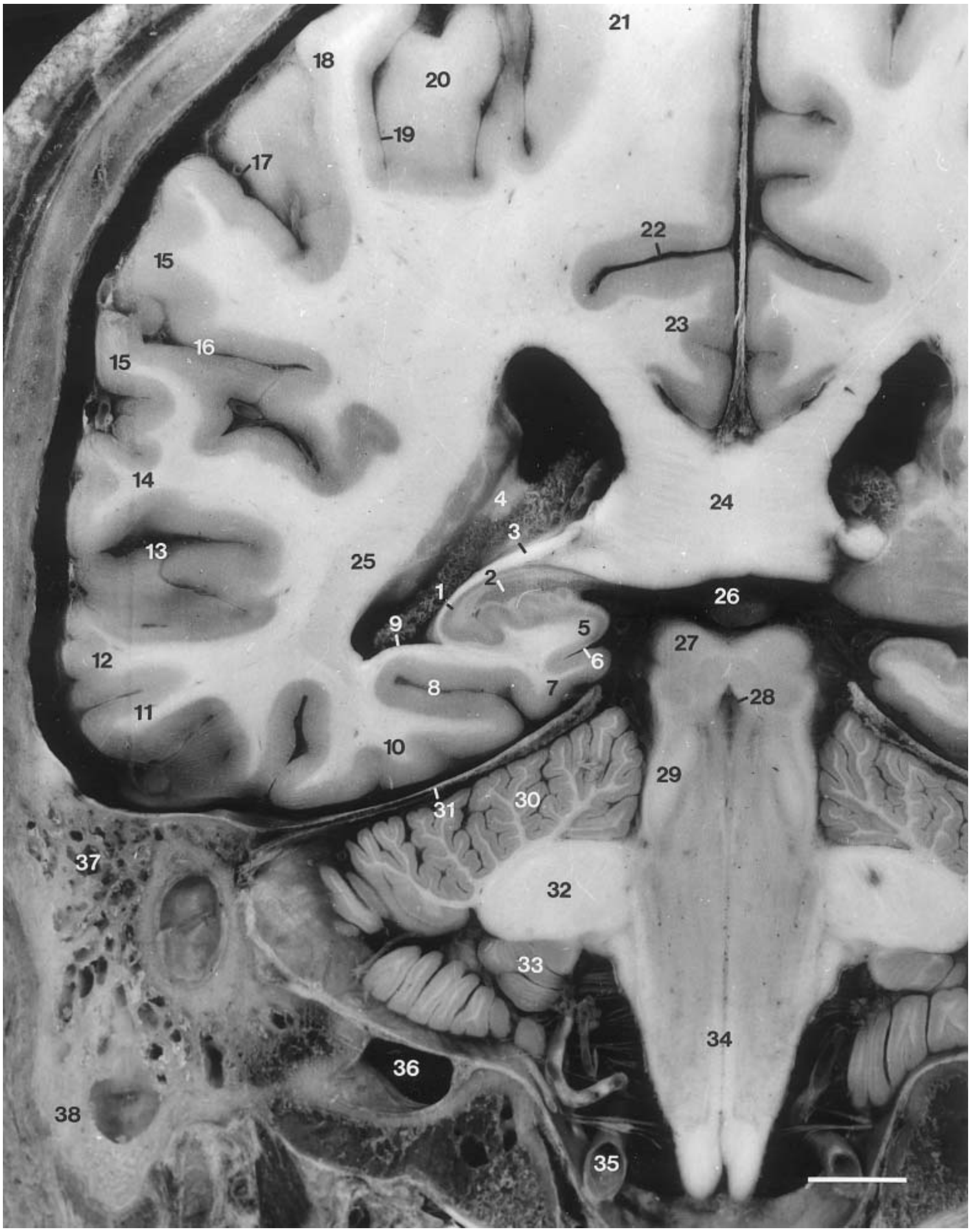

Fig. 108. D Head section, posterior view of the section. **Bar**, 10 mm

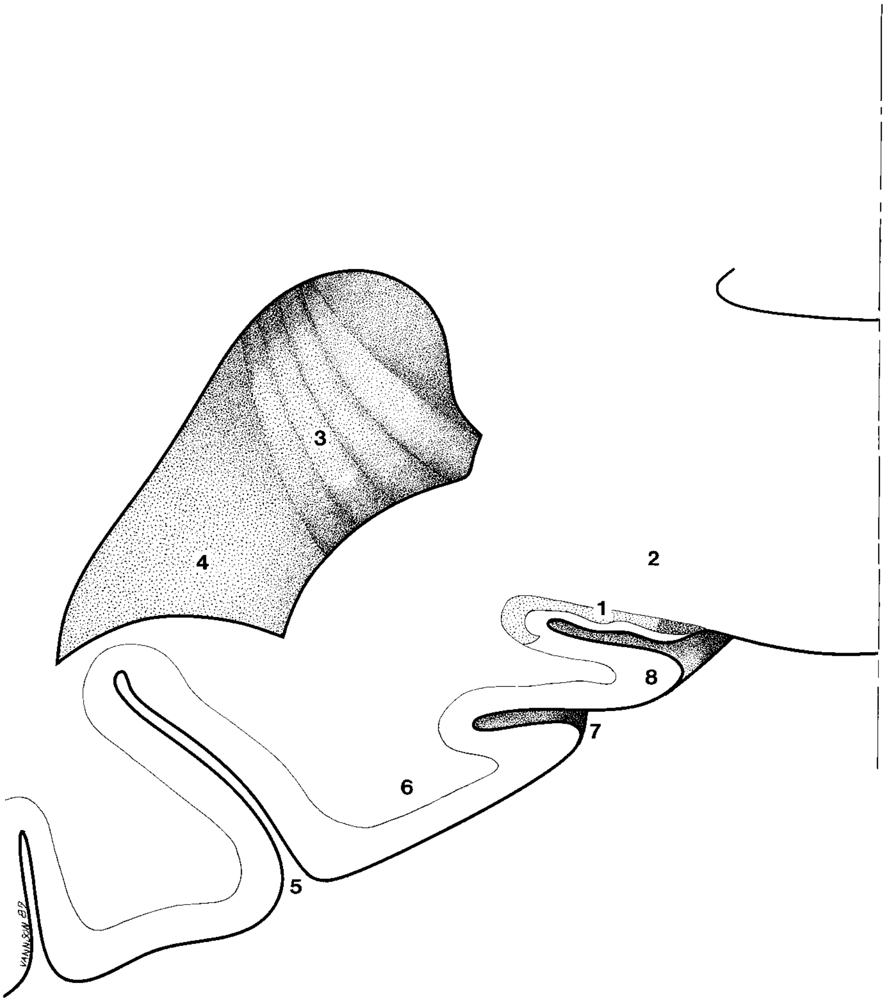

Fig. 109. A Coronal section of terminal segment of the hippocampal tail, showing plane of section **1**, cornu Ammonis (subsplenial gyrus); **2**, splenium; **3**, calcar avis; **4**, collateral trigone; **5**, collateral sulcus; **6**, parahippocampal gyrus (posterior part); **7**, anterior calcarine sulcus; **8**, isthmus

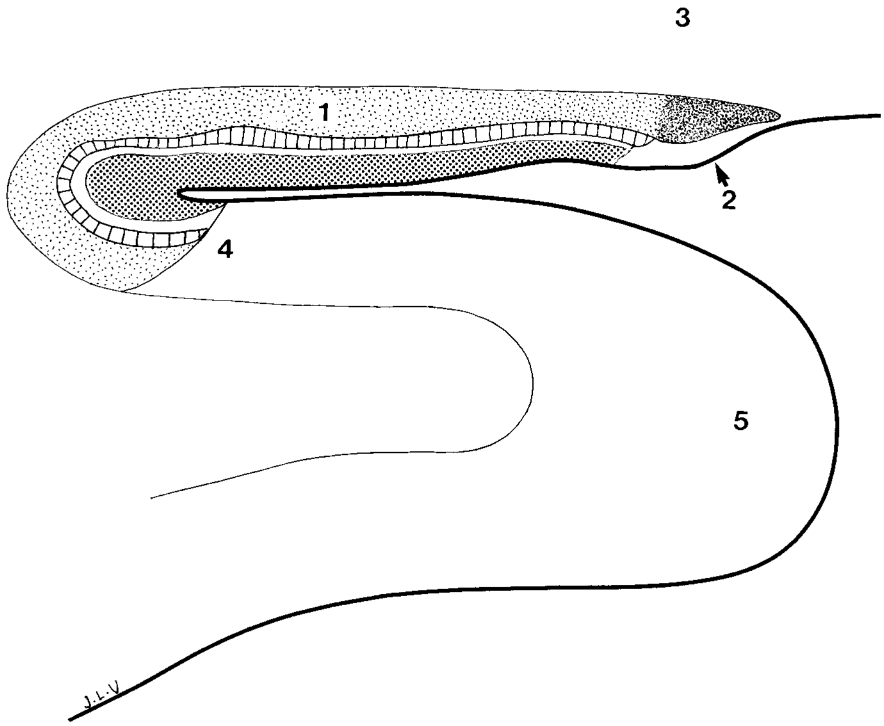

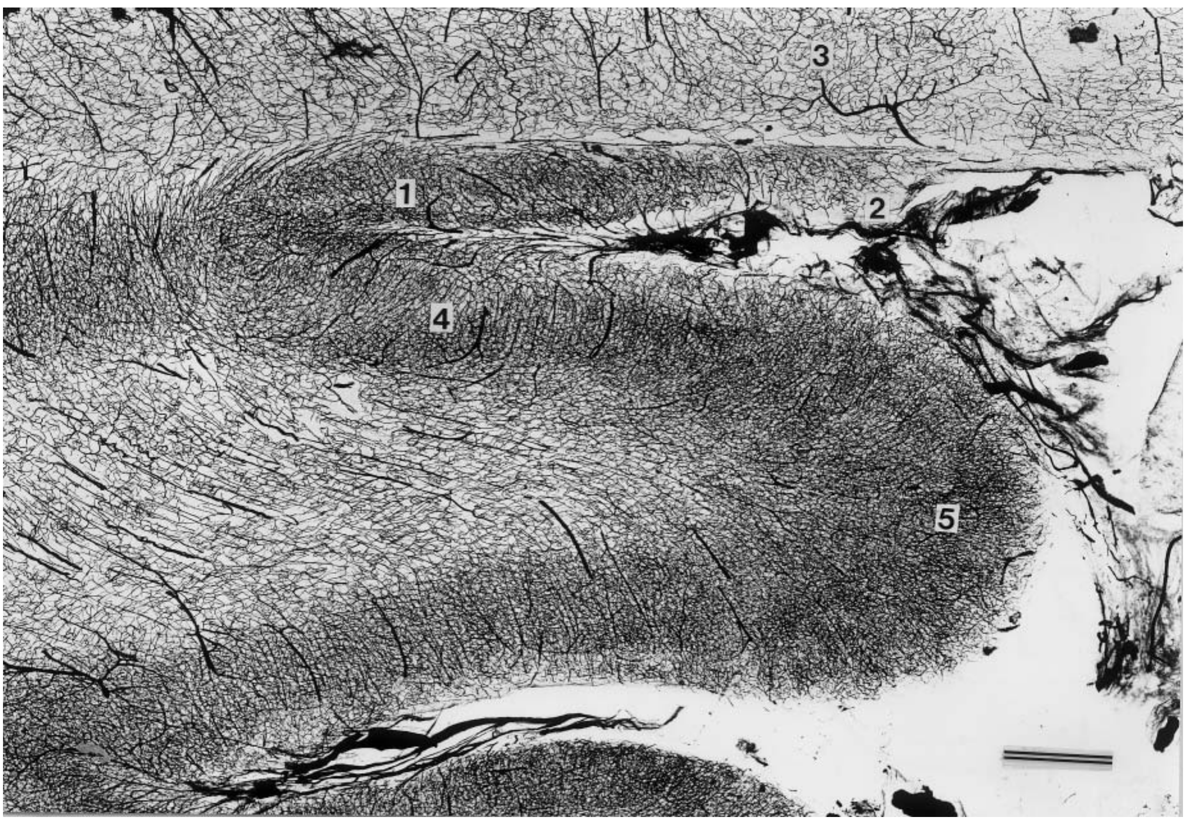

Fig. 109. B Coronal section of the hippocampal tail. Intravascular India ink injection with explanatory diagram. **Bar,** 1 mm **1**, cornu Ammonis (subsplenial gyrus; CA1, CA3); **2**, longitudinal striae; **3**, splenium; **4**, subiculum; **5**, isthmus

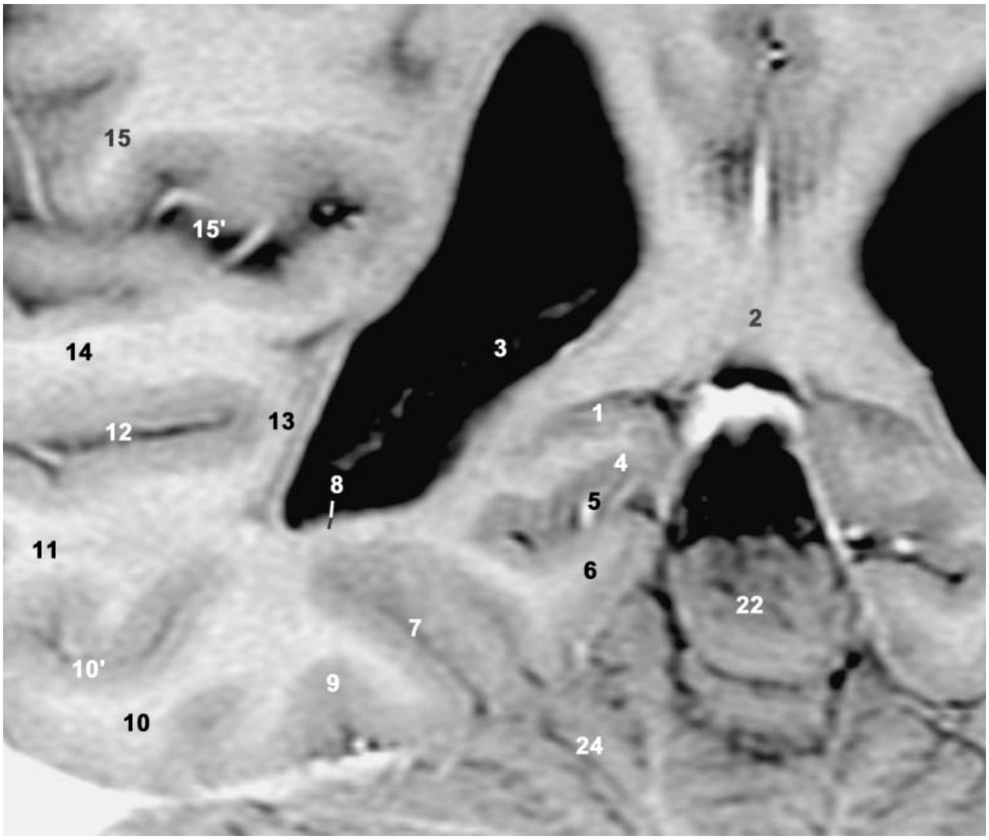

Fig. 109. C 3T MRI view

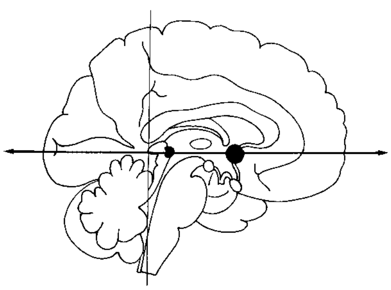

1, cornu Ammonis (subsplenial gyrus); **2**, splenium; **3**, atrium of the lateral ventricle; **4**, isthmus; **5**, anterior calcarine sulcus; **6**, parahippocampal gyrus; **7**, collateral sulcus; **8**, collateral trigone; **9**, fusiform gyrus; **10**, inferior temporal gyrus; **10′**, inferior temporal sulcus; **11**, middle temporal gyrus; **12**, superior temporal sulcus; **13**, optic radiations; **14**, superior temporal gyrus; **15**, supramarginal gyrus; **15′**, lateral fissure, posterior ascending segment; **16**, intraparietal sulcus; **17**, postcentral gyrus; **18**, central sulcus; **19**, precentral gyrus; **20**, cingulate sulcus; **21**, cingulate gyrus; **22**, central lobule; **23**, tentorium cerebelli; **24**, quadrangular lobule; **25**, superior semilunar lobule; **26**, brachium pontis; **27**, fourth ventricle; **28**, biventer lobule; **29**, transverse sinus

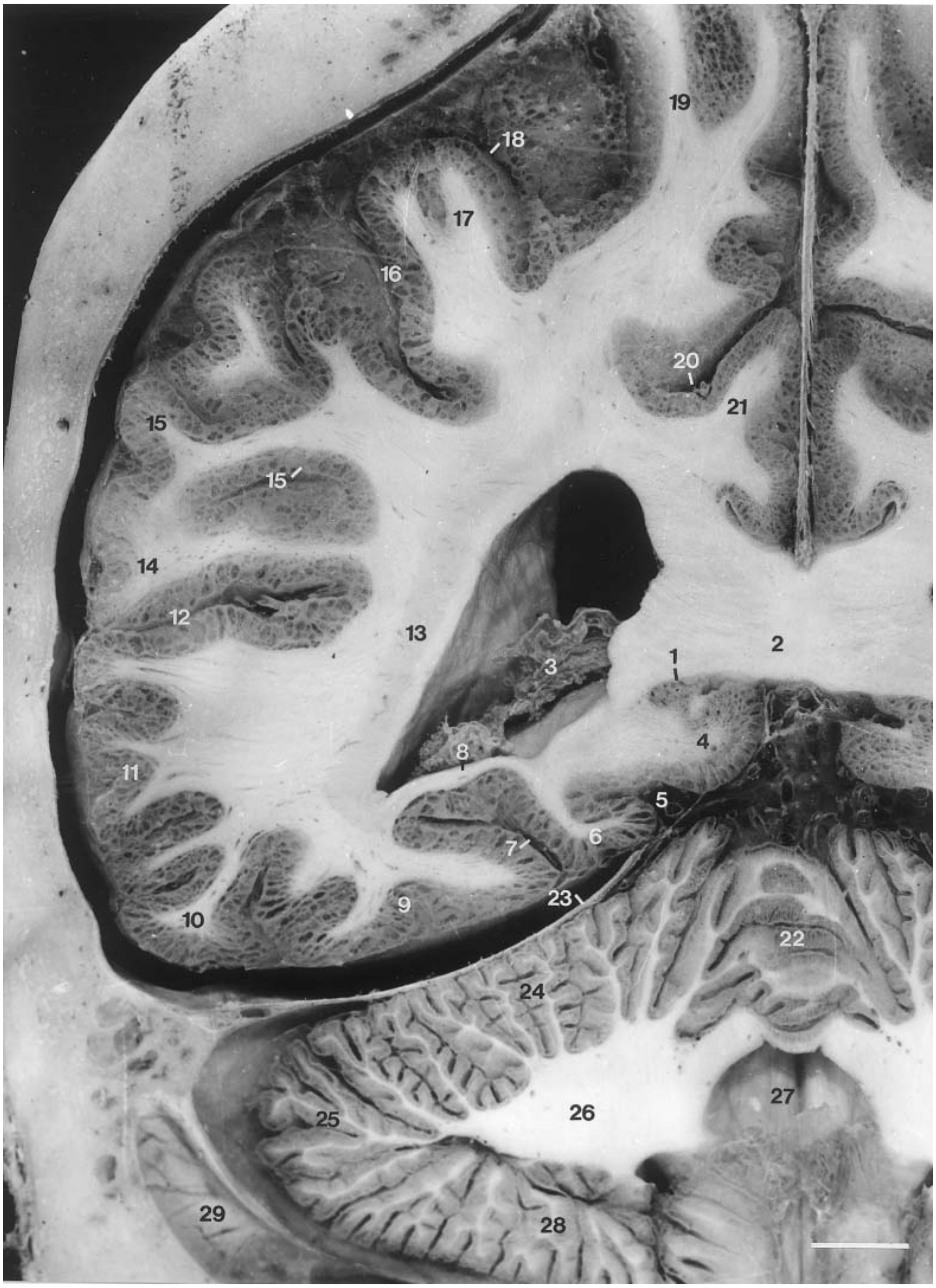

Fig. 109. D Head section, posterior view of the section **Bar,** 10 mm

7.2 Sagittal Sections

Figures 112 – 117 show sagittal sections of the hippocampus from medial to lateral levels.

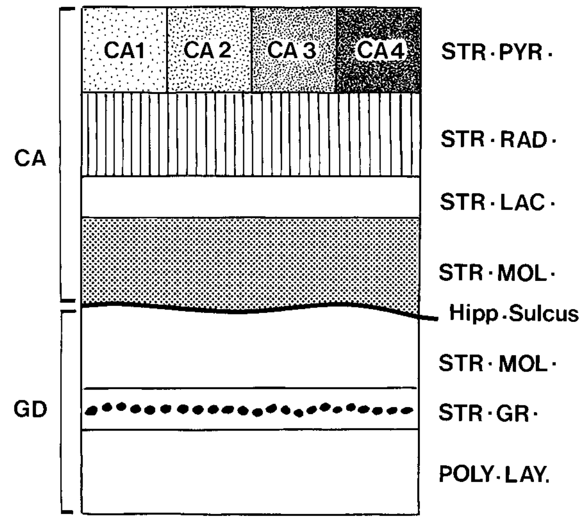

Fig. 110. Structure of the hippocampus
CA, cornu Ammonis; **STR. PYR.**, stratum pyramidale; **STR. RAD.**, stratum radiatum; **STR. LAC.**, stratum lacunosum; **STR. MOL.**, stratum moleculare; **Hipp. Sulcus**, vestigial hippocampal sulcus; **GD**, gyrus dentatus; **STR. MOL.**, stratum moleculare; **STR. GR.**, stratum granulosum; **POLY.LAY.**, polymorphic layer

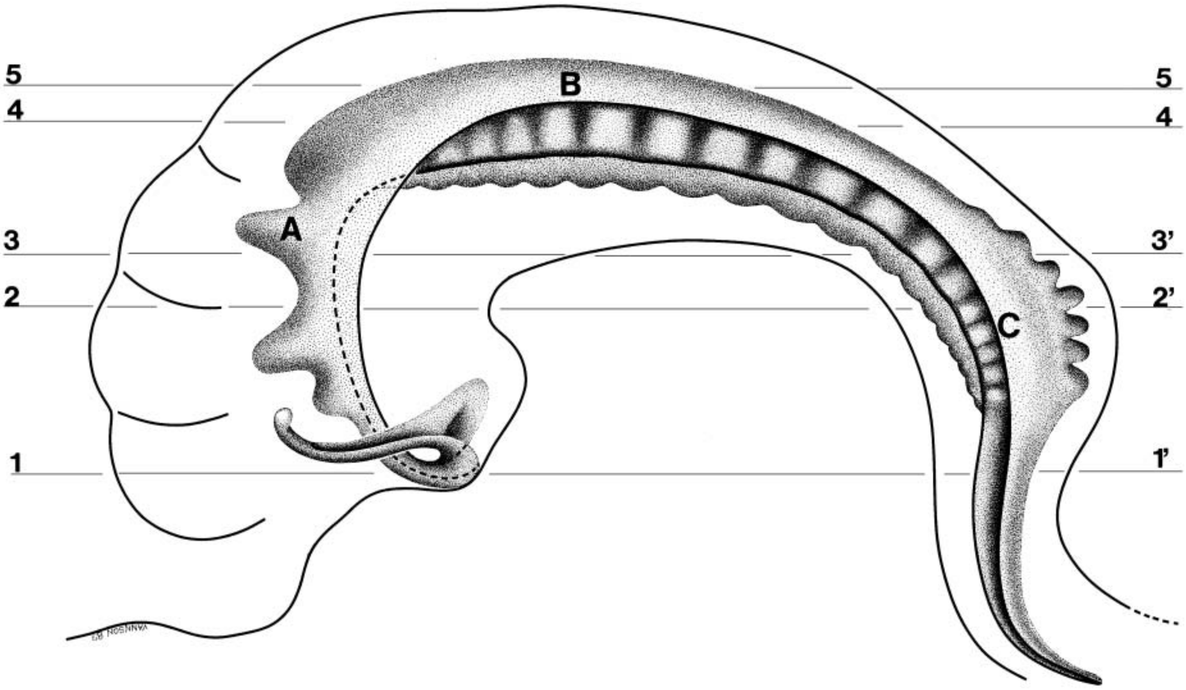

Fig. 111. A, B. General position of the gyrus dentatus in the head (**A**), body (**B**), and tail (**C**) of the hippocampus.
1 to **5**, successive planes of sections shown in Fig. 111B

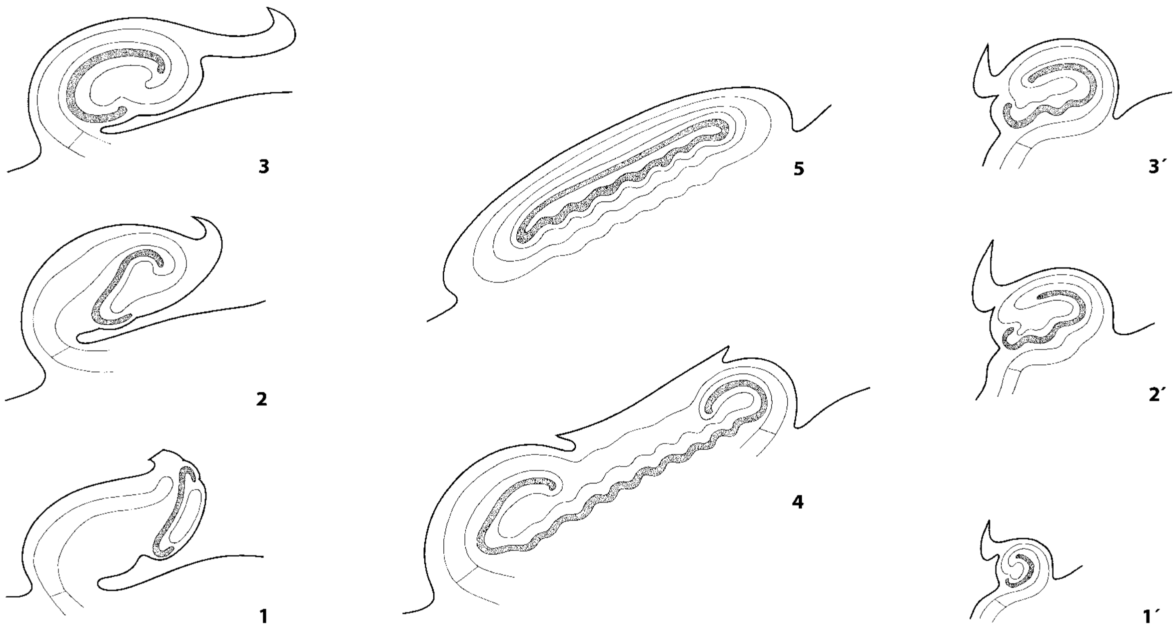

Fig. 111 B

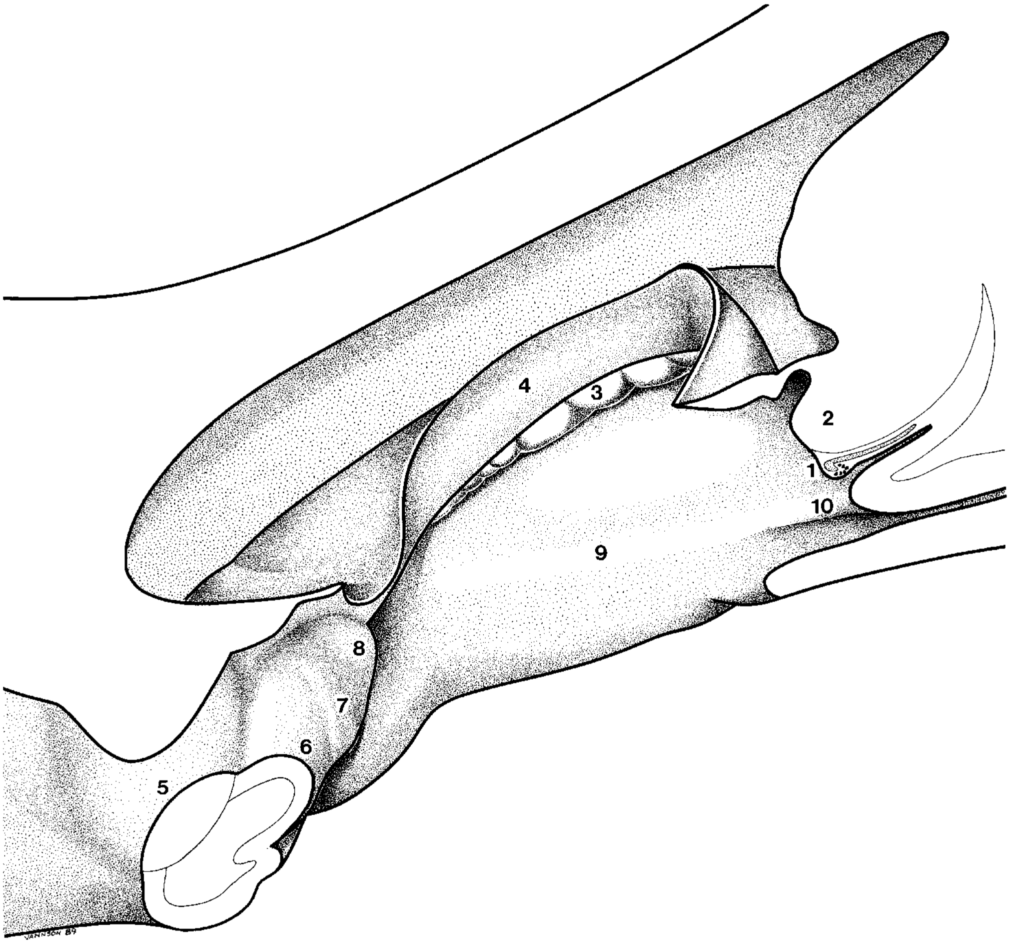

Fig. 112. A Sagittal section of hippocampus, showing plane of section
1, hippocampal tail; **2**, splenium; 3, margo denticulatus; **4**, fimbria; **5**, semilunar gyrus; **6**, uncinate gyrus; **7**, band of Giacomini; **8**, uncal apex; **9**, parahippocampal gyrus; **10**, isthmus

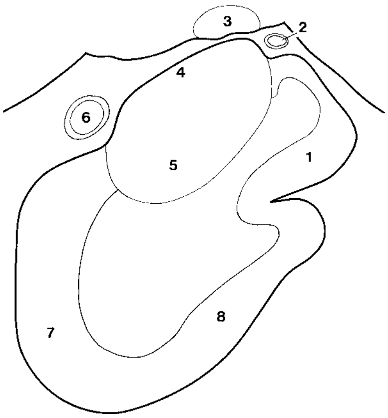

Fig. 112. B Sagittal section of uncus. Intravascular India ink injection with explanatory diagram. **Bar,** 2 mm
1, uncinate gyrus; **2**, anterior choroidal artery; **3**, optic tract; **4**, cortical nucleus of amygdala; **5**, accessory basal nucleus of amygdala; **6**, middle cerebral artery; **7**, ambient gyrus; **8**, parahippocampal gyrus

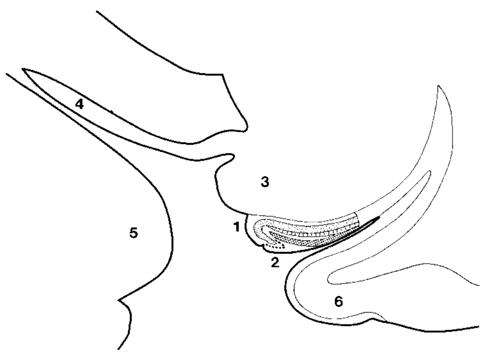

Fig. 112. C Sagittal section of hippocampal tail. Intravascular India ink injection with explanatory diagram. **Bar,** 2 mm

1, gyrus fasciolaris; **2**, fasciola cinerea; **3**, splenium; **4**, fornix; **5**, pulvinar; **6**, isthmus

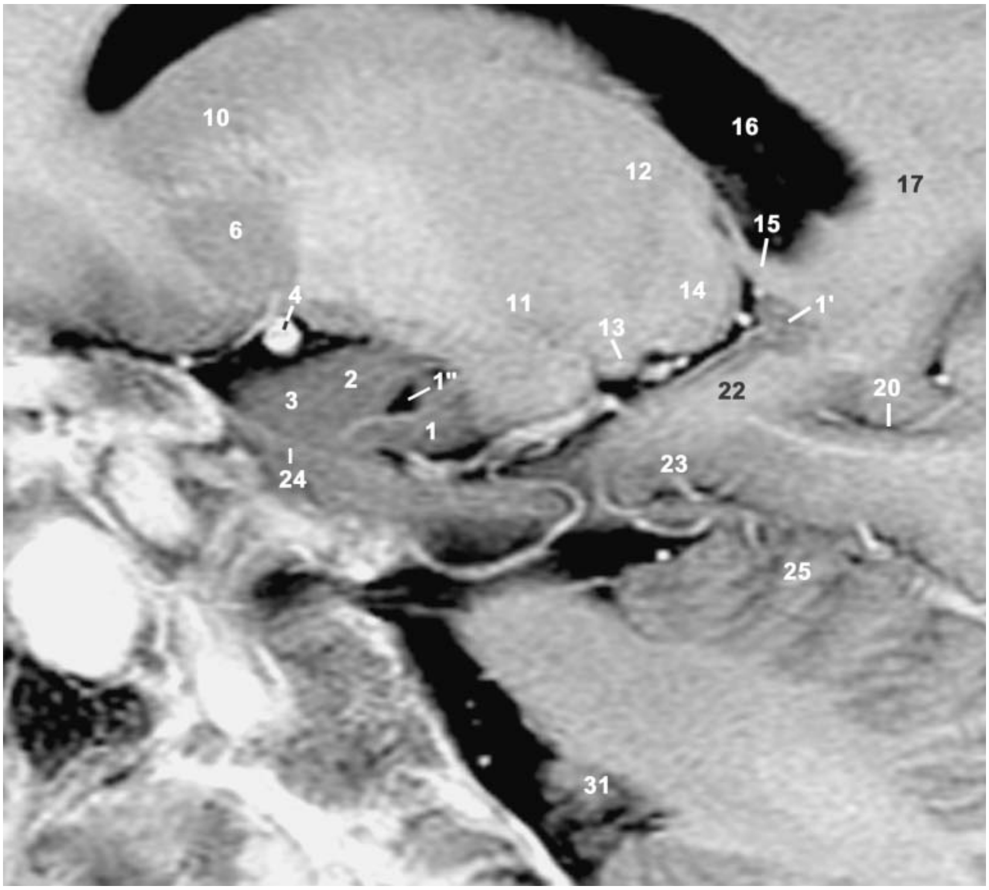

Fig. 112. D 3T MRI view

1, uncinate gyrus (head of hippocampus); **1′**, hippocampal tail; **1″**, uncal recess of the temporal horn; **2**, amygdala; **3**, ambient gyrus; **4**, middle cerebral artery; **5**, optic tract; **6**, putamen; **7**, anterior commissure, lateral part; **8**, globus pallidus, lateral part; **9**, globus pallidus, medial part; **10**, caudate nucleus; **11**, internal capsule, posterior limb; **12**, lateral posterior thalamic nucleus; **13**, medial geniculate body; **14**, pulvinar; **15**, crus of fornix; **16**, lateral ventricle; **17**, corpus callosum; **18**, parieto-occipital fissure; **19**, cuneus; **20**, calcarine sulcus and striate cortex; **21**, lingual gyrus; **22**, isthmus; **23**, parahippocampal gyrus; **24**, tentorium cerebelli; **25**, quadrangular lobule; **26**, simple lobule; **27**, superior semilunar lobule; **28**, horizontal fissure; **29**, inferior semilunar lobule; **30**, biventer lobule; **31**, flocculus; **32**, trigeminal nerve; **33**, trigeminal cave; **34**, temporal, petrous part; **35**, internal carotid artery; **36**, dentate nucleus

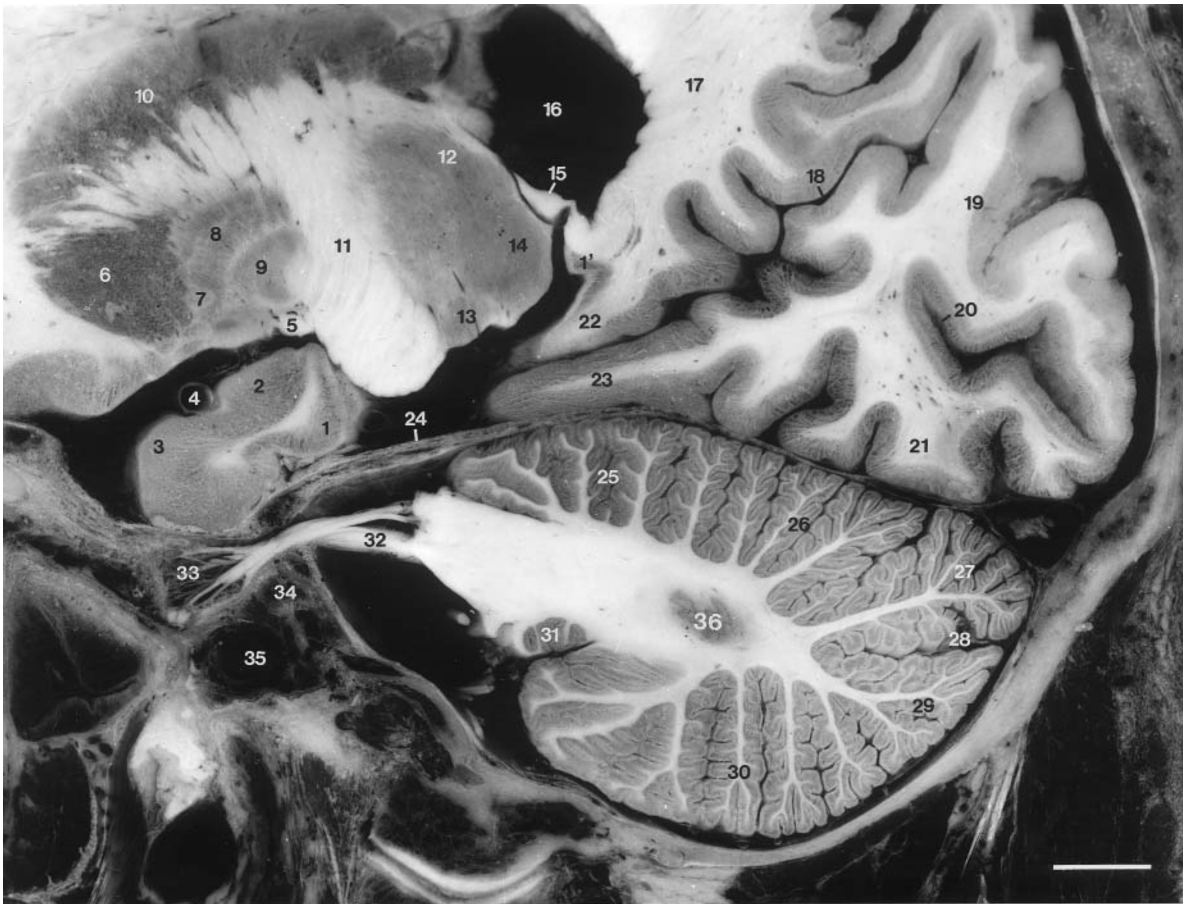

Fig. 112. E Head section. **Bar**, 10 mm

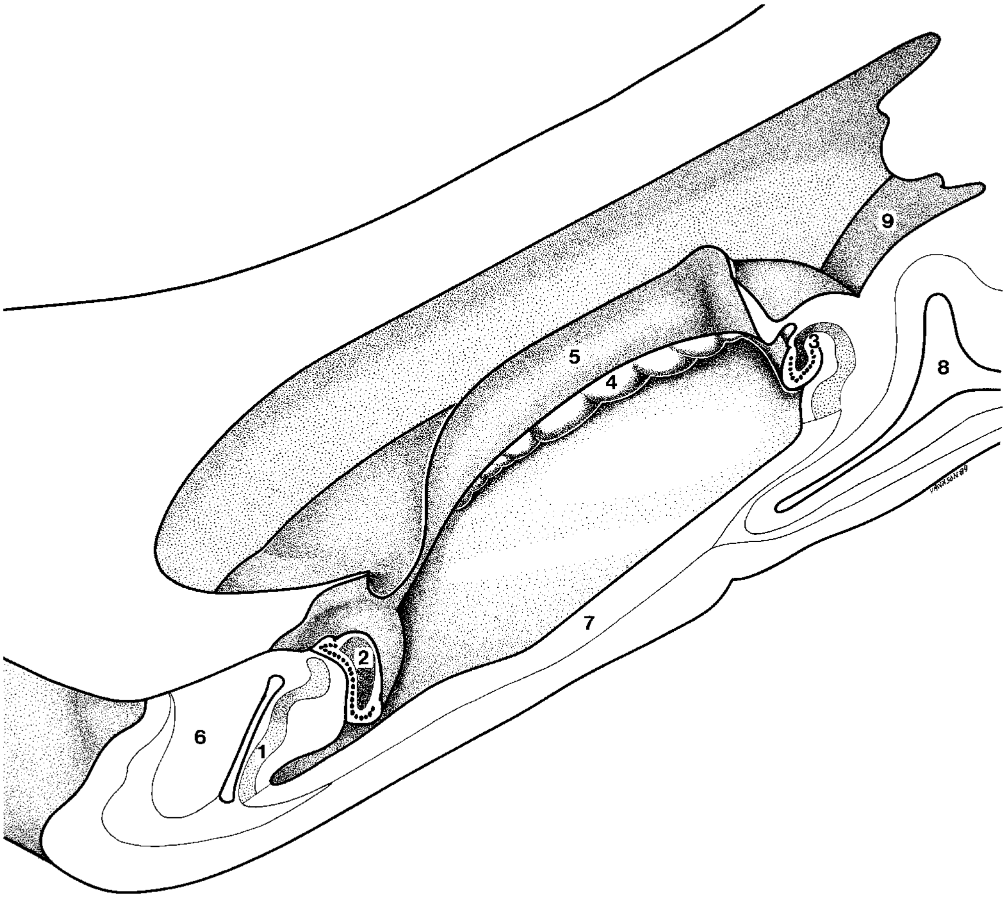

Fig. 113. A Sagittal section of hippocampus, showing plane of section
1, hippocampal head; **2**, uncal apex; **3**, hippocampal tail; **4**, margo denticulatus; **5**, fimbria; **6**, amygdala; **7**, parahippocampal gyrus; **8**, anterior calcarine sulcus; **9**, calcar avis

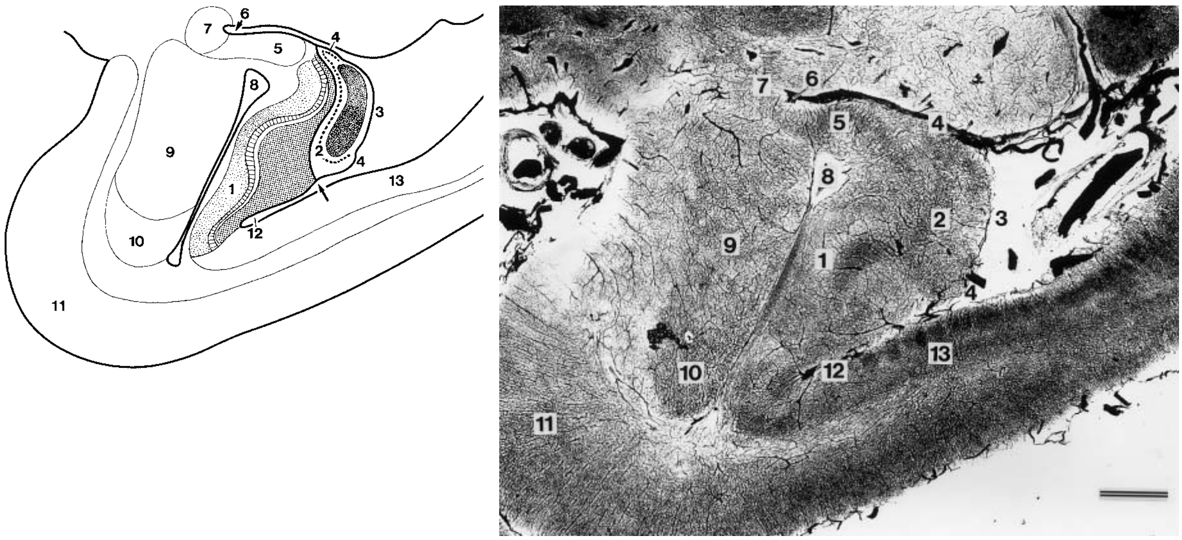

Fig. 113. B Sagittal section of hippocampal head. Intravascular India ink injection with explanatory diagram. Note the maculate aspect of the vascular network of the presubiculum (**13**) in relation to its nervous structure (see p. 9). The **arrow** indicates the superficial hippocampal sulcus. **Bar,** 2.4 mm

1, cornu Ammonis (CA1, CA2); **2**, gyrus dentatus; **3**, uncal apex (CA3, CA4); **4**, band of Giacomini; **5**, cortical nucleus of amygdala; **6**, endorhinal sulcus; **7**, medial nucleus of amygdala; **8**, temporal horn of the lateral ventricle; **9**, accessory basal nucleus of amygdala; **10**, basal nucleus of amygdala; **11**, ambient gyrus; **12**, uncal sulcus; **13**, presubiculum

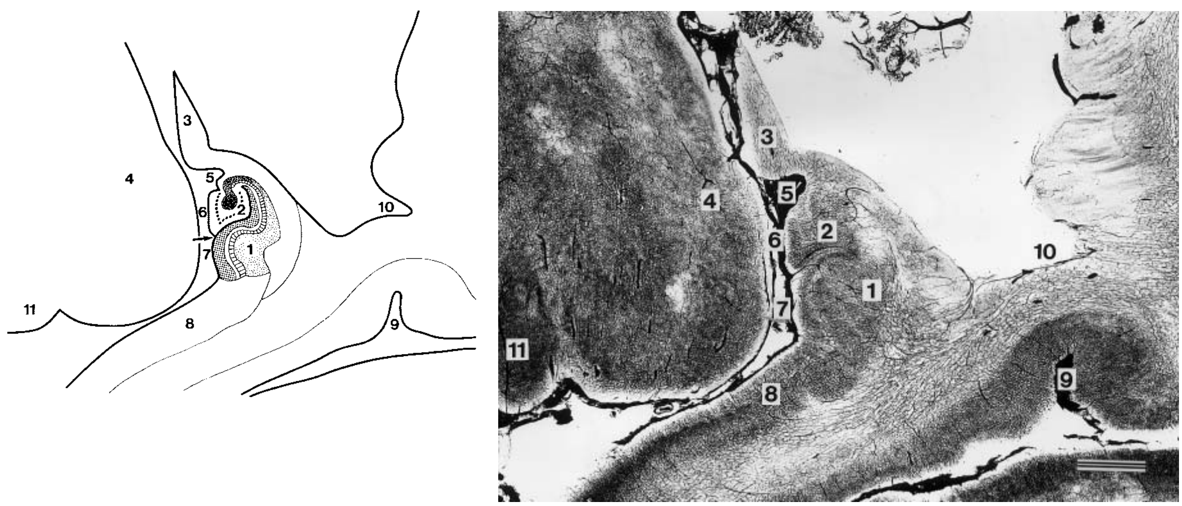

Fig. 113. C Sagittal section of hippocampal tail (middle segment). Vascular India ink injection with explanatory diagram. The **arrow** indicates the superficial hippocampal sulcus. **Bar,** 2.3 mm

1, cornu Ammonis (CA1 – CA4); **2**, gyrus dentatus; **3**, fimbria; **4**, pulvinar; **5**, gyrus fasciolaris; **6**, fasciola cinerea; **7**, gyri of Andreas Retzius; **8**, subiculum; **9**, anterior calcarine sulcus; **10**, calcar avis; **11**, lateral geniculate body

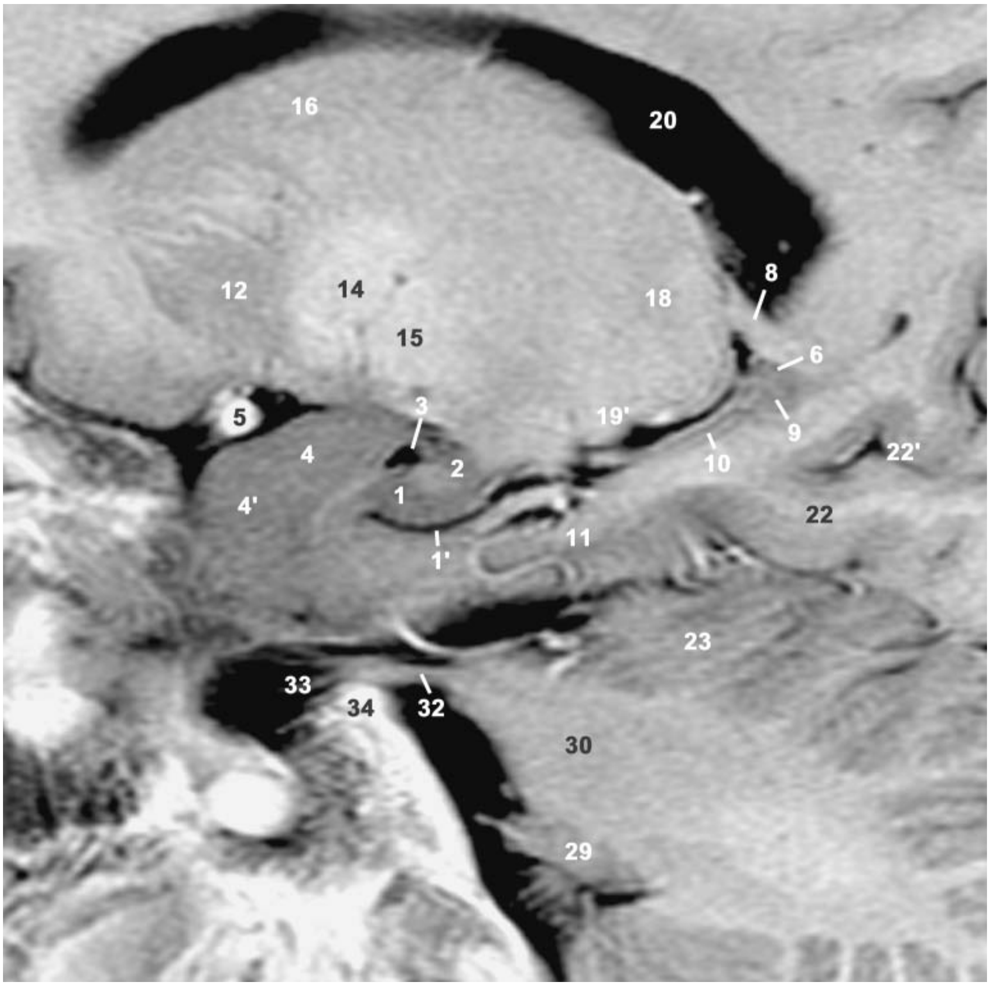

Fig. 113. D 3T MRI view

1, hippocampal head, cornu Ammonis; **1′**, uncal sulcus; **2**, hippocampal head, uncal apex; **3**, temporal (inferior) horn of the lateral ventricle; **4**, amygdala; **4′**, ambient gyrus; **5**, middle cerebral artery; **6**, hippocampal tail, cornu Ammonis; **7**, hippocampal tail, fasciola cinerea; **8**, fimbria; **9**, gyri of Andreas Retzius; **10**, subiculum; **11**, parahippocampal gyrus; **12**, putamen; **13**, anterior commissure, lateral part; **14**, globus pallidus, lateral part; **15**, globus pallidus, medial part; **16**, caudate nucleus; **17**, internal capsule, posterior limb; **18**, pulvinar; **19**, lateral geniculate body; **19′**, medial geniculate body; **20**, lateral ventricle; **21**, superior occipital gyrus; **22**, lingual gyrus; **22′**, calcarine sulcus; **23**, quadrangular lobule; **24**, simple lobule; **25**, superior semilunar gyrus; **26**, horizontal fissure; **27**, inferior semilunar gyrus; **28**, biventer lobule; **29**, flocculus; **30**, brachium pontis; **31**, tentorium cerebelli; **32**, trigeminal nerve; **33**, trigeminal cave; **34**, temporal, petrous part; **35**, internal cerebral artery

Fig. 113. E Head section. **Bar**, 10 mm

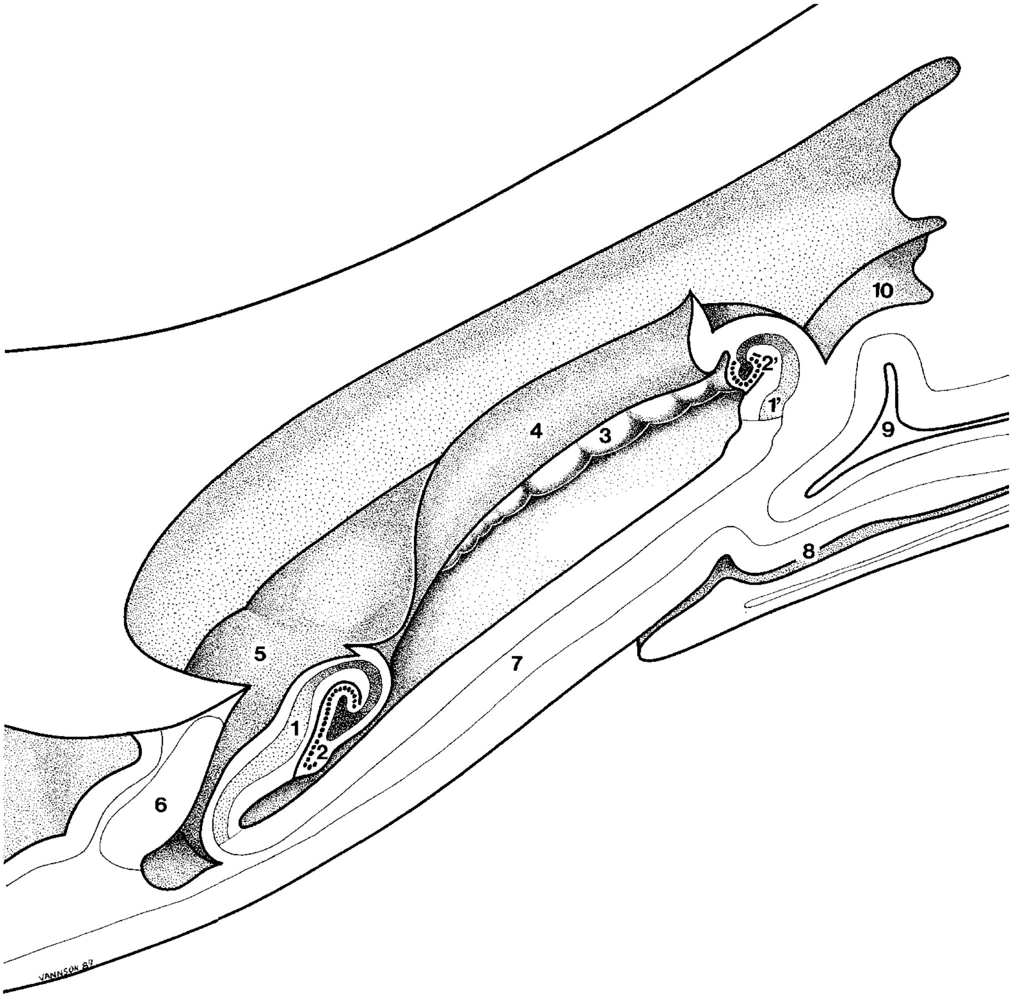

Fig. 114. A Sagittal section of hippocampus, showing plane of section
1, cornu Ammonis in the head; **1′**, cornu Ammonis in the tail; **2**, gyrus dentatus in the head; **2′**, gyrus dentatus in the tail; **3**, margo denticulatus; **4**, fimbria; **5**, digitationes hippocampi; **6**, amygdala; **7**, parahippocampal gyrus; **8**, collateral sulcus; **9**, anterior calcarine sulcus; **10**, calcar avis

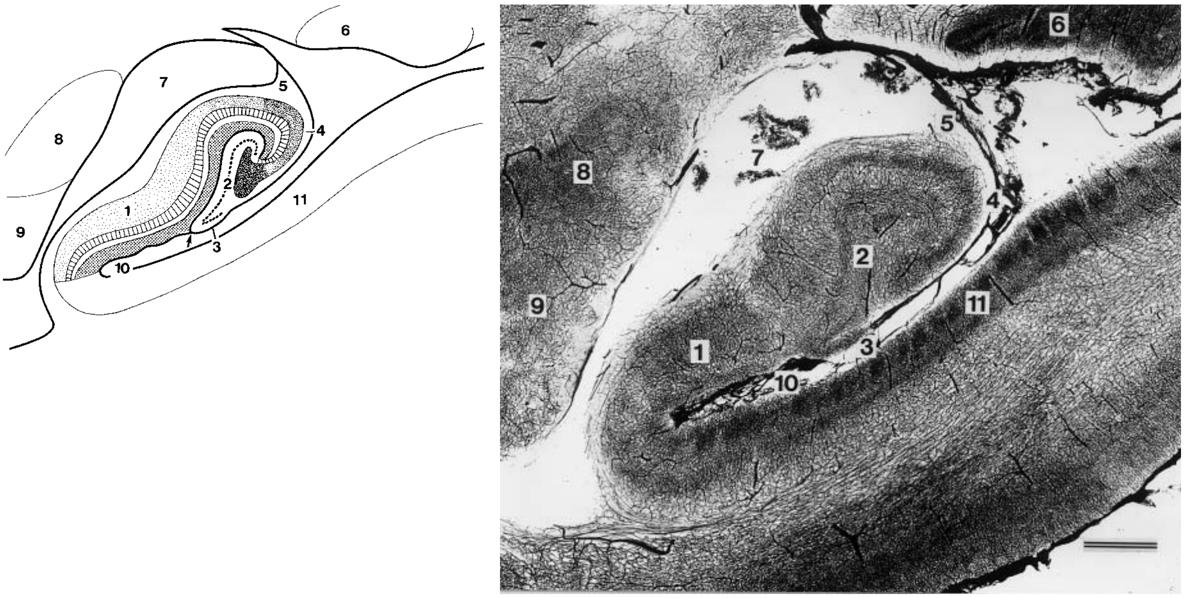

Fig. 114. B Sagittal section of hippocampal head. Intravascular India ink injection with explanatory diagram. The **arrow** indicates the superficial hippocampal sulcus. Note the maculate aspect of the capillary network in relation to the structure of the presubiculum (**11**) (see p. 9). **Bar,** 2.2 mm

1, cornu Ammonis (CA1 – CA4); **2**, gyrus dentatus; **3**, band of Giacomini; **4**, uncal apex; **5**, fimbria; **6**, lateral geniculate body; **7**, temporal horn of lateral ventricle; **8**, basal nucleus of amygdala; **9**, lateral nucleus of amygdala; **10**, uncal sulcus; **11**, presubiculum

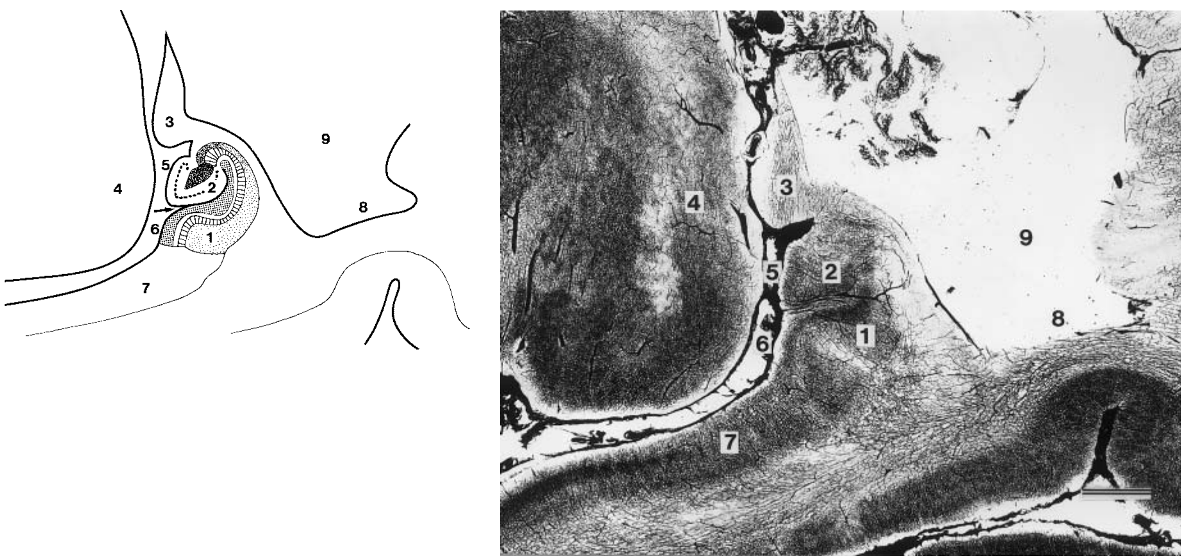

Fig. 114. C Sagittal section of hippocampal tail (middle segment). Intravascular India ink injection with explanatory diagram. The **arrow** indicates the superficial hippocampal sulcus. **Bar,** 2 mm

1, cornu Ammonis (CA1 – CA4); **2**, gyrus dentatus; **3**, fimbria; **4**, pulvinar; **5**, fasciola cinerea; **6**, gyri of Andreas Retzius; **7**, subiculum; **8**, calcar avis; **9**, atrium

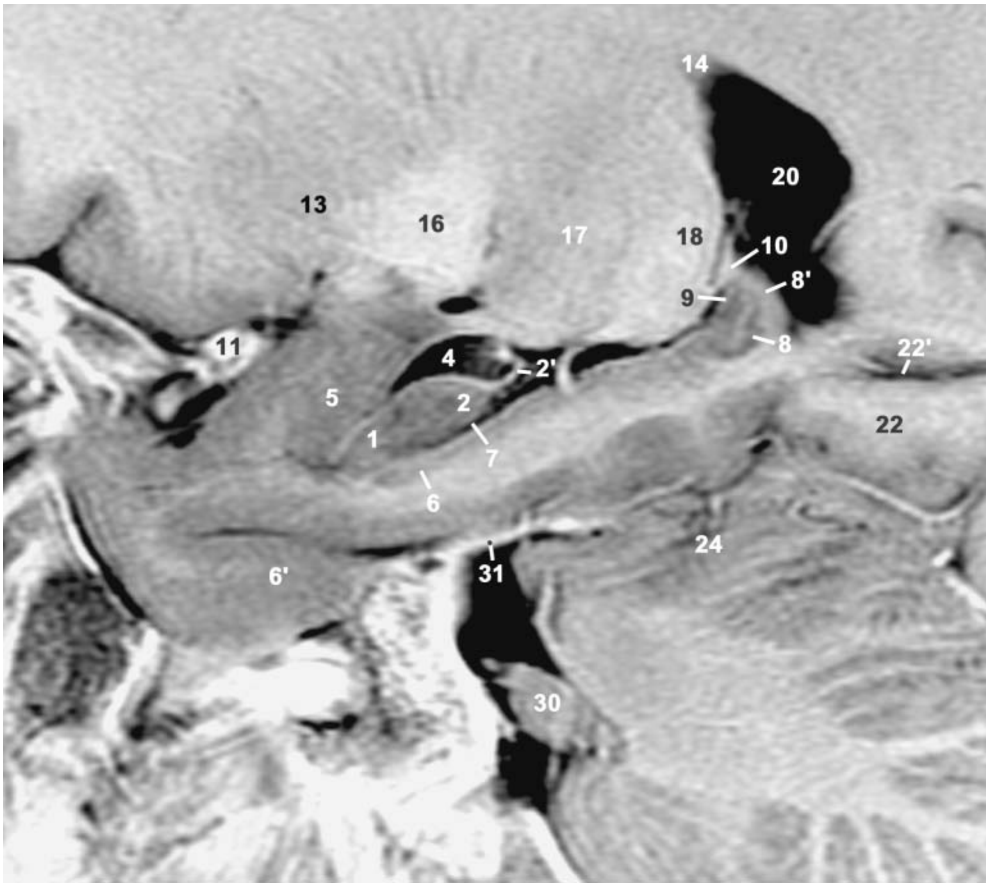

Fig. 114. D 3T MRI view

1, hippocampal head, cornu Ammonis; **2**, hippocampal head, gyrus dentatus; **2′**, fimbria; **3**, uncal apex; **4**, temporal (inferior) horn of the lateral ventricle; **5**, amygdala; **6**, subiculum; **6′**, ambient gyrus (entorhinal area); **7**, uncal sulcus; **8**, hippocampal tail, cornu Ammonis; **8′**, alveus; **9**, hippocampal tail, gyrus dentatus; **10**, fimbria; **11**, middle cerebral artery; **12**, anterior commissure, lateral part; **13**, putamen; **14**, caudate nucleus; **15**, globus pallidus, lateral part; **16**, globus pallidus, medial part; **17**, internal capsule, posterior limb; **18**, pulvinar; **19**, lateral geniculate body; **20**, lateral ventricle; **21**, superior occipital gyrus; **22**, lingual gyrus; **22′**, calcarine sulcus; **23**, transverse sinus; **24**, quadrangular lobule; **25**, simple lobule; **26**, superior semilunar lobule; **27**, horizontal fissure; **28**, inferior semilunar lobule; **29**, biventer lobule; **30**, flocculus; **31**, tentorium cerebelli; **32**, trigeminal nerve; **33**, temporal, petrous part; **34**, trigeminal cave; **35**, internal carotid artery

Fig. 114. E Head section. Bar, 10 mm

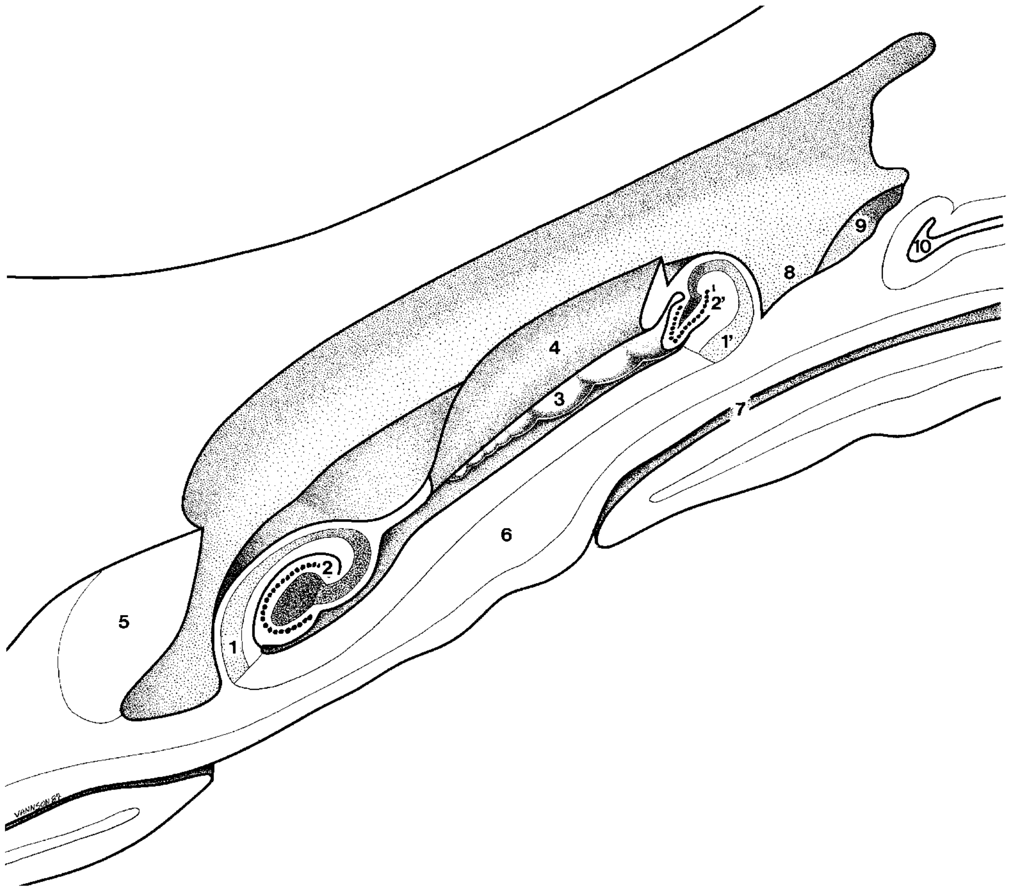

Fig. 115. A Sagittal section of hippocampus, showing plane of section
1, cornu Ammonis in the head; **1′**, cornu Ammonis in the tail; **2**, gyrus dentatus in the head; **2′**, gyrus dentatus in the tail; **3**, margo denticulatus; **4**, fimbria; **5**, amygdala; **6**, parahippocampal gyrus; **7**, collateral sulcus; **8**, collateral trigone; **9**, calcar avis; **10**, calcarine sulcus

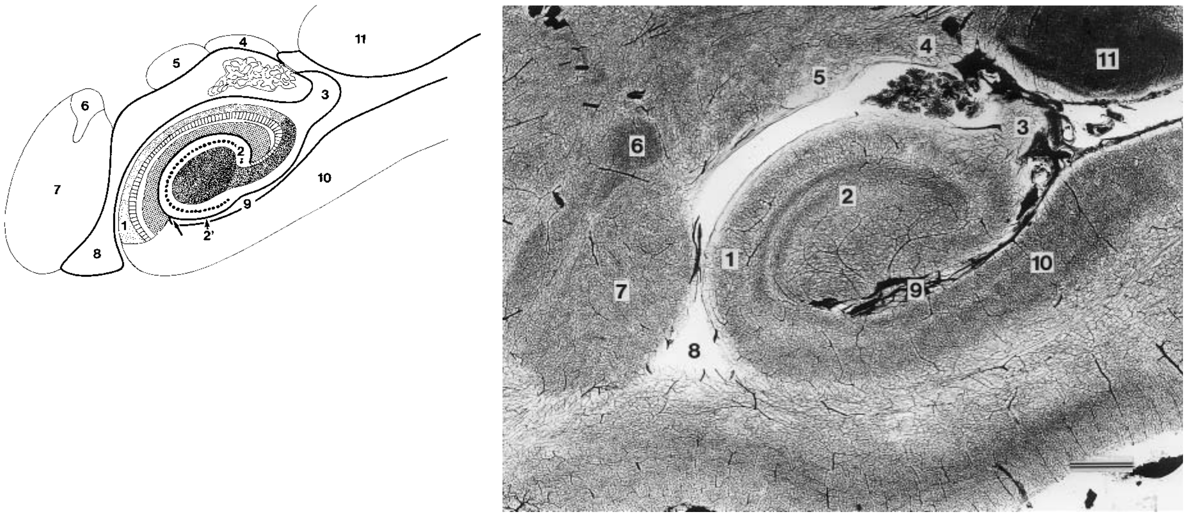

Fig. 115. B Sagittal section of hippocampal head. Intravascular India ink injection with explanatory diagram. **Arrow** indicates the superficial hippocampal sulcus. Bar, 2 mm

1, cornu Ammonis (CA1 – CA4); **2**, gyrus dentatus; **2′**, band of Giacomini; **3**, fimbria; **4**, stria terminalis; **5**, tail of caudate nucleus; **6**, basal nucleus of amygdala; **7**, lateral nucleus of amygdala; **8**, temporal horn of lateral ventricle (uncal recess); **9**, uncal sulcus; **10**, subiculum; **11**, lateral geniculate body

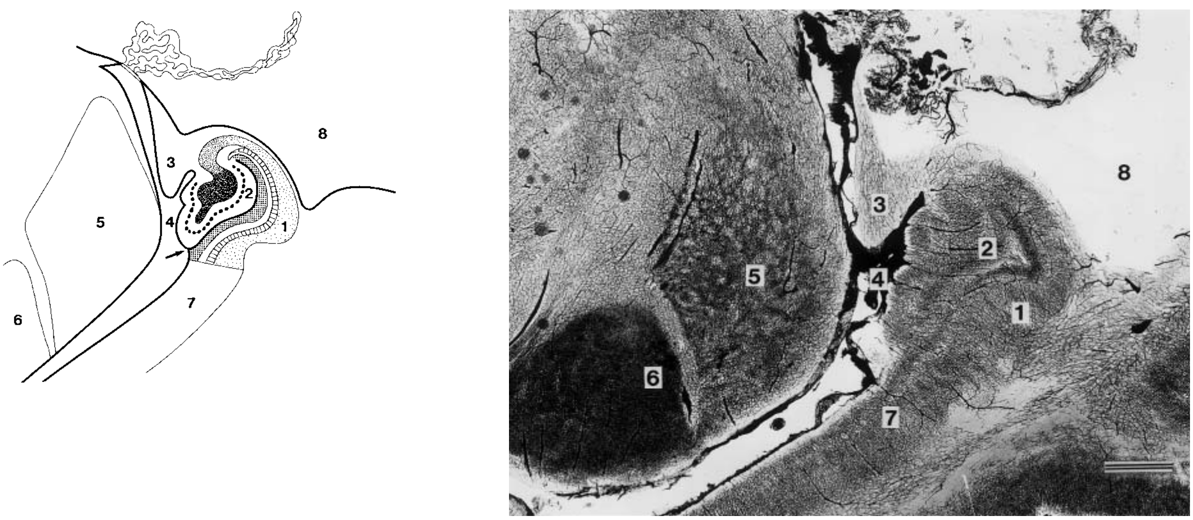

Fig. 115. C Sagittal section of hippocampal tail (initial segment following the hippocampal body). Vascular injection with explanatory diagram. **Arrow** indicates the superficial hippocampal sulcus. **Bar**, 2.5 mm

1, cornu Ammonis (CA1 – CA4); **2**, gyrus dentatus; **3**, fimbria; **4**, margo denticulatus; **5**, pulvinar; **6**, lateral geniculate body; **7**, subiculum; **8**, atrium

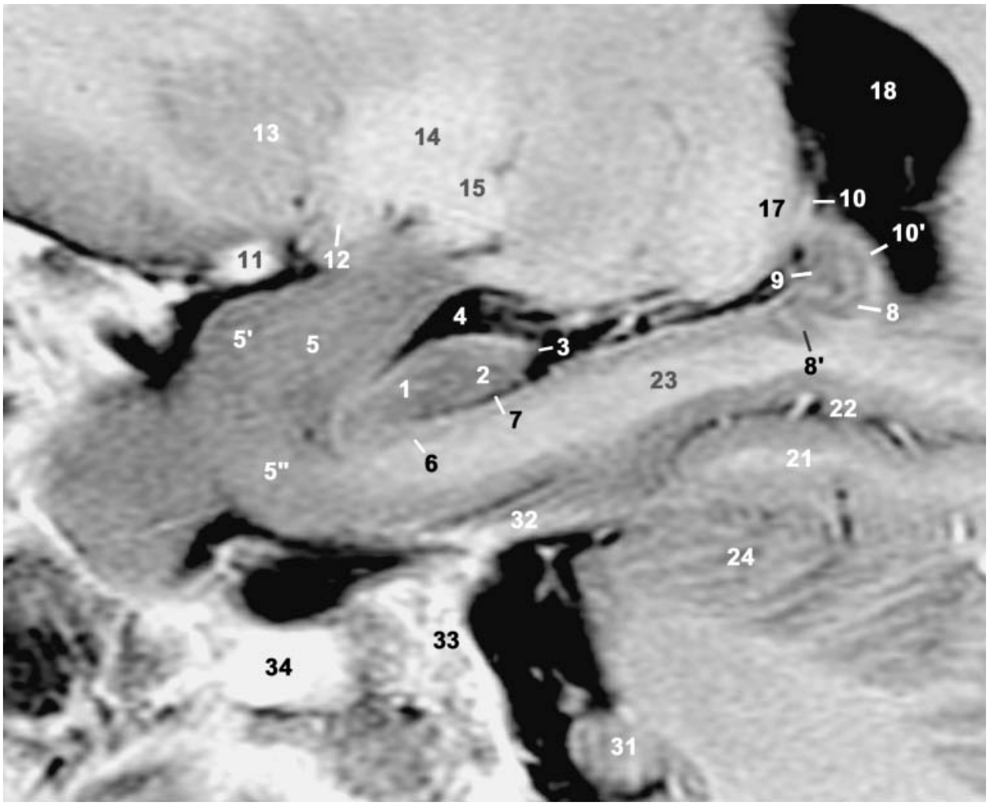

Fig. 115. D 3T MRI view

1, hippocampal head, cornu Ammonis; **2**, hippocampal head, gyrus dentatus; **3**, fimbria; **4**, temporal (inferior) horn of the lateral ventricle; **5**, amygdala; **5′**, semilunar gyrus; **5″**, ambient gyrus; **6**, subiculum; **7**, uncal sulcus; **8**, hippocampal tail, cornu Ammonis; **8′**, gyri of Andreas Retzius; **9**, hippocampal tail, gyrus dentatus; **10**, fimbria; **10′**, alveus; **11**, middle cerebral artery; **12**, anterior commissure, lateral part; **13**, putamen; **14**, globus pallidus, lateral part; **15**, globus pallidus, medial part; **16**, caudate nucleus; **17**, pulvinar; **18**, lateral ventricle; **19**, middle occipital gyrus; **20**, inferior occipital gyrus; **21**, fusiform gyrus; **22**, collateral sulcus; **23**, parahippocampal gyrus; **24**, quadrangular lobule; **25**, simple lobule; **26**, superior semilunar lobule; **27**, transverse sinus; **28**, horizontal fissure; **29**, inferior semilunar lobule; **30**, biventer lobule; **31**, flocculus; **32**, tentorium cerebelli; **33**, temporal, petrous part; **34**, internal carotid artery; **35**, auditory tube

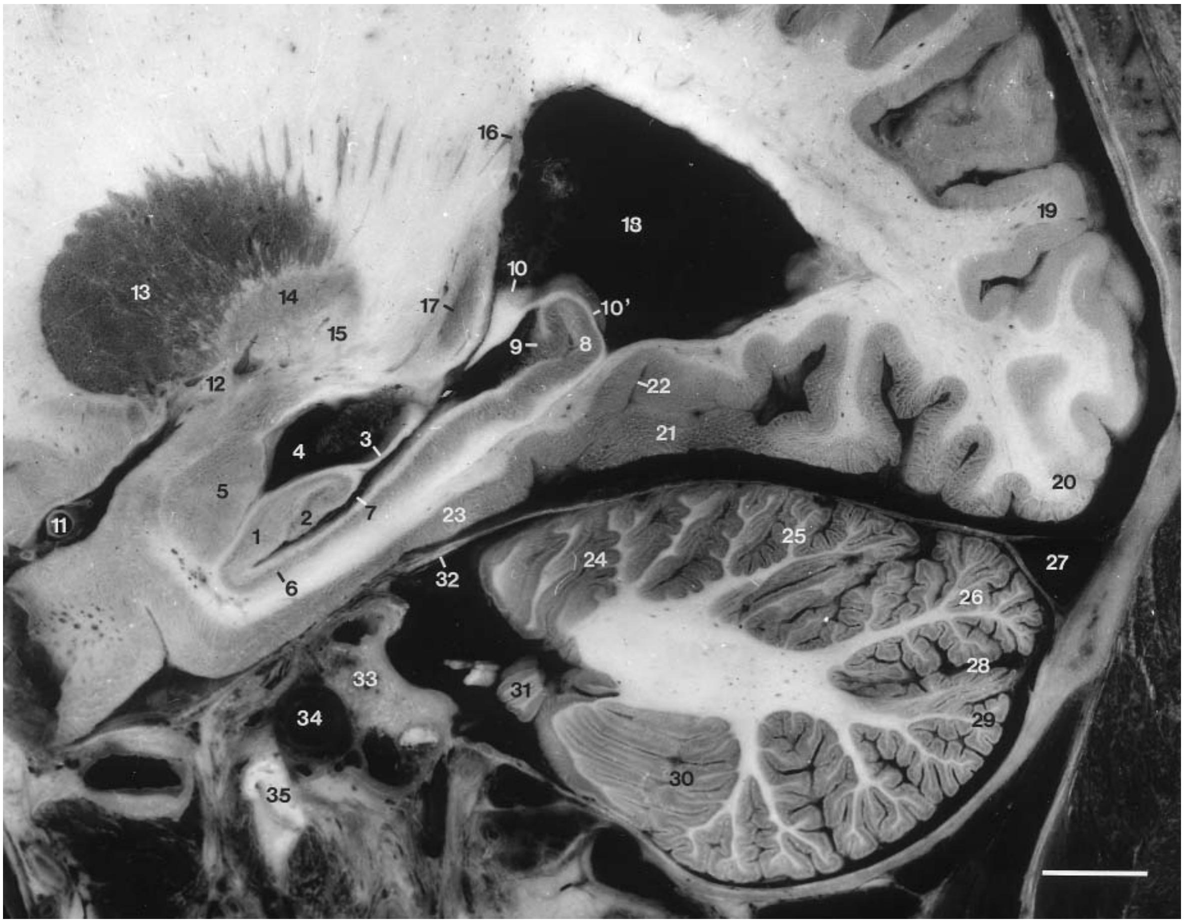

Fig. 115. E Head section. **Bar**, 10 mm

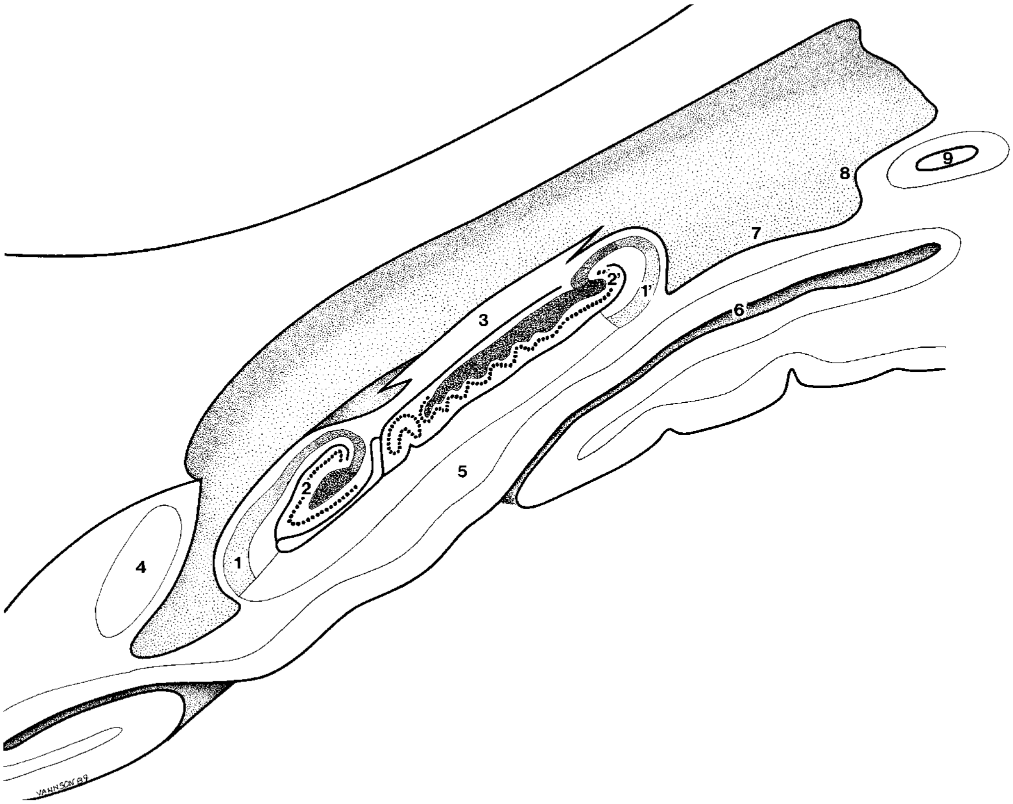

Fig. 116. A Sagittal section of hippocampus, showing plane of section
1, cornu Ammonis in the head; **1′**, cornu Ammonis in the body; **2**, gyrus dentatus in the head; **2′**, gyrus dentatus in the body; **3**, fimbria; **4**, amygdala; **5**, parahippocampal gyrus; **6**, collateral sulcus; **7**, collateral trigone; **8**, calcar avis; **9**, calcarine sulcus

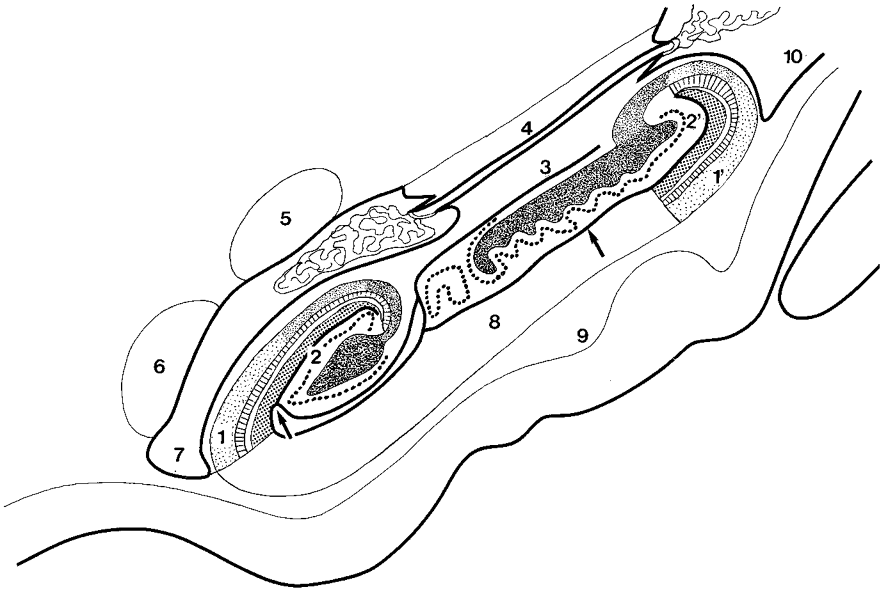

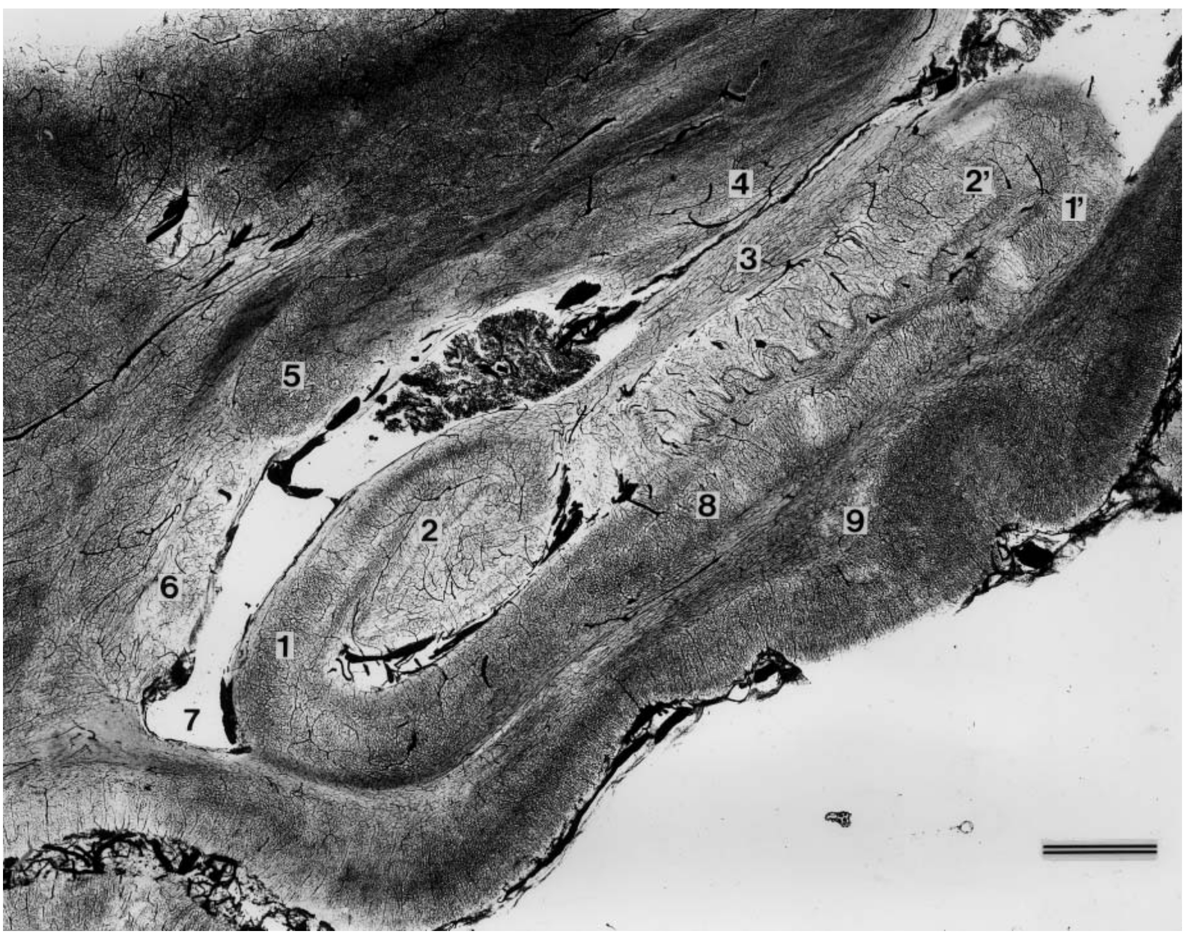

Fig. 116. B Sagittal section of hippocampus. Intravascular India ink injection with explanatory diagram. **Arrows** indicate the superficial hippocampal sulcus. **Bar,** 3 mm
1, cornu Ammonis in the head (CA1-CA4); **1′**, cornu Ammonis in the body (CA1 – CA4); **2**, gyrus dentatus in the head; **2′**, gyrus dentatus in the body; **3**, fimbria; **4**, stria terminalis; **5**, caudate nucleus; **6**, lateral nucleus of amygdala; **7**, temporal horn of lateral ventricle (uncal recess); **8**, subiculum; **9**, parahippocampal gyrus; **10**, collateral trigone

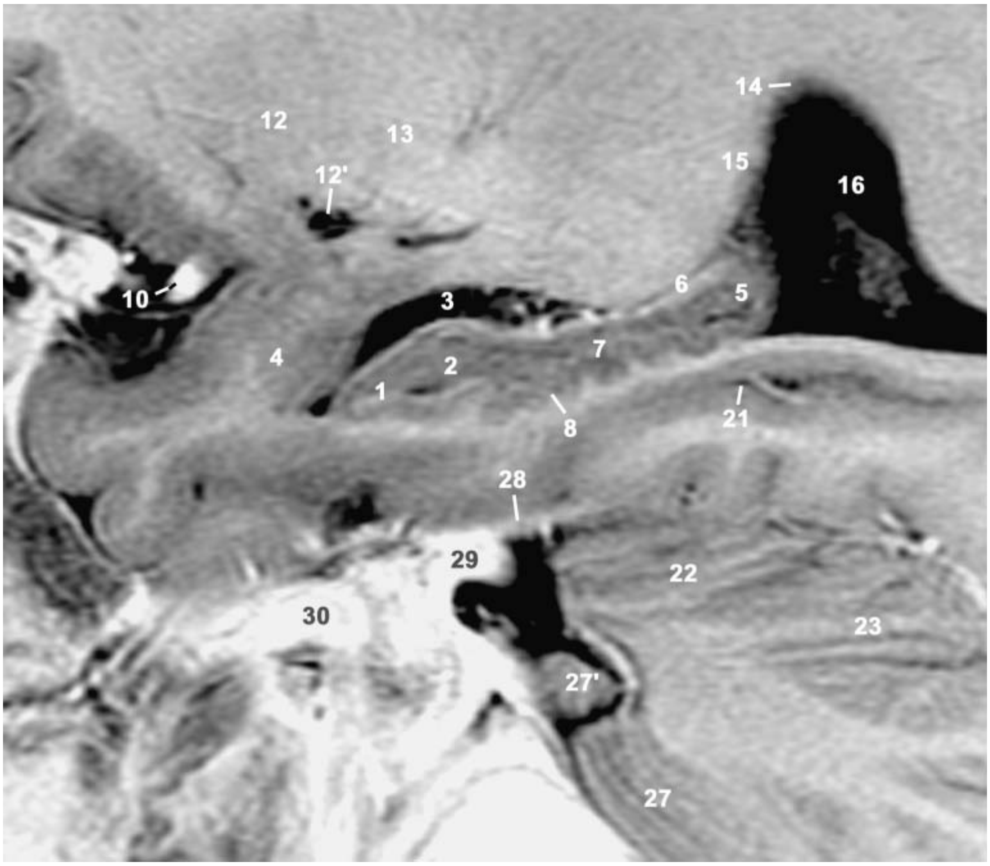

Fig. 116. C 3T MRI view

1, hippocampal head, cornu Ammonis; **2**, hippocampal head, gyrus dentatus; **3**, temporal (inferior) horn of the lateral ventricle; **4**, amygdala; **5**, hippocampal body, cornu Ammonis; **6**, fimbria; **6′**, alveus; **7**, margo denticulatus (gyrus dentatus); **8**, subiculum; **9**, parahippocampal gyrus; **10**, middle cerebral artery; **11**, anterior commissure, lateral part; **12**, putamen; **12′**, striate vessels; **13**, globus pallidus, lateral part; **14**, caudate nucleus; **15**, pulvinar; **16**, lateral ventricle; **17**, middle occipital gyrus; **18**, inferior occipital gyrus; **19**, transverse sinus; **20**, fusiform gyrus; **21**, collateral sulcus; **22**, quadrangular lobule; **23**, simple lobule; **24**, superior semilunar lobule; **25**, horizontal fissure; **26**, inferior semilunar lobule; **27**, biventer lobule; **27′**, flocculus; **28**, tentorium cerebelli; **29**, temporal, petrous part; **30**, internal carotid artery; **31**, auditory tube

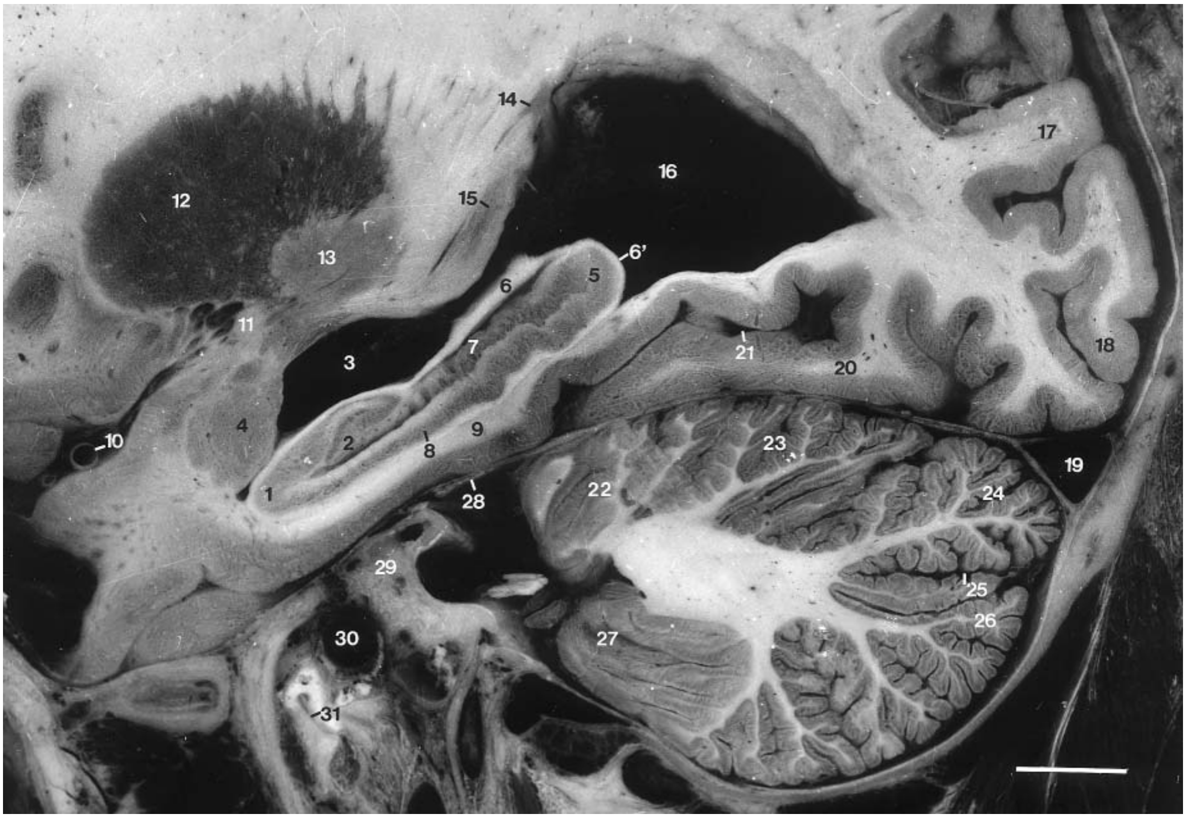

Fig. 116. D Head section. **Bar**, 10 mm

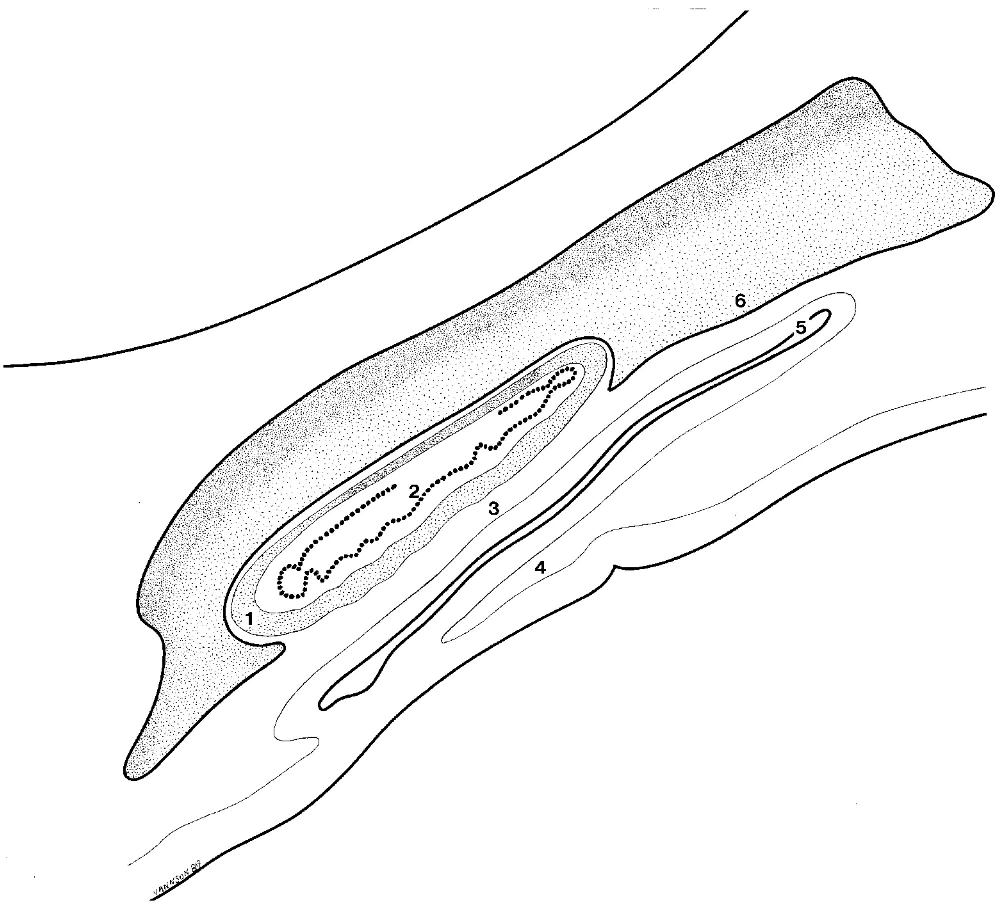

Fig. 117. A Sagittal section of hippocampus, showing plane of section
1, cornu Ammonis in the body; **2**, gyrus dentatus; **3**, parahippocampal gyrus; **4**, fusiform gyrus; **5**, collateral sulcus; **6**, collateral trigone

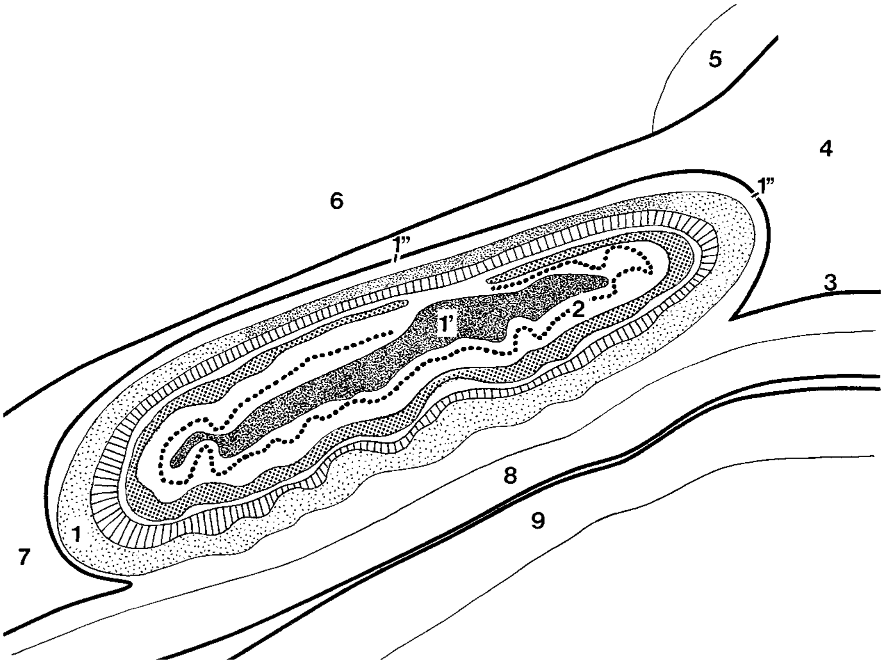

Fig. 117. B Sagittal section of hippocampus. Intravascular India ink injection with explanatory diagram. **Bar**, 3 mm
1, cornu Ammonis (CA1, CA2); **1′**, cornu Ammonis (CA4); **1″**, alveus; **2**, gyrus dentatus; **3**, collateral trigone; **4**, atrium; **5**, caudate nucleus; **6**, optic radiations; **7**, temporal horn; **8**, parahippocampal gyrus; **9**, fusiform gyrus

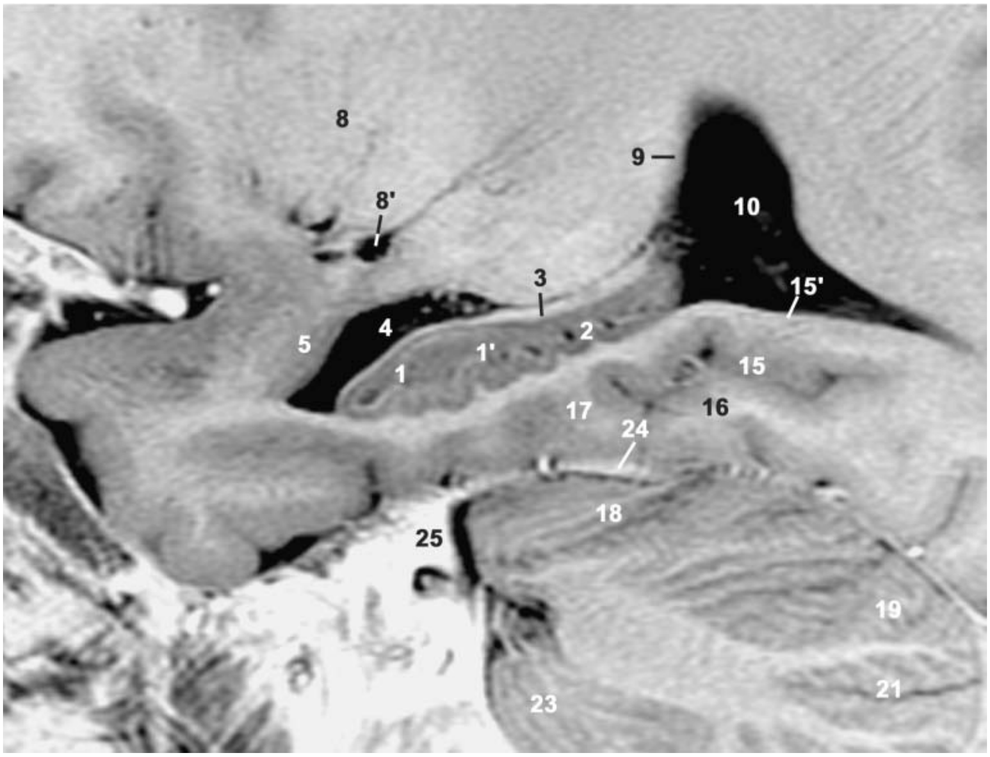

Fig. 117. C 3T MRI view

1, cornu Ammonis (CA1); **1′**, cornu Ammonis (CA4); **2**, gyrus dentatus; **3**, alveus; **4**, temporal (inferior) horn of the lateral ventricle; **5**, amygdala; **6**, claustrum; **7**, insula; **8**, putamen; **8′**, striate vessels; **9**, caudate nucleus; **10**, atrium of the lateral ventricle; **11**, superior occipital gyrus; **12**, middle occipital gyrus; **13**, inferior occipital gyrus; **14**, fourth occipital gyrus; **15**, collateral sulcus; **15′**, collateral trigone; **16**, fusiform gyrus; **17**, parahippocampal gyrus; **18**, simple lobule; **19**, superior semilunar lobule; **20**, transverse sinus; **21**, horizontal fissure; **22**, inferior semilunar lobule; **23**, biventer lobule; **24**, tentorium cerebelli; **25**, temporal, petrous part

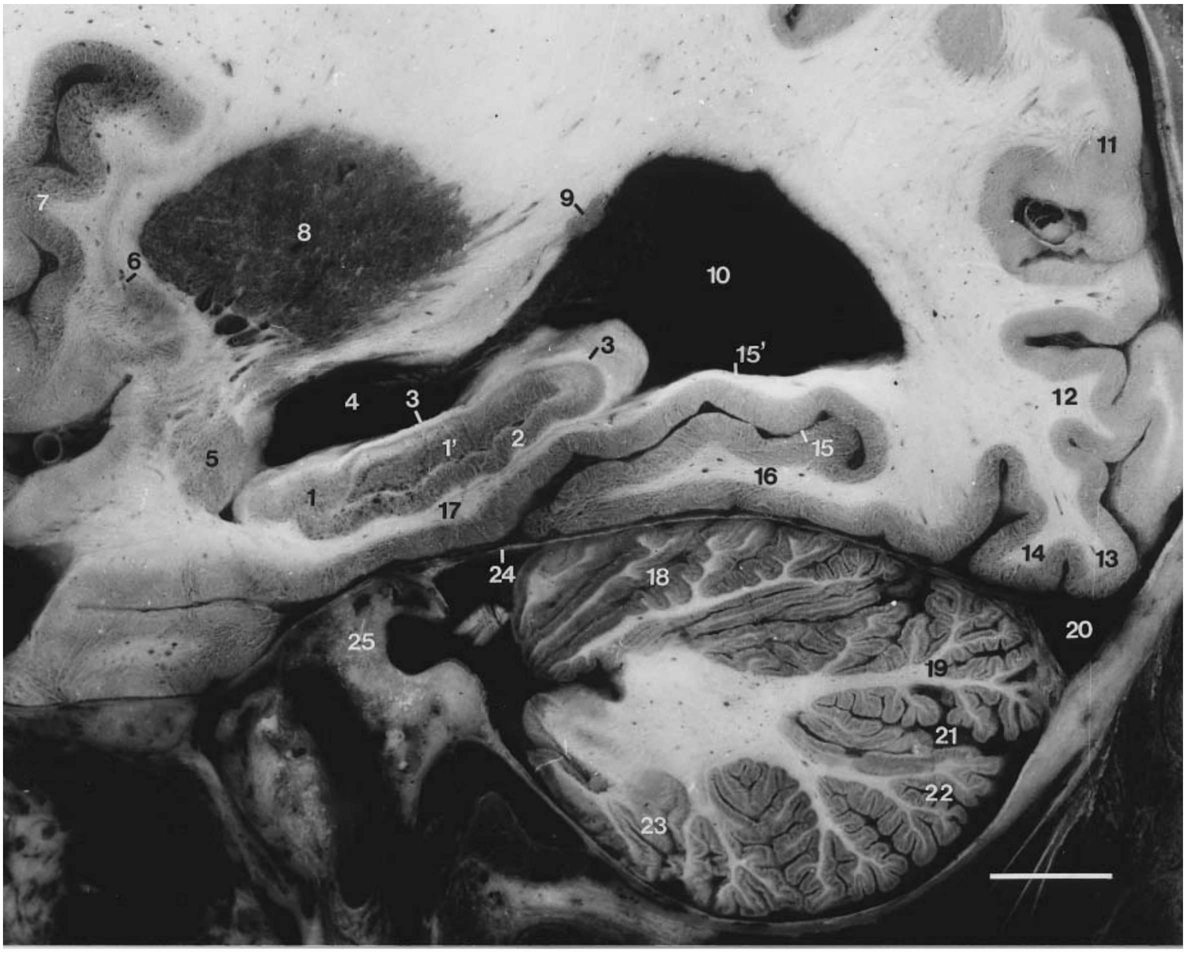

Fig. 117. D Head section. **Bar,** 10 mm

7.3 Axial Sections

Figures 119–124 show serial axial sections of the hippocampus from upper to lower levels.

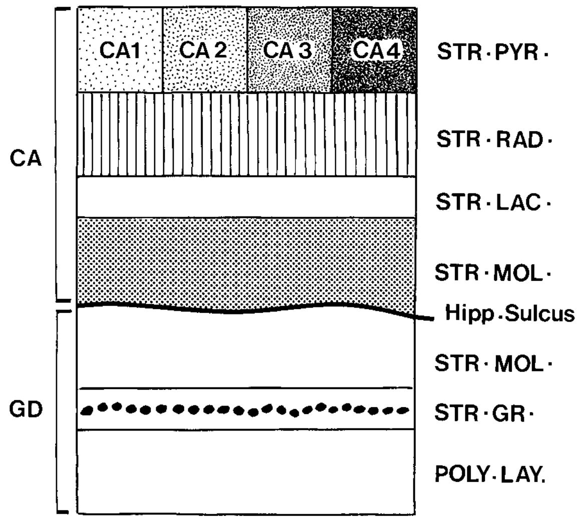

Fig. 118. Structure of the hippocampus
CA, cornu Ammonis; STR. PYR., stratum pyramidale; STR. RAD., stratum radiatum; STR. LAC., stratum lacunosum; STR. MOL., stratum moleculare; Hipp. Sulcus, vestigial hippocampal sulcus; GD, gyrus dentatus; STR. GR., stratum granulosum; POLY. LAY., polymorphic layer

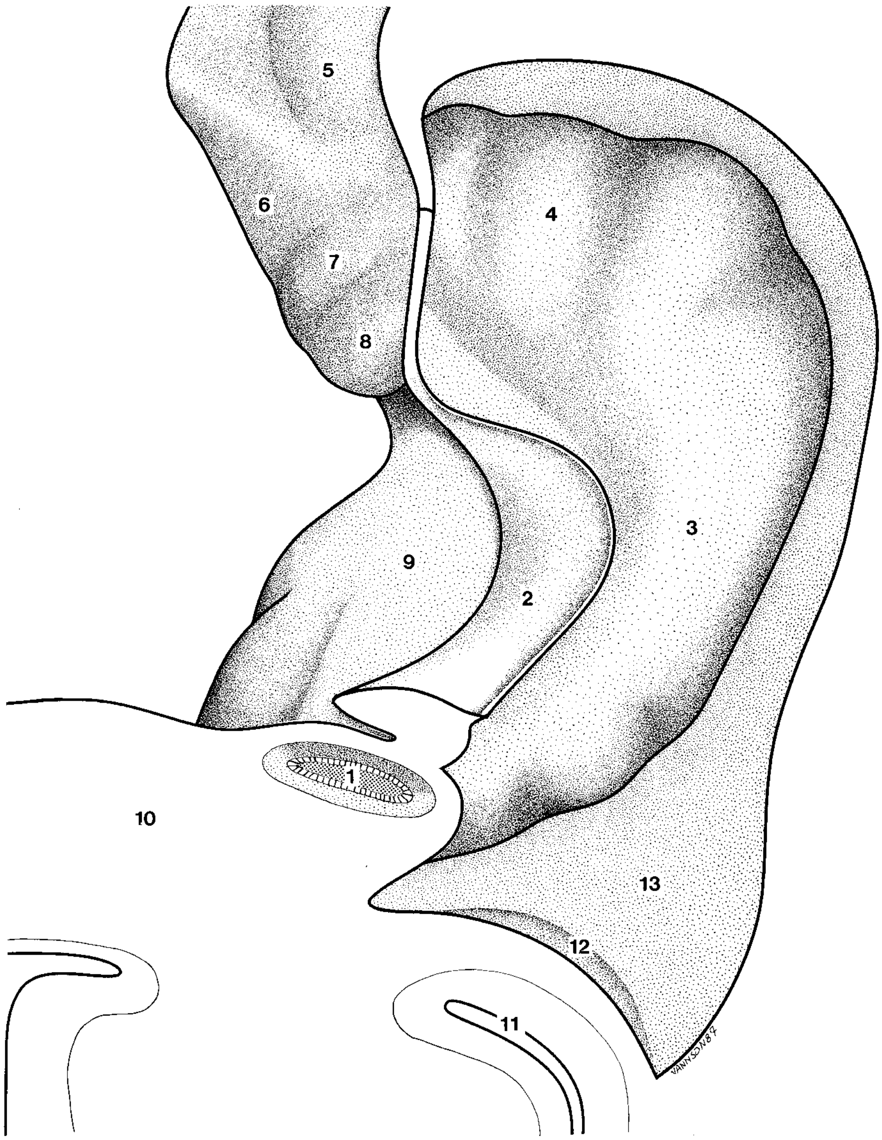

Fig. 119. A Axial section of hippocampal tail, showing plane of section and structure **1**, hippocampal tail, cornu Ammonis (CA1, CA3); **2**, fimbria; **3**, hippocampal body; **4**, hippocampal head (digitationes hippocampi); **5**, semilunar gyrus; **6**, uncinate gyrus; **7**, band of Giacomini; **8**, uncal apex; **9**, parahippocampal gyrus; **10**, splenium; **11**, anterior calcarine sulcus; **12**, calcar avis; **13**, collateral trigone

Fig. 119. B Axial section of hippocampal tail. Intravascular India ink injection. **Bar,** 2.3 mm

1, cornu Ammonis; **2**, fimbria; **3**, atrium of the lateral ventricle; **4**, caudate nucleus; **5**, pulvinar; **6**, transverse fissure, lateral part; **7**, splenium

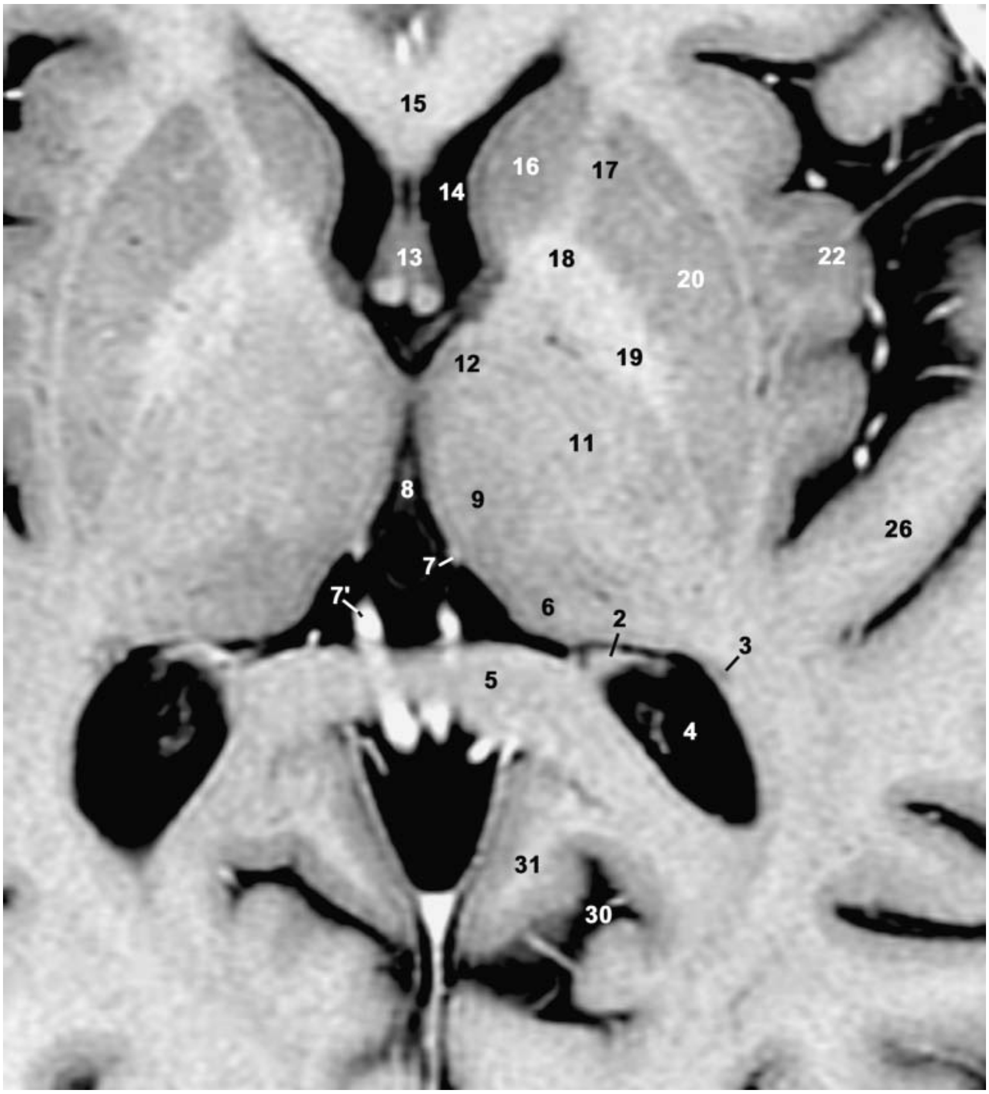

Fig. 119. C 3T MRI view

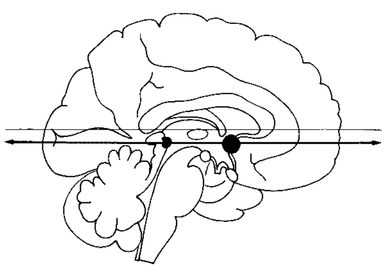

1, hippocampal tail, cornu Ammonis; **2**, fimbria; **3**, tail of caudate nucleus; **4**, atrium of the lateral ventricle; **5**, splenium of corpus callosum; **6**, pulvinar; **7**, stria medullaris; **7′**, internal cerebral veins; **8**, third ventricle; **9**, dorsomedial thalamic nucleus; **10**, lateral posterior thalamic nucleus; **11**, ventral lateral thalamic nucleus; **12**, anterior thalamic nucleus; **13**, fornix; **14**, frontal (anterior) horn of the lateral ventricle; **15**, genu of corpus callosum; **16**, head of caudate nucleus; **17**, internal capsule, anterior limb; **18**, internal capsule, genu; **19**, internal capsule, posterior limb; **20**, putamen; **21**, claustrum; **22**, insula; **23**, precentral gyrus; **24**, central sulcus; **25**, postcentral gyrus; **26**, superior temporal gyrus; **27**, superior temporal sulcus; **28**, middle temporal gyrus; **29**, calcarine sulcus and striate cortex; **30**, parieto-occipital fissure; **31**, cingulate gyrus

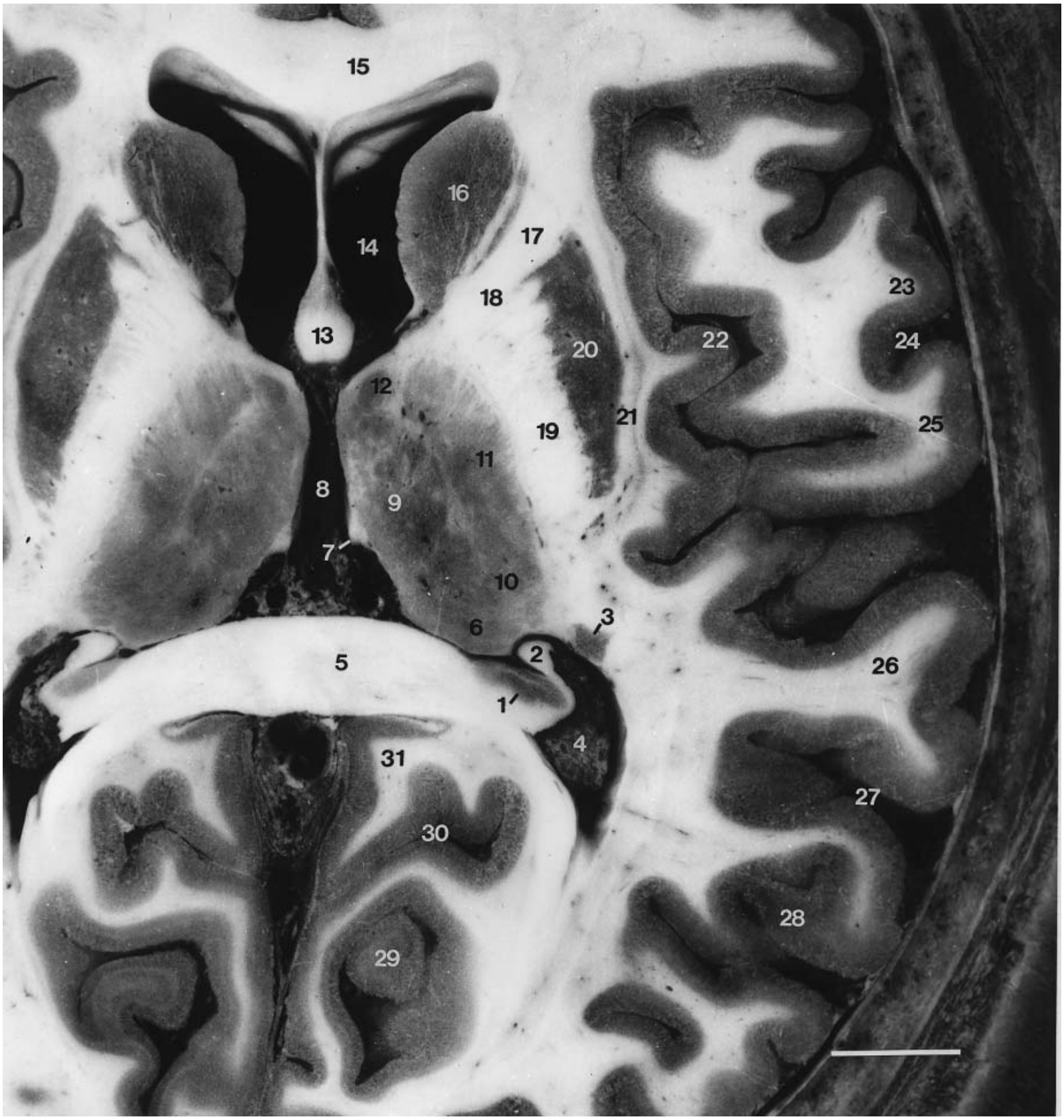

Fig. 119. D Head section. **Bar,** 10 mm

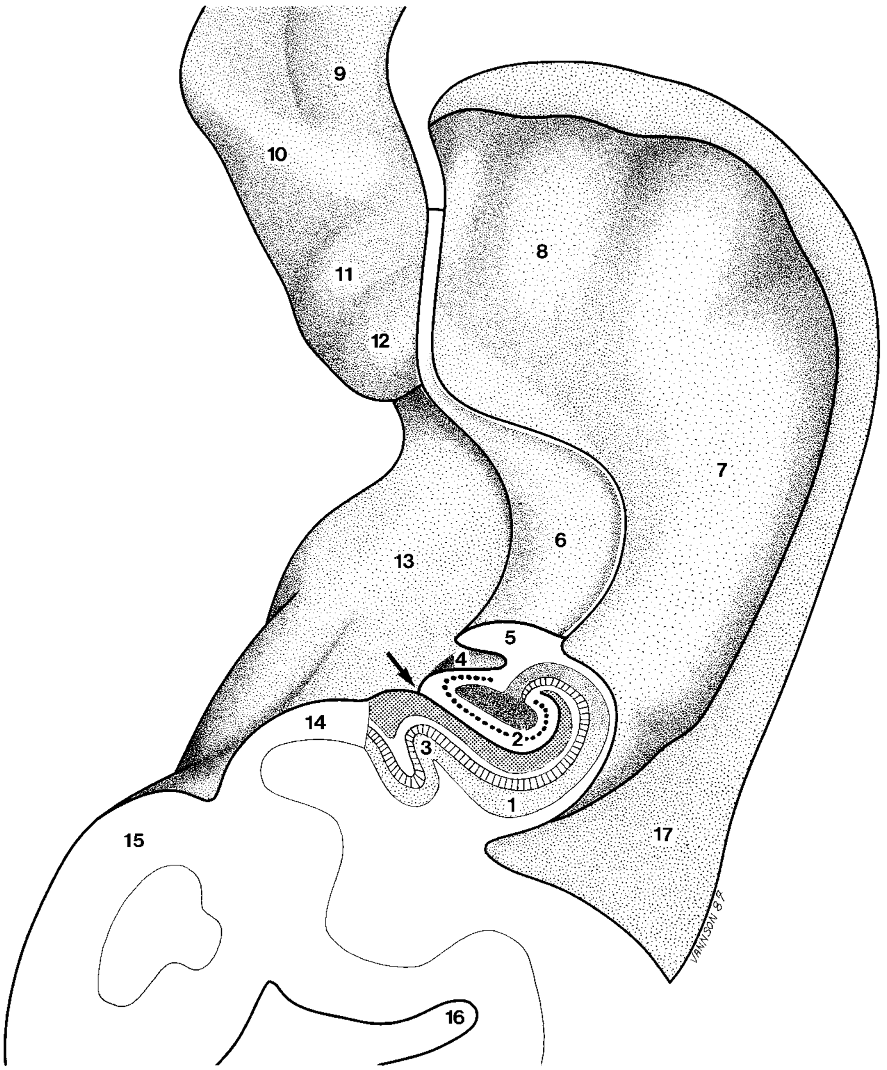

Fig. 120. A Axial section of hippocampal tail, showing plane of section and structure. **Arrow** indicates the superficial hippocampal sulcus
1, cornu Ammonis (CA1 – CA4); **2**, gyrus dentatus; **3**, fold of CA1 and gyri of Andreas Retzius (not clearly visible at the surface here); **4**, margo denticulatus; **5**, cut surface of the fimbria; **6**, fimbria; **7**, hippocampal body; **8**, hippocampal head (digitationes hippocampi); **9**, semilunar gyrus; **10**, uncinate gyrus; **11**, band of Giacomini; **12**, uncal apex; **13**, parahippocampal gyrus; **14**, subiculum; **15**, isthmus; **16**, anterior calcarine sulcus; **17**, collateral eminence

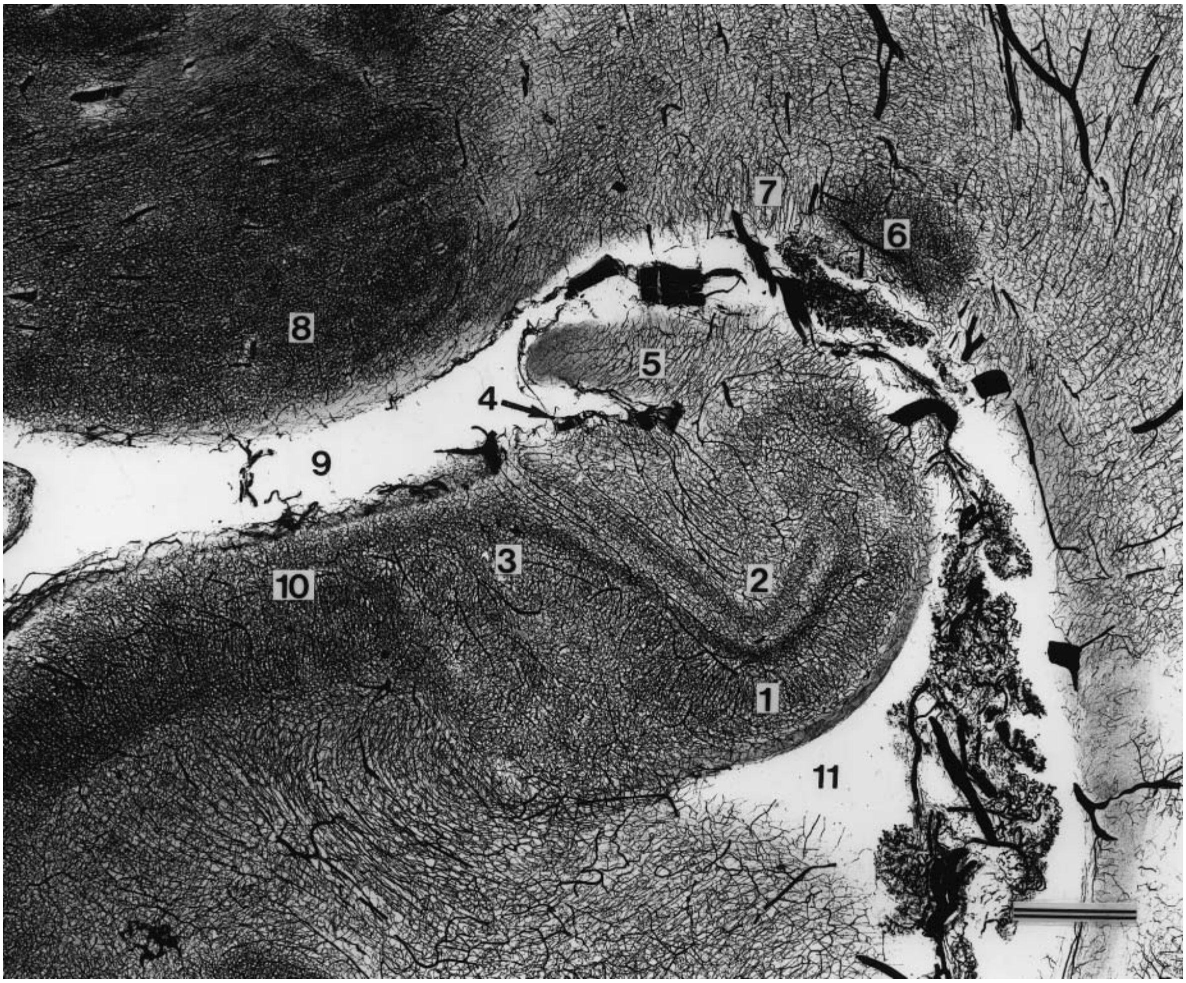

Fig. 120. B Axial section of hippocampal tail. Intravascular India ink injection. **Bar**, 2 mm
1, cornu Ammonis; **2**, gyrus dentatus; **3**, fold of CA1 and gyri of Andreas Retzius (not clearly visible at the surface here); **4**, margo denticulatus; **5**, fimbria; **6**, tail of caudate nucleus; **7**, stria terminalis; **8**, pulvinar; **9**, transverse fissure, lateral part; **10**, subiculum; **11**, temporal horn of the lateral ventricle

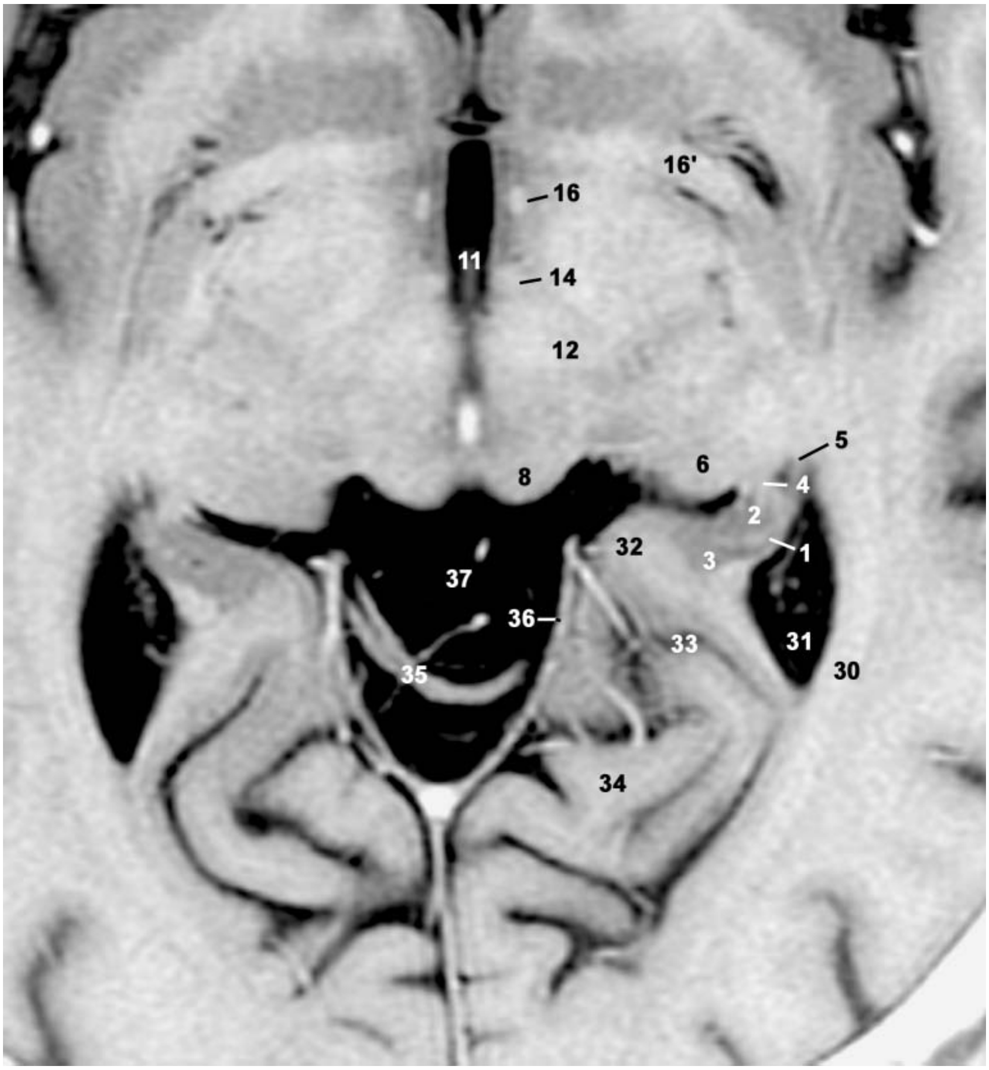

Fig. 120. C 3T MRI view

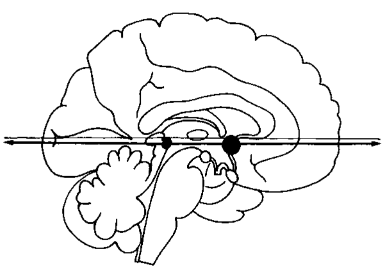

1, hippocampal tail, cornu Ammonis; **2**, hippocampal tail, gyrus dentatus; **3**, gyrus of Andreas Retzius; **4**, fimbria; **5**, tail of caudate nucleus; **6**, pulvinar; **7**, ventral posterolateral thalamic nucleus; **8**, superior colliculus; **9**, pineal gland; **10**, posterior commissure; **11**, third ventricle; **12**, dorsomedial thalamic nucleus; **13**, ventral lateral thalamic nucleus; **14**, mamillothalamic tract; **15**, interthalamic adhesion; **16**, column of fornix; **16′**, anterior commissure, lateral part; **17**, lateral ventricle, frontal horn; **18**, head of caudate nucleus; **19**, internal capsule, anterior limb; **20**, claustrum; **21**, insula; **22**, putamen; **23**, globus pallidus, lateral part; **24**, globus pallidus, medial part; **25**, internal capsule, posterior limb; **26**, lateral fissure; **27**, superior temporal gyrus; **28**, superior temporal sulcus; **29**, middle temporal gyrus; **30**, optic radiations; **31**, occipital horn of the lateral ventricle; **32**, isthmus; **33**, anterior calcarine sulcus; **34**, lingual gyrus; **35**, culmen; **36**, tentorium cerebelli; **37**, quadrigeminal cistern

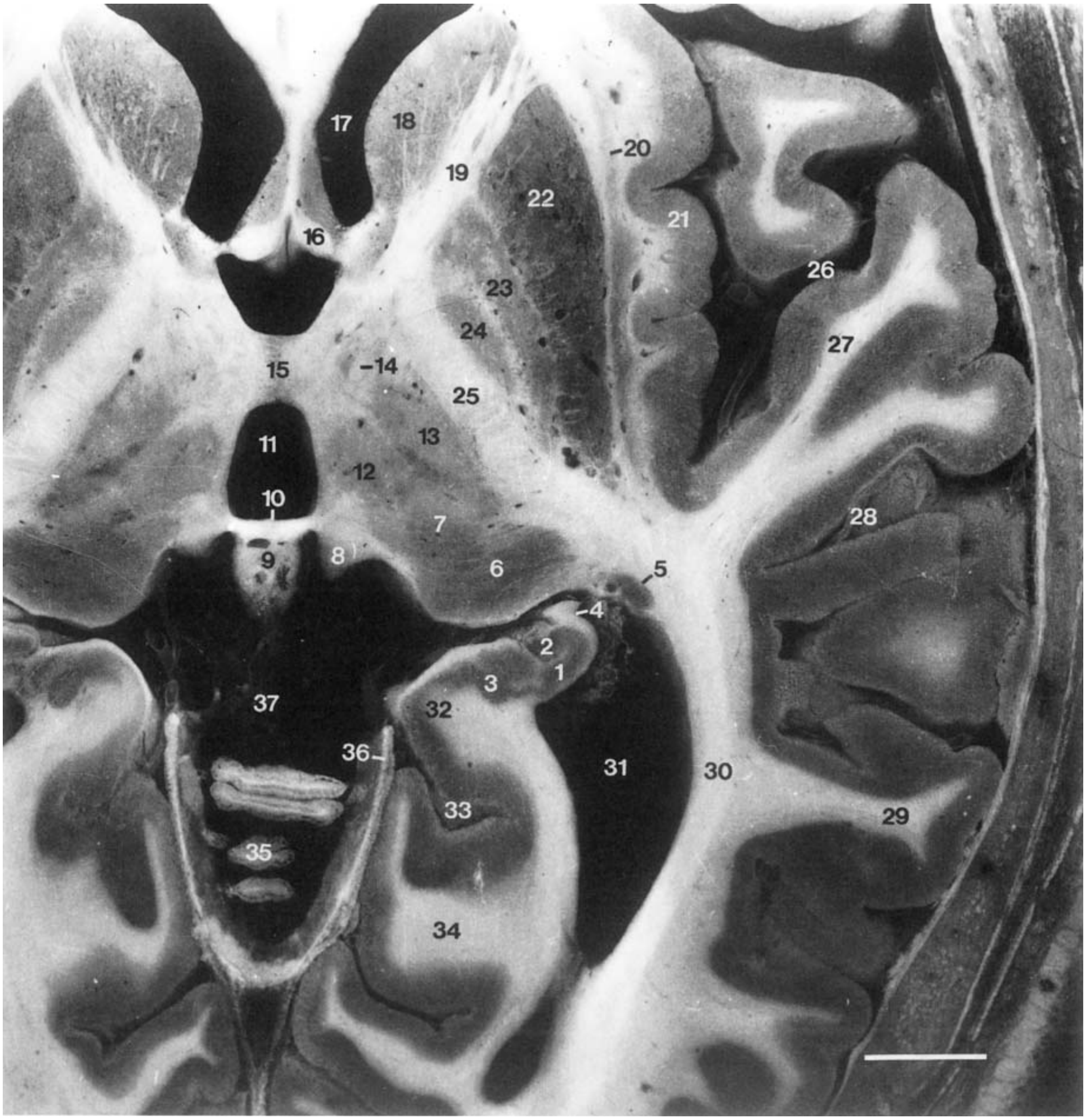

Fig. 120. D Head section. **Bar**, 10 mm

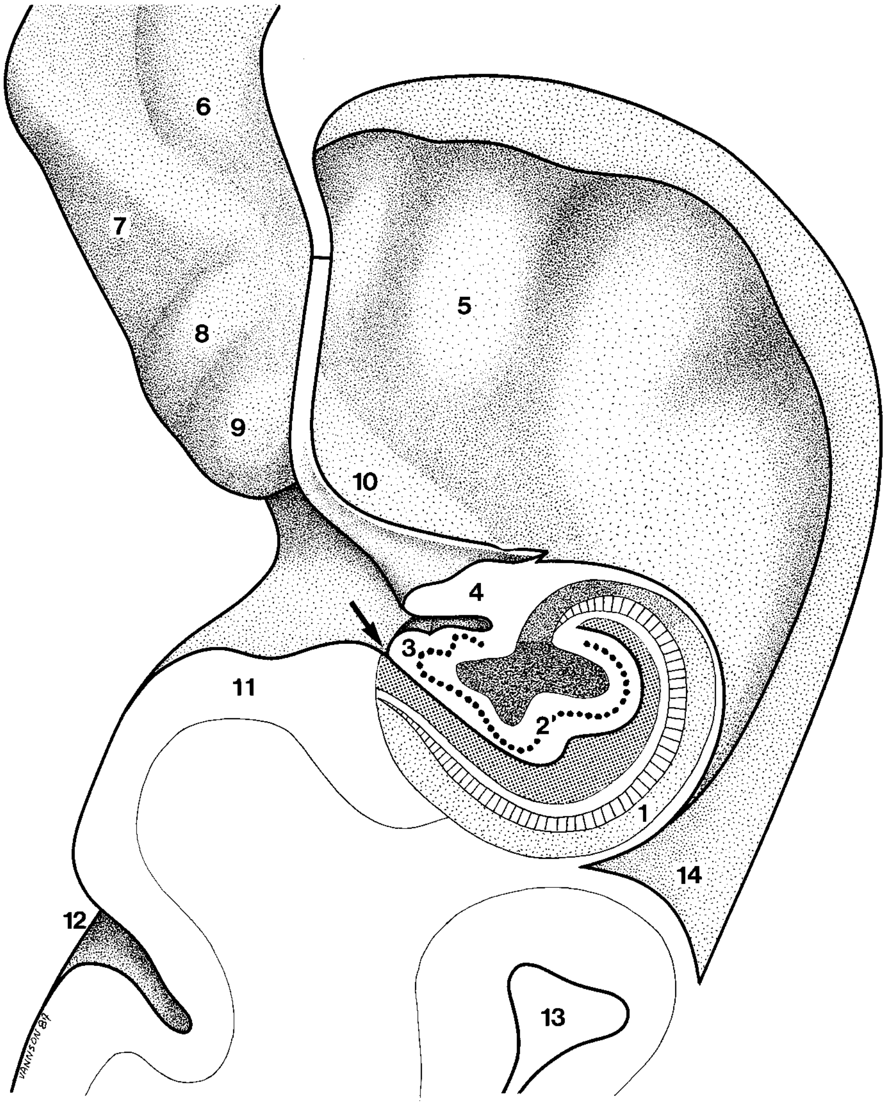

Fig. 121. A Axial section of hippocampal body, showing plane of section and structure. **Arrow** indicates the superficial hippocampal sulcus
1, cornu Ammonis (CA1 – CA4); **2**, gyrus dentatus; **3**, margo denticulatus; **4**, cut surface of fimbria; **5**, hippocampal head (digitationes hippocampi); **6**, semilunar gyrus; **7**, uncinate gyrus; **8**, band of Giacomini; **9**, uncal apex; **10**, fimbria; **11**, subiculum; **12**, anterior calcarine sulcus; **13**, collateral sulcus; **14**, collateral eminence

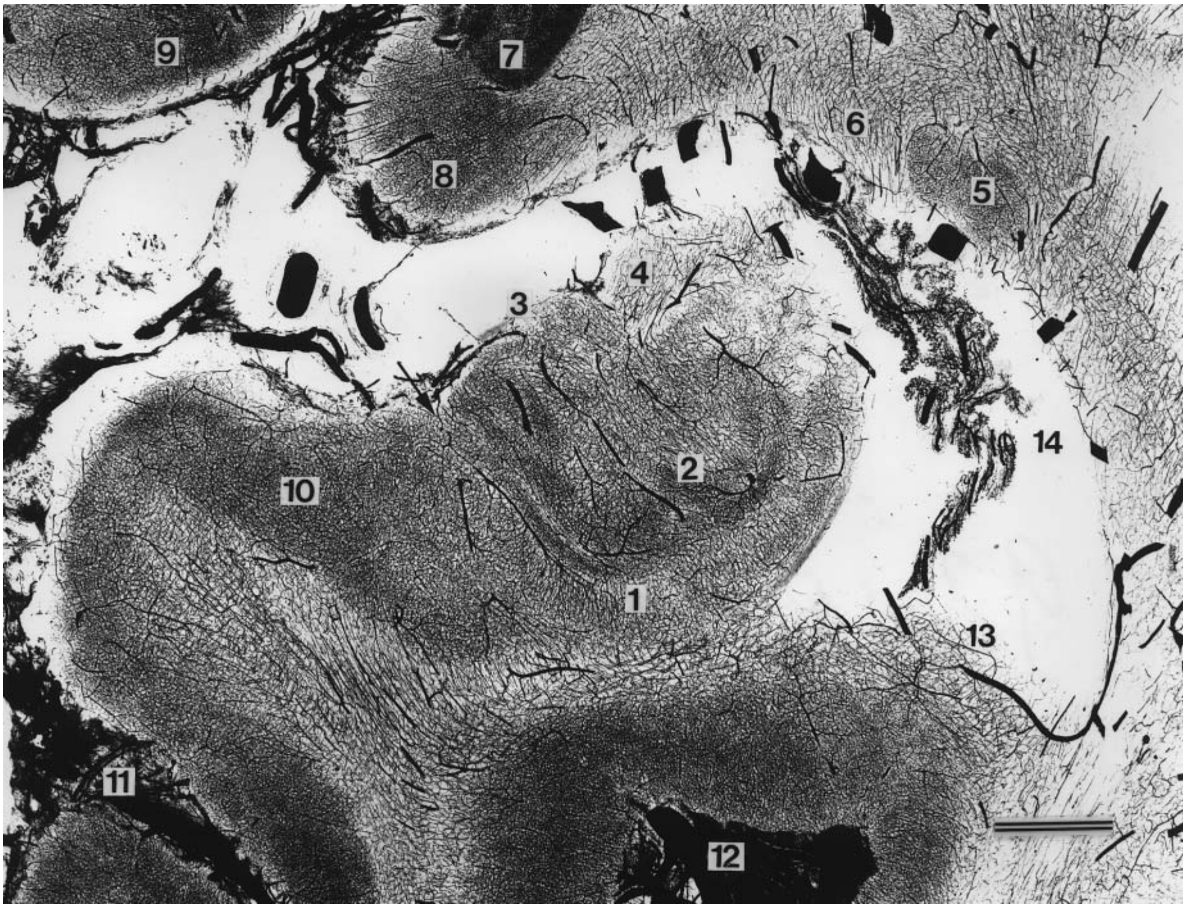

Fig. 121. B Axial section of hippocampal body. Intravascular India ink injection. **Bar**, 2.3 mm
1, cornu Ammonis; **2**, gyrus dentatus; **3**, margo denticulatus; **4**, fimbria; **5**, tail of caudate nucleus; **6**, stria terminalis; **7**, lateral geniculate body; **8**, pulvinar; **9**, medial geniculate body; **10**, subiculum; **11**, anterior calcarine sulcus; **12**, collateral sulcus; **13**, collateral eminence; **14**, temporal horn of the lateral ventricle

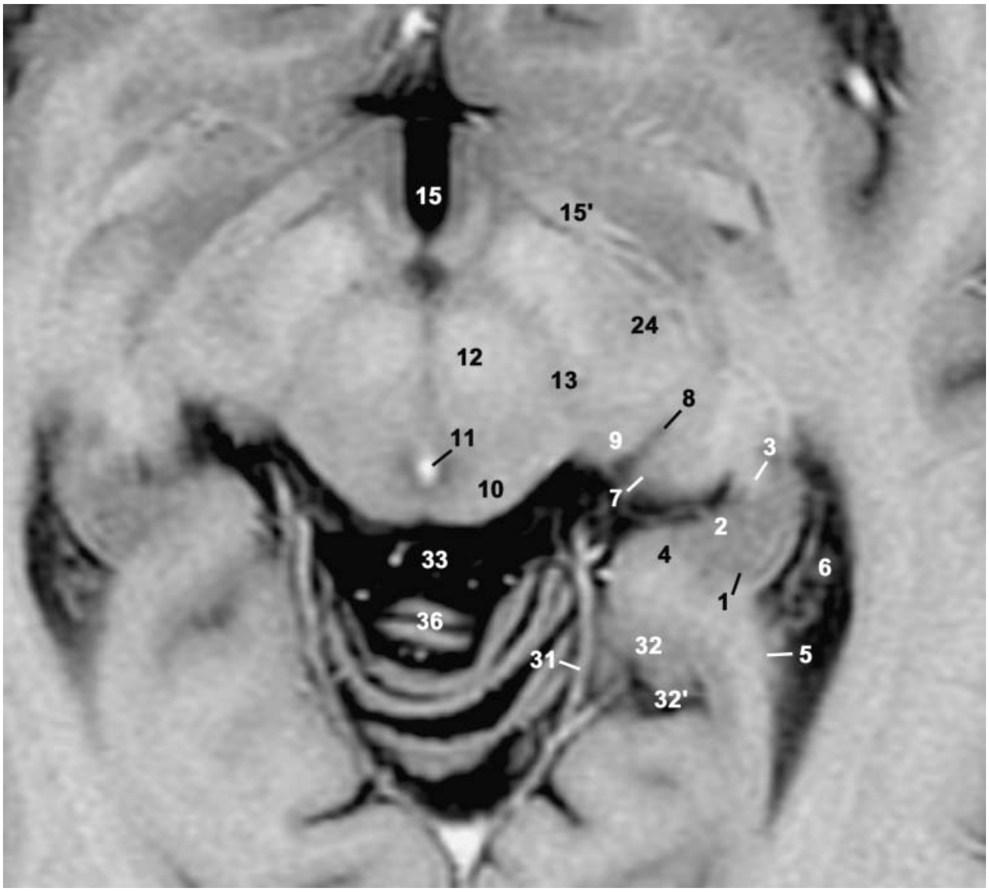

Fig. 121. C 3T MRI view

1, hippocampal body, cornu Ammonis; **2**, hippocampal body, gyrus dentatus; **3**, fimbria; **4**, subiculum; **5**, collateral eminence; **6**, temporal (inferior) horn of the lateral ventricle; **7**, pulvinar; **8**, lateral geniculate body; **9**, medial geniculate body; **10**, superior colliculus; **11**, cerebral aqueduct; **11′**, periaqueductal grey matter; **12**, red nucleus; **13**, substantia nigra; **14**, mamillothalamic tract; **15**, third ventricle; **15′**, optic tract; **16**, column of fornix; **17**, anterior commissure, medial part; **17′**, anterior commissure, lateral part; **18**, caudate nucleus; **19**, claustrum; **20**, insula; **21**, putamen; **22**, globus pallidus, lateral part; **23**, globus pallidus, medial part; **24**, internal capsule, posterior limb; **25**, lateral fissure; **26**, superior temporal gyrus; **27**, superior temporal sulcus; **28** middle temporal gyrus; **29** collateral sulcus; **29′**, lingual sulcus; **30**, lingual gyrus; **31**, tentorium cerebelli; **32**, parahippocampal gyrus; **32′**, anterior calcarine sulcus; **33**, quadrigeminal cistern; **34**, ambient cistern; **35**, wing of ambient cistern; **36**, culmen

Fig. 121. D Head section. Bar, 10 mm

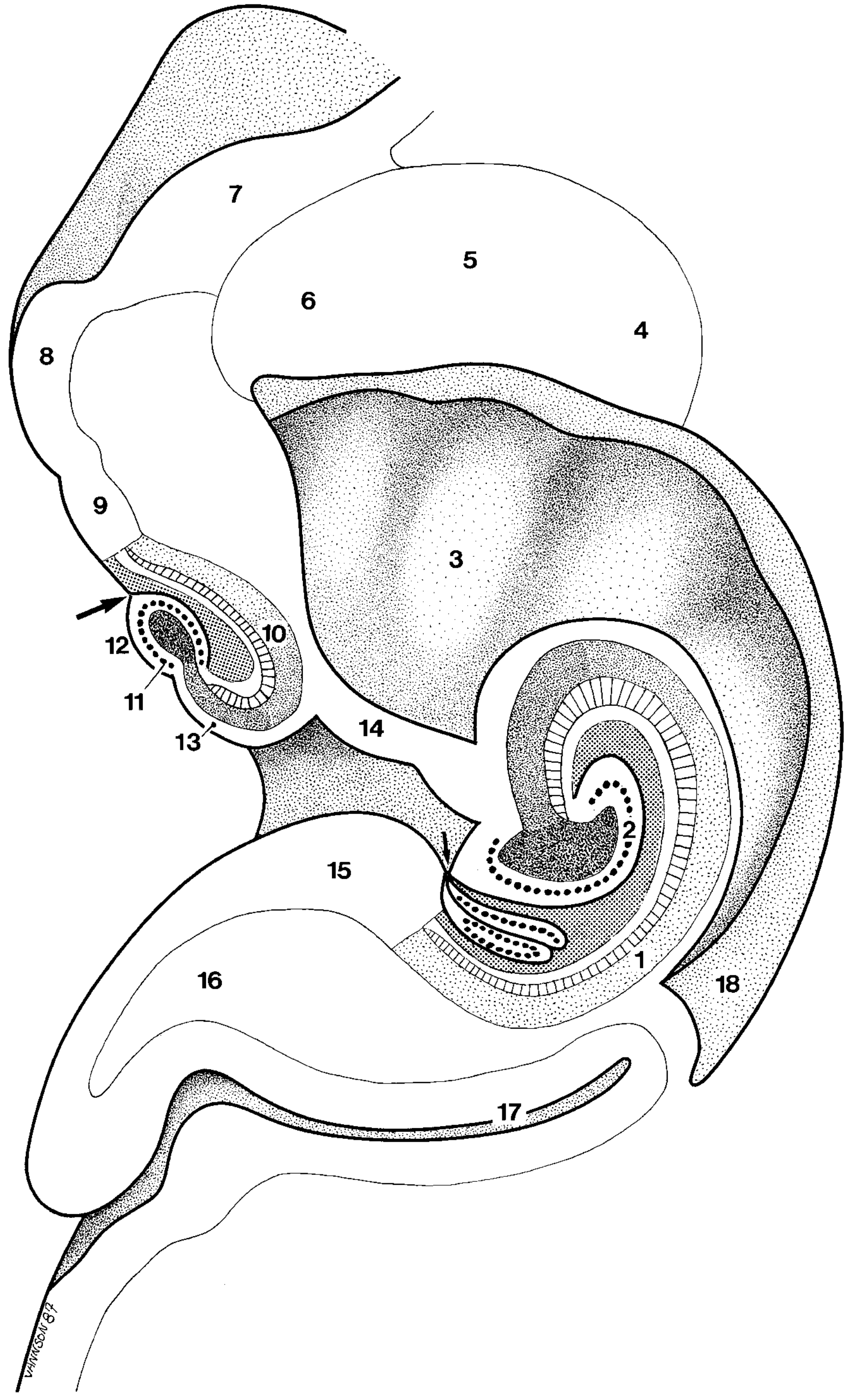

Fig. 122. A Axial section of the hippocampal body and head, showing plane of section and structure. **Arrows** indicate the superficial hippocampal sulcus
1, cornu Ammonis in the body (CA1 – CA4); **2**, gyrus dentatus in the body; **3**, hippocampal head (digitationes hippocampi); **4**, lateral nucleus of amygdala; **5**, basal nucleus of amygdala; **6**, accessory basal nucleus of amygdala; **7**, cortical nucleus of amygdala; **8**, uncinate gyrus; **9**, subiculum; **10**, cornu Ammonis in the uncus (CA1 – CA4); **11**, gyrus dentatus in the uncus; **12**, band of Giacomini; **13**, uncal apex covered with alveus; **14**, fimbria; **15**, subiculum; **16**, parahippocampal gyrus; **17**, collateral sulcus; **18**, collateral eminence

Fig. 122. B Axial section of the hippocampal body and head. Intravascular India ink injection. **Bar**, 2.6 mm
1, cornu Ammonis in the body; **2**, gyrus dentatus in the body; **3**, tail of caudate nucleus; **4**, lateral nucleus of amygdala; **5**, basal nucleus of amygdala; **6**, accessory basal nucleus of amygdala; **7**, cortical nucleus of amygdala; **8**, uncinate gyrus; **9**, subiculum in the uncinate gyrus; **10**, cornu Ammonis in the uncus; **11**, gyrus dentatus in the uncus; **12**, band of Giacomini; **13**, uncal apex; **14**, fimbria; **15**, temporal horn of the lateral ventricle and choroid plexuses; **16**, subiculum

Fig. 122. C 3T MRI view

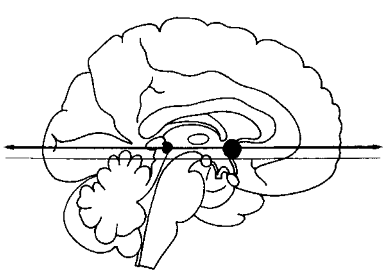

1, hippocampal body, cornu Ammonis; **1′**, digitationes hippocampi; **2**, hippocampal body, gyrus dentatus; **3**, subiculum; **4**, temporal (inferior) horn of the lateral ventricle; **5**, hippocampal head, uncal apex; **6**, amygdala, lateral nucleus; **7**, amygdala, basal nucleus; **8**, amygdala, cortical nucleus; **9**, optic tract; **9′**, optic chiasma; **10**, mamillary body; **11**, tuber; **12**, third ventricle; **13**, anterior perforated substance; **14**, nucleus accumbens; **15**, claustrum; **16**, insula; **17**, lateral fissure; **18**, superior temporal gyrus; **19**, superior temporal sulcus; **20**, middle temporal gyrus; **21**, collateral sulcus; **22**, lingual gyrus; **23**, parahippocampal gyrus; **24**, tentorium cerebelli; **25**, culmen; **26**, quadrigeminal cistern; **27**, cerebral acqueduct; **27′**, periaqueductal grey matter; **28**, brachium conjunctivum; **29**, red nucleus; **30**, substantia nigra; **31**, crus cerebri; **32**, crural cistern; **33**, ambient cistern

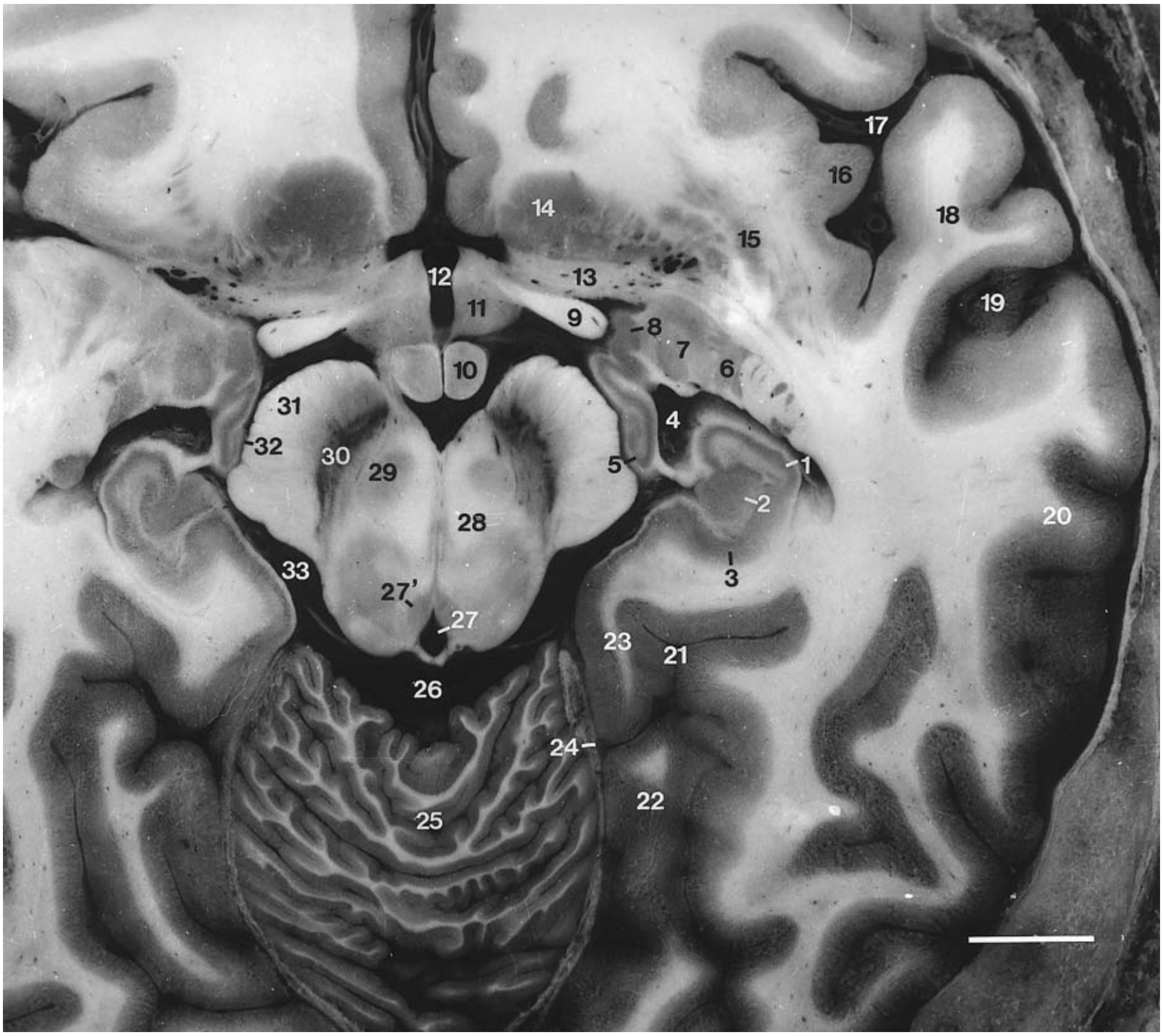

Fig. 122. D Head section. **Bar**, 10 mm

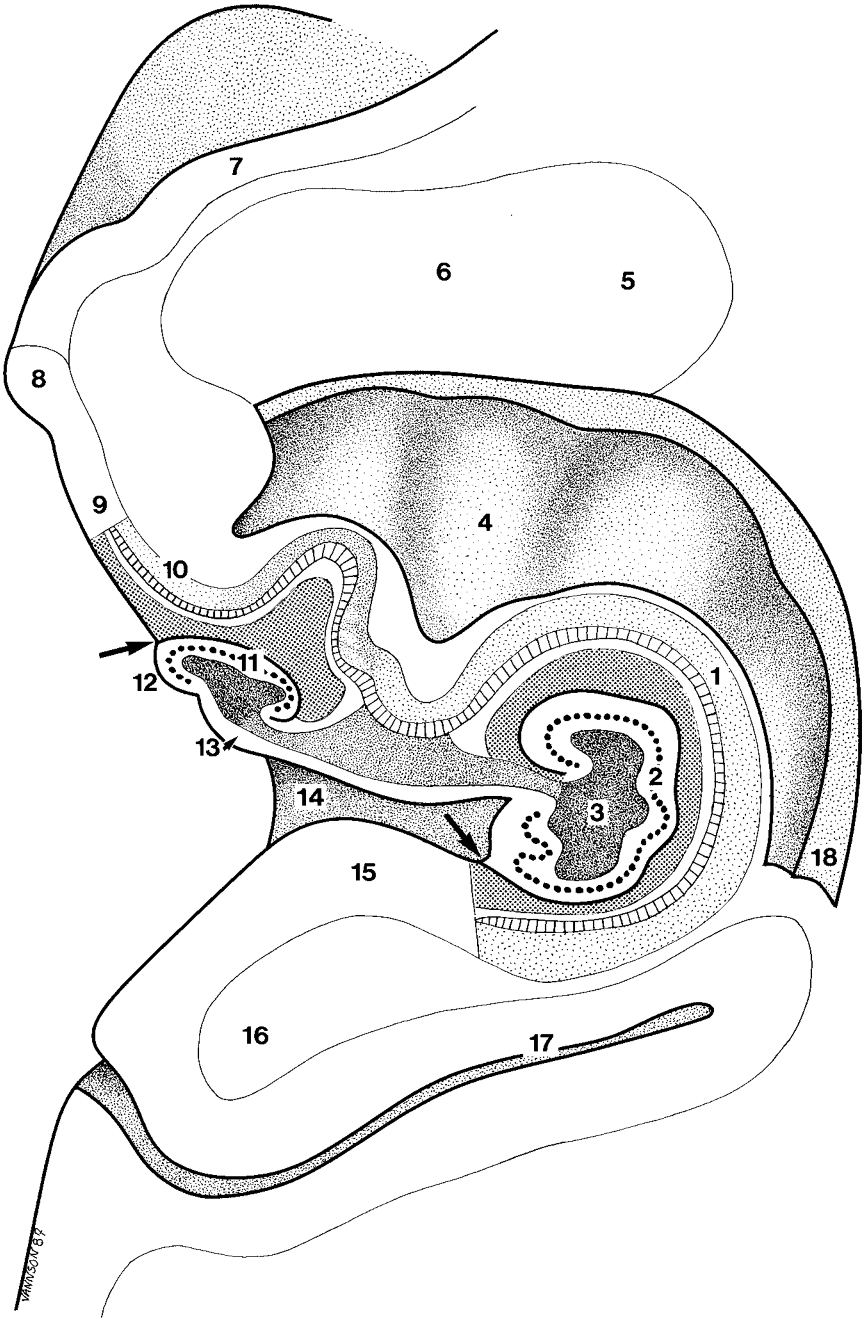

Fig. 123. A Axial section of hippocampal head, showing plane of section and structure. **Arrows** indicate the superficial hippocampal sulcus
1, cornu Ammonis (CA1) in digitationes hippocampi (internal digitations); **2**, gyrus dentatus; **3**, CA4 field of cornu Ammonis; **4**, digitationes hippocampi (internal digitations); **5**, lateral nucleus of amygdala; **6**, basal nucleus of amygdala; **7**, ambient gyrus; **8**, uncinate gyrus; **9**, subiculum in the uncinate gyrus; **10**, cornu Ammonis in the uncinate gyrus (CA1); **11**, gyrus dentatus in the uncal apex; **12**, band of Giacomini; **13**, uncal apex covered with alveus; **14**, uncal sulcus; **15**, subiculum; **16**, parahippocampal gyrus; **17**, collateral sulcus; **18**, collateral eminence

Fig. 123. B Axial section of hippocampal head. Intravascular India ink injection. **Bar**, 2.6 mm
1, cornu Ammonis; **2**, gyrus dentatus; **3**, CA4 field; **4**, digitationes hippocampi (internal digitations); **5**, lateral nucleus of amygdala; **6**, basal nucleus of amygdala; **7**, ambient gyrus; **8**, uncinate gyrus; **9**, subiculum in the uncinate gyrus; **10**, cornu Ammonis in the uncinate gyrus; **11**, gyrus dentatus; **12**, band of Giacomini; **13**, uncal apex covered with alveus; **14**, uncal sulcus; **15**, subiculum; **16**, posterior cerebral artery; **17**, parahippocampal gyrus; **18**, collateral sulcus; **19**, collateral eminence; **20**, temporal horn of the lateral ventricle

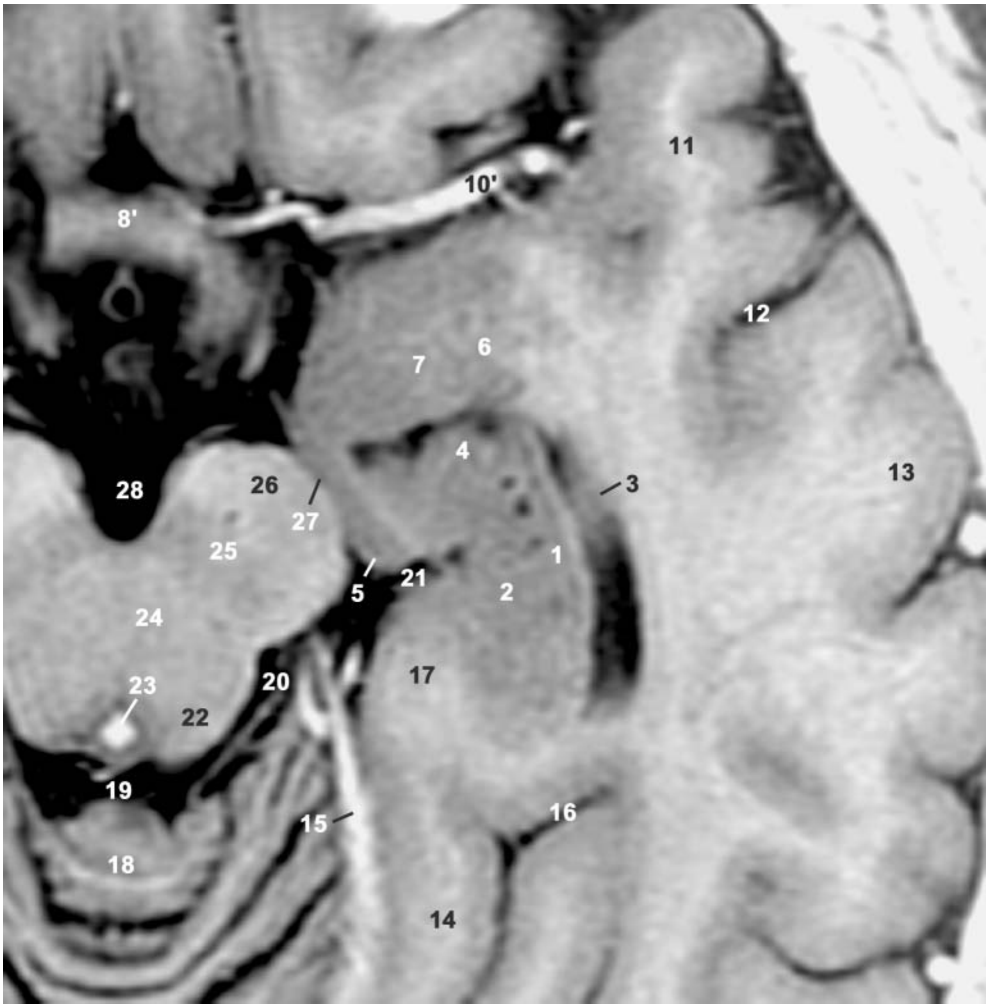

Fig. 123. C 3T MRI view

1, hippocampal head, cornu Ammonis; **2**, hippocampal head, gyrus dentatus; **3**, temporal (inferior) horn of the lateral ventricle; **4**, digitationes hippocampi (internal digitations); **5**, uncal apex; **6**, amygdala, lateral nucleus; **7**, amygdala, basal nucleus; **8**, optic tract; **8′**, optic chiasma; **9**, nucleus accumbens; **10**, insula; **10′**, lateral fissure and middle cerebral artery; **11**, superior temporal gyrus; **12**, superior temporal sulcus; **13**, middle temporal gyrus; **14**, lingual gyrus; **15**, tentorium cerebelli; **16**, collateral sulcus; **17**, parahippocampal gyrus; **18**, culmen; **19**, quadrigeminal cistern; **20**, ambient cistern; **21**, wing of ambient cistern; **22**, superior colliculus; **23**, cerebral aqueduct; **24**, brachium conjunctivum (superior cerebellar peduncle); **25**, substantia nigra; **26**, crus cerebri; **27**, crural cistern; **28**, intercrural (interpeduncular) cistern; **29**, mamillary body; **30**, tuber; **31**, third ventricle; **32**, lamina terminalis

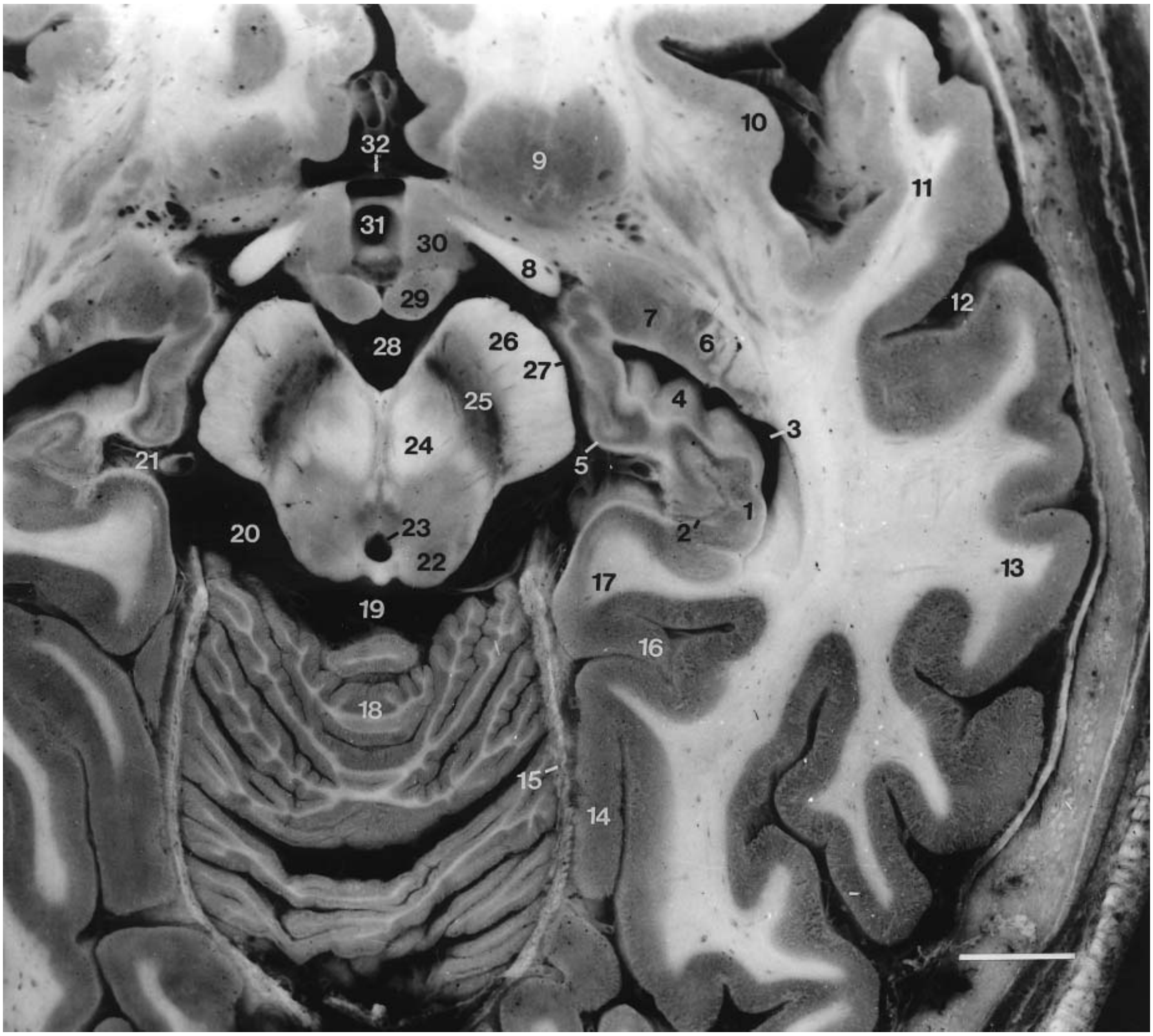

Fig. 123. D Head section. **Bar**, 10 mm

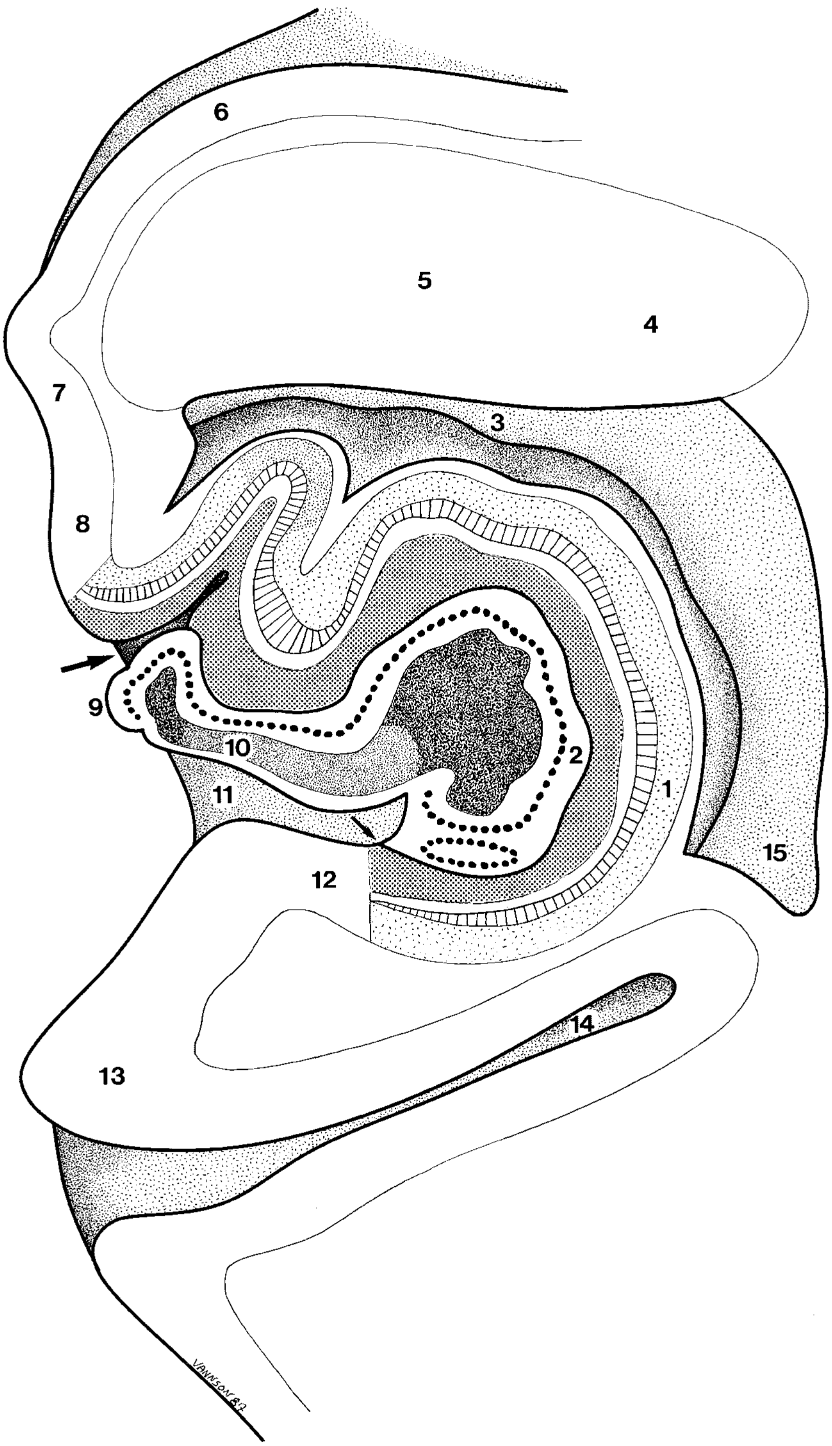

Fig. 124. A Axial section of hippocampal head, showing plane of section and structure. **Arrows** indicate the superficial hippocampal sulcus
1, cornu Ammonis (CA1) in digitationes hippocampi; **2**, gyrus dentatus; **3**, uncal recess of temporal horn; **4**, lateral nucleus of amygdala; **5**, basal nucleus of amygdala; **6**, ambient gyrus; **7**, uncinate gyrus; **8**, subiculum in the uncinate gyrus; **9**, band of Giacomini; **10**, uncal apex; **11**, uncal sulcus; **12**, subiculum; **13**, parahippocampal gyrus; **14**, collateral sulcus; **15**, collateral eminence

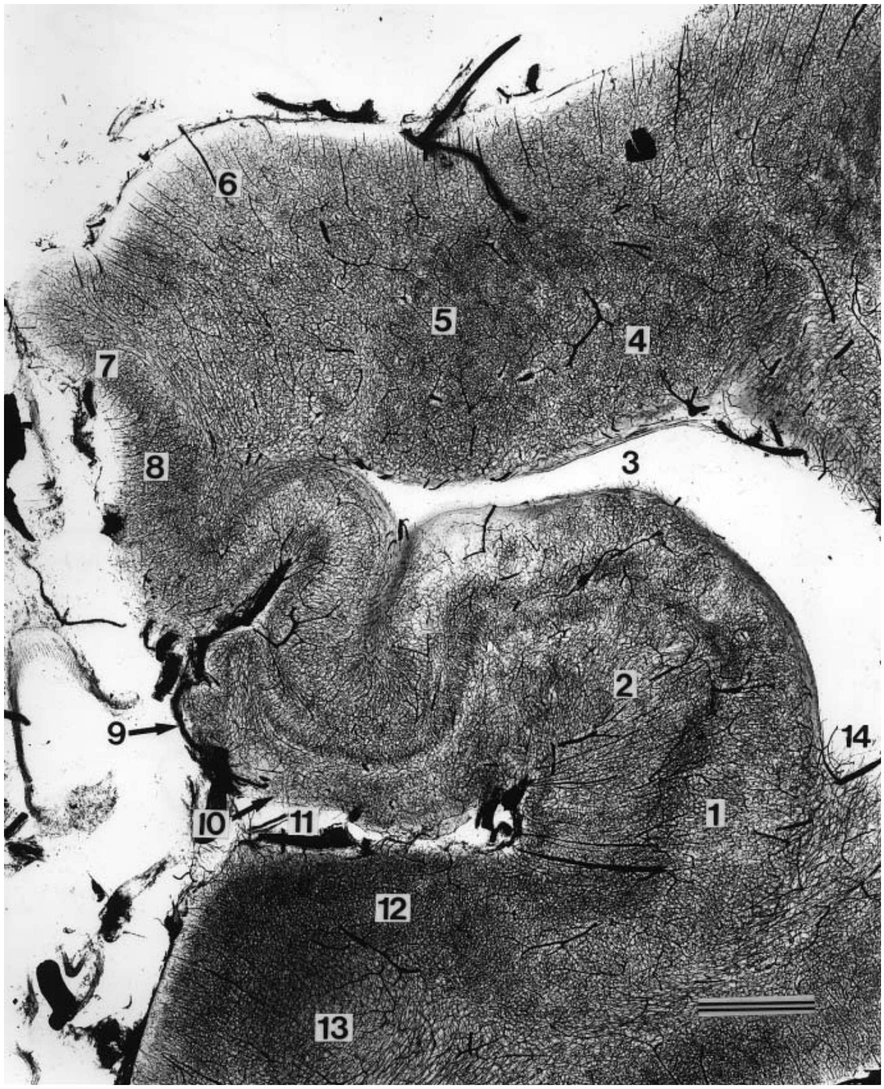

Fig. 124. B Axial section of hippocampal head. Intravascular India ink injection. **Bar**, 2.4 mm
1, hippocampal head, cornu Ammonis; **2**, hippocampal head, gyrus dentatus; **3**, temporal horn (uncal recess); **4**, lateral nucleus of amygdala; **5**, basal nucleus of amygdala; **6**, ambient gyrus; **7**, uncinate gyrus; **8**, subiculum in the uncinate gyrus; **9**, band of Giacomini; **10**, uncal apex; **11**, uncal sulcus; **12**, subiculum; **13**, parahippocampal gyrus; **14**, collateral eminence

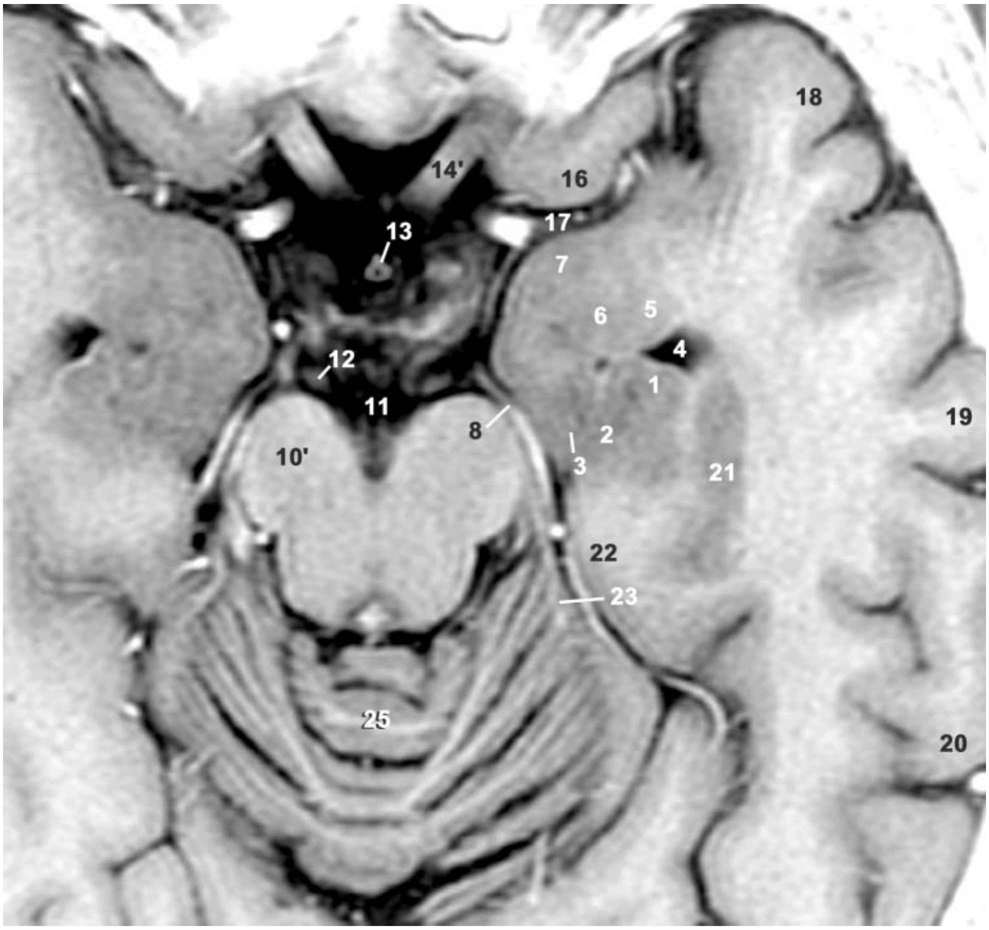

Fig. 124. C 3T MRI view

1, hippocampal head, digitationes hippocampi; **2**, hippocampal head, gyrus dentatus; **3**, uncal apex; **4**, temporal (inferior) horn of the lateral ventricle; **5**, amygdala, lateral nucleus; **6**, amygdala, basal nucleus; **7**, ambient gyrus; **8**, crural cistern and posterior cerebral artery; **9**, brachium conjunctivum; **10**, pons, upper part; **10′**, crus cerebri; **11**, intercrural (interpeduncular) cistern and basilar artery; **12**, oculomotor nerve; **13**, hypophysial stalk; **14**, optic chiasma; **14′**, optic nerve; **15**, gyrus rectus; **16**, posterior orbital gyrus; **17**, lateral fissure, basal part and middle cerebral artery; **18**, superior temporal gyrus; **19**, middle temporal gyrus; **20**, inferior temporal gyrus; **21**, collateral sulcus; **22**, parahippocampal gyrus; **23**, tentorium cerebelli; **24**, culmen; **25**, central lobule

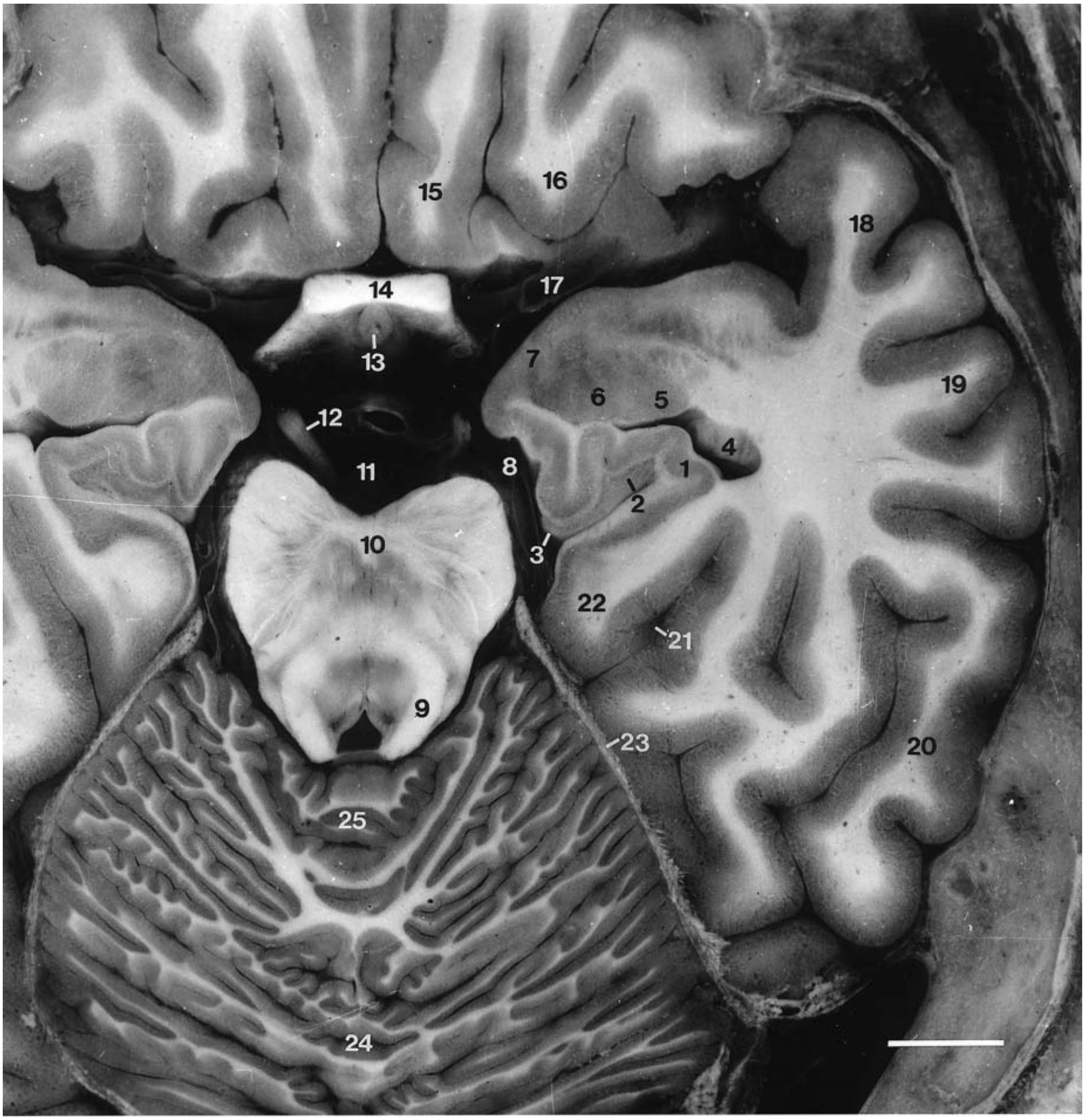

Fig. 124. D Head section. **Bar,** 10 mm

References

Addison WHF (1915) On the rhinencephalon of Delphinus delphis. J Comp Neurol 25: 497–522

Adolphs R, Tranel D, Damasio H, Damasio AR (1995) Fear and the human amygdala. J Neurosci 15 (9): 5879–5891

Aeby CH (1871) Der Bau des menschlichen Körpers. Vogel, Leipzig

Aggleton JP (1986) A description of the amygdalo-hippocampal interconnections in the macaque monkey. Exp Brain Res 64: 515–526

Aggleton JP (1992) The amygdala: neurobiological aspects of emotion, memory and mental dysfunction. Wiley-Liss, New York, p 615

Alonso JR, Hoi Sang U, Amaral DG (1996) Cholinergic innervation of the primate hippocampal formation. II. Effects of fimbria/fornix transection. J Comp Neurol 375: 527–551

Altschul R (1939) Zur Angioarchitectonik des Gehirns. Anat Anz 88: 23–24

Amaral DG, Campbell MJ (1986) Transmitter systems in the primate dentate gyrus. Hum Neurobiol 5: 169–180

Amaral DG, Insausti R (1990) Hippocampal formation. In: Praxinos G (ed) The human nervous system. Academic, San Diego, pp 711–755

Amaral DG, Witter MP (1989) The three-dimensional organization of the hippocampal formation: a review of anatomical data. Neuroscience 31 (3): 571–591

Amaral DG, Insausti R, Cowan WM (1984) The commissural connections of the monkey hippocampal formation. J Comp Neurol 224: 307–336

Amaral DG, Insausti R, Cowan WM (1987) The entorhinal cortex of the monkey. I. Cytoarchitecture organization. J Comp Neurol 264: 326–355

Amaral DG, Price JL, Pitkänen A, Carmichael ST (1992) Anatomical organization of the primate amygdaloid complex. In: Aggleton JP (ed) The amygdala: neurobiological aspects of emotion, memory and mental dysfunctions. Wiley-Liss, New York, pp 1–66

Andersen P (1975) Organization of hippocampal neurons and their interconnections. In: Isaacson RL, Pribram KH (eds) The hippocampus. I. Structure and development. Plenum, New York, pp 155–175

Andersen P, Bliss TVP, Skrede KK (1971) Lamellar organization of hippocampal excitatory pathways. Exp Brain Res 13: 222–238

Andersen RA, Asanuma C, Essick G, Siegel RM (1990) Corticocortical connections of anatomically and physiologically defined subdivisions within the inferior parietal lobule. J Comp Neurol 296: 65–113

Andrew J, Watkins ES (1969) A stereotaxic atlas of the human thalamus and adjacent structures. Williams and Wilkins, Baltimore, p 257

Angevine JB (1975) Development of the hippocampal region. In: Isaacson RL, Pribram KH (eds) The hippocampus. I. Structure and development. Plenum, New York, pp 61–94

Anthony J (1947) Morphologie externe du cerveau des singes platyrhiniens. Ann Sci Nat (Zool) VIII: 1–150

Arïens Kappers CH, Huber GC, Crosby EC (1967) The comparative anatomy of the nervous system of vertebrates, including man, vol 3. Hafner, New York, pp 1413–1429

Babb TL, Brown WJ, Pretorius J, Davenport C, Lieb JP, Crandall PH (1984) Temporal lobe volumetric cell densities in temporal lobe epilepsy. Epilepsia 25 (6): 729–740

Bär TH (1980) The vascular system of the cerebral cortex . In: Advances in anatomy, embryology and cell biology, vol 59. Springer, Berlin Heidelberg New York, p 62

Bargmann W (1964) Histologie und mikroskopische Anatomie des Menschen, 5th edn. Thieme, Stuttgart

Bell MA, Ball MJ (1981) Morphometric comparison of hippocampal microvasculature in ageing and demented people: diameters and densities. Acta Neuropathol 53: 299–318

Benninghoff A (1940) Lehrbuch der Anatomie des Menschen, vol 2. II. Nervensystem, Haut und Sinnesorgane. Lehmanns, Munich

Bentivoglio M, Kultas-Ilinsky K, Ilinsky I (1993) Limbic thalamus: structure, intrinsic organization and connections. In: Vogt BA, Gabriel M (eds) Neurobiology of cingulate cortex and limbic thalamus. Birkhäuser, Boston, pp 71–123

Bilkey D, Goddard GV (1985) Medial septal facilitation of hippocampal granule cell activity is mediated by inhibition of inhibitory interneurons. Brain Res 361: 99–106

Bischoff S (1986) Mesohippocampal dopamine system. Characterization, functional and clinical implications. In: Isaacson RL, Pribram KH (eds) The hippocampus, vol. 3. Plenum, New York, pp 1–32

Blackstad TW (1956) Commissural connections of the hippocampal region in the rat, with special reference to their mode of termination. J Comp Neurol 105: 417–538

Blackstad TW (1958) On the termination of some afferents to the hippocampus and fascia dentata. Acta Anat 35: 202–214

Blackstad TW, Brink K, Hem J, Jeune B (1970) Distribution of hippocampal mossy fibers in the rat. An experimental study with silver impregnation methods. J Comp Neurol 138: 433–450

Bland BH (1986) The physiology and pharmacology of hippocampal formation theta rhythms. Prog Neurobiol 26: 1–54

Braak H (1974) On the structure of the human archicortex. I. The cornu ammonis. A Golgi and pigment architectonic study. Cell Tissue Res 152: 349–383

Braak H (1980) Architectonics of the human telencephalic cortex. Studies of brain function, vol 4, Springer, Berlin Heidelberg New York, pp 24–62

Braak H, Braak E (1983) Neuronal types in the basolateral amygdaloid nuclei of man. Brain Res Bull 11: 349–365

Bratz E (1899) Ammonshornbefunde der Epileptischen. Arch Psychiatr Nervenkr 31: 820–836

Broca P (1878) Anatomie comparée des circonvolutions cérébrales. Le grand lobe limbique et la scissure limbique dans la série des mammifères. Rev Anthropol 1: 385–498

Brodal A (1947) The hippocampus and the sense of smell. A review. Brain 70: 179–222

Buckmaster PS, Soltesz I (1996) Neurobiology of hippocampal interneurons. A workshop review. Hippocampus 6: 330–339

Carpenter MB, Sutin J (1983) Human neuroanatomy, 8th edn. Williams and Wilkins, Baltimore, pp 612–642

Carpenter MB, Noback CR, Moss ML (1954) The anterior choroidal artery. Its origins, course, distribution, and variations. AMA Arch Neurol Psychiatry 71: 714–722

Cerbone A, Patacchioli FR, Sadile AG (1993) A neurogenetic and morphogenetic approach to hippocampal functions based on individual differences and neurobehavioral covariations. Behav Brain Res 55: 1–16

Cervos-Navarro J, Rozas I (1978) The arteriole as a site of metabolic exchange. Adv Neurol 20: 17–24

Chan Palay V (1987) Somatostatin immunoreactive neurons in the human hippocampus and cortex shown by immunogold/silver intensification on vibratome sections: coexistence with neuropeptide Y neurons, and effects in Alzheimer-type dementia. J Comp Neurol 260 (2): 201–224

Chronister RB, White LE (1975) Fiber architecture of the hippocampal formation: anatomy, projections and structural significance. In: Isaacson RL, Pribram KH (eds) The hippocampus. I. Structure and development. Plenum, New York, pp 9-39

Clara M (1959) Das Nervensystem des menschen, 3rd edn. Barth, Leipzig, p 808

Cobb S (1929) The cerebral circulation. VIII. A quantitative study of the capillaries in the hippocampus. Arch Surg 18: 1200–1209

Collins RC (1986) Selective vulnerability of brain: new insights from the excitatory synapse. Metab Brain Dis 1 (4): 231–240

Corsellis JAN (1958) Individual variation in the size of the tentorial opening. J Neurol Neurosurg Psychiatry 21: 279–283

Corsellis JAN, Bruton CJ (1983) Neuropathology of status epilepticus in humans. Adv Neurol 34: 129–139

Corsellis JAN, Meldrum BS (1976) Epilepsy. In: Blackwood W, Corsellis JAN (eds) Greenfield's neuropathology, 4th edn. Arnold, London, pp 771–795

Craigie EH (1945) The architecture of the cerebral capillary bed. Biol Rev 20: 133–146

Crosby RC, Humphrey T, Lauer EW (1962) Correlative anatomy of the nervous system. Macmillan, New York, p 731

Crunelli V, Forda S, Kelly JS (1985) Excitatory amino acids in the hippocampus: synaptic physiology and pharmacology. TINS: 26–30

Davis JN, Nishimo K, Moore K (1989) Noradrenergic regulation of delayed neuronal death after transient forebrain ischemia. In: Ginsberg MD, Dietrich WD (eds) Cerebrovascular diseases. Raven, New York, pp 109–116

De Armond SJ, Fusco MM, Dewey MM (1974) Structure of the human brain. A photographic atlas. Oxford University Press, New York, p 166

De Garengeot RJ (1742) Splanchnologie ou l'anatomie des viscères, vol 2, 2nd edn. Osmont, Paris, pp 250–251

Dejerine J (1980) Anatomie des centres nerveux, vol 1. Masson, Paris, p 816

Delay J, Brion S (1969) Le syndrome de Korsakoff. Masson, Paris

De Reuck J, van Kerckvoorde L, de Coster W, van der Eecken (1979) Ischemic lesions of the hippocampus and their relation to Ammon's horn sclerosis. J Neurol 220: 157–168

Devinsky O, Luciano D (1993) The contributions of cingulate cortex to human behavior. In: Vogt BA, Gabriel M (eds) Neurobiology of cingulate cortex and limbic thalamus. Birkhäuser, Boston, pp 527-556

Diamond DM, Fleshner M, Ingersoll N, Rose GM (1996) Psychological stress impairs spatial working memory: relevance to electrophysiological studies of hippocampal function. Behav Neurosci 110 (4): 661–672

Doebler JA, Markesbery WR, Anthony A, Rhoads RE (1987) Neuronal RNA in relation to neuronal loss and neurofibrillary pathology in the hippocampus in Alzheimer's disease. J Neuropathol Exp Neurol 46 (1): 28–39

Du F, Whetsell WO, Abou-Khalil B, Blumenkopf B, Lothman EW, Schwarcz R (1993). Preferential neuronal loss in layer III of the entorhinal cortex in patients with temporal lobe epilepsy. Epilepsy Res 16: 223–233

Dunning HS, Wolff HG (1937) The relative vascularity of various parts of the central and peripheral nervous system of the cat and its relation to function. J Comp Neurol 67: 433–450

Duval M (1881–1882) La corne d'Ammon. Arch Neurol 2: 3

Duvernoy H (1972) The vascular architecture of the median eminence. In: Knigge KM, Scott DE, Weindl A (eds) Brain-endocrine interaction. Median eminence: structure and function. International Symposium, Munich 1971. Karger, Basel, pp 79–108

Duvernoy H (1975) The superficial veins of the human brain. Veins of the brain stem and of the base of the brain. Springer, Berlin Heidelberg New York, p 110

Duvernoy H (1988) The human hippocampus. An atlas of applied anatomy. Bergmann, Munich

Duvernoy H (1995a) The human brain stem and cerebellum. Surface, structure, vascularization and three dimensional sectional anatomy with MRI. Springer, Wien New York

Duvernoy H (1995b) Brain anatomy. In: Kuzniecky RI, Jacqson GD (eds) Magnetic resonance in epilepsy. Raven, New York, pp 49–105

Duvernoy H (1999a) Human brainstem vessels, 2nd edn. Springer, Berlin Heidelberg New York, p 261

Duvernoy H (1999b) The human brain. Surface, blood supply and three-dimensional sectional anatomy, 2nd edn. Springer, Wien New York, p 491

Duvernoy H, Koritke JG (1964) Contribution à l'étude de l'angioarchitectonie des organes circumventriculaires. Arch Biol (Liège) 75: 849–904

Duvernoy H, Koritke JG (1965) Recherches sur la vascularisation de l'organe subfornical. J Med Besançon 2: 115–130

Duvernoy H, Kortike JG, Monnier G (1969) Sur la vascularisation de la lame terminale humaine. Z Zellforsch 102: 49–77

Duvernoy H, Koritke JG, Monnier G (1971) Sur la vascularisation du tuber postérieur chez l'homme et sur les relations vasculaires tubéro-hypophysaires. J Neurovisc Relat 32: 112–142

Duvernoy H, Koritke JG, Monnier G, Jacquet G (1972) Sur la vascularisation de l'area postrema et de la face postérieure du bulbe chez l'homme. Z Anat Entwickl Gesch 138: 41–66

Duvernoy H, Delon S, Vannson JL (1981) Cortical blood vessels of the human brain. Brain Res Bull 7: 519–579

Duvernoy H, Delon S, Vannson JL (1983) The vascularization of the human cerebellar cortex. Brain Res Bull 11 (4): 419–480

Duvernoy H, Parratte B, Tatul and Vuillier F (2000) The human pineal gland: Relationships with surrounding structures and blood supply. Neurological Research 22: 747–790

Earle KM, Baldwin M, Penfield W (1953) Incisural sclerosis and temporal lobe seizures produced by hippocampal herniation at birth. Arch Neurol Gen Psychiatry 69: 27–42

Eichenbaum H, Otto T, Cohen NJ (1994) Two functional components of the hippocampal memory system. Behav Brain Sci 17: 449–518

Elliot Smith G (1896) The fascia Dentata. Anat Anz 12: 119–126

Elliot Smith G (1897) The morphology of the indusium and striae lancisii. Anat Anz 13: 23–27

Elliot Smith G (1898) The relation of the fornix to the margin of the cerebral cortex. J Anat 32: 23–58

Erdem A, Yasargil G, Roth P (1993) Microsurgical anatomy of the hippocampal arteries. J Neurosurg 79: 256–265

Fleischhauer K (1959) Zur Chemoarchitektonik der Ammonsformation. Nervenarzt 194: 300–301

Francis PT, Cross AJ, Bowen DM (1994) Neurotransmitters and neuropeptides. In: Terry RD, Katzman R, Bick KL (eds) Alzheimer disease. Raven, New York, pp 247–261

Frederikson CJ, Klitenick MA, Manton WI, Kirkpatrick JB (1983) Cytoarchitectonic distribution of zinc in the hippocampus of man and the rat. Brain Res 273: 335–339

Friede RL (1966) The histochemical architecture of the Ammon's horn as related to its selective vulnerability. Acta Neuropathol 6: 1–13

Fujii K, Lenkey C, Rhoton AL Jr (1980) Microsurgical anatomy of the choroidal arteries: lateral and third ventricles. J Neurosurg 52: 165–188

Gaffan D, Lim C (1991) Hippocampus and the blood supply to TE: parahippocampal pial section impairs visual discrimination learning in monkeys. Exp Brain Res 87: 227–231

Gallagher M, Holland PC (1994) The amygdala complex: multiple roles in associative learning and attention. Proc Natl Acad Sci USA 91: 11771–11776

Gastaut H, Lammers JH (1961) Anatomie du rhinencéphale. Masson, Paris

Giacomini CH (1884) Fascia dentata du grand hippocampe dans le cerveau de l'homme. Arch Ital Biol 5: 1–16, 205–219, 396–417

Gluhbegovic N, Williams TH (1980) The human brain. A photographic guide. Harper and Row, Hagerstown, p 176

Goldberg H (1974) The anterior choroidal artery. In: Newton TH, Potts DG (eds) Radiology of the skull and brain, vol II, book 2. Mosby, St Louis, pp 1628–1658

Grassé PP (1972) Traité de zoologie. Anatomie, systématique, biologie, vol XVI, part IV. Masson, Paris, p 1077

Graybiel AM, Aosaki T, Flaherty AW, Kimura M (1994) The basal ganglia and adaptative motor control. Science 265: 1826–1831

Green JD, Arduini A (1954) Hippocampal electrical activity in arousal. J Neurophysiol 17: 533–557

Green RC, Mesulam MM (1988) Acetylcholinesterase fiber staining in the human hippocampus and parahippocampal gyrus. J Comp Neurol 273: 488–499

Groenewegen HJ, Berendse HW, Meredith GE, Haber SN, Voorn P, Wolters JG, Lohman AHM (1991) Functional anatomy of the ventral limbic system-innervated striatum. In: Willner P, Scheel-Krüger J (eds) The mesolimbic dopamine system: from motivation to action. Wiley, Chichester, pp 19–59

Haber SN, Lynd-Balta E, Mitchell SJ (1993) The organization of the descending ventral pallidal projections in the monkey. J Comp Neurol 329: 111–128

Haefely W, Polc P (1986) Physiology of GABA enhancement by benzodiazepines and barbiturates. In: Olsen J (ed) Benzodiazepine/GABA receptors and chloride channels: structural and functional properties. Liss, New York, pp 97–133

Haigler HJ, Cahill L, Crager M, Charles E (1985) Acetylcholine, aging and anatomy: differential effects in the hippocampus. Brain Res 362: 157–160

Haines DE (1987) Neuroanatomy. An atlas of structures, sections and systems, 2nd edn. Urban and Schwarzenberg, Baltimore, p 236

Hasegava T, Ravens JR, Toole JF (1967) Precapillary arteriovenous anastomoses. "Thouroughfare channels" in the brain. Arch Neurol 16: 217–224

Hassler O (1967) Arterial deformities in senile brains. Acta Neuropathol 8: 219–229

Heiman M (1938) Über Gefässstudien am aufgehellten Gehirn. I. Die Gefässe des Ammonshornes. Schweiz Arch Neurol Psychiatr 40: 277–301

Hens L, Van den Bergh R (1977) Vascularization and angioarchitecture of the human pes hippocampi. Eur Neurol 15: 264–274

Herman JP, Schäfer MKH, Young EA, Thompson R, Douglass J, Akil H, Watson SJ (1989) Evidence for hippocampal regulation of neuroendocrine neurons of the hypothalamo-pituitary-adrenocortical axis. J Neurosci 9: 3072–3082

Hevner RF, Wong-Riley MT (1992) Entorhinal cortex of the human, monkey, and rat: metabolic map as revealed by cytochrome oxidase. J Comp Neurol 326: 451–469

Hjorth-Simonsen A, Jeune B (1972) Origin and termination of the hippocampal perforant path in the rat studied by silver impregnation. J Comp Neurol 144: 215–232

Howe ML, Courage ML (1993) On resolving the enigma of infantile amnesia. Psychol Bull 113: 305–326

Huang YP, Wolf BS (1974) The basal cerebral vein and its tributaries. In: Newton TH, Potts DG (eds) Radiology of the skull and brain, vol 2, book 3. Angiography. Mosby, St. Louis, pp 2111–2154

Humphrey T (1967) The development of the human hippocampal fissure. J Anat 101 (4): 655–676

Hussein S, Renella RR, Dietz H (1988) Microsurgical anatomy of the anterior choroidal artery. Acta Neurochir (Vienna) 92: 19–28

Hyman BT, Van Hoesen GW, Kromer LJ, Damasio AR (1986) Perforant pathway changes and the memory impairment of Alzheimer's disease. Ann Neurol 20: 472–481

Ikonomovic MD, Sheffield R, Armstrong DM (1995) AMPA-selective glutamate receptor subtype immunoreactivity in the aged human hippocampal formation. J Comp Neurol 359: 239–252

Insausti R, Tunon T, Sobreviela T, Insausti AM, Gonzalo LM 1995. The human entorhinal cortex: a cytoarchitectonic analysis. J Comp Neurol 355: 171–198

Isaacson RL (1974) The limbic system. Plenum, New York, p 292

Jacobs MS, Mc Farland WL, Morgane PJ (1979) The anatomy of the brain of the bottlenose dolphin (Tursiops truncatus). Rhinic lobe (rhinencephalon): the archicortex. Brain Res Bull 4 [Suppl 1]:1–108

Johansen FF, J¢rgensen MB, Ekström von Lubits DKJ, Diemar NH (1984) Selective dendrite damage in hippocampal CA1 stratum radiatum with unchanged axon ultrastructure and glutamate uptake after transient cerebral ischaemia in the rat. Brain Res 291: 373–377

Kahle W (1986) Nervous system and sensory organs. In: Kahle W, Leonhardt H, Platzer W (eds) Color atlas and textbook of human anatomy, vol 3, 3rd edn. Thieme, Stuttgart, p 374

Kartsounis LD, Rudge P, Stevens JM (1995) Bilateral lesions of CA1 and CA2 fields of the hippocampus are sufficient to cause a severe amnesic syndrome in humans. J Neurol Neurosurg Psychiatry 59: 95 – 98

Kennady JC, Taplin GV (1967) Shunting in cerebral microcirculation. Am Surg 33 (10): 763 – 771

Kesner RP (1994) Hippocampus and memory for time. Behav Brain Sci 17: 485 – 486

Khan NM (1969) The blood supply of the midbrain in man and monkey. PhD thesis, Guy's Hospital Medical School, London

Khazipov R, Bregestovski P, Ben-Ari Y (1993) Hippocampal inhibitory interneurons are functionally disconnected from excitatory inputs by anoxia. J Neurophysiol 70 (6): 2251 – 2259

Kier L, Fulbright RK, Bronen RA (1995) Limbic lobe embryology and anatomy: dissection and MR of the medial surface of the fetal cerebral hemisphere. Am J Neuroradiol 16: 1847 – 1853

Kirino T (1982) Delayed neuronal death in the gerbil hippocampus following ischemia. Brain Res 239: 57 – 69

Kirino T, Tamura A, Sano K (1986) A reversible type of neuronal injury following ischemia in the gerbil hippocampus. Stroke 17 (3): 455 – 459

Klinger J (1948) Die makroskopische Anatomie der Ammonsformation. Denkschriften der Schweizerischen Naturforschenden Gesellschaft, vol 78 (1). Fretz, Zurich, p 82

Klosovskii BN (1963) Fundamental principles of the development, structure and function of the vaso-capillary network of the brain. In: Klosovskii BN (ed) The development of the brain and its disturbance by harmful factors. Pergamon, Oxford, pp 44 – 54

Köhler C, Eriksson L, Davies S, Chan Palay V (1986) Neuropeptide Y innervation of the hippocampal region in the rat and monkey brain. J Comp Neurol 244: 384 – 400

König JFR, Klippel RA (1963) The rat brain. A stereotaxic atlas. Williams and Wilkins, Baltimore, p 162

Kopelman MD (1993) The neuropsychology of remote memory. In: Boller F, Grafman J (eds) Handbook of neuropsychobiology, vol 8. Elsevier, Amsterdam, pp 215 – 238

Kopsch F (1940) Nervensystem – Sinnesorgane. In: Rauber A, Kopsch F (eds) Lehrbuch und Atlas der Anatomie des Menschen, vol III, 15th edn. Thieme, Leipzig, p 562

Koritké JG, Sick H (1982) Atlas de coupes sériées du corps humain. 1. Tête, cou, thorax. Urban and Schwarzenberg, Munich, p 165

Kotapka MJ, Graham DI, Adams JH, Gennarelli TA (1994) Hippocampal pathology in fatal human head injury without high intracranial pressure. J Neurotrauma 11 (3) 317 – 324

Kudo Y, Takeda K, Yamazaki K (1990) Quin2 protects against neuronal cell death due to Ca2+ overload. Brain Res 528: 48 – 54

Kuhlenbeck H (1954) The human diencephalon. Confin Neurol 14 [Suppl]: 230

Lang J (1981) Klinische Anatomie des Kopfes. Neurokranium – Orbita – Kraniozervikaler Übergang. Springer, Berlin Heidelberg New York, pp 286 – 287

Lang J (1985) Anatomy of the tentorial margin. Adv Neurosurg 13: 173 – 181

Lavin A, Grace AA (1994) Modulation of dorsal thalamic cell activity by the ventral pallidum: its role in the regulation of thalamocortical activity by the basal ganglia. Synapse 18: 104 – 127

Lazorthes G, Gouaze A, Salamon G (1976) Vascularisation et circulation de l'encéphale. I. Anatomie descriptive et fonctionnelle. Masson, Paris

Lecaque G, Scialfa G, Salamon G, Szikla G, Hori T, Petrov V (1978) Les artères du gyrus parahippocampique. J Radiol 5: 3 – 12

LeDoux JE (1989) Cognitive emotional interactions in the brain. Cogn Emotion 3: 267 – 289

LeDoux JE (1993) Emotional memory systems in the brain. Behav Brain Res 58: 69 – 79

Leonard BW, Amaral DG, Squire LR, Zola-Morgan S (1995) Transient memory impairment in monkeys with bilateral lesions of the entorhinal cortex. J Neurosci 15 (8) 5637 – 5659

Lewis FT (1923) The significance of the term hippocampus. J Comp Neurol 35: 213 – 230

Lierse W (1963) Die Gefässversorgung des Archipallium. Abt Anz 112: 265 – 269

Liliequist B (1959) The subarachnoid cisterns. An anatomic and roentgenologic study. Acta Radiol [Suppl] 185: 61 – 71

Lindenberg R (1957) Die Gefässversorgung und ihre Bedeutung für Art und Ort von kreislaufbedingten Gewebeschäden und Gefässprozessen. In: Scholz (ed) Handbuch der speziellen pathologischen Anatomie und Histologie, vol XIII/1B: Erkrankungen des Nervensystems. Springer, Berlin, pp 1093 – 1095

Lopes da Silva FH, Arnolds DEAT (1978) Physiology of the hippocampus and related structures. Ann Rev Physiol 40: 185 – 216

Lopes da Silva FH, Groenewegen HJ, Holshiemer J, Room P, Witter MP, van Groen TH, Wadman SJ (1985) The hippocampus as a set of partially overlapping segments with a topographically organized system of inputs and ouputs: the entorhinal cortex as a sensory gate, the medial septum as a gainsetting system and the ventral striatum as a motor interface. In: Buzsaki G, Vanderwolf CH (eds) Electrical activity of the archicortex. Akadémiai Kiado, Budapest, pp 83 – 106

Lopez da Silva FH, Wadman WJ, Arnolds DEAT, Veeken C, Holsheimer J (1984) Hippocampus: behavior and modulation of local circuits. In: Reinoso-Suarez F, Ajmone-Marsan C (eds) Cortical integration. Raven, New York, pp 147 – 170 (International brain research organisation, monograph series, vol II)

Lorente de No R (1928) Ein Beitrag zur Kenntnis der Gefässverteilung in der Hirnrinde. J Psychol Neurol 35: 19 – 31

Lorente de No R (1934) Studies on the structure of the cerebral cortex. II. Continuation of the study of the Ammonic system. J Psychol Neurol 46 (2): 113 – 177

Lynch G, Cotman CW (1975) The hippocampus as a model for studying anatomical plasticity in the adult brain. In: Isaacson RI, Pribram KH (eds) The hippocampus. I. Structure and development. Plenum, New York, pp 123 – 154

Lynch G, Rose G, Gall C (1978) Anatomical and functional aspects of the septo-hippocampal projections. Ciba Found Symp 58: 5 – 24

Macchi G (1951) The ontogenic development of the olfactory telencephalon in man. J Comp Neurol 95: 245 – 305

Maclean PD (1992) The limbic system concept. In: Trimble MR, Bolwig TG (eds) The temporal lobes and the limbic system. Wrightson Biomedical, pp 1 – 265

MacLean PF (1970) The triune brain, emotion of scientific bias. In: Schmitt FO (ed) The neurosciences, second study program. Rockefeller University Press, New York, pp 336 – 349

Mani RB, Lohr JB, Jeste DV (1986) Hippocampal pyramidal cells and aging in the human: a quantitative study of neuronal loss in sectors CA1 to CA4. Exp Neurol 94: 29 – 40

Margerison JH, Corsellis JAN (1966) Epilepsy and the temporal lobes. Brain 89: 499:536

Margolis MT, Newton TH, Hoyt WF (1974) The posterior cerebral artery. II. Gross and roentgenographic anatomy. In Newton T, Potts DG (eds) Radiology of the skull and brain, vol II, book 2. Mosby, St. Louis, pp 1551–1579

Marinkovic S, Milisavljevic M, Puskas L (1992) Microvascular anatomy of the hippocampal formation. Surg Neurol 37: 339–349

Mark LP, Daniels DL, Naidich TP, Yetkin Z, Borne JA (1993) Anatomic moment. The hippocampus. Am J Neuroradiol 14: 709–712

Markowitsch HJ (1995a) Which brain regions are critically involved in the retrieval of old episodic memory? Brain Res Rev 21 (2): 117–127

Markowitsch HJ (1995b) Anatomical basis of memory disorders. In: Gazzaniga MS (ed) The cognitive neurosciences. MIT Press, Cambridge, pp 765–779

Martin LJ, Powers RE, Dellovade TL, Price DL (1991) The bed nucleus-amygdala continuum in human and monkey. J Comp Neurol 309: 445–485

McLardy T (1962) Zinc enzymes and the hippocampal mossy fibre system. Nature 194: 300–302

Meyer A (1971) Historical aspect of cerebral anatomy. Oxford University Press, London, p 230

Milisavljevic M, Marinkovic S, Lolic-Draganic V (1986) Anastomoses in the territory of the posterior cerebral arteries. Acta Anat 127: 221–225

Miller RA, Burack E (1977) Atlas of the central nervous system in man, 2nd edn. Williams and Wilkins, Baltimore, p 63

Moore RY (1975) Monoamine neurons innervating the hippocampal formation and septum: organization and response to injury. In: Isaacson RL, Pribram KH (eds) The hippocampus, vol II. Plenum, New York, pp 215–238

Morandi X, Brassier G, Darnault P, Mercier P, Scarabin JM, Duval JM (1996) Microsurgical anatomy of the anterior choroidal artery. Surg Radiol Anat 18: 275–280

Mountcastle VB (1995) The parietal system and some higher brain functions. Cerebral cortex 5: 377–390

Mouritzen Dam A (1979) The density of neurons in the human hippocampus. Neuropathol Appl Neurobiol 5: 249–264

Muller J, Shaw L (1965) Arterial vascularization of the human hippocampus. Arch Neurol 13: 45–47

Mutel M (1923) Etudes morphologiques sur le rhinencéphale de l'homme et des mammifères. Humblot, Nancy, p 233

Nagata S, Rhoton AL, Barry M (1988) Microsurgical anatomy of the choroidal fissure. Surg Neurol 30: 3–59

Naidich TP, Daniels DL, Haughton VM, Williams A, Pojunas K, Palacios E (1987) Hippocampal formation and related structures of the limbic lobe; anatomic-MR correlation. I. Surface features and coronal sections. Radiology 162: 747–754

Nauta WJH (1958) Hippocampal projections and related neural pathways to the midbrain in the cat. Brain 81: 319–340

Nieuwenhuys R (1985) Chemoarchitecture of the brain. Springer, Berlin Heidelgerg New York, pp 181–183

Nieuwenhuys R, Voogd J, van Huijzen CH (1988) The human central nervous system. A synopsis and atlas, 3rd edn. Springer, Berlin Heidelberg New York, pp 293–363

Nilges RG (1944) The arteries of the mammalian cornu ammonis. J Comp Neurol 80: 177–190

Noël P, Cornil A, Chailly P, Flament-Durand J (1977) Mesial temporal haemorrhage, consequence of status epilepticus. J Neurol Neurosurg Psychiatry 40: 932–935

Nunzi MG, Milan F, Polato P, Gorio A (1986) GABAergic neurons and coexistence of GABA and neuropeptides in the hippocampal microcircuitry. In: Ion channels in neural membranes. Liss, New York, pp 333–345

O'Keefe J, Nadel L (1978) The hippocampus as a cognitive map. Oxford University Press, Oxford, p 570

Olbrich HG, Braak H (1985) Ratio of pyramidal cells versus non-pyramidal cells in sector CA1 of the human Ammon's horn. Anat Embryol 173 (1): 105–110

Olivier A (1996) Surgery of the mesial temporal epilepsy. In: Shorvon S, Dreifuss F, Fish D, Thomas D (eds) The treatment of epilepsy. Blackwell, London, pp 689–698

Olney JW, Sesma MA, Wozniak DF (1993) Glutamatergic, cholinergic, and GABAergic systems in posterior cingulate cortex: interactions and possible mecanisms of limbic system disease. In: Vogt BA, Gabriel M (eds) Neurobiology of cingulate cortex and limbic thalamus. Birkhäuser, Boston, pp 557–580

Olszewski J (1952) The thalamus of the Macaca mulatta. An atlas for use with the stereotaxic instrument. Kager, Basel, p 93

Ono T, Nishijo H, Uwano T (1995) Amygdala role in conditioned associative learning. Prog Neurobiol 46: 401–422

Onodera H, Sato G, Kogure K (1986) Lesions to Schaffer collaterals prevent ischemic death of CA1 pyramidal cells. Neurosci Lett 68: 169–174

Papez JW (1937) A proposed mechanism of emotion. Arch Neurol Psychiatry 38: 725–743

Penfield W, Jasper H (1954) Epilepsy and the functional anatomy of the human brain. Little Brown, Boston, p 896

Petsche H, Stumpf C, Gogolak G (1962) The significance of the rabbit's septum as a relay station between the midbrain and the hippocampus. I. The control of hippocampus arousal activity by the septum cells. Electroencephalogr Clin Neurophysiol 14: 202–211

Pfeifer RA (1930) Grundlegende Untersuchungen für die Angioarchitektonik des menschlichen Gehirns. Springer, Berlin

Pinard E, Tremblay E, Ben-Ari Y, Seylaz J (1984) Blood flow compensates oxygen demand in the vulnerable CA3 region of the hippocampus during kainate-induced seizures. Neuroscience 13 (4): 1039–1049

Poirier P, Charpy A (1921) Traité d'anatomie humaine, vol 3, parts 1 and 2. Masson, Paris

Powell EW, Hines G (1975) Septohippocampal interface. In: Isaacson RL, Pribram KH (eds) The hippocampus. I: Structure and development. Plenum, New York, pp 41–59

Rakic P, Nowakowski RS (1981) The time of origin of neurons in the hippocampal region of the rhesus monkey. J Comp Neurol 196: 99–128

Ramon y Cajal S (1909–1911) Histologie du système nerveux de l'homme et des vertébrés, vols I, II. Maloine, Paris

Ramon y Cajal S (1968) The structure of Ammon's horn. Thomas, Springfield, p 78

Ravens JR (1974) Anastomoses in the vascular bed of the human cerebrum. In: Cervos Navarro J (ed) Pathology of cerebral microcirculation. De Gruyter, Berlin, pp 26–38

Retzius G (1896) Das Menschenhirn. Nordstedt and Söner, Stockholm

Rhoton AL Jr, Fujii K, Fradd B (1979) Microsurgical anatomy of the anterior choroidal artery. Surg Neurol 12: 171–187

Ridley RM, Baker HF, Harder JA, Pearson C (1996) Effects of lesions of different parts of the septo-hippocampal system in primates on learning and retention of information acquired before or after surgery. Brain Res Bull 40 (1): 21–32

Riley HA (1960) An atlas of the basal ganglia, brain stem and spinal cord based on myelin-stained material. Hafner, New York, p 709

Roberts M, Hanaway J (1970) Atlas of the human brain in section. Lea and Febiger, Philadelphia, p 95
Rose M (1927) Allocortex bei Tier und Mensch. Die sogenannte Riechrinde beim Menschen und beim Affen. J Psychol Neurol 34: 261 – 401
Rosene DL, van Hoesen GW (1987) The hippocampal formation of the primate brain. A review of some comparative aspects of cytoarchitecture and connections. In: Jones EG, Peters A (eds) Cerebral cortex, vol 6. Further aspects of cortical function, including hippocampus. Plenum, New York, pp 345-456
Rothman SM (1984) Synaptic release of excitatory amino acid neurotransmitter mediates anoxic neuronal death. J Neurosci 4: 1884 – 1891
Rutecki PA, Grossman RG, Armstrong D, Irish-Loewen S (1989) Electrophysiological connections between the hippocampus and entorhinal cortex in patients with complex partial seizures. J Neurosur 70: 667 – 675
Sakamoto N, Michel JP, Kopp N, Tohyama M, Pearson J (1987) Substance P and enkephalin immunoreactive neurons in the hippocampus and related areas of the human infant brain. Neuroscience 22 (3): 801 – 812
Salamon G, Huang YP (1976) Radiologic anatomy of the brain. Springer, Berlin Heidelberg New York, p 404
Salamon G, Huang YP (1980) Computed tomography of the brain. Atlas of normal anatomy. Springer, Berlin Heidelberg New York, p 359
Samson Y, Wu JJ, Friedman AH, Davis JN (1990) Catecholaminergic innervation of the hippocampus in the cynomolgus monkey. J Comp Neurol 298: 250 – 263
Sasaki M, Sone M, Ehara S, Tamakawa Y (1993) Hippocampal sulcus remnant: potential cause of change in signal intensity in the hippocampus. Radiology 188: 743 – 746
Saunders RL de CH, Bell MA (1971) X-ray microscopy and histochemistry of the human cerebral blood vessels. J Neurosurg 35: 128 – 140
Schaffer K (1892) Beitrag zur Histologie der Ammonshornformation. Arch Mikrosk Anat 39: 611 – 632
Scharrer E (1940) Vascularization and vulnerability of the cornu ammonis in the opossum. Arch Neurol Psychiatry 44 (3): 483 – 506
Scharrer E (1944) The blood vessels of the nervous tissue. Q Rev Biol 19: 308 – 318
Schmidt-Kastner R, Freund TF (1991) Selective vulnerability of the hippocampus in brain ischemia. Neuroscience 40: 599 – 636
Schreiber SS, Baudry M (1995) Selective neuronal vulnerability in the hippocampus. A role for gene expression? TINS 18 (10): 446 – 451
Schwerdtfeger WK (1979) Direct efferent and afferent connections of the hippocampus with the neocortex in the marmoset monkey. Am J Anat 156: 77 – 82
Schwerdtfeger WK (1984) Structure and fiber connections of the hippocampus. A comparative study. Adv Anat Embryol Cell Biol 83: 74
Schwerdtfeger WK (1986) Light and electron microscopic data on field CA1 of the hippocampus of the squirrel monkey, Saimiri sciureus. J Hirnforsch 27: 521 – 532
Sheps JG (1945) The nuclear configuration and cortical connections of the human thalamus. J Comp Neurol 83: 1 – 53
Siggins GR, Henriksen SJ, Chavkin C, Gruol D (1986) Opioid peptides epileptogenesis in the limbic system: cellular mechanisms. Adv Neurol 44: 501 – 512
Simic G, Kostovic I, Winblad B, Bogdanovic N (1997) Volume and number of neurons of the human hippocampal formation in normal aging and Alzheimer's disease. J Comp Neurol 379: 482 – 494
Singer M, Yakovlev PI (1964) The human brain in sagittal section. Thomas, Springfield, p 81
Solodkin A, Van Hoesen GW (1996) Entorhinal cortex modules of the human brain. J Comp Neurol 365: 610 – 627
Sommer W (1880) Erkrankung des Ammonshorns als aetiologisches Moment der Epilepsie. Arch Psychiatr 10: 631 – 675
Spielmeyer W (1927) Die Pathogenese des epileptischen Krampfes. Z Dtsch Ges Neurol Psychiatr 109: 501 – 520
Spielmeyer W (1930) The anatomic substratum of the convulsive state. Arch Neurol Psychiatry 23: 869 – 875
Squire LR (1986) Mechanisms of memory. Science 232 (4758): 1612 – 1619
Squire LR, Zola-Morgan S (1988) Memory: brain systems and behavior. TINS 11 (4): 170 – 175
Squire LR, Zola-Morgan S, Alvarez P (1994) Functional distinctions within the medial temporal lobe memory system: what is the evidence. Behav Brain Sci 17 (3): 495 – 496
Stackman RW, Walsh TJ (1995) Distinct profile of working memory errors following acute or chronic disruption of the cholinergic septohippocampal pathway. Neurobiol Learn Mem 64: 226 – 236
Stephan H (1975) Allocortex. In: Bargmann W (ed) Handbuch der mikroskopischen Anatomie des Menschen, vol 4. Nervensystem, part 9. Springer, Berlin Heidelberg New York, pp 50 – 58
Stephan H (1983) Evolutionary trends in limbic structures. Neurosci Biobehav Rev 7: 367 – 374
Stephan H, Manolescu J (1980) Comparative investigations on hippocampus in insectivores and primates. Z Mikrosk Anat Forsch 94 (6): 1025 – 1050
Stephens RG, Stilwell DL (1969) Arteries and veins of the human brain. Thomas, Springfield, pp 96 – 99
Suzuki WA (1994) What can neuroanatomy tell us about the functional components of the hippocampal memory system ? Behav Brain Sci 17 (3): 496 – 498
Suzuki WA, Amaral DG (1993) The organization of cortical inputs to the perirhinal cortices in the monkey. Abstr Soc Neurosci 16: 53
Suzuki WA, Amaral DG (1994) Perirhinal and parahippocampal cortices of the macaque monkey: cortical afferents. J Comp Neurol 350: 494 – 533
Swanson LW (1978) The anatomical organization of septo-hippocampal projections. Ciba Found Symp 58: 25 – 48
Swanson LW (1983) The hippocampus and the concept of the limbic system. In: Seifert (ed) Neurobiology of the hippocampus. Academic, London, pp 3 – 20
Talairach J, Szikla G (1967) Atlas d'anatomie stéréotaxique du télencéphale. Etudes anatomo-radiologiques. Masson, Paris, p 326
Talairach J, Tournoux P (1988) Co-planar stereotaxic atlas of the human brain 3-dimensional proportional system. An approach to cerebral imaging. Thieme, Stuttgart
Testut L, Latarjet A (1948) Traité d'Anatomie humaine, 9th edn, vol 2. Angéiologie, système nerveux central. Doin, Paris, p 1277
Teyler TJ, DiScenna P (1984) The topological anatomy of the hippocampus: a clue to its function. Brain Res Bull 12: 711 – 719
Teyler TJ, DiScenna P (1985) The role of hippocampus in memory: a hypothesis. Neurosci Biobehav Rev 9: 377 – 389
Teyler TJ, Vardaris RM, Lewis D, Rawitch AB (1980) Gonadal steroid: effects of excitability of hippocampal pyramidal cells. Science 209: 1017 – 1019

Tilney F (1939) The hippocampus and its relations to the corpus callosum. J Nerv Ment Dis 89 (1): 433 – 513
Treves A (1995) Quantitative estimate of the information relayed by the Schaffer collaterals. J Comput Neurosci 2: 259 – 272
Trillet M (1992) Neurobiologie de la mémoire. Encéphale 18: 295 – 303
Tryhubczak A (1975) Myeloarchitectonics of the hippocampal formation in the dog. Fol Biol 23 (2): 177 – 188
Turner BH (1981) The cortical sequence and terminal distribution of sensory related afferents to the amygdaloid complex of the rat and monkey. In: Ben Ari Y (ed) The amygdaloid complex. INSERM Symposium no. 20. Elsevier, Amsterdam, pp 51 – 62
Turner W (1891) The convolutions of the brain. A study in comparative anatomy. J Anat Physiol 25: 105 – 153
Uchimura J (1928) Über die Gefässversorgung des Ammonshornes. Z Gesamte Neurol Psychiatr 112: 1 – 19
Unsöld R, Ostertag CB, DeGroot J, Newton TH (1982) Computer reformations of the brain and skull base. Anatomy and clinical application. Springer, Berlin Heidelberg New York, p 234
Van Buren JM, Borke RC (1972) Variations and connections of the human thalamus. 2. Variations of the human diencephalon. Springer, Berlin Heidelberg New York, p 116
Vanderwolf CH, Leung LWS, Stewart DJ (1985) Two afferent pathways mediating hippocampal rhythmical slow activity. In: Buzsaki G, Vanderwolf CH (eds) Electrical activity of the archicortex. Akadémiai Kiado, Budapest, pp 47 – 66
Van Hoesen GW (1982) The parahippocampal gyrus. New observations regarding its cortical connections in the monkey. TINS 5 (10): 345 – 350
Van Hoesen GW (1985) Neural systems of the non-human primate forebrain implicated in memory. Ann NY Acad Sci 444: 97 – 112
Veazey RB, Amaral DG, Cowan WM (1982) The morphology and connections of the posterior hypothalamus in the Cynomolgus monkey (Macaca fascicularis). II. Efferent connections, J Comp Neurol 207: 135 – 156
Vertes RP (1985) Brainstem-septohippocampal circuits controlling the hippocampal EEG. In: Buzsaki G, Vanderwolf CH (eds) Electrical activity of the archicortex. Akadémiai Kiado, Budapest, pp 33 – 45
Villiger R, Ludwig E (1946) Gehirn und Rückenmark. Schwabe, Basel, p 481
Vogt BA (1993) Structural organization of cingulate cortex: areas, neurons, and somatodendritic transmitter receptors. In: Vogt BA, Gabriel M (eds) Neurobiology of cingulate cortex and limbic thalamus. A comprehensive handbook. Birkhäuser, Boston, pp 19 – 70
Vogt BA, Sikes RW, Vogt LJ (1993) Anterior cingulate cortex and the medial pain system. In: Vogt BA, Gabriel M (eds) Neurobiology of the cingulate cortex and limbic thalamus. Birkhäuser, Boston, pp 313 – 344
Vogt C, Vogt O (1937) Sitz und Wesen der Krankheiten im Lichte der topistischen Hirnforschung und des Varierens der Tiere, part 1. Barth, Leipzig, p 457
Walaas I (1983) The hippocampus. In: Emson PC (ed) Chemical neuroanatomy. Raven, New York, pp 337 – 358
West MJ (1993) Regionaly specific loss of neurons in the aging human hippocampus. Neurobiol Aging 14: 287 – 293
West MJ, Schwerdtfeger WK (1985) An allometric study of hippocampal components. Brain Behav Evol 27: 93 – 105
Wieser HG, Yasargil MG (1982) Selective amygdalohippocampectomy as a surgical treatment of mesiobasal limbic epilepsy. Surg Neurol 17: 445 – 457
Williams PL (1995) Gray's anatomy, 38th edn, Churchill Livingstone, New York, pp 1115 – 1141
Wilson CL, Isokawa-Akesson M, Babb TL, Engel J, Cahan LD, Crandall PH (1987) A comparative view of local and interhemispheric limbic pathways in humans: an evoked potential analysis. In: Engel J et al (eds) Fundamental mechanisms of human brain function. Raven, New York, pp 27 – 38
Winslow JB (1752) Exposition anatomique de la structure du corps humain, 2nd edn. Duchenne, Amsterdam
Witter MP, Groenewegen HJ (1992) Organizational principles of hippocampal connections. In: Trimble MR, Bolwig (eds) The temporal lobes and the limbic system. Wrightson Biomedical, pp 37 – 60
Wolf BS, Huang YP (1964) The subependymal veins of the lateral ventricles. Am J Roentgenol 91 (2): 406 – 426
Wolff HG (1938) The cerebral blood vessels. Anatomical principles. Proc Assoc Res Nerv Ment Dis XVIII: 29 – 67
Wolff JR (1976) An ontogenetically defined angioarchitecture of the neocortex. Arzneimittel-Forsch 26: 1239
Wolfram-Gabel R (1983) La vascularisation de la toile choroïdienne du troisième ventricule chez l'homme. Thesis, Amiens
Yasargil MG (1984) Microneurosurgery. I. Microsurgical anatomy of the basal cisterns and vessels of the brain, diagnostic studies, general operative techniques and pathological considerations of the intracranial aneurysms. Thieme, Stuttgart, p 371
Yasargil MG (1987) Microsurgical anatomy of the brain. In: Yasargil MG (ed) Microneurosurgery. IIIA. AVM of the brain history, embryology, pathological considerations, hemodynamics, diagnostic studies, microsurgical anatomy. Thieme, Stuttgart, pp 284 – 337
Yates PO (1976) Vascular disease of the central nervous system. In: Blackwood W, Corsellis JAN (eds) Greenfield's neuropathology, 4th edn. Arnold, London, pp 86 – 147
Zola-Morgan S, Squire LR, Amaral DG (1986) Human amnesia and the medial temporal region: enduring memory impairment following a bilateral lesion limited to field CA1 of the hippocampus. J Neurosci 6 (10): 2950 – 2967
Zola-Morgan S, Squire LR, Amaral DG, Suzuki WA (1989) Lesions of perirhinal and parahippocampal cortex that spare the amygdala and hippocampal formation produce severe memory impairment. J Neurosci 9 (12): 4355 – 4370
Zola-Morgan S, Squire LR, Rempel NL, Clower RP, Amaral DG (1992) Enduring memory impairment in monkeys after ischemic damage to the hippocampus. J Neurosci 12 (7): 2582 – 2596
Zuckerkandl E (1887) Über das Riechzentrum. Enke, Stuttgart

Index